Universidade de Aveiro Departamento de Química
2013

Ana Isabel Martins Novais Padrão

Plasticidade mitocondrial em condições patofisiológicas

Mitochondrial plasticity in pathophysiological conditions

Universidade de Aveiro Departamento de Química
2013

Ana Isabel Martins Novais Padrão

Plasticidade mitocôndrial em condições patofisiológicas

Mitochondrial plasticity in pathophysiological conditions

Tese apresentada à Universidade de Aveiro para cumprimento dos requisitos necessários à obtenção do grau de Doutor em Bioquímica, realizada sob a orientação científica do Doutor Francisco Manuel Lemos Amado, Professor Associado da Escola Superior de Saúde da Universidade de Aveiro e da Doutora Rita Maria Pinho Ferreira, Professora Auxiliar Convidada do Departamento de Química da Universidade de Aveiro

Apoio financeiro da FCT e do FSE no âmbito do III Quadro Comunitário de Apoio através da bolsa SFRH/BD/66642/2009 e do projecto FCT (PTDC/DES/114122/2009), COMPETE e FEDER (FCOMP-01-0124-FEDER-014707).

Dedico este trabalho aos meus pais.

o júri

presidente

Doutor Joaquim Manuel Vieira
professor catedrático da Universidade de Aveiro

Doutor Francisco Manuel Pereira Peixoto
professor associado com agregação da Universidade de Trás-Os-Montes e Alto Douro

Doutor Francisco Manuel Lemos Amado
professor associado da Universidade de Aveiro

Doutora Rita Maria Pinho Ferreira
professora auxiliar convidada da Universidade de Aveiro

Doutor Carlos Pedro Fontes Oliveira
investigador auxiliar da Faculdade de Ciências da Saúde da Universidade da Beira Interior

Doutora Maria João Garrett Silveirinha Sottomayor Neuparth
professor coordenadora do Instituto Politécnico de Saúde do Norte, CESPU CRL.

agradecimentos

Este trabalho representa a conjugação de esforços de muitas pessoas que nos últimos anos contribuíram para encontrar o melhor rumo, fazer as melhores opções e tomar as melhores decisões. Assim, ao concluir esta etapa deixo apenas algumas palavras, não suficientes, mas um sentido e profundo sentimento de reconhecido agradecimento.

Aos meus orientadores, Professor Doutor Francisco Amado e Professora Doutora Rita Ferreira, agradeço a inexcedível orientação científica e toda a confiança que depositaram em mim. Espero ser capaz de corresponder a todas as expectativas. Um agradecimento especial à Professora Doutora Rita Ferreira por toda a motivação e entusiasmo que sempre me transmitiu e por todos os "empurrões" que me deu. Obrigada pela disponibilidade e celeridade que demonstraram durante as correções da tese.

Ao Doutor Rui Vitorino, agradeço pela colaboração e pelos valiosos ensinamentos que muito elevaram os meus conhecimentos científicos. Pelo exemplo de profissionalismo, determinação e entusiasmo que muito me inspiraram.

Ao Professor Doutor José Alberto Duarte, ao Daniel Gonçalves e à D. Celeste Resende, pelo apoio na elaboração e manutenção do protocolo animal.

Ao Professor Doutor Pedro Domingues e Professora Doutora Rosário Domingues, agradeço pela disponibilidade e simpatia com que sempre me receberam e pelo exemplo de dedicação.

Aos meus colegas do Departamento de Química, Alexandre Ferreira, André Silva, Armando Caseiro, Catarina Ramos, Cláudia simões, Cristina Barros, Miguel Aroso, Rita Ferreira, Susana Aveiro, Virgínia Carvalhais, Renato Alves e Zita Cotrim pela amizade, companheirismo e disponibilidade. Obrigada pelos bons momentos quer nas horas de trabalho quer nas de lazer.

Aos meus pais por sempre terem acreditado em mim, por sempre me terem apoiado, mesmo nas decisões mais difíceis. Por me terem ensinado a nunca desistir. À minha irmã e ao meu cunhado por estarem sempre presentes.

Ao Rui, por teres caminhado sempre a meu lado durante esta etapa académica. Por teres aturado os meus dias de mau humor, nem sempre foi fácil. Obrigada pelo teu apoio incondicional, amizade e carinho.

Aos meus amigos de longa data, obrigada por compreenderem as minhas ausências.

Por fim, agradeço também à Fundação para a Ciência e Tecnologia pelo financiamento através da bolsa de doutoramento SFRH/BD/6642/2009, sem o qual este trabalho não teria sido possível.

Palavras-chave Mitocôndria, músculo estriado, envelhecimento, cancro, diabetes mellitus

resumo

O músculo-esquelético e o músculo cardíaco consomem diariamente grandes quantidades de ATP para a contração, pelo que não é de surpreender que a morfologia, a distribuição e a funcionalidade mitocondrial sejam importantes para a manutenção da sua homeostasia. Mais ainda, o músculo estriado apresenta duas populações de mitocôndrias, as intermiofibrilares (IMF), presentes em maior quantidade, e as subsarcolemais (SS). Na presente tese foram estudados, utilizando modelos animais, os mecanismos moleculares localizados na mitocôndria do músculo estriado para melhor compreender o papel da plasticidade mitocondrial em resposta a várias condições patofisiológicas nomeadamente o envelhecimento, a diabetes *mellitus* e o cancro.

A análise bioquímica das populações de mitocôndrias isoladas do coração evidenciou uma maior atividade da cadeia respiratória nas mitocondriais IMF em comparação com as SS. A maior suscetibilidade das subunidades dos complexos da cadeia respiratória das mitocôndrias SS à carbonilação, mas não à nitração, parece justificar a menor atividade da cadeia respiratória observada nesta população de mitocôndrias.

No estudo da adaptação mitocondrial ao envelhecimento verificou-se a acumulação de mitocôndrias disfuncionais no coração. A diminuição da atividade da cadeia respiratória parece ser justificada, pelo menos em parte, pelo aumento da suscetibilidade de proteínas mitocondriais a modificações oxidativas. Adicionalmente verificou-se que um estilo de vida sedentário tem um impacto negativo na funcionalidade mitocondrial do coração de animais idosos.

No músculo-esquelético de animais com diabetes *mellitus* tipo 1 induzida pela administração de streptozotocina, verificou-se uma acumulação de mitocôndrias disfuncionais devido, pelo menos em parte, ao comprometimento do sistema de controlo de qualidade proteica mitocondrial. Efetivamente, a diminuição da atividade e da expressão de proteases AAA foi acompanhada pela acumulação de proteínas mitocondriais oxidadas.

No músculo-esquelético de animais com caquexia associada ao carcinoma urotelial também se verificou a ocorrência de disfunção mitocondrial associada ao comprometimento do sistema de controlo de qualidade proteica, envolvendo as proteases mitocondriais paraplegina e Lon, com consequente acumulação de proteínas mitocondriais oxidadas. A disfunção mitocondrial observada no músculo *gastrocnemius* de animais com cancro ocorreu em paralelo com o aumento do catabolismo muscular e consequente perda de massa corporal.

No global, os resultados sugerem que independentemente do estímulo patofisiológico que promove uma resposta adaptativa da mitocôndria no músculo estriado existem semelhanças no padrão de plasticidade mitocondrial. A redução da capacidade de produção de ATP parece ser devida ao aumento dos danos oxidativos das proteínas mitocondriais, nomeadamente das subunidades dos complexos da cadeia respiratória, de proteínas metabólicas e da MnSOD com consequente comprometimento das vias moleculares em que estão envolvidas. Os nossos resultados evidenciaram, pela primeira vez, a contribuição da disfunção do sistema de controlo de qualidade proteica mitocondrial para a acumulação de proteínas oxidadas e, consequentemente, para a disfunção mitocondrial.

keywords Mitochondria, striated muscle, aging, cancer, diabetes mellitus

abstract

Both skeletal and cardiac muscles daily burn tremendous amounts of ATP to meet the energy requirements for contraction. So, it is not surprising that the maintenance of mitochondrial morphology, number, distribution and functionality in striated muscle are important for muscle homeostasis. In these tissues mitochondria present the added dimension of two populations, the intermyofibrillar (IMF) and the subsarcolemmal (SS) mitochondria, being IMF the most abundant one. In the present thesis, the molecular mechanisms harboured in mitochondria of striated muscles were studied using animal models, to better comprehend the role of mitochondrial plasticity in several pathophysiological conditions such as aging, diabetes mellitus and bladder cancer.

The comparative analysis of IMF and SS populations isolated from heart evidenced a higher respiratory chain activity of mitochondria interspersed in the contractile apparatus. The higher susceptible of SS respiratory chain complexes subunits to carbonylation, but not to nitration, seems to justify the lower respiratory chain activity observed in this mitochondrial population.

Our results showed that in heart from aged mice there is an accumulation of dysfunctional mitochondria. The age-related decrease of oxidative phosphorylation activity seems to be justified, at least partially, by the increased proneness of mitochondrial proteins as OXPHOS subunits and MnSOD to oxidative modifications. Moreover, a sedentary lifestyle seems to worsen the functional consequences of aging in heart by increasing mitochondrial proteins susceptibility to nitration.

In skeletal muscle from rats with type 1 diabetes mellitus induced by streptozotocin administration, we verified the accumulation of dysfunctional mitochondria due, at least in part, to the impairment of PQC system. Indeed, the decreased activity of AAA proteases was accompanied by the accumulation of oxidatively modified mitochondrial proteins with impact in respiratory chain activity.

The diminishing of mitochondria activity also underlies cancer-induced muscle wasting. Indeed, using a rat model of chemically induced urothelial carcinoma we verified that the loss of *gastrocnemius* mass was related to mitochondrial dysfunction due to, at least partially, the down-regulation of PQC system involving the mitochondrial proteases paraplegin and Lon. PQC impairment resulted in the accumulation of oxidatively modified mitochondrial proteins.

In overall, regardless the pathophysiological stimuli that promote mitochondrial alterations, there are similarities in the pattern of disease-related mitochondrial plasticity. The diminished capacity for ATP production in striated muscle seems to be due to increased oxidative damage of mitochondrial proteins, namely subunits of respiratory chain complexes, metabolic proteins and MnSOD. Our data highlighted, for the first time, the impact of mitochondrial PQC system impairment in the accumulation of oxidized proteins, exacerbating the dysfunction of this organelle in striated muscle in several pathophysiological conditions.

TABLE OF CONTENTS

LIST OF FIGURES

Chapter I

Chapter II

Chapter III

Chapter IV

Study I

Study II

Study III

Study IV

Chapter V

Appendix- Supplementary data

Study II

Study III

LIST OF TABLES

Chapter I

Chapter II

Chapter III

Chapter IV

Study I

Study II

Study III

Study IV

Appendix- Supplemtary data

Study I

LIST OF ABBREVIATIONS

4E-BP1	Eukaryotic translation initiator factor 4E binding protein 1
AAA	ATPases associated with a variety of cellular activities
ACTRII	Type UU activin receptor
ADP	Adenosine Diphosphate
Afg312	ATP family gene 3-like 2
AIF	Apoptosis-induced factor
ATP	Adenosine triphosphate
BN-PAGE	Blue native polyacrylamide gel electrophoresis
CAT	Catalase
Ccp1	Cytochrome c peroxidase
CoQ	Coenzyme Q
Cyt c	Cytochrome c
DNA	Deoxyribonucleic acid
E1	Ubiquitin activating enzyme
E2	Ubiquitin carrier protein
E3	Ubiquitin protein ligase
eIF-4E	Eukaryotic translation initiator factor 4E
ETC	Electron transport chain
$FADH_2$	Flavin adenine dinucleotide
FeS	Iron sulfur centers
FoxO	Transcription factor Forkhead box O
GPx	Glutathione peroxidase
H_2O_2	Hydrogen peroxide
HNE	2-hydroxy-4-nonenal
$HO^{\bullet}$	Hydroxil radical
***i*-AAA**	intermembrane space-ATPase Associated with various cellular Activities
IM	Inner membrane
IMF	Intermyofibrillar mitochondria
IMS	Intermembrane space
kDA	KiloDalton
***m*-AAA**	matrix-ATPase Associated with various cellular Activities
MDA	Malondialdehyde
MnSOD	Manganese superoxide dismutase
MPTP	Mitochondrial permeability transition

mtDNA	Mitochondrial DNA
mTOR	Mammalian target of rapamycin
MuRF-1	E-3 ligases Muscle Ring Finger 1
NADH	Nicotinamide adenine dinucleotide
NF-κB	Transcription factor nuclear factor kappaB
$NO^{\bullet}$	Nitric oxide
$O_2^{\bullet-}$	Superoxide radical
OM	Outer membrane
$ONOO^-$	Peroxynitrite
OXPHOS	Oxidative phosphorylation
PGC-1-α	Peroxisome proliferator-activator receptor gamma coactivator 1α
PI3K	Insulin activate phosphatidylinositol-3 kinase
PIF	Proteolysis-inducing factor
PKB	Protein Kinase B
PQC	Protein quality control
PTMs	Post-translational modifications
RNA	Ribonucleic acid
RONS	Reactive oxygen and nitrogen species
ROS	Reactive oxygen species
SIRT	Sirtuin
SOD	Superoxide dismutase
SS	Subsarcolemmal mitochondria
STZ	Streptozotocin
T1DM	Type 1 diabetes mellitus
T2DM	Type 2 diabetes mellitus
TCA	Citric Acid Cycle
TEM	Transmission electron microscopy
Tfam	Mitochondrial transcription factor A
TGF-β	Transforming growth factor-beta
TPPII	Tripeptidyl peptidase II
UCP	Uncoupling protein
UCP-DTA	Uncoupling protein diphtheria toxin A chain
WT	Wild-type
YMEP1L1	Yeast Mitochondrial Escape Protein-1-Like 1

CHAPTER I

STATE OF THE ART

1. General Introduction

Mitochondria are crucial organelles involved in energy production, metabolism and intracellular signaling (Benard and Rossignol 2008). These organelles vary in shape, number and activity to regulate several cellular physiological processes, like ATP production, redox status and calcium homeostasis. Both skeletal and cardiac muscles are extremely energy demanding tissues, highly reliant on mitochondrial oxidative metabolism (Sandri 2008). These muscles rapidly respond to metabolic challenges like exercise, inactivity or disease, being morphological, biochemical and functional alterations of mitochondria key factors in cellular metabolic adaptation. This mitochondrial remodeling is generally designated as "mitochondrial plasticity", which is defined as changes of this organelle activity, content or oxidative phosphorylation capacity due to altered metabolic conditions (Hoppeler and Fluck 2003; Pagel-Langenickel, Schwartz et al. 2007) induced by aging or diseases like diabetes mellitus and cancer.

Studies in striated muscle present the added dimension of two distinct mitochondrial populations that exist as a dynamic network. Mitochondria differ in their subcellular localization, morphology and biochemical properties. Subsarcolemmal (SS) mitochondria are located just underneath the sarcolemma and have a large, lamellar shape. In contrast, the intermyofibrillar (IMF) mitochondria are smaller, more compact, and are located between the contractile filaments. These two spatially distinct mitochondrial populations possess precise functional and biochemical properties and respond differently to external stimuli. Whereas IMF mitochondria are mainly devoted to the energy supply of myosin and SR-ATPases, SS mitochondria support other processes such as ion homeostasis or signaling pathways (Palmer, Tandler et al. 1977; Hoppeler 1986; Hoppeler and Fluck 2003; Riva, Tandler et al. 2005; Hoppel, Tandler et al. 2009).

Impairment of mitochondrial plasticity in striated muscle has been observed in various disorders, including diabetes mellitus, cancer as well as aging (Cohen 1995; Mahgoub and Abd-Elfattah 1998; Hayat, Patel et al. 2004; Boudina and Abel 2007). Underlying these pathophysiological conditions it has been reported changes in mitochondrial morphology, number, distribution and function (Hoppeler and Fluck 2003; Pagel-Langenickel, Schwartz et al. 2007). Mitochondrial dysfunction is usually related to enhanced oxidative stress (Raha and Robinson 2000), oxidative damage of biomolecules, decreased activities of the

electron transport chain (ETC) complexes (Mandavilli, Santos et al. 2002) and decreased ability for ATP synthesis (Chang, Van Remmen et al. 2003). The accumulation of oxidized proteins in mitochondria is avoided by defense systems (Tatsuta and Langer 2008) as Protein Quality Control (PQC) system (Langer, Kaser et al. 2001; Voos and Rottgers 2002; Koppen and Langer 2007; Baker and Haynes 2011), which comprises a multitude of complexes that, among other roles, are involved in the specific proteolytic removal of terminally damaged polypeptides. However, in many pathophysiologic conditions PQC system is defective or overwhelmed (Koppen and Langer 2007). Either the case, the net result is mitochondrial dysfunction. So, PQC players might be seen as potential therapeutic targets to restore mitochondria functionality in pathophysiological conditions.

Generally, it seems that mitochondrial plasticity is a key element in striated muscle adaptation under stress. In such conditions, the molecular mechanisms underlying mitochondrial plasticity might be overcome, explaining why mitochondrial dysfunction is an early event in the pathogenesis of diseases as for example diabetes mellitus (Ferreira et al., 2013). Despite the importance of mitochondrial plasticity in cell fate, its role as a determinant of cell viability is yet poorly understood.

2. State of the art

2.1. Mitochondria in striated muscle

Mitochondria play critical roles in both life and death of striated muscle. This organelle not only produce ATP via oxidative phosphorylation for tissue survival and functionality, but also is involved in multiple cell signalling cascades and in the regulation of cellular metabolism, development, ion homeostasis and apoptosis (Benard, Faustin et al. 2006; Logan 2006; Benard and Rossignol 2008; Nunnari and Suomalainen 2012). Figure 1 summarizes the metabolic pathways harbored in mitochondria, the regulatory mechanisms of protein import, apoptosis, proteolysis, redox, and of calcium levels.

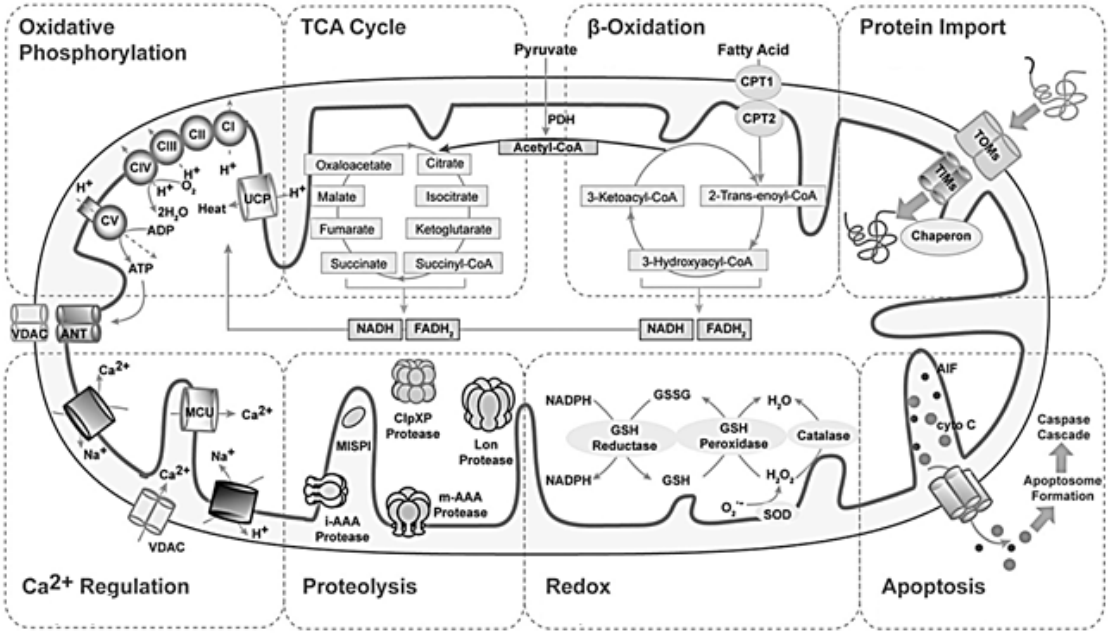

Figure 1: Overview of mitochondria-related processes.
A schematic cross-section of a mitochondrion is shown, with the proteins and protein complexes that are involved in various cellular pathways and processes. Mitochondrial pathways responsible for crucial cellular functions within cell, including protein import, OXPHOS, TCA cycle, β-oxidation, apoptosis, proteolysis, redox and calcium regulation are detailed.
VDAC, voltage-dependent anion exchanger; ANT, adenine nucleotide exchanger; TOMs, translocases of the outer membrane; TIMs, translocase of the inner membrane; Cyto C, cytochrome c; AIF, apoptosis-induced factor; UCP, uncoupling protein; i-AAA, proteases of the AAA family in the inner membrane; m-AAA, proteases of the AAA family in the matrix; GSSG, glutathione disulfide; GSH, glutathione; ClpXP, ATP-dependent Clp protease ATP-binding subunit clpX-like; MCU, mitochondrial calcium uniporter, PDH, pyruvate dehydrogenase; C-I, respiratory chain complex I; C-II, complex II; C-III, complex III; C-IV, complex IV; C-V, complex V; NADH, nicotinamide adenine dinucleotide; $FADH_2$- flavin adenine dinucleotide; SOD- superoxide dismutase, CPT1, Carnitine palmitoyltransferase I, CPT2, Carnitine palmitoyltransferase II; MISPI, mitochondrial intermembrane space protease (adapted from Zhang, Lin et al. 2012).

Mitochondria are highly dynamic, pleomorphic organelles which fuse and divide in response to environment stimuli, development status, and energy requirement of the cell (Chan 2006; Frazier, Kiu et al. 2006; Campello and Scorrano 2010). Some authors argue that in most cells, mitochondria form a reticular network that radiate from the nucleus, creating an interconnected system that supplies the cell with energy and essential metabolites (Liesa, Palacin et al. 2009; Westermann 2010). Nevertheless, electron microscopy of mitochondrion defined their basic morphology as double-membrane organelle, typically rod-shaped and about 1-2 μm in length and 0.1-0.5 μm in width (reviewed by Logan 2006), presenting an outer membrane (OM) and an inner membrane (IM) with folded cristae that give rise to two aqueous compartments, the intermembrane

space (IMS) and the matrix (Duchen 2004; Logan 2006; Navarro and Boveris 2007; Benard and Rossignol 2008; Stowe and Camara 2009), as represented in figure 1. The OM surrounds the organelle, whereas the IM surrounds the central matrix space. The IMS is located between two membranes. The OM is relatively permeable to small molecules and ion species (Duchen 2004; Navarro and Boveris 2007), which move through transmembrane channels formed by a family of integral membrane proteins called porins. The microenvironment space that comprises IMS contains a distinct group of proteins which play major roles in cell physiology, in mitochondrial energetics and in cell death. The IM is largely impermeable and forms the barrier between the cytosol and the mitochondrial matrix. It is composed of segments of inner boundary membrane, parallel to the OM, that join the cristae at cristae junctions. The cristae contain the ETC and phosphorylation apparatus, and several membrane transporters (Lesnefsky, Moghaddas et al. 2001; Gilkerson, Selker et al. 2003; Duchen 2004; Logan 2006). The structure and number of cristae seem to vary enormously between different tissues (Duchen 2004), and seem dependent of the metabolic state of the tissue (Logan 2006; Stowe and Camara 2009). For instance, mitochondria from heart muscle have more cristae than those from liver (Distler, Kerner et al. 2008). These differences occur to fulfill the distinct ATP demands of different cell types. The matrix is considered a highly functional zone of mitochondria once it harbors several metabolic pathways as Krebs cycle (Krebs 1940). Mitochondrial matrix also contains mitochondrial DNA, RNA and ribosome special carriers (Distler, Kerner et al. 2008).

The mammalian mitochondrion contains 4 to 5 copies of its own circular DNA molecule (mtDNA). This small molecule of 16 kb encodes for 37 genes, from which 13 are proteins, all belonging to the respiratory chain (seven proteins from complex I, one from complex 3, three from complex IV, and two from complex V), 2 are rRNA (16S and 12S) and the remainder are mitochondrial tRNAs) (Wallace, Brown et al. 1999; Duchen 2004). mtDNA is traditionally considered “naked” due to the lack of histones and therefore less protected from oxidative damage than nuclear DNA (Duchen 2004). The mtDNA has a significant contribution for mitochondrial function and integrity (Joseph, Rungi et al. 2004; Zeviani and Di Donato 2004). Defects in the synthesis of one of the 13 mtDNA-encoded respiratory subunits can lead to respiratory chain dysfunction and to a wide range of

pathogenic conditions, some of which affect skeletal and cardiac muscles. Although mitochondria contain their own genome and protein synthesizing machinery they are only semi-autonomous (Logan 2006). Proteomic cataloguing studies estimated that mitochondria contain about 1000 (yeast) to 1500 (human) different proteins (Sickmann, Reinders et al. 2003; Perocchi, Jensen et al. 2006; Reinders, Zahedi et al. 2006; Pagliarini, Calvo et al. 2008) with the vast majority (~98%) encoded within the nucleus (synthesized upon cytosolic ribosomes and imported to mitochondria by an elaborate network of translocases and sorting machineries) (Koehler 2000; Neupert and Herrmann 2007; Ryan and Hoogenraad 2007; Chacinska, Koehler et al. 2009). Therefore, the mitochondrial proteome should be viewed as a dynamic program generated by a cross-talk between the two genomes and able to adapt to tissue needs or disease states (Poyton and McEwen 1996; Ryan and Hoogenraad 2007; Dimmer and Rapaport 2008). Changes in the mitochondrial proteome exert influences over mitochondrial homeostasis, underlying diseases and controlling natural processes as development and aging (Wallace 1999; Duchen 2004; Lowell and Shulman 2005).

Mitochondria are highly plastic in terms of shape, number and distribution between tissues and cells types (Yaffe 1999; Logan 2006; Vafai and Mootha 2012). The number of mitochondria *per* cell is variable, depending on cell type and pathophysiological state (Logan 2006; Stowe and Camara 2009; Zick, Rabl et al. 2009; Vafai and Mootha 2012). Tissues with highly energetic demands have great number of mitochondria (Duchen 2004; Vafai and Mootha 2012). Liver cells have 1000–2000 mitochondria *per* cell, making up 20% of the cell volume, and the IM (cristae) area is about 5 times greater than that of the OM. In cardiac mitochondria, the cristae area is much larger, and the mitochondrial volume can reach 30% of cell volume (Stowe and Camara 2009). Indeed, the mammalian heart is a hotspot of metabolic activity, consuming each day 100 times its own weight in ATP (Dorn 2013). Striated muscles are highly reliant on mitochondria and skeletal muscle accounts for approximately 40% of total body mass, being a major site of metabolic activity (Romanello and Sandri 2013). In striated muscles there are two distinct populations of mitochondria that exist as a dynamic network. Mitochondria differ in their subcellular localization, morphology and biochemical properties and they constantly adapt to cellular needs. SS mitochondria are located just beneath the sarcolemma whereas the

smaller IMF mitochondria, which account for 80% of mitochondria, is interspersed in the contractile filaments (Palmer, Tandler et al. 1977; Hoppeler 1986; Hoppeler and Fluck 2003; Riva, Tandler et al. 2005; Hoppel, Tandler et al. 2009). It has been suggested that SS mitochondria provide energy for membrane-related events like signalling and transport of ions and others subtracts, while IMF mitochondria supply ATP for the interaction of myosin with actin leading to muscle contraction (Romanello and Sandri 2013). The two populations differ in structure, size, ATP levels, protein import rates, substrate utilization, and other biochemical properties. IMF mitochondria have a higher rate of oxygen consumption, ATP content, protein import rates, and enzyme activities when compared with SS mitochondria (Palmer, Tandler et al. 1977; Cogswell, Stevens et al. 1993; Takahashi and Hood 1996). In cardiac muscle the specific activity of many mitochondrial enzymes like succinate dehydrogenase and citrate synthase is greater in IMF than in SS mitochondria (Palmer, Tandler et al. 1977). In the cardiac muscle, the rate of oxidative phosphorylation is 1.5 times higher in IMF mitochondria (Palmer, Tandler et al. 1977), supporting the ATP needs for muscle contraction (Ferreira, Vitorino et al. 2012). In skeletal muscle, state 3 respiration (ADP-stimulated respiration) is 2.3- to 2.8-fold greater in IMF than in SS mitochondria and IMF mitochondria show 3 fold greater ATP synthesis rates, indicating that SS and IMF mitochondria have distinct energetic characteristics. Besides bioenergetic differences, cardiac mitochondria populations have different cristae morphology. SS mitochondria present lamelliform cristae whereas in IMF mitochondria predominates tubular cristae (Riva, Tandler et al. 2005), which might reflect compositional differences between mitochondria populations. In skeletal muscle endogenous mitochondrial protein synthesis is 1.8-fold higher in IMF than in SS mitochondria. Moreover, IMF mitochondria have 3–4-fold greater protein import rates of the precursor malate dehydrogenase and ornithine-carbamoyltransferase than SS (Takahashi and Hood 1996). Higher amounts of mitofilin, the mitochondrial-associated protein involved in the regulation of cristae morphology, were observed in IMF mitochondria compared to SS, being more pronounced in cardiac tissue than in *gastrocnemius* muscle (Ferreira, Vitorino et al. 2012). Furthermore, the two mitochondrial subpopulations respond differently to distinct metabolic challenges, including exercise (Krieger, Tate et al. 1980), aging (Fannin, Lesnefsky et al. 1999; Suh, Heath et al. 2003; Ljubicic, Joseph et al. 2009), obesity and type 2 diabetes (Ritov, Menshikova et al. 2005), fasting (Lionetti, Mollica et al. 2007), and

apoptosis (Adhihetty, Ljubicic et al. 2007). Cardiac SS mitochondria seem to be more prone to ischemia damage, due to an increased loss of cardiolipin, reduced oxidative phosphorylation and reactive oxygen species (ROS) production (Lesnefsky, Slabe et al. 2001). In contrast, cardiac IMF mitochondria seem to be more susceptibility to aging and heart failure due to increased oxidative stress (Rosca, Minkler et al. 2011). However, there is no consensus on the functional identity of SS and IMF mitochondria and on the significance of the differential response to pathophysiologic stimuli.

2.1.1. Mitochondrial oxidative phosphorylation system

Mitochondria have a key role in cellular metabolism, harboring the enzymatic reactions underlying the metabolism of carbohydrates, fats and proteins, which intermediate metabolites are selectively imported into the mitochondrial matrix and further metabolized into nicotinamide adenine dinucleotide (NADH) and/or flavin adenine dinucleotide ($FADH_2$). The electrons released by the oxidation of NADH and $FADH_2$ are transferred via the ETC to the final electron acceptor molecular oxygen, which is reduced to water (Poyton and McEwen 1996; Benard and Rossignol 2008; Huttemann, Lee et al. 2008). ETC consists in four major multi-subunit complexes (complexes I-IV), which are localized in the IM. ETC also involves two electron transport carriers: ubiquinone or coenzyme Q10, embedded in the membrane lipid bilayer, and cytochrome c, localized on the external surface of the IM (Poyton and McEwen 1996; Benard and Rossignol 2008). Together with a fifth complex, the ATP synthase (complex V), they are responsible for the production of energy to the cell in the form of ATP and constitute the mitochondrial oxidative phosphorylation (OXPHOS) (Benard and Rossignol 2008). The complexes that establish the ETC are multi-subunits protein complexes associated with prosthetic groups that allow the electrons to flow. Interestingly, the proteins from complex II are entirely encoded by the nucleus, while all the other complexes represent a mixture of proteins encoded by nuclear and mitochondrial DNA (Benard and Rossignol 2008).

Complex I (NADH-ubiquinone oxidoreductase; NADH dehydrogenase) is the largest respiratory complex, with a molecular mass greater than 1000 kDa, and in heart of bovine comprises 46 different subunit peptides, including flavin mononucleotide (FMN) moiety and seven to nine iron-sulfur centers (FeS) and up to three detectable ubisemiquinone species. These complexes catalyze the oxidation of NADH to NAD^+, transferring two

electrons to ubiquinone. This process is coupled to the translocation of four protons across the membrane out mitochondria matrix. Complex I has a L-shaped form, with a long hydrophobic arm and a short hydrophilic arm with the FMN and the NADH active centers that extends the protein complex into the matrix, (Janssen, Nijtmans et al. 2006; Navarro and Boveris 2007).

Complex II (succinate dehydrogenase; succinate-ubiquinone reductase) is a succinate:ubiquinone oxidoreductase that reduces succinate to fumarate, transferring two electrons to ubiquinone. This complex is simultaneously part of the ETC and TCA cycle. In eukaryotes this oligomeric complex is composed of 4 subunits namely a flavoprotein, with a FAD molecule covalently bound, an iron-sulfur protein and two hydrophobic smaller peptides that serve as membrane anchors (Cecchini 2003; Navarro and Boveris 2007; Rutter, Winge et al. 2010). Succinate dehydrogenase is the only respiratory complex that does not pump protons across the IM during its catalytic cycle (Dudkina, Sunderhaus et al. 2008; Rutter, Winge et al. 2010). The mobile carrier between complex I/complex II and complex III is a lipid soluble benzoquinone with a long isoprenoid side chain that may exist in three oxidation states: ubiquinone – fully oxidized, semiquinone – semi-oxidized, or ubiquinol – fully reduced. The most common form in mammals has 10 isoprene units and is referred as Coenzyme Q10 (Navarro and Boveris 2007).

Complex III (cytochrome bc1 complex; ubiquinol-cytochrome c oxidoreductase) is a multisubunit integral membrane complex of the mitochondrial transport chain, which catalyzes electron transfer from ubiquinol to cytochrome c and couples this process to electrogenic translocation of protons across the IM (Brandt and Trumpower 1994; Berry, Guergova-Kuras et al. 2000). This complex in mammalian is composed by 11 polypeptides, 3 of which are associated with the redox centers b_{562}, b_{566} and c_1 heme and an iron-sulfur cluster (Cecchini 2003). The membrane spanning region of complex III consists of 13 transmembrane helices, eight of which belong to cytochrome b. Cytochrome c (cyt c) is a small peptide bound to a heme c group that is associated to the IM, facing the IMS. It is reduced by the electrons transferred from complex III, transporting them to complex IV (Navarro and Boveris 2007; Lenaz and Genova 2009).

Complex IV (cytochrome c oxidase, cytochrome oxidase; ferrocytochrome c: oxygen oxidoreductase) is the final catalyst of the ETC, being located in the inner mitochondrial membrane (Diaz, Fukui et al. 2006). This 200 kDa multicomponent protein reduces O_2 to

H_2O, consuming four protons from the matrix (Navarro and Boveris 2007; Fontanesi, Soto et al. 2008). The enzyme in mammalian contains 13 different subunits, 3 of which are mitochondrially encoded (Cecchini 2003). The redox centers of complex IV are two heme a centres, heme a and heme a_3, located in two different environments, each one associated to a copper atom, respectively, CuA and CuB (Navarro and Boveris 2007).
The electrochemical gradient of protons generated by the pumping activity of complexes I, III and IV is used by ATP synthase to synthesize ATP from ADP and phosphate, which is coupled to the backflow of protons to the matrix (Huttemann, Lee et al. 2008). Most of the cellular ATP of eukaryote cells is synthesized by the F1F0-ATPase complex present in the mitochondrial inner membrane during oxidative phosphorylation. Mitochondrial ATP synthase, F1-F0-ATPase or complex V is formed by 15-18 distinct subunits. It is composed of two distinct functionally and physically components: F1, peripheral to membrane, and F0, integral at the inner membrane (Weber 2006; Fontanesi, Soto et al. 2008).

The organization of the OXPHOS system within the IM appears to be far more complicated than previously thought. There are two main explanations for the interactions between complexes: the fluid state and the solid state models. The fluid state organization model supports that electron transport through the ETC was thought to occur through random interactions of individual protein complexes and the mobile carriers coenzyme Q and cyt c in the IM. This model is based on the finding that all individual protein complexes of the OXPHOS system can be purified in enzymatically active form and on lipid dilution experiments (Acin-Perez, Fernandez-Silva et al. 2008; Schon and Dencher 2009). More recently, this model was confronted with an alternative view, the solid state in which individual complexes are physically grouped into supercomplexes within the IM that transport electrons more efficiently (Lenaz and Genova 2007). Schagger (2001) found structural evidences of specific OXPHOS complexes associations in yeast and mammalian mitochondria using Blue-Native electrophoresis (BN-PAGE), and so introduced the model of the “respirasome”, confirming earlier observations favoring specific inter-complex interactions (Schagger and von Jagow 1991; Schagger 2001). However, OXPHOS supercomplexes and individual OXPHOS complexes co-exist within the IM into a dynamic process that depends on the physiological state (Dudkina, Sunderhaus et al. 2008). Indeed,

such associations may promote stability and substrate channeling while minimizing ROS formation (Shoubridge 2012).

2.1.2. Mitochondrial oxidative stress

In addition to ATP production for cell survival, the mitochondria are also a major source of ROS/RONS. Normally, up to 5% of the oxygen consumed by the mitochondrial respiratory chain undergoes one electron reduction, typically at complexes I, II or III, generating superoxide ($O_2^{\bullet -}$) and hydroxyl ($HO^{\bullet}$) radicals, and hydrogen peroxide (H_2O_2) (Kirkinezos and Moraes 2001; Turrens 2003; Muller, Liu et al. 2004; Ott, Gogvadze et al. 2007; Murphy 2009). Superoxide can also react with nitric oxide ($NO^{\bullet}$) to form peroxynitrite ($ONOO^-$). These metabolic by-products have important physiological functions (e.g. inflammation) but might also be powerful cell-damaging oxidants, though can be neutralized by antioxidant enzymes, as manganase superoxide dismutase (MnSOD) and glutathione peroxidase (GPx) (Ott, Gogvadze et al. 2007). In recent years, there is increasing evidence that ROS are not only toxic but also needed for healthy life (Veal, Day et al. 2007; Brigelius-Flohe 2009; Hamanaka and Chandel 2010; Bae, Oh et al. 2011; Sena and Chandel 2012) (Figure 2). Controlled produced ROS act as a secondary messenger amplifying signals that are crucial for normal cell function (cell proliferation and differentiation). An induction of ROS production will lead to adaptative programs including the transcriptional upregulation of antioxidant genes. In contrast, an overt imbalance between ROS production and the antioxidant defense systems leads to the breakage of normal homeostasis (oxidative stress) and will signal the initiation of the senescence and apoptosis. Non-signaling, irreversible damage to cellular components (e.g. proteins, nucleic acids, and lipids) is only observed under the highest levels of cellular ROS and are closely related to a wide range of pathophysiogical conditions, such as cancer, cardiovascular diseases, aging, diabetes mellitus and neurodegenerative diseases (Hamanaka and Chandel 2010; Bae, Oh et al. 2011; Verdejo, del Campo et al. 2012). Therefore, mitochondria can be seen as a main source of ROS production under pathophysiological conditions as well as primary target of its damaging effects (Turrens 2003).

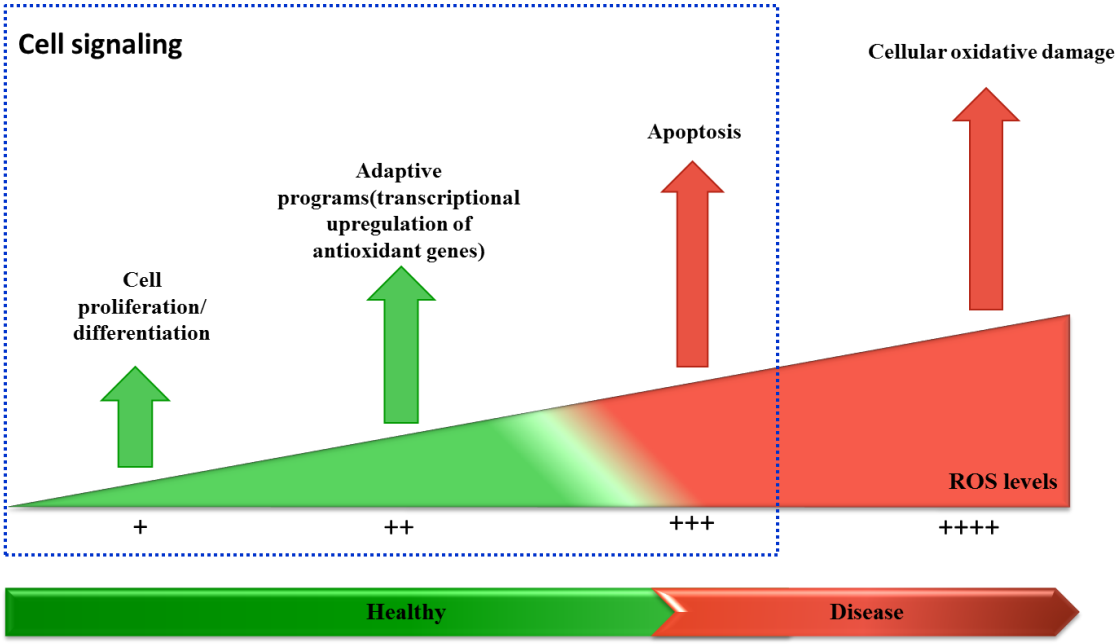

Figure 2: Mitochondrial ROS levels are crucial for cellular signaling.
Low levels of mitochondrial ROS are required for cellular processes such as proliferation and differentiation. An induction in ROS production will lead to adaptive programs including the transcriptional up-regulation of antioxidant genes. Higher levels of ROS will signal the initiation of senescence and apoptosis. Non-signaling, irreversible damage to cellular components is only observed under the highest levels of cellular ROS (adapted from Hamanaka and Chandel 2010).

ROS signaling contributes to muscle homeostasis, maintaining normal striated muscle structure and function (Droge 2002; Smith and Reid 2006; Brigelius-Flohe 2009; Musaro, Fulle et al. 2010). ROS levels augment in response to both increased contractile activity (i.e. muscular exercise) and prolonged periods of muscle disuse (e.g. immobilization). These seemingly contradictory signaling functions of ROS are probably due to differences in both the magnitude and the temporal pattern of ROS generation. For example, a moderate increase in skeletal muscle ROS production during a short time period (e.g. minutes) can activate signaling pathways leading to cellular adaptation and protection against future stresses (Powers and Jackson 2008; Jackson 2009; Ristow, Zarse et al. 2009; Silva, Pinho et al. 2009; Strobel, Peake et al. 2011). In contrast, high levels of ROS over long time periods (e.g. hours) may result in chronic activation of signaling pathways that promote proteolysis and potentially cell death (Sastre, Asensi et al. 1992; Vina, Gimeno et al. 2000; Palazzetti, Richard et al. 2003; Ji, Gomez-Cabrera et al. 2006; Silva, Pinho et al. 2009) but also positive adaptations following moderate exercise (Ristow, Zarse et al. 2009).

2.1.3. Mitochondrial protein quality control system

Mitochondria integrity and function are regulated by defense processes (Tatsuta and Langer 2008), being the PQC system the major biochemical process that contributes to the maintenance of cellular functions under normal and stress conditions (Langer, Kaser et al. 2001; Voos and Rottgers 2002; Koppen and Langer 2007; Baker and Haynes 2011). In general, PQC comprises a multitude of complexes and interdependent biochemical reactions that contribute to the functional integrity of proteins, ranging from the support of protein (re)folding, the protection against aggregation to the specific proteolytic removal of terminally damaged polypeptides. PQC proteins are activated by the accumulation of misfolded proteins within mitochondria in order to balance the homeostasis (Baker and Haynes 2011).

PQC comprises two major pathways that avoid irreversible protein aggregation. Firstly, chaperones (Hsp60, Hsp70 and Hsp100 families) recognize misfolded proteins, bind and try to refold them into their native form thus reconstituting protein function. However, if refolding fails to occur, proteases of the AAA family (ATPases associated with a variety of cellular activities) eliminate misfolded proteins by degrading them into small fragments and amino acids, which are transported out of mitochondria and are then available for *de novo* protein synthesis in the cytoplasm (Langer, Kaser et al. 2001; Goldberg 2003; Voos 2009; Luce, Weil et al. 2010; Baker and Haynes 2011; Sauer and Baker 2011; Lionaki and Tavernarakis 2013). AAA^+ proteins convert the energy derived from ATP hydrolysis into mechanical work and mediate remodeling of macromolecular structures, thereby controlling a variety of cellular processes (Tatsuta and Langer 2009). During organelle biogenesis and in stress conditions, unfolded or misfolded proteins can accumulate in each compartment of mitochondria, and so compartment-specific PQC machinery is needed to prevent protein aggregation (Baker and Haynes 2011) (Figure 3).

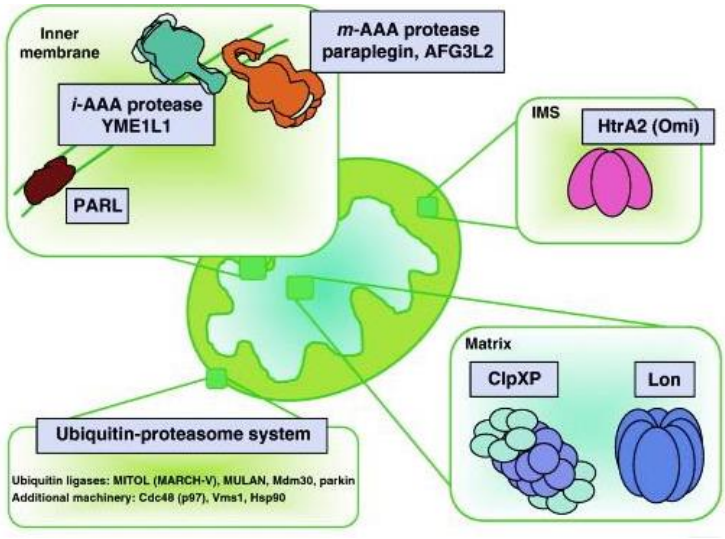

Figure 3: Protein quality control system monitors the four mitochondrial compartments.
Localized quality control proteases monitor and protect all mitochondrial compartments against deleterious accumulation of misfolded, misassembled or unfolded proteins. The inner membrane contains two proteases, each oriented with its respective catalytic site facing the matrix or intermembranar space side of the membrane. The m-AAA has a hetero-oligomeric assembly composed of paraplegin and AFG3L2 and i-AAA has homo-oligomeric assembly composed of YME1L1. The matrix is monitored by two different AAA proteases, ClpXP and Lon, whereas the intermembranar space is monitored by HtrA2 (Omi). The rhomboid protease PARL resides in the IM where it is involved in intramembrane proteolysis of substrates including PINK1. Less is known about protein QC of the mitochondrial OM or protein import into the organelle, but the cytosol-localized ubiquitin–proteasome system is probably involved (adapted fromBaker and Haynes 2011).
PARL, Presenilins-associated rhomboid-like protein; ClpXP, ATP-dependent Clp protease ATP-binding subunit clpX-like ; HtrA2(Omi); m-AAA, matrix-ATPase associated with various cellular activities; i-AAA, intermembranar space-ATPase associated with various cellular activities; YME1L1, yeast mitochondrial escape protein-1 like 1; IMS- intermembranar space; AFG3L2, ATP family gene 3-like 2.

The inner mitochondrial membrane is the protein-richest cellular membrane and contains the OXPHOS, which homeostasis is of major importance to maintain mitochondrial function. The membrane-bound ATP-dependent proteases, AAA proteases, mediate the proteolytic breakdown of membrane proteins. Two AAA proteases, which expose their catalytic sites to opposite membrane surfaces, are apparently ubiquitously present in the inner membrane: the *i*-AAA protease active in the intermembrane space and *m*-AAA protease in the matrix. (Kaser and Langer 2000; Koppen and Langer 2007; Baker and Haynes 2011). Both of these proteases mediate the ATP-dependent dislocation of substrate proteins from the membrane allowing their degradation in a hydrophilic environment (Leonhard, Guiard et al. 2000). The *i*-AAA protease complex is a homo-oligomeric formed by six subunits of the Yeast Mitochondrial Escape protein-1-Like 1 (YME1L1) (Leonhard,

Herrmann et al. 1996). In human mitochondria, *m*-AAA can be organized in hetero- or homo-oligomeric assemblies composed of paraplegin and ATPase family gene 3-like 2 (Afg312) and it is essential for the maintenance of oxidative phosphorylation (Kaser and Langer 2000; Tatsuta 2009). Within mitochondria, m-AAA proteases have versatile activities, being not only quality control enzymes that completely degrade non-assembled or misfolded polypeptides (Arlt, Tauer et al. 1996), but can also act as processing enzymes specifically cleaving mitochondrial proteins with regulatory functions, having a chaperone-like activity (Koppen and Langer 2007; Koppen, Bonn et al. 2009).

Paraplegin is a subunit of the hetero-oligomeric m-AAA protease, localized in the inner mitochondrial membrane, with the active site in the mitochondrial matrix (Gerdes, Tatsuta et al. 2012; Rugarli and Langer 2012). Paraplegin has three domains, one of which has an AAA_+ module, making this protease part of the AAA_+ superfamily (Karlberg, van den Berg et al. 2009). This protein forms cylindrical hetero-hexamers to become active, a known feature from AAA_+ proteins family (Karata, Inagawa et al. 1999). The m-AAA protein complex is both responsible for PQC in the IM and protein activation, and specifically, paraplegin is involved in the degradation of misfolded proteins, cleavage of mitochondrial targeting sequences, mitochondrial ribosome maturation (Nolden, Ehses et al. 2005) and is also linked to the proteolytic processing of OPA1, a GTPase in the IM, which alteration cause optical atrophy (Ishihara, Fujita et al. 2006). In addition to its function in PQC, the m-AAA proteases control the biogenesis of the OXPHOS complexes. A nuclear encoded subunit of mitochondrial ribosome, MrpL32, is matured by m-AAA proteases, having in this case the role of processing this ribosomal subunit and not of a PQC enzyme (Nolden, Ehses et al. 2005). Being MrpL32 processing a prerequisite for its assembly into ribosomes and mitochondrial translation, the m-AAA protease directly regulates the synthesis of mtDNA-encoded OXPHOS subunits within mitochondria (Tatsuta and Langer 2008). It is important to note that both regulatory and PQC functions of the m-AAA protease are interdependent and may compete with each other. While m-AAA degrades substrates resultant from aging and ROS production, it will not assemble MrpL32, resulting in the inhibition of OXPHOS proteins translation (Nolden, Ehses et al. 2005). The m-AAA protease also presents a protective function regarding OXPHOS complexes, mediating the maturation of the ROS scavenger cytochrome c peroxidase (Ccp1) in the mitochondrial intermembrane space. This peroxidase is processed by the m-

AAA protease and the rhomboid protease Pcp1, an intramembrane-cleaving peptidase in the inner membrane (Esser, Tursun et al. 2002). Two different ATP-dependent proteases have been identified in the matrix, the Lon/Pim1 protease (Suzuki, Suda et al. 1994; Van Dyck, Pearce et al. 1994) and the ClpXP protease (de Sagarra, Mayo et al. 1999; Santagata, Bhattacharyya et al. 1999). While the Lon protease contains proteolytic and ATPase activities on the same polypeptide, the ClpP protease has to form a protein complex with the mitochondrial ClpX chaperone that provides ATPase activity and is responsible for substrate recognition (Santagata, Bhattacharyya et al. 1999; Kang, Ortega et al. 2002). Besides the requirement of mitochondrial ClpXP in the unfolded protein response, its role within mitochondria is still poorly comprehended (Zhao, Wang et al. 2002; Haynes, Petrova et al. 2007). Lon is a serine protease that forms soluble heptameric complexes in the MM (Stahlberg, Kutejova et al. 1999) and has been demonstrated to mediate the proteolysis of misfolded and unassembled matrix proteins (Bota, Van Remmen et al. 2002). Lon is involved in the removal of damaged proteins including oxidized proteins, and thereby prevents the extensive accumulation of protein aggregates (Bota, Van Remmen et al. 2002; Bota, Ngo et al. 2005). Besides its role in protein quality control, studies in yeast suggest an essential function of Lon in mtDNA maintenance (Suzuki, Suda et al. 1994; Van Dyck, Pearce et al. 1994) and in organelle biogenesis and maintenance (Bender, Leidhold et al. 2010; Baker and Haynes 2011). In contrast to matrix and IM proteolysis, little is known about the turnover of proteins localized in the IMS and the OM. A putative candidate for the surveillance of protein quality in the IMS is HtrA2/Omi, a member of a conserved family of serine proteases. In mammals, HtrA2/Omi is up-regulated in response to several stress stimuli (Faccio, Fusco et al. 2000; Gray, Ward et al. 2000). In contradiction to a potential protective role, several studies proposed HtrA2/Omi to promote cell death (Suzuki, Imai et al. 2001; Hegde, Srinivasula et al. 2002; van Loo, van Gurp et al. 2002). Following apoptotic stimuli, HtrA2/Omi is released from mitochondria into the cytosol where it facilitates apoptosis through its protease activity.

Preserving the integrity of proteins, biomolecules prone to molecular damage, is a fundamental function of all biological systems. Impaired quality control of mitochondria might contribute to the build-up of oxidized proteins and impairment of mitochondrial redox homeostasis associated to aging and various diseases, including prevalent

neurological disorders like Parkinson's disease and spinocerebellar ataxia (Koppen and Langer 2007; Rugarli and Langer 2012).

2.2. The role of the post-translational modifications in the regulation of mitochondrial plasticity

Mounting evidence suggests that post-translational modifications (PTMs) of mitochondrial proteins play an important role in organelle homeostasis and adaptation to biomechanical stressors. PTMs can be either narrowly restricted to rapid and reversible modifications (e.g. phosphorylation and acetylation), often mediated by specific enzymes, or broadly extended to include non-enzymatic processes such as carbonylation and nitration that might lead to protein oxidative damage and proteolysis, affecting protein levels, localization and/or function. Both types of PTMs are important to consider in pathophysiologic conditions, once the interplay between regulatory PTMs and the ones causal of mitochondrial dysfunction might modulate the extent of disease progression (Foster, Van Eyk et al. 2009; Kerner, Lee et al. 2011). Due to the regulatory role of PTMs (Grimsrud, Carson et al. 2012; Sack 2012), recent studies have investigated its effects on striated muscle mitochondrial plasticity.

Reversible phosphorylation and acetylation tightly regulate mitochondrial processes leading to energy production and synthesis of mitochondrially-encoded components of OXPHOS complexes (Aponte, Phillips et al. 2009; Balaban 2010; Guan and Xiong 2011). It is not surprising that altered levels of phosphorylation and acetylation have been linked to diseases, such as cancer, diabetes mellitus and aging (Cohen 2002). Reversible phosphorylation of proteins is the most common and one of the best understood signaling mechanisms that regulate and connect many metabolic pathways. Indeed, using ATP as substrate, kinases transfer phosphate groups to serine, threonine and tyrosine residues generating negatively charged side chains, which significantly impacts the structural properties of those amino acid residues (Koc and Koc 2012). With the recent advent of mass spectrometry-based technologies applied to the study of proteins' phosphorylation, a new vision has emerged of an extensively phosphorylated and dynamically regulated mitochondrial proteome (Pagliarini and Dixon 2006; Agnetti, Kane et al. 2007). Mitochondrial phosphoproteome dynamics in cardiac (Boja, Phillips et al. 2009; Deng, Zhang et al. 2011; Phillips, Aponte et al. 2011) and in skeletal muscle (Zhao, Leon et al.

2011) is critically reviewed in Chapter III taking in consideration current data on protein phosphorylation profiling in mitochondria, the potential kinases involved and how pathophysiological conditions modulate the mitochondrial phosphoproteome.

Reversible acetylation on the ε-amino group of internal lysine residues (hereinafter referred to as acetylation) has emerged as a PTM with a crucial role in regulating target protein functions, akin to phosphorylation. This modification neutralizes the positive charges of ε -amino groups of lysine residues and usually result in the inhibition of metabolic enzymes activities (Fritz, Galligan et al. 2012), including the activities of glutamate dehydrogenase, long chain fatty acid dehydrogenase, and nuclear encoded subunits of the electron transport chain complexes, complexes I and II (Ahn, Kim et al. 2008; Cimen, Han et al. 2010; Finley, Haas et al. 2011). Over 20-30 % of all proteins in the mitochondria are acetylated, of which the majority are involved in metabolic pathways as fatty acid oxidation, amino acid oxidation, the TCA cycle, urea cycle, and oxidative phosphorylation (Bao and Sack 2010; Fritz, Galligan et al. 2012; Koc and Koc 2012). Despite intensive studies aiming the identification of acetyltransferases in mammalian mitochondria, no protein acetyltransferase activity has been detected to date (Koc and Koc 2012). The regulation of acetylation is mediated by NAD^+-dependent protein deacetylases called the Sirtuin (SIRT) family, being SIRT3 one of the most studied in the control of mitochondrial proteins deacetylation (Bao and Sack 2010; Fritz, Galligan et al. 2012). The mitochondrial sirtuins (SIRT3, SIRT4 and SIRT5) are vital for cell survival and act in a NAD^+-dependent manner, using NAD^+ as a co-substrate in deacetylation and ADP-ribosylation reactions (Verdin, Hirschey et al. 2010). SIRT3 has shown to be the major deacetylase that modulates mitochondrial functions in response to [NADH]/[NAD^+] ratio by regulating the activities of several key metabolic enzymes while SIRT4 and SIRT5 have fewer known substrates in mammalian mitochondria (Lombard, Alt et al. 2007; Yang, Yang et al. 2007). In the absence of SIRT3, mitochondrial proteins become hyperacetylated, which impairs their function, contributing to mitochondrial dysfunction. SIRT3 expression was reported to decrease in mouse models of T2DM (Palacios, Carmona et al. 2009; Jing, Emanuelli et al. 2011). Moreover, SIRT3 appears to be regulated by exercise in skeletal muscle and by pressure overload in the heart (Sack 2011). Nevertheless, the regulatory role of protein lysine residues acetylation in the control of mitochondrial homeostasis is only beginning to be explored.

Since mitochondria is a major source of RONS, mitochondrial proteins are especially exposed to oxidative modifications, being the elimination of modified proteins crucial for the maintenance of this organelle's integrity. Hence, the failure of functional protein maintenance and accumulation of oxidized proteins has been reported in several pathophysiological conditions. Post-translational oxidative modifications of proteins, manifested as carbonylation and nitration, appear to be a key mechanism underlying impaired functional and/or structural protein integrity leading to mitochondrial dysfunction (Turko, Li et al. 2003; Kanski, Behring et al. 2005; Choksi and Papaconstantinou 2008). Protein carbonylation has been subject of great interest, because it is irreversible and results in protein irreparable damage. This type of oxidative modification occurs when proteins directly react with ROS, leading to the formation of protein derivatives or peptide fragments containing highly reactive carbonyl groups, such as aldehydes and ketones (Dalle-Donne, Rossi et al. 2003; Stadtman and Levine 2003). Among the main carbonyl products of metal-catalyzed oxidation of proteins are glutamic and aminoadipic semialdehydes (Requena, Chao et al. 2001; Requena, Levine et al. 2003; Babusikova, Jesenak et al. 2008). Lysine, arginine, proline, and threonine residues of proteins are particularly sensitive to metal-catalyzed oxidation, leading in each case to the formation of carbonyl derivatives. Peptide carbonyl derivatives are also obtained as fragmentation products of peptide bond cleavage reactions or can be formed by the interaction of protein amino acid side chains (cysteine sulfhydryl groups, histidine imidazole groups, and lysine amino groups) with lipid peroxidation products, including 4-hydroxy-2-nonenal, acrolein, and malondialdehyde. Glycation/glycoxidation reactions can also lead directly to carbonyl adducts and indirectly to the formation of N-carboxymethyl-lysine derivatives that, because of their strong chelating ability, are able to promote the generation of carbonyl groups by metal-catalyzed reactions (Stadtman and Levine 2003; Stadtman 2006). Indeed, protein carbonyl content is actually the most general indicator and by far the most commonly used marker of protein oxidation, and accumulation of carbonylated proteins in mitochondria is undoubtedly associated with impaired respiratory function, playing a crucial role in the cellular response to pathophysiological stimuli (Feng, Xie et al. 2008; Alves, Vitorino et al. 2010).

Protein tyrosine nitration is a covalent protein modification resulting from the addition of a nitro ($-NO_2$) group onto one of the two equivalent *ortho* carbons of the aromatic ring of

tyrosine residues (Abello, Kerstjens et al. 2009). Many diseases are associated with increased levels of protein-bound nitrotyrosine, which has also been used as a marker of oxidative damage. Protein tyrosine nitration was reported in mitochondria of striated muscle in diabetes mellitus (Turko, Li et al. 2003; Dabkowski, Baseler et al. 2010; Ferreira, Guerra et al. 2013) and aging (Kanski, Behring et al. 2005). Although used as a marker of pathological disease processes and of oxidative stress, some authors argue that protein tyrosine nitration can be selective, dynamic and reversible and seems to fulfill the criteria of a regulatory physiological signal (Aulak, Koeck et al. 2004; Gow, Farkouh et al. 2004; Yakovlev and Mikkelsen 2010).

2.3. Mitochondrial plasticity of striated muscle in response to pathophysiological conditions

Striated muscle daily burns tremendous amounts of ATP to meet the energy requirements for contraction. In this sense, it is not surprising that maintenance of mitochondrial morphology, number, distribution and function in cardiac and skeletal tissues are important to preserve muscle function (Romanello and Sandri 2013). In order to fulfill tissue's needs, mitochondria have a considerable plasticity, responding rapidly and adequately when challenged by physiological or pathological stimuli. Mitochondrial plasticity is defined as changes of mitochondrial activity, content or oxidative phosphorylation capacity due to altered metabolic conditions (Hoppeler and Fluck 2003; Pagel-Langenickel, Schwartz et al. 2007) induced by cellular aging or by several diseases like diabetes mellitus and cancer. Among the several methodological approaches used to study mitochondrial plasticity, mass spectrometry-based proteomics presents the added dimension of allowing the large-scale characterization of mitochondrial protein profile. The comparative analysis of mitochondrial proteome in distinct conditions might contribute to the understanding of the relationship between mitochondrial dysfunction and diseases. The proteomics-based methodological approaches used in the study of mitochondrial plasticity in pathophysiological conditions are reviewed in Chapter II. In this section, the main findings on mitochondrial plasticity in cardiac and skeletal muscles are examined in diabetes mellitus, cancer and aging.

2.3.1. Mitochondrial plasticity in Diabetes mellitus

Mitochondria have an essential role in fatty acid and glucose metabolism and thus are likely to be impacted by impaired metabolism related to diabetes mellitus (Duncan 2011). Several studies on mitochondrial plasticity in cardiac and skeletal muscles further support a connection between mitochondrial dysfunction and both type 1 diabetes mellitus (T1DM) (Dabkowski, Williamson et al. 2009; Ferreira, Guerra et al. 2013) and type 2 diabetes mellitus (T2DM) (Ritov, Menshikova et al. 2005; Dabkowski, Baseler et al. 2010) and related complications, as cardiomyopathy. Indeed, cardiomyopathy is a common complication among diabetics, leading to increased heart failure and ultimately to death (Sander and Giles 2003; Shen, Zheng et al. 2004; Duncan 2011; Maisch, Alter et al. 2011). The mechanisms responsible for this pathological condition are complex and continue to be elucidated (Boudina and Abel 2010; Maisch, Alter et al. 2011). Altered energy metabolism towards increased rate of fatty acid oxidation, enlarged ROS production, impaired mitochondrial calcium handling and altered lipid content are among the mechanisms that may contribute to mitochondrial dysfunction in the diabetic heart (Duncan 2011). Skeletal muscle is the most insulin-sensitive tissue and is the source for more than 80% of insulin-stimulated glucose uptake in humans (Patti and Corvera 2010), being the predominant site of insulin-resistance in T2DM (Mogensen, Sahlin et al. 2007). Indeed, diabetes mellitus induces diverse structural, metabolic and functional changes in skeletal muscle. Briefly, diabetes mellitus diminish the functional capacity of skeletal muscle leading to muscle weakness, causes metabolic disturbance characterized by reduced cellular glucose uptake and fatty acid oxidation, and structural changes as muscle atrophy, augmented lipid deposition as well as muscle fiber changes (Sun, Liu et al. 2008).

Studies with human subjects and animal models provide evidences of altered mitochondrial morphology in skeletal muscle and heart mitochondria in response to T2DM and T1DM. Electron microscopy of skeletal muscle biopsies from obese subjects with T2DM revealed mitochondria of smaller size and number *per* volume (density) compared with those in lean controls (Kelley, He et al. 2002). These findings were supported by others (Morino, Petersen et al. 2005) but counteracted by Phielix *et al*. (2008) that reported no differences of mtDNA copy number between T2DM patients, insulin-resistant first-degree relatives of T2DM patients, and age and body mass index matched controls. Studies

with transmission electron microscopy (TEM) also revealed a significantly reduced numbers of SS mitochondria in skeletal muscle of T2DM and obese subjects, which was associated with reduced electron transport activity *per* unit mtDNA, suggestive of functional impairment (Ritov, Menshikova et al. 2005). Similarly, in heart muscle, SS mitochondria from *db/db* animals presented altered morphology, including a decrease in size and internal complexity, whereas IMF showed increased internal complexity (Dabkowski, Baseler et al. 2010).

T1DM was also associated to alterations in mitochondrial content and morphology. Skeletal muscle mitochondria of insulin-deficient rats due to administration of streptozotocin (STZ) showed loss of cristae and increased electron-dense granules along with the accumulation of lipid droplets around mitochondria (Chao, Ianuzzo et al. 1976), an increased number of disarrayed cristae and mitochondrial swelling (Chen and Ianuzzo 1982; Bonnard, Durand et al. 2008). Cardiac muscle cells from STZ-treated rats also presented swollen mitochondria, clearing of mitochondrial matrix and incorporation of lysosomal membranes into mitochondria matrix (Seager, Singal et al. 1984). Dabkowski, Williamson et al. (2009) analyzed mitochondrial populations from heart STZ diabetic rats and verified decreases in both size and complexity of IMF, with no significant effect on SS mitochondria. In insulin-deficient Akita mice, that develop diabetes as a result of a mutation in the insulin gene, unchanged mitochondrial content was reported in heart mitochondria when compared to wild-type (WT) mice, despite reduced cristae density and greater mean area (Bugger, Boudina et al. 2008). In other studies, an increase in mitochondria number was reported in insulin-deficient Akita mice (Bugger, Chen et al. 2009), in *db/db* obese diabetic mice and in OVE26 mice (Shen, Zheng et al. 2004). *db/db* mice have a defect in the leptin receptor, leading to obesity and hyperinsulinemia (as opposed to the insulin-defective Akita mice) that result in cardiac steatosis. These alterations of mitochondrial content were paralleled by changes in the content of mitochondrial transcription factor A (Tfam), which was found up-regulated by 4-weeks of STZ (Kanazawa, Nishio et al. 2002) and 5-months old OVE26 (Shen, Zheng et al. 2004); however, opposite findings were reported in STZ- heart mitochondria (Ferreira, Guerra et al. 2013). Others studies showed that the peroxisome proliferator-activated receptor gamma coactivator 1α (PGC-1α), a crucial regulator of mitochondrial metabolism, was reduced in skeletal muscle of T2DM patients (Mootha, Lindgren et al. 2003; Patti, Butte et

al. 2003) and in heart muscle of type 1 diabetic Akita mice (Bugger, Chen et al. 2009). However, in the diabetic heart muscle of insulin-resistant uncoupling protein diphtheria toxin A chain (UCP-DTA) (Duncan, Fong et al. 2007) and of leptin receptor–deficient *db/db* mice (Boudina, Sena et al. 2007), mitochondrial biogenesis was accompanied by a significant increase in PGC-1α.

The morphological alterations reported in striated muscle mitochondria from diabetic subjects are accompanied by impaired mitochondrial functionality, manifested by reduced NADH oxidoreductase and citrate synthase activities (Kelley, He et al. 2002). T2DM-related OXPHOS impairment was paralleled by increased lipid content in myocytes, as well as by a relative decrease in the proportion of enzymes regulating oxidative as opposed to glycolytic metabolism (He, Watkins et al. 2001; Ritov, Menshikova et al. 2005). The comparative analysis of mitochondria subpopulations showed that SS mitochondria but not IMF mitochondria displayed reduced ETC activity in T2DM (Ritov, Menshikova et al. 2005). Dabkowski, Baseler *et al*. (2010) observed a decrease of OXPHOS complexes I, III, IV and V activities and mitochondrial membrane potential, and increased oxidative damage exclusively in SSM of *db/db* mice. Furthermore, inner mitochondrial membrane proteins, including those from electron transport chain, ATP synthesis, and mitochondrial protein import machinery, were predominantly decreased. Despite being consistent the impaired mitochondrial function *per* unit muscle tissue, controversy exists regarding whether mitochondria *per se* are defective or whether the problem is restricted to mitochondrial number. Mogensen, Sahlin *et al.* (2007) reported a small but significant reduction in mitochondrial respiration rate *per* mitochondrion in skeletal muscle from T2DM patients. Moreover, reduced oxygen use under conditions of ADP stimulation (coupled respiration) and maximal uncoupling by carbonyl cyanide *p*-[trifluoromethoxy]-phenyl-hydrazone were reported in permeabilized skeletal muscle fibers of human patients with type 2 diabetes compared with non-diabetic controls (Boushel, Gnaiger et al. 2007). However, when data was normalized to mtDNA or to citrate synthase activity no differences were noticed, suggesting that T2DM-related blunted mitochondrial respiration in muscle is due to a lower mitochondrial content rather than to an intrinsic organelle defect (Boushel, Gnaiger et al. 2007). These results were recently supported by other studies (Rabol, Larsen et al. 2010; Larsen, Stride et al. 2011).

Regarding T1DM, in heart mitochondria isolated from STZ rats (Pierce and Dhalla 1985) and from type 1 diabetic Akita mice (Bugger, Chen et al. 2009) a depressed state 3 respiration and lower ATP synthesis were showed. Mitochondrial calcium uptake was also decreased in hyperglycemic rats, being the change fully reverted by 2 weeks of insulin administration. Mitochondrial calcium uptake was also reduced in mitochondria from diabetic hyperglycemic hearts (Tanaka, Konno et al. 1992; Flarsheim, Grupp et al. 1996). Heart mitochondria from STZ-treated diabetic rats not only presented decreased mitochondrial respiration but also increased induction of the calcium-mediated mitochondrial permeability transition (MPTP) (Oliveira, Seica et al. 2003). Goto-Kakizaki rats seem less susceptible to the induction of MPTP, showing larger calcium accumulation before the overall loss of mitochondrial impermeability (Oliveira, Rolo et al. 2001). The effect of hyperglycemia in STZ heart mitochondrial populations was also studied and decreased electron transport chain complex II respiratory activity in diabetic SS and IMF was observed, with the decrease being greater in IMF. Furthermore, complexes I and III activities were decreased in IMF but were unchanged in SS mitochondria from diabetics (Dabkowski, Williamson et al. 2009). The majority of hyperglycemia-induced cardiac mitochondrial alterations occur in IMF, which is critical for the process of energy generation for muscle contractility (Dabkowski, Williamson et al. 2009; Lumini-Oliveira, Magalhaes et al. 2011). In skeletal muscle the maximal rate of oxidative ATP synthesis was reduced in male patients with T1DM compared to non-diabetes subjects, suggesting that reduced muscle mitochondrial capacity in conjunction with increased glycolytic flux represents a significant metabolic shift in T1DM (Crowther, Milstein et al. 2003).

Studies have suggested that the decreased respiratory capacity of mitochondria in diabetic striated muscles is due to increased mitochondrial ROS production or alteration in antioxidant defense systems or both (Maxwell, Thomason et al. 1997; Rosen, Nawroth et al. 2001; Scheede-Bergdahl, Penkowa et al. 2005; Phielix, Schrauwen-Hinderling et al. 2008). Mitochondrial ROS activate multiple pathways that lead to cellular damage in the setting of hyperglycemia. Several studies reported an association between increased ROS production and the progression of diabetic complications in various tissues including heart and skeletal muscle (Marra, Cotroneo et al. 2002; Russell, Gastaldi et al. 2003). Tyrosine nitration of mitochondrial proteins is a common mechanism by which oxidative stress

causes dysfunctional mitochondria, with particular relevance in diabetic heart. A proteomic approach carried out by Turko, Li *et al.* (2003) revealed tyrosine nitration of several cardiac proteins in rats with alloxan-induced T1DM, including proteins involved in energy metabolism (succinyl- CoA:3-oxoacid CoA transferase, creatine kinase). More recently, Ferreira, Guerra *et al.* (2013) reported an increase of STZ-related mitochondrial protein nitration, being OXPHOS subunits and metabolic proteins from the Krebs cycle and fatty acid oxidation particularly susceptible to this protein modification. The accumulation of carbonylated mitochondrial proteins has also been associated to impaired respiratory chain activity in diabetes mellitus (Bonnard, Durand et al. 2008; Ferreira, Guerra et al. 2013), playing a crucial role in the pathogenesis of diabetes-related cardiomyopathy. Moreover, increased mitochondrial 4-hydroxy-2-nonenal (4-HNE) accumulation has been related to the impairment of OXPHOS complex II activity in STZ-induced T1DM (Lashin, Szweda et al. 2006). Nevertheless, the overexpression of catalase or MnSOD seems to restore the T1DM-induced impaired mitochondrial morphology and normalize cardiomyocyte contractility (Ye, Metreveli et al. 2004; Shen, Zheng et al. 2006).

2.3.2. Mitochondrial plasticity in Aging

Aging is a complex biological process, characterized by general time-dependent declines in the physiological and biochemical functions of many tissues (Harman 1981; Kirkwood 2005), with marked effect on heart and skeletal muscle function. Mitochondria are severely affected by aging, being proposed that the dysfunction of this organelle in particular plays a key role in age-related muscle function decline (Trifunovic and Larsson 2008). The role of mitochondria in the process of age-dependent deterioration of heart and skeletal muscle has become the focus of many studies with the gradually accepted idea that mitochondria dysfunction is a major contributor to aging (Cadenas and Davies 2000; Kwong and Sohal 2000; Short, Bigelow et al. 2005; Figueiredo, Ferreira et al. 2008; Figueiredo, Powers et al. 2009) and that age-related oxidative damage to mitochondrial DNA, lipids and proteins is a key mechanism underlying loss of function (Sohal 2002; Short, Bigelow et al. 2005). Several changes can be observed during aging, including a reduced capacity to use oxygen along with impaired cardio-circulatory capacity, and degeneration in muscle mass characterized by a reduction in muscle fiber diameters and by qualitative and quantitative

alterations in muscle fibers (D'Antona, Pellegrino et al. 2003; Doria, Buonocore et al. 2012).

Skeletal muscle is one of the most adversely affected tissues with increasing age (Booth, Weeden et al. 1994; Carmeli, Coleman et al. 2002) and its functionality has been reported to decline 3-10% *per* decade after the age of 25 (Rogers, Hagberg et al. 1990; Short, Bigelow et al. 2005). The hallmarks of aging are a decrease in both skeletal muscle fiber number and fiber cross sectional area, known as sarcopenia (Thompson 2009; Calvani, Joseph et al. 2013). This age-related skeletal muscle weakness leads to a substantially impaired mobility, locomotion, and quality of life (Morley, Abbatecola et al. 2011). Cardiac aging is a complex process which includes deposition of extracellular matrix, a decrease in cardiomyocites number and an increase in cardiomyocytes size. This age-related changes leads to cardiac functional decline and is associated with diminished ability to meet increased demand (Fares and Howlett 2010; Papp, Czuriga et al. 2012).

The content, morphology, and functional properties of mitochondria decay in striated muscle during aging (Shigenaga, Hagen et al. 1994; Huang and Hood 2009; Lanza and Sreekumaran Nair 2010; Terman, Kurz et al. 2010; Cheng, Ito et al. 2013). Several studies in old human subjects and animal models showed evidences of age-related changes in mitochondrial phenotype of striated muscles. TEM analyses revealed that the mitochondrial volume density within skeletal muscle changes with age (Conley, Jubrias et al. 2000; Corsetti, Pasini et al. 2008). In aged subjects, it is widely accepted that a significant proportion of the skeletal muscle mitochondria are abnormally enlarged, disrupted and more rounded in shape (Shigenaga, Hagen et al. 1994; Tonkonogi, Fernstrom et al. 2003; Terman, Kurz et al. 2010). Similarly, TEM of cardiac mitochondria from aged and newborn rats revealed that mitochondria were elongated in newborn mice, and gradually became rounded in older mice (Cheng, Ito et al. 2013). Vacuolization of the matrix and shortened mitochondrial cristae (Beregi, Regius et al. 1988; Shigenaga, Hagen et al. 1994) and giant mitochondria were reported in aged skeletal muscle mitochondria (Beregi, Regius et al. 1988) and in mitochondria of senescent cardiomyocytes (Coleman, Silbermann et al. 1987). Coupled with these morphological alterations, a decline in mitochondrial content, as represented by mitochondrial mtDNA copy number or CS activity, has also been demonstrated in skeletal muscle (Barazzoni, Short et al. 2000; Short,

Bigelow et al. 2005; Lyons, Mathieu-Costello et al. 2006; Menshikova, Ritov et al. 2006; Gouspillou, Bourdel-Marchasson et al. 2013) although this idea is not consensual (Picard, Ritchie et al. 2010). These findings are expected due, at least partially, to a decreased capacity for mitochondrial biogenesis (Reznick, Zong et al. 2007; Koltai, Szabo et al. 2010; Joseph, Adhihetty et al. 2012; Koltai, Hart et al. 2012). Indeed, regarding skeletal muscle, several studies has been reported an age-associated downregulation of PGC-1α (Reznick, Zong et al. 2007; Koltai, Szabo et al. 2010; Joseph, Adhihetty et al. 2012; Koltai, Hart et al. 2012), as well as its upstream regulators AMPK and SIRT1 (Reznick, Zong et al. 2007; Koltai, Szabo et al. 2010; Koltai, Hart et al. 2012), but accompained by an opposite trend by nuclear respiratory factors and Tfam (Lezza, Pesce et al. 2001; Koltai, Hart et al. 2012). Unlike skeletal muscle, it has been demonstrate that mitochondrial biogenesis increases in the aged heart, as indicated by the increase in mtDNA copy number concomitant with significant upregulation of the PGC-1α and its downstream effectors, Tfam and nuclear respiratory factors. Indeed, it has been suggest that increased mitochondrial biogenesis in aged heart represents a compensatory maladaptive response in reaction ATP deficiency, which is also stimulated by age-related oxidative damage to mitochondria (Dai and Rabinovitch 2009).

Given the central role of mitochondria in energy production it is not surprising that striated muscle mitochondrial bioenergetics became compromised with age (Short, Bigelow et al. 2005), considering the decreased mitochondrial respiratory capacity and ETC enzyme activities reported in aged skeletal muscle (Tonkonogi, Fernstrom et al. 2003; Nair 2005; Short, Bigelow et al. 2005; Conley, Jubrias et al. 2007). Functional analysis revealed age-related reduced activities of complex I and/or complex IV in humans (Coggan, Spina et al. 1992; Cooper, Mann et al. 1992; Boffoli, Scacco et al. 1994; Rooyackers, Adey et al. 1996; Short, Vittone et al. 2003; Tonkonogi, Fernstrom et al. 2003; Chabi, Mousson de Camaret et al. 2005; Crane, Devries et al. 2010; Joseph, Adhihetty et al. 2012) and in animal models (Sugiyama, Takasawa et al. 1993; Desai, Weindruch et al. 1996; Lenaz, Bovina et al. 1997; Barazzoni, Short et al. 2000; Kwong and Sohal 2000; Kerner, Turkaly et al. 2001; Kumaran, Subathra et al. 2004; Baker, Betik et al. 2006; Mansouri, Muller et al. 2006; Choksi, Nuss et al. 2008; Picard, Ritchie et al. 2010). Nevertheless, some contradictory data was reported (Pastoris, Boschi et al. 2000; Gianni, Jan et al. 2004; Capel, Rimbert et

al. 2005; O'Connell and Ohlendieck 2009; Picard, Ritchie et al. 2010). Complex II activity was showed to be unchanged with age in skeletal muscle mitochondria (Sugiyama, Takasawa et al. 1993; Pastoris, Boschi et al. 2000; Fattoretti, Vecchiet et al. 2001; Kerner, Turkaly et al. 2001; Capel, Buffiere et al. 2004; Chabi, Mousson de Camaret et al. 2005; Picard, Ritchie et al. 2010) but some studies reported opposite findings (Coggan, Spina et al. 1992; Boffoli, Scacco et al. 1994; Kumaran, Subathra et al. 2004; Choksi, Nuss et al. 2008; O'Connell and Ohlendieck 2009). Data regarding complex III activity are inconsistent, with some studies reporting a decrease of its activity (Kumaran, Subathra et al. 2004; Chabi, Mousson de Camaret et al. 2005; Choksi, Nuss et al. 2008), but others observed no changes (Sugiyama, Takasawa et al. 1993; Pastoris, Boschi et al. 2000; Kerner, Turkaly et al. 2001; Capel, Rimbert et al. 2005). Divergent subjects' characteristics (e.g. different animal models, wide variation in age subjects across studies, sample size) and analytical techniques (e.g. isolation mitochondria) might justify the discrepancies among studies regarding aging of striated muscle.

As a result of impaired enzymes and complexes activities, ATP synthesis diminishes within aged skeletal muscle (Drew, Phaneuf et al. 2003; Mansouri, Muller et al. 2006), and the whole body maximal oxygen consumption (VO_2max) declines (Tonkonogi, Fernstrom et al. 2003; Capel, Rimbert et al. 2005; Short, Bigelow et al. 2005). The assessment of mitochondrial respiration stimulated with a variety of substrates in the presence of ADP revealed that state 3 respiration, respiratory control ratio and ADP/O ratio parameters decreased in aged skeletal muscle (Kumaran, Panneerselvam et al. 2005). At rest, muscle ATP synthesis was reduced in 30-month, compared to 7-month-old mice, and a lower ATP/ADP ratio in 30-month-old mice was reported (Marcinek, Schenkman et al. 2005). The age-related decrease of mitochondrial state 3 respiration (Faist, Koenig et al. 1998; Figueiredo, Ferreira et al. 2008; Figueiredo, Powers et al. 2009), and of state 4 respiration (Kerner, Turkaly et al. 2001) was associated to increased levels of uncoupling protein 2 (UCP-2) (Barazzoni and Nair 2001) and to decreased content of UCP-3 (Kerner, Turkaly et al. 2001) or unchanged UCP-3 (Barazzoni and Nair 2001) in skeletal muscle. These results suggest that increased UCP-2 levels potentially increase the uncoupling of mitochondrial respiration to limit ATP production in aging skeletal muscle. However, UCP-3 expression may reflect mitochondrial substrate utilization and may be influenced by muscle fiber composition and metabolic characteristics. Moreover, a decreased state 4 respiration and

UCP-3 content emerge as a likely mechanism of age-related oxidative damage to tissue (Lesnefsky and Hoppel 2006).

Similarly to skeletal muscle, it is generally believed that mitochondrial function in heart declines with age; however, controversies remains (Manzelmann and Harmon 1987; Takasawa, Hayakawa et al. 1993; Delaval, Perichon et al. 2004; Yan, Ge et al. 2004; Cocco, Sgobbo et al. 2005; Judge, Jang et al. 2005; Wagatsuma and Sakuma 2012). Some studies have demonstrated a decline in oxygen consumption in aged heart (Delaval, Perichon et al. 2004; Yan, Ge et al. 2004), but others have reported no changes (Manzelmann and Harmon 1987; Cocco, Sgobbo et al. 2005). Moreover, some authors have shown a differential effect of the aging process on the two mitochondrial populations within the cardiac muscle (Fannin, Lesnefsky et al. 1999; Lesnefsky, Moghaddas et al. 2001; Moghaddas, Stoll et al. 2002; Judge, Jang et al. 2005; Das and Muniyappa 2013). Fannin, Lesnefsky *et al.* (1999) found that IMF mitochondria but not SS mitochondria from aged rat hearts exhibited less protein yield and oxidative phosphorylation rates, compared with those from adult rat heart. These resultas have been confirmed by others (Lesnefsky, Gudz et al. 2001; Moghaddas, Stoll et al. 2002; Das and Muniyappa 2013). Regarding ETC complexes, complex I activity appears to be the most susceptible to age-related decline in the heart (Sugiyama, Takasawa et al. 1993; Castelluccio, Baracca et al. 1994; Lenaz, Bovina et al. 1997; Andreu, Arbos et al. 1998; Petrosillo, Matera et al. 2009; Choksi, Nuss et al. 2011; Das and Muniyappa 2013), although some studies reported no significant changes (Kwong and Sohal 2000; Miro, Casademont et al. 2000). Moreover, the activities of complexes III (Castelluccio, Baracca et al. 1994; Lesnefsky, Gudz et al. 2001; Moghaddas, Stoll et al. 2002; Tatarkova, Kuka et al. 2011) and IV (Sugiyama, Takasawa et al. 1993; Castelluccio, Baracca et al. 1994; Andreu, Arbos et al. 1998; Fannin, Lesnefsky et al. 1999; Kwong and Sohal 2000; Moghaddas, Stoll et al. 2002; Choksi, Nuss et al. 2011; Tatarkova, Kuka et al. 2011; Cheng, Ito et al. 2013; Das and Muniyappa 2013) have been reported to decrease with aging. Contraditory studies have shown that complex II activity appears to be unaffected (Sugiyama, Takasawa et al. 1993; Miro, Casademont et al. 2000) or rather enhanced (Castelluccio, Baracca et al. 1994; Kwong and Sohal 2000) or even decreased with aging (Tatarkova, Kuka et al. 2011; Das and Muniyappa 2013). All these contraditory findings in heart aging mitochondria seem to reflect variability in subjects characteristics (e.g. animal model, age of subjects, sample size) and variability in

experimental procedures (e.g. mitochondrial isolation, enzyme assay) to asses mitochondrial function within cardiac muscle. Gomez, Monette *et al.* (2009) demonstrated that the formation of supercomplexes involving complexes I, III, and IV decrease in rat aged heart. The heart age-related reduction of mitochondrial cardiolipin, which is located in the inner mitochondrial membrane, seems to be closely associated to the decrease of complex III activity (Paradies, Ruggiero et al. 1998; Lesnefsky, Minkler et al. 2009) and is related with a diminished complex I activity (Paradies, Petrosillo et al. 2002; Petrosillo, Matera et al. 2009). Complex V activity was also reported to decline in aged heart (Guerrieri, Capozza et al. 1993; Davies, Poljak et al. 2001; Yarian, Toroser et al. 2006).

Studies have suggested that the decreased mitochondrial bioenergetic capacity of aged striated muscles is due to increased mitochondrial ROS production or changes in antioxidant defense systems (Yarian, Toroser et al. 2006). One of the best-known markers of age-related protein oxidation is the carbonyl group content, which was reported to increase in skeletal muscle (Alves, Vitorino et al. 2010) and in heart in an age-dependent way (Yarian, Toroser et al. 2006; Choksi, Nuss et al. 2008). Other types of protein modifications, such as 3-nitrotyrosine, was also found in subunits of OXPHOS complexes (Kanski, Behring et al. 2005). Indeed, the decline of complexes I and V activities in aged mouse heart was related with their higher susceptibility to oxidative damage without repercurssions in protein expression levels (Choksi, Nuss et al. 2008). A marked age-dependent increase in the main antioxidant enzymes (SOD, CAT, GPx) has been shown in rat *soleus* muscle (Ji, Dillon et al. 1990). Concerning SOD activity, several studies showed an age-dependent reduction of total SOD and MnSOD in rat skeletal muscle (Lammi-Keefe, Swan et al. 1984), while other studies did not find changes in the activity of total SOD, but reported an increase in MnSOD with age (Carrillo, Kanai et al. 1992). In humans, an increased age-dependent activity of MnSOD was particularly evident in several types of skeletal muscle (Marzani, Felzani et al. 2005; Barreiro, Coronell et al. 2006). Contraditory results have been reported for CAT actitity; however, some studies showed no changes (Marzani, Felzani et al. 2005)s, while others described a significant increase (Barreiro, Coronell et al. 2006) or decrease (Pansarasa, Felzani et al. 2002).

2.3.3. Mitochondrial plasticity in Cancer

Studies focused on mitochondria plasticity in striated muscle of individuals with cancer are scarce and mainly target cancer cachexia. Although the cellular and molecular mechanisms of cachexia are incompletely understood, some studies have suggested mitochondria as the place of energy wasting in cancer cachexia (Julienne, Dumas et al. 2012). Most of the data on mitochondrial plasticity in cancer cachexia was retrieved from studies with preclinical models and mainly targeted skeletal muscle since muscle loss is an important factor affecting cancer patients' survival. Cancer cachexia-related muscle atrophy contributes to physical disability, weakness and decreased capacity of wound healing and reduces responsiveness to chemotherapy (Julienne, Dumas et al. 2012). Cardiac dysfunction was recently suggested as an overlooked morbidity related to cancer that may occur in tandem with cachexia (Tian, Nishijima et al. 2010; Tian, Asp et al. 2011). Heart contractile dysfunction in mice with C26 tumor-induced cachexia was related to increased fibrosis, deranged myocardium structure, and altered gene expression of contractile proteins (Tian, Nishijima et al. 2010; Tian, Asp et al. 2011). However, the contribution of mitochondria to cancer-induced heart remodeling was never studied.

In cancer-related skeletal muscle wasting it was recently reported that mitochondria presents altered morphology, decreased OXPHOS activity and increased proteolysis and biogenesis (White, Baltgalvis et al. 2011; Shum, Mahendradatta et al. 2012; Wang, Pickrell et al. 2012; Fermoselle, Garcia-Arumi et al. 2013). The morphological changes are characterized by the presence of electron-lucent areas, which correspond to the loss of mitochondria cristae and swelling (Shum, Mahendradatta et al. 2012). TEM analysis of skeletal muscle mitochondria from tumor-bearing mice revealed the presence of giant mitochondria (Tzika, Fontes-Oliveira et al. 2013). The activation of TNF-alpha-induced NF-κB was shown to result in the decreased expression of regulator factors involved in mitochondrial biogenesis (e.g. PGC-1α, PPARα, and Tfam) and to affect downstream oxidative proteins (citrate synthase, and cytochrome *c* oxidase), disturbing muscle oxidative capacity (Remels, Gosker et al. 2010).Wang, Pickrell *et al.* (2012), using a transgenic tumor-bearing mice over-expressing PGC-1α in skeletal muscle, verified that the increased mitochondrial biogenesis was not sufficient to alter the levels of pro-inflammatory cytokines and prevent the mass loss. Moreover, the higher expression of PGC-1α in muscle was suggested to lead to the development of larger tumors.

Ushmorov, Hack et al. (1999) were the firsts to investigate mitochondrial oxidative phosphorylation in skeletal muscle using a mouse model of cancer cachexia (mice bearing fibrosarcoma MCA- 105) and showed a 25% reduction in oxygen consumption and a reduction in cytochrome c oxidase activity. More recently, Julienne, Dumas et al. (2012) confirmed the reduction of complex IV activity in cachectic rats with peritoneal carcinogenesis, that was also related to decreased levels of cytochrome c in skeletal muscle. A significant reduction in cytochrome-c oxidase complex subunit IV protein expression and in cytochrome c protein was reported in the skeletal muscle of ApcMin/+ cachectic mice, an animal model of colorectal cancer that develops cachexia (White, Baltgalvis et al. 2011). Decrease of ETC complexes I, II, and IV activities and of mitochondrial respiratory chain oxygen consumption was also observed in the *gastrocnemius* of cachectic mice-bearing LP07 lung tumor (Fermoselle, Garcia-Arumi et al. 2013)

Similarly to the observed in other pathophysiological conditions, mitochondrial dysfunction in wasted muscle seems to be related to increased oxidative stress, manifested by increased levels of malondialdehyde (MDA) (Gomes-Marcondes and Tisdale 2002), greater protein susceptibility to carbonylation and nitration, and increased content of 2-hydroxy-4-nonenal- (HNE-) and MDA-protein adducts (Barreiro, de la Puente et al. 2005). Among mitochondrial proteins, the ones involved in oxidative phosphorylation seem to be more prone to oxidative damage in tumor bearing rat skeletal muscle (Marin-Corral, Fontes et al. 2010). Indeed, reactive carbonyl groups and MDA adducts of ATP synthase were significantly increased in *gastrocnemius* of tumor bearing rats. Higher levels of HNE- and MDA-protein adducts were also reported in *tibialis anterior*, *soleus*, and heart of cachectic animals (Marin-Corral, Fontes et al. 2010). Moreover, the same authors reveal that the levels of MnSOD were significantly greater in heart of tumor bearing rats. However, no studies have evaluated markers of oxidative stress in mitochondria isolated from striated muscle of cancer cachectic subjects.

2.3.4. Integrative overview of striated muscle mitochondrial plasticity in pathophysiological conditions

Alterations in morphological, biochemical and functional properties of mitochondria in striated muscle mitochondria have been reported in several pathophysiologic conditions as

aging, diabetes mellitus and, more recently, in cancer. The alterations that ultimately impact cellular functions are overviewed in table 1.

Table 1: **Summary of striated muscle mitochondrial alterations in response to aging, diabetes mellitus and cancer.**

Mitochondrial plasticity		Morphologic changes	Number	Bioenergetics	Biogenesis	Oxidative stress	Antioxidant systems
Aging	**Skeletal muscle**	↓ density ↓ volume Vacuolization of matrix ↓ cristae	↑/↓	↑/↓	↓	↑	↑
	Cardiac muscle	Giant Vacuolization of matrix ↓cristae	↓	↑/↓	↑	↑	?
T1DM	**Skeletal muscle**	Swelling Vacuolization of matrix ↓cristae	?	↑/↓	?	↑	?
	Cardiac muscle	Swelling Vacuolization of matrix ↓cristae	?	↑/↓	?	↑	?
T2DM	**Skeletal muscle**	Smaller ↓Density	↑/↓	↑/↓	↑/↓	↑	?
	Cardiac muscle	Smaller ↓ Density	?	↑/↓	?	↑	↑
Cancer	**Skeletal muscle**	Giant Swelling ↓cristae	?	↑/↓	↑/↓	↑	?
	Cardiac muscle	?	?	?	?	?	?

T1DM,Type 1 diabetes mellitus; T2DM, Type 2 diabetes mellitus;↑, increase; ↓, decrease; ?, ↑/↓, inconsistent results; ?, no information.

Regardless the pathophysiological stimuli that triggers mitochondrial plasticity, there are some similarities in the pattern of disease-related mitochondrial changes. Alterations in mitochondria morphology have been reported in all the pathophysiological conditions analyzed, including vacuolization of the matrix, shortened cristae and enlargement. No studies are known that performed morphological characterization of mitochondria from cardiac muscle in cancer. It is widely accepted that the number of cardiac muscle mitochondria is diminished with age. Except for cardiac muscle, data are not consistent over different studies, possibly justified by the different methods used for its assessment, namely in sample preparation. Moreover, once mitochondria are isolated and removed from the *in vivo* environment or fixed within tissue preparations, factors such as osmotic

forces, tissue turgor, or membrane integrity may be altered and might easily affect mitochondrial morphology, mitochondrial size and number.

Perturbed mitochondrial biogenesis has been suggested to cause reduced mitochondrial number as well as reduced capacity for oxidative phosphorylation in several pathophysiological conditions. Despite increased cardiac mitochondrial biogenesis, the number of mitochondria seems to reduce with aging. Nevertheless, changes in muscle mitochondrial biogenesis in pathophysiological conditions remain a controversial issue, as mitochondrial functionality. Most studies reported the impairment of mitochondrial functionality with age, diabetes mellitus and cancer based on the experimental assessment of oxidative phosphorylation activity or oxygen consumption. However, it is unclear which specific mitochondrial complexes are impacted by these pathophysiological conditions. Some of discrepancies among studies may be explained by differences in mitochondrial isolation procedure and/or methodologies used for measurement of mitochondrial energy production (Picard, Ritchie et al. 2010).

Mitochondrial impairment in striated muscle from aged subjects, with diabetes or with cancer seems related to increased oxidative stress, manifested by enlarged levels of oxidized mitochondrial proteins. Among mitochondrial proteins more susceptible to oxidative damage in such conditions are subunits of OXPHOS complexes and metabolic proteins. Concerning antioxidant systems, the overexpression of MnSOD have been reported in aged skeletal muscle mitochondria in cardiac mitochondria of T2DM subjects. This overexpression might reflect an attempt to restore mitochondria functionality, impacted by these conditions. No studies are known that measured the antioxidant capacity of mitochondria isolated from striated muscle in cancer and T1DM.

Regarding the multiple pathways underlying mitochondrial impairment in striated muscle, pharmacological and non-pharmacological therapeutic strategies targeting these molecular processes might be envisioning(Judge and Leeuwenburgh 2007; Toledo, Menshikova et al. 2008; Rabol, Svendsen et al. 2009; Meex, Schrauwen-Hinderling et al. 2010). Among non-pharmacological strategies, exercise has been proposed to either prevent or counteract striated muscle mitochondrial damage. The benefits of exercise in promoting health are well documented (Lee, Shiroma et al. 2012). Adaptations to physical activity include increased mitochondrial biogenesis and function, and improvement in antioxidant network,

leading to a more effective control of RONS production (Ji, Wu et al. 1991; Judge, Jang et al. 2005; Rabol, Svendsen et al. 2009; Alves, Vitorino et al. 2010; Meex, Schrauwen-Hinderling et al. 2010; Phielix, Meex et al. 2010).

Despite the considerable efforts made in the study of mitochondrial plasticity in the pathophysiological conditions here reviewed, many unanswered questions remains. First, it is unclear which specific molecular mechanisms are responsible for mitochondrial plasticity in response to aging, diabetes mellitus and cancer. Second, it is unknown whether SS and IMF mitochondria are equal contributors to the mitochondrial dysfunction in these pathophysiologies.

2.4. The contribution of mitochondria signaling to striated muscle wasting

Muscle dysfunction represents a clinical feature of muscle wasting and is defined as the presence of low muscle mass and low muscle function (strength or performance), which might occur as a consequence of aging, and it may also result from prolonged periods of rest or as a consequence of a sedentary lifestyle (Sakuma and Yamaguchi 2012). Moreover, muscle dysfunction accompanies many chronic disease such as chronic heart failure, chronic kidney disease, cancer, human immunodeficiency virus (HIV), sepsis, immune disorders, and dystrophies (Thomas 2007; Fanzani, Conraads et al. 2012; Gea, Casadevall et al. 2012). When muscle wasting is related to chronic diseases is usually referred as cachexia and when is consequence of normal aging the term sarcopenia is used (Sakuma and Yamaguchi 2012).

Both, cardiac and skeletal muscles have limited proliferative capacity, thus the regulation of their size is mostly based on protein turnover (Bergmann, Bhardwaj et al. 2009). Protein synthesis and degradation are tightly coupled biological processes, which balance impacts muscle contraction. An altered protein turnover, secondary to the catabolic/anabolic imbalance due to decreased protein synthesis or increased protein degradation, results in the loss of muscle mass. The two processes are tightly regulated and interrelated (Sandri 2008; Schiaffino, Dyar et al. 2013). Muscle wasting occurs when protein degradation rates exceed protein synthesis, and may be induced in striated muscle by a variety of conditions, including starvation, denervation, cancer cachexia, heart failure and aging. Figure 4

presents an overview of the main signaling pathways suggested to underlie muscle wasting.

In cardiac and skeletal muscles, two major signaling pathways control protein synthesis, the IGF1–Akt–mTOR pathway, acting as a positive regulator, and the myostatin–Smad2/3 pathway, acting as a negative regulator (Rommel, Bodine et al. 2001; Sandri, Sandri et al. 2004; Stitt, Drujan et al. 2004; Fanzani, Conraads et al. 2012). In normal conditions, both IGF-1 and insulin activate phosphatidylinositol-3 kinase (PI3K) which in turn activates Akt [also known as protein kinase B (PKB)]. Activated Akt stimulates mammalian target of rapamycin (mTOR) to facilitate protein synthesis (Bodine, Stitt et al. 2001) through the phosphorylation and activation of p70S6 kinase, and phosphorylation of eukaryotic translation initiator factor 4E binding protein 1 (4E-BP1), which reliefs the repression of the protein initiation factor eukaryotic translation initiator factor 4E (eIF-4E) (Glass 2003). In addition, activated Akt phosphorylates the transcription factor Forkhead box O (FoxO) sequestering FoxO to the cytoplasm, preventing the transcription of key genes involved in protein degradation, such as the E-3 ligases Muscle Ring Finger 1 (MuRF-1) and atrogin-1 (also called Muscle Atrophy F-box (MAFbx)) in proteasome mediated proteolysis (Sandri, Sandri et al. 2004) and Bnip3 in lysosome mediated proteolysis (Zhao, Brault et al. 2007). Muscle wasting due to reduced Akt signaling was observed in different pathophysiological conditions (Price, Bailey et al. 1996; Penna, Bonetto et al. 2010; Toth, Ward et al. 2011).

A negative regulator of muscle bulk is myostatin, also known as member of transforming growth factor-beta (TGF-β) family, which is expressed predominantly in skeletal muscle (Springer, Adams et al. 2010; Elkina, von Haehling et al. 2011). Upon binding to its type II activin receptor (ACTRII), it phosphorylates and activates transcription factors Smad2/3, inhibiting Akt activity (Amirouche, Durieux et al. 2009; Trendelenburg, Meyer et al. 2009; Argiles, Orpi et al. 2012). Interruption of myostatin's gene expression leads to muscle hypertrophy and hyperplasia (McPherron et al., 1997). Another pathway playing a consistent role in muscle wasting relies on the activity of the transcription factor nuclear factor-kappaB (NF-κB) (Kandarian and Jackman 2006), which is activated by several pro-inflammatory cytokines (e.g. TNF-α, IL-6) as well as tumor-derived factor proteolysis-inducing factor (PIF). Activated NF-κB translocates into the nucleus and initiates the transcription of E3 ligases as well as other subunits involved in proteasome mediated proteolysis, such as ubiquitin and proteasome subunits (Tisdale 2009).

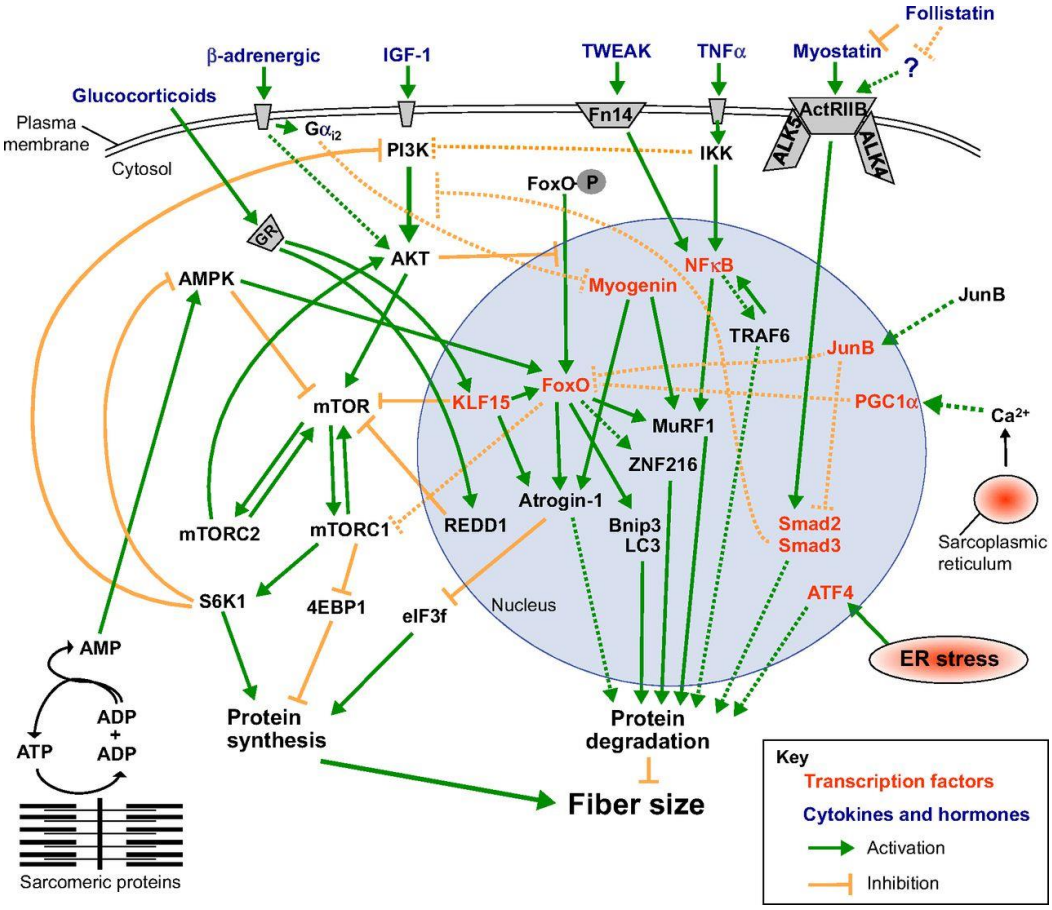

Figure 4: Overview of the molecular pathways involved in muscle wasting, which can be viewed as the result of protein synthesis/degradation imbalance.
Protein synthesis and degradation are regulated by several multiple signaling pathways, many of which converge at common intermediates and/or crosstalk with one another. Dotted lines depict pathways whose molecular mechanisms and role in muscle have yet to be completely defined. GR, glucocorticoid receptor; ER, endoplasmic reticulum (adapted from Bonaldo and Sandri 2013).

Another pathway that promotes enhanced proteolysis in striated muscle is the AMP kinase (AMPK)-FoxO3 axis (Romanello, Guadagnin et al. 2010; Romanello and Sandri 2010). Specifically, AMPK is a cellular sensor of energy levels, and active AMPK modulates FoxO3 action independently of Akt (Greer, Oskoui et al. 2007; Romanello, Guadagnin et al. 2010). Increased cellular levels of active AMPK results in the activation of the transcriptional activating factor FoxO3, resulting in increased expression of atrogin-1, MuRF-1, LC3, and Bnip3 that play role in in the degradation of contractile proteins via the ubiquitin-proteasome system and autophagy (Greer, Oskoui et al. 2007; Romanello,

Guadagnin et al. 2010). Therefore, AMPK activation of FoxO3 can accelerate muscle protein breakdown via both the ubiquitin- proteasome system and autophagy.

The degradation of striated muscle proteins is controlled by three major proteolytic systems, the lysosomal protease system, the calcium-activated system (calpains) and ATP-dependent ubiquitin-proteasome system. These systems work together to degrade muscle proteins and involve a variety of atrophy related genes or atrogenes, which are controlled by specific transcription factors, such as FoxO3 (Tisdale 2005; Powers, Kavazis et al. 2007; Fanzani, Conraads et al. 2012; Bonaldo and Sandri 2013). Lysosomal cathepsins are mainly responsible for degrading extracellular proteins and cell receptors. Calcium activated system calpains are involved in myofibrillar disassembly, releasing myofibrils for the ubiquitin-proteasome system, which plays a predominant role in the degradation of myofibrillar proteins. Ubiquitin might be covalently attached to a lysine residue of the target protein under the sequential function of a series of enzymes: ubiquitin activating enzyme (E1), the ubiquitin carrier protein (E2), and ubiquitin protein ligase (E3) (Pickart 2001). Two E3 ligases, atrogin-1 (or MAFbx) and MuRF-1 are highly induced during skeletal muscle wasting (Bodine, Stitt et al. 2001; Gomes, Lecker et al. 2001). Attachment of multiple ubiquitin molecules (called polyubiquitination) is a tag in the protein for its recognition and degradation by the 26S proteasome (Baumeister, Walz et al. 1998). The 26S proteasome has three types of proteolytic activity: chymotrypsin-like, trypsin-like and caspase-like activities, and the combination converts protein into peptides with six to nine amino acids. The peptides are further degraded to amino acids by other enzymes, such as tripeptidyl peptidase II (TPPII). Other findings also suggest a role of autophagy-lysosome system, where damaged organelles and proteins are degraded in skeletal muscle (Vicencio, Galluzzi et al. 2008). The overexpression of the autophagy marker Bnip3 *per se* could stimulate autophagy in the skeletal muscle, and similar to E3-ligases, Bnip3 expression is regulated by FoxO in skeletal muscle wasting (Mammucari, Schiaffino et al. 2008).

The involvement of mitochondria in muscle wasting seems a common feature (Adhihetty, Ljubicic et al. 2005; Marzetti, Hwang et al. 2010; Romanello, Guadagnin et al. 2010; Romanello and Sandri 2010; Powers, Smuder et al. 2011; Singh and Hood 2011; White, Baynes et al. 2011). The loss of mitochondria in wasted muscles, changes in organelle morphology, increased mitochondrial ROS production, and impaired ATP production

might produce signals that contribute to muscle wasting (Powers, Wiggs et al. 2012). The increased mitochondrial ROS production seems to promote muscle wasting by enhancing proteolysis and depressing protein synthesis. Indeed, increased ROS levels have been shown to activate both calpains and caspase-3, and increase the expression of key E3 ligases, leading to increased muscle protein degradation by the ubiquitin-proteasome system (Li, Chen et al. 2003; McClung, Whidden et al. 2008; Powers and Jackson 2008; Powers, Smuder et al. 2011). Exposure of cardiac myocytes to H_2O_2 can depress protein synthesis by 49% (Pham, Sugden et al. 2000), being predicted to occur at the level of mRNA translation, due, in part, to a decrease in Akt/mTOR signaling (Powers, Smuder et al. 2011).

Several factors, including increased mitochondrial ROS production, can promote the permeabilization of the OM and the consequent release of pro-apoptotic factors such as apoptosis-inducing factor (AIF) and cytochrome c (Adhihetty, Ljubicic et al. 2005; Tait and Green 2010). In cytoplasm, cytochrome c can activate caspase-3 and lead to muscle protein breakdown. In skeletal muscle, the activation of apoptosis leads to decreased myonuclear number, which was reported in inactivity, in chronic heart failure and aging (Allen, Linderman et al. 1997; Adams, Jiang et al. 1999; Leeuwenburgh, Gurley et al. 2005; Siu, Pistilli et al. 2005). The reduction in the number of nuclei in muscle fibers would decrease its transcriptional capacity and therefore reduce the overall protein synthesis (Powers, Wiggs et al. 2012). Experiments with caspase-3 knockout animals suggest that the absence of caspase-3 protects against denervation-induced muscle wasting by suppressing apoptosis and protecting against the loss of myonuclei (Plant, Bain et al. 2009). Accumulating evidence suggests that enhanced activation of apoptosis takes place in aged skeletal muscle, likely contributing to the development of sarcopenia (Marzetti and Leeuwenburgh 2006). In this scenario, mitochondrial apoptotic signaling might be seen as a central mechanism underlying the pathogenesis of age-related muscle atrophy (Adhihetty, O'Leary et al. 2008). Other findings suggest that inactivity-induced mitochondrial energy stress can promote enhanced proteolysis via the AMP kinase (AMPK)-FoxO3 axis (Romanello, Guadagnin et al. 2010; Romanello and Sandri 2010). Despite being recognized as a major factor contributing to muscle wasting, the signaling mechanisms that lead to mitochondrial dysfunction are just starting to be disclosed.

3. Aims of the study

Regarding the role of mitochondria in striated muscle adaptation to aging, diabetes mellitus and cancer, the general goal of the present thesis was to characterize the mitochondrial plasticity in skeletal and cardiac muscles in these pathophysiological conditions. To accomplish this, specific purposes were outlined in the different original research articles (Papers I - IV) that comprise chapter IV:

i) Identify the main mitochondrial protein targets to oxidation and nitration in heart of young, old active and old sedentary mice, and relate it with mitochondrial respiratory chain activity (Paper I).

ii) Evaluate the influence of cellular location of mitochondria in respiratory chain activity and OXPHOS subunits' susceptibility to oxidative and nitrative stress in rat cardiac muscle (Paper II).

iii) Determine whether IMF mitochondria protein quality control system is affected by STZ-induced hyperglycemia and how they relate to mitochondrial dysfunction in rat skeletal muscle (Paper III).

iv) Investigate the interplay between urothelial carcinoma-induced catabolic profile and skeletal muscle phenotype focusing on mitochondrial plasticity in *gastrocnemius* muscle. Analyse the potential regulatory role of protein quality control system in mitochondria activity and in mitochondrial proteins' susceptibility to oxidation (Paper IV).

List of Studies:

Theoretical Background

Book Chapter

Padrão, A.I., Vitorino,R., Nogueira-Ferreira, R., Almeida, V., Henriques-Coelho, T., Duarte, J.A., Ferreira, R., Amado, F. (2013). "Mitochondria protein profiling in striated

muscle: insights into pathophysiological conditions". In In Ming D. Li (Eds), *Recent Advances in Proteomics Research*, Nova Science Publishers, ISBN: 978-1-62948-218-7.

Review

Padrão, A.I., Ferreira, R., Duarte, J.A., Vitorino,R., Amado, F. (2013). "Unraveling the phosphoproteome dynamics in mammals mitochondria from a network perspective". *Journal of Proteome* Research, 12 (10):4257–4267.

Original research papers

Paper I

Padrao, A. I., Ferreira, R., Vitorino, R., Alves, R. M., Figueiredo, P., Duarte, J. A., Amado, F. (2012). "Effect of lifestyle on age-related mitochondrial protein oxidation in mice cardiac muscle". *European Journal of Applied Physiology*, 112(4): 1467-1474.

Paper II

Padrao, A. I., Ferreira, R. M., Vitorino, R., Alves, R. M., Neuparth, M. J., Duarte, J. A., Amado, F. (2011) "OXPHOS susceptibility to oxidative modifications: the role of heart mitochondrial subcellular location". *Biochimica et Biophysica Acta*, 1807(9): 1106-1113.

Paper III

Padrao, A. I., Carvalho, T., Vitorino, R., Alves, R. M., Caseiro, A., Duarte, J. A., Ferreira, R., Amado, F. (2012) "Impaired protein quality control system underlies mitochondrial dysfunction in skeletal muscle of streptozotocin-induced diabetic rats". *Biochimica et Biophysica Acta*, 1822(8): 1189-1197.

Paper IV

Padrao, A. I., Oliveira, P., Vitorino, R., Colaco, B., Pires, M.J., Castellanos, E., Neuparth, M. J., Teixeira, C., Costa, C., Moreira-Gonçalves, D., Cabral, S., Duarte, J. A., Lara-Santos, L., Amado, F., Ferreira, R., Bladder cancer-induced skeletal muscle wasting: Disclosing the role of mitochondria plasticity. *The International Journal of Biochemistry & Cell Biology*, 45(7): 1399-1409.

CHAPTER II

BOOK CHAPTER

MITOCHONDRIA PROTEIN PROFILING IN STRIATED MUSCLE: INSIGHTS INTO PATHOPHYSIOLOGICAL CONDITIONS

In Ming D. Li (Eds), *Recent Advances in Proteomics Research*, Nova Science Publishers, ISBN 978-1-62948-218-7

Chapter

MITOCHONDRIA PROTEIN PROFILING IN STRIATED MUSCLE: INSIGHTS INTO PATHOPHYSIOLOGICAL CONDITIONS

Ana Isabel Padrão,[1] Rui Vitorino,[1,] Rita Nogueira-Ferreira,[1,2] Vanessa Almeida,[1] Tiago Henriques-Coelho,[2] José A. Duarte,[3] Francisco Amado,[1,4] and Rita Ferreira[1]*

[1]QOPNA, Mass Spectrometry Group,
University of Aveiro, Aveiro, Portugal
[2]Department of Physiology and Cardiothoracic Surgery,
Faculty of Medicine, University of Porto, Porto, Portugal
[3]CIAFEL, Faculty of Sports, University of Porto, Porto, Portugal
[4]School of Health Sciences, University of Aveiro, Portugal

ABSTRACT

Striated muscle is highly reliant on mitochondria where essential mechanisms of energy production, signaling, biosynthesis and apoptosis are contained and so, the orchestration of these pathways plays a critical role in cell physiology. Mitochondrial proteome are adjusted to the specific needs of the muscle and to the environmental conditions that it faces. Cumulative evidences have linked mitochondrial dysfunction to the pathogenesis of cardiovascular diseases, diabetes mellitus, cancer and aging. Progress on mass spectrometry-based proteomics and bioinformatics made possibly the large-scale characterization of mitochondrial proteome and its dynamics under pathophysiological conditions. This chapter focuses on principles and technical considerations of state-of-the-art mitochondrial proteomics, and on its applications to the proteome characterization of mitochondria isolated from skeletal and cardiac muscles. The comparative analysis of mitochondrial proteome with mass spectrometry-based proteomics towards the understanding of the relationship between mitochondrial dysfunction and diseases is explored as well as the challenges and future perspectives in this field.

* Corresponding author: Rui Vitorino, Address: Department of Chemistry, University of Aveiro, 3810-193, Aveiro, Portugal. E-mail: rvitorino@ua.pt; Fax: +351234370084.

Keywords: Mitochondrial plasticity; Proteomics; Pathophysiological conditions, Skeletal and cardiac muscles

1. INTRODUCTION

Mitochondria are the powerhouses of the cell, being the major site of ATP production via oxidative phosphorylation (OXPHOS) for tissue survival and functionality. Besides their key role in energy producing, mitochondria are critical organelles involved in multiple cell signalling cascades and in the regulation of cellular metabolism, development, calcium homeostasis and apoptosis (McBride et al. 2006; Benard et al. 2006; Benard and Rossignol 2008). Some tissues like the striated muscles are highly reliant on mitochondria. Indeed, the mammalian heart is a hotspot of metabolic activity, consuming each day 100 times its own weight in ATP (Dorn 2013). Skeletal muscle accounts for approximately 40% of total body mass, being a major site of metabolic activity (Romanello and Sandri 2013).

In striated muscles there are two distinct populations of mitochondria that differ in their subcellular localization, morphology and biochemical properties. Subsarcolemmal (SS) mitochondria are located just beneath the sarcolemma whereas the smaller intermyofibrillar (IMF) mitochondria, which account for 80% of mitochondria, are interspersed in the contractile filaments (Riva et al. 2005; Hoppel et al. 2009; Hoppeler and Fluck 2003; Palmer et al. 1977; Hoppeler 1986). The plasticity of these mitochondrial populations was studied in response to distinct stimuli using proteomic approaches relied on mass spectrometry and expression differences were related to the location of mitochondria in the cell (Dabkowski et al. 2009; Baseler et al. 2011; Ferreira et al. 2010).

Proteomic cataloguing studies show that mitochondria contain about 1000 (yeast) to 1500 (human) different proteins (Pagliarini et al. 2008; Perocchi et al. 2006; Sickmann et al. 2003; Reinders et al. 2006). The vast majority (~98%) of the total protein composition of the organelle is encoded within the nucleus, synthesized upon cytosolic ribosomes and imported to submitochondrial destinations by an elaborate network of translocases and sorting machineries (Koehler 2000; Chacinska et al. 2009; Ryan and Hoogenraad 2007; Neupert and Herrmann 2007). A remaining minority of the proteome is encoded by mitochondrion's own genome, which encodes only a few components of the respiratory chain complexes (13 in humans) (Duchen 2004). Therefore, the mitochondrial proteome should be viewed as a dynamic program generated by the cross-talk between the two genomes and able to adapt to tissue's needs or disease states (Ryan and Hoogenraad 2007; Dimmer and Rapaport 2008). Changes in the mitochondrial proteome exert influences over mitochondrial homeostasis, leading to disease in addition to disturb natural processes as development and ageing (Duchen 2004; Lowell and Shulman 2005; Wallace 1999).

2. MITOCHONDRIAL PROTEOME CHARACTERIZATION IN STRIATED MUSCLE

The mitochondrial proteome is unique, complex and dynamically regulated as it adapts to the needs of tissues, like the striated muscles, or disease states (Johnson et al. 2007; Balaban

2010; Zhang et al. 2008). Besides alterations in protein levels, these conditions might regulate posttranslational modifications (PTMs) such as glycosylation, acetylation, phosphorylation and even ubiquitination (Witze et al. 2007; Kerner et al. 2011; Koc and Koc 2012). These modifications might affect protein folding and, consequently, organelle function. Such high complexity might explain the wide heterogeneity of mitochondrial proteome reported in different studies and highlights the technical challenges in proteome characterization (Warda et al. 2013). Over the last decade, great progresses were achieved in mass spectrometry-based approaches for the study of whole mitochondrial proteome, sub-proteome, mitochondrial protein complexes and their molecular organization, and for the characterization of mitochondrial protein PTMs in both physiological and pathological conditions.

The workflow for mitochondrial proteomics includes the isolation of mitochondria from tissues or cultured cells, large-scale separation of mitochondrial proteins, protein identification and quantification by MS, and bioinformatic analysis (figure 1). Large-scale proteome profiling started with the classic two-dimensional electrophoresis (2-DE), which combines isoelectric focusing (IEF) and polyacrylamide gel electrophoresis in denaturating conditions (SDS-PAGE). This approach was optimized with the use of fluorescent dyes, Differential Gel Electrophoresis (DIGE), for comparative quantitative analysis. New approaches have been proposed and include gel-free analysis of mitochondrial proteins (MudPIT) with novel peptide labeling techniques for quantitation, and complementary functional analysis (e.g. Blue Native PAGE).

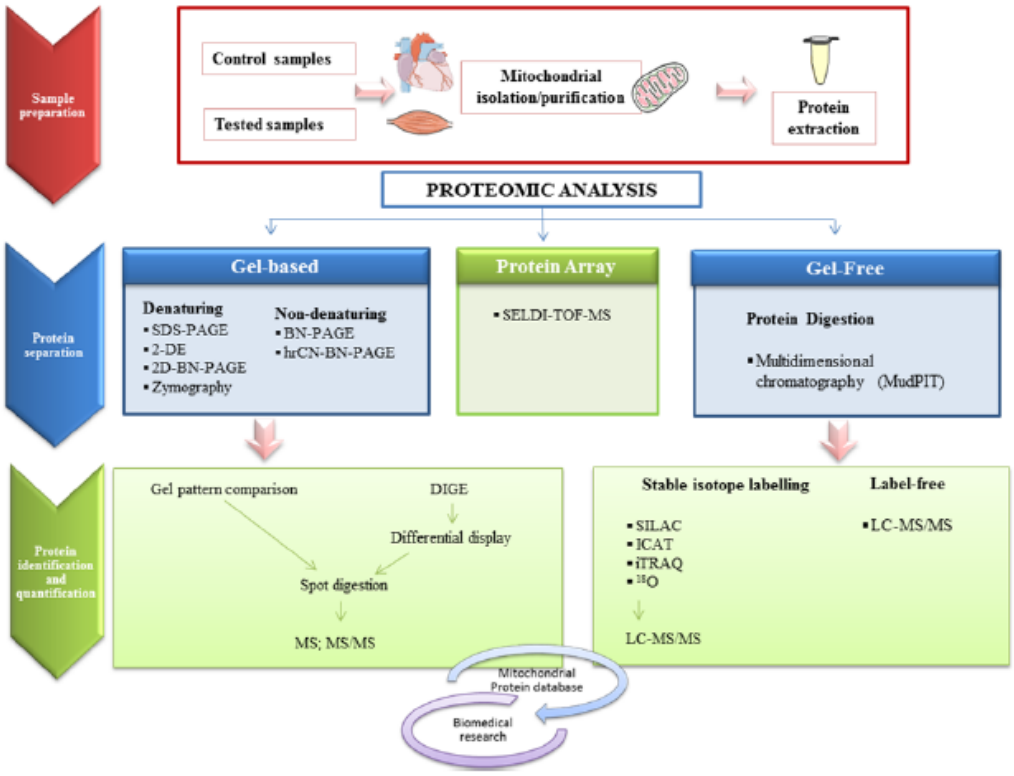

Figure 1.

Finally, data integration with bioinformatic tools gives a broad range perspective of the mitochondrial proteome plasticity in response to pathophysiological conditions.

2.1. Mitochondrial Isolation and Purification Methods for Proteomics

Preparation of pure and functionally viable mitochondria is an important step to achieve reliable and reproducible proteomic outputs (Zhang et al. 2012). Mitochondrial fractionation consists of two major steps: disruption of the cellular organization (homogenization of tissue) and differential centrifugation of the homogenate (Huber et al. 2003). Homogenization buffers usually contain ethylene glycol tetraacetic acid (EGTA) and delipidated BSA to avoid mitochondrial swelling and the uncoupling of mitochondria respiration by free fatty acids, respectively (Graham 1993).

The most effective method for mitochondrial isolation is differential centrifugation, although several other techniques such as free-flow electrophoresis (Zischka et al. 2003), kit-based methods (Hartwig et al. 2009) have been applied to these types of studies (Kang et al. 2008; Jung et al. 2000). In 1948 it was proposed the first protocol to isolate rat liver mitochondria based on a differential centrifugation (Hogeboom et al. 1948). Then, isolation methods have been modified and tailored to tissues and animal species analyzed.

Compared with free-flow electrophoresis, density gradient centrifugation has great advantages both in obtaining functional mitochondria and good yields (Hartwig et al. 2009), it is easily set up, and ideally combined with analytical techniques (Huber et al. 2003). To reduce "contaminating" organelles like endoplasmic reticulum or lysosomes, mitochondria are further purified using density gradients, which are usually set up with sucrose (Meisinger et al. 2000; Hanson et al. 2001; Rezaul et al. 2005), Percoll (Ferreira et al. 2010; Pagliarini et al. 2008; Millar et al. 2001; Mootha et al. 2003; Werhahn et al. 2001; Fukada et al. 2004), Nycodenz (Jiang et al. 2004; Li et al. 2009) or Metrizamide (Taylor et al. 2003; Fountoulakis and Schlaeger 2003).

Purification of mitochondria can also be performed by immunoisolation using mitochondria-specific antibodies (Herrnstadt et al. 1999; Lee et al. 2010). This method leads to highly purified preparations, but has the disadvantage of being expensive and large amounts of sample are lost (Herrnstadt et al. 1999).

More recently, protocols performing mild proteolytic treatments have been reported to the analysis of cytoplasm-exposed mitochondrial proteins by proteomics (Forner et al. 2006), a method based on flow field-flow fractionation for size-based separation of mitochondria prior to proteomic analysis (Kang et al. 2008).

After purification, mitochondrial purity and intactness must be validated by immunoblotting using specific markers of mitochondria and of other common contaminating organelles (Zhang et al. 2008; Chen et al. 2010), by membrane potential measurements, respiratory control index assessments, and/or morphology evaluation by electron microscopy (Zhang et al. 2008).

Sample subfractionation might also be performed to reduce sample complexity before MS analyses and so increase the number of identified proteins; however, high amounts of sample are required and usually involves ultracentrifugation combined with density gradients (Ferreira et al. 2010; Forner et al. 2006).

2.2. Mitochondrial Protein Separation Approaches

The most widespread protein separation approaches used in mitochondrial proteomics can be divided in two main categories: gel-based and gel-free strategies (figure 1), which application to mitochondria proteome is reviewed in this section.

2.2.1. Gel-Based Approaches

Since it was first introduced in 1975 (O'Farrell 1975), 2-DE has evolved at different levels and became the workhorse of protein separation and the method of choice for differential protein expression analysis. It separates a complex protein mixture based upon two intrisic protein characteristics, net charge (isoelectric point, p*I*) and molecular weight (MW). This approach provides the highest resolution in soluble protein separation, and resolves hundreds or thousands of proteins at once (Mathy and Sluse 2008; Schulze and Usadel 2010; Lilley et al. 2002). In many cases it is possible to separate different isoforms of a given protein, which can be due to sequence variations or to PTMs (Roepstorff 2012). Nevertheless, 2-DE has lately come under assault due to its known limitations and in part to the development of alternative MS-based approaches. Any of the reasons behind this trend include issues related to reproducibility (Lilley et al. 2002), poor representation of low abundant proteins (Gygi et al. 2000), highly acidic/basic proteins, or proteins with extreme size or hydrophobicity (Ong and Pandey 2001; Gorg et al. 1997; Wilkins et al. 1998), and difficulties in automation of the gel-based techniques (Tonge et al. 2001). Moreover, the comigration of multiple proteins in a single spot renders comparative quantification rather inaccurate (Abdallah et al. 2012). Mitochondrial proteins appear mostly within the pH range of 3-11 and within the 15 to 100 kDa molecular mass range (Mathy and Sluse 2008). In fact, some proteins have a p*I* too alkaline to be well resolved on a typical wide range IPG strips (Kane et al. 2006), as for example, cytochrome c (p*I* = 10.3) (Flatmark 1966). A large percentage of mitochondrial proteins, such as the ones from electron transporter chain (ETC), which represent about 40% of inner membrane proteins (Schwerzmann et al. 1986), have high hydrophobic properties, making isoelectric focusing difficult (Hanson et al. 2001; Santoni et al. 2000). To avoid the limitations of 2-DE in the analysis of specific classes of mitochondrial proteins, SDS-PAGE coupled to liquid chromatography and to tandem MS (LC-MS/MS) has been applied in large-scale mitochondrial proteome research (Taylor et al. 2002; Padrao et al. 2012) since it takes advantage of the resolving power of electrophoresis in a single dimension.

Development of several fluorescent staining methods and protein labeling prior to 2-DE separation as the Difference Gel Electrophoresis (DIGE) method (Unlu et al. 1997), responded to specific concerns about the qualitative and quantitative limitations of protein spot detection (Van den Bergh and Arckens 2004). This technique is based on the incorporation of different fluorescent cyanide dyes (Cydye) in protein's lysine residues (Minden 2007; Marouga et al. 2005) and is therefore compatible with in-gel digestion and MS analysis (Lilley et al. 2002). After electrophoresis, the gel is scanned, fluorescent excitation from each distinct Cydye is captured and overlapped for the comparison of spot density between the other dyes and the standard signal, avoiding possible intra-gel variability (Mathy and Sluse 2008; Lilley and Friedman 2004). Comparing with coomassie- or silver-staining methods the sensitivity of the 2-DE-DIGE method is very high, with a detection limit of ~1 ng and a dynamic range of ~10^5 (Lilley et al. 2002; Tonge et al. 2001; D'Hertog et al. 2006).

DIGE offered the advantage of multiplexing, supressing inter-gel variability and reducing the number of gels required (Shaw et al. 2003), being strongly recommended for protein quantification and comparison (Mathy and Sluse 2008). So, 2-DE-DIGE has captured a lot of attention in the field of mitochondrial proteome research (Baseler et al. 2011; Meng et al. 2009; Egan et al. 2011).

Membrane-bound mitochondrial protein complexes may be analyzed from a functional perspective with special in-gel approaches. Schagger and von Jagow (1991) developed a method named Blue-Native Electrophoresis (BN-PAGE) that allow the separation of intact membrane protein complexes (e.g. mitochondrial respiratory chain complexes). A charge shifting agent, the dye Coomassie Brilliant Blue G-250, is added to the cathode buffer in order to stick to proteins conferring a uniform electric charge without unfold the protein. Thus, intact protein complexes can be separated on a nondenaturing gradient gel according to their MW, though the size and shape of each complex also influence how far that complex migrates into the gel. Moreover, 2D blue-native polyacrylamide gel electrophoresis (2D-BN-PAGE) has been successfully used to resolve mitochondrial membrane proteins (Schagger and von Jagow 1991; Devreese et al. 2002). Denaturing conditions are employed to separate complexes' individual subunits in the second dimension, based on their MW (Nijtmans et al. 2002). Several authors (Padrao et al. 2011; Brookes et al. 2002) have shown the great potential of this technique in functional proteomics for the analysis of mitochondrial molecular signaling, protein-to-protein interaction and posttranslational modifications, especially in respiratory chain proteins from the mitochondrial membrane (Abdallah et al. 2012). Among the limitations associated to BN-PAGE is its low resolving power for some proteins that cannot bind coomassie blue and so present a neutral or basic p*I*, and the interference of coomassie blue with some fluorimetric and catalytic assays (Wittig and Schagger 2008). In an attempt to overcome these disadvantages, a new methodology named high resolution clear-native electrophoresis (hrCN-PAGE) was developed (Wittig and Schagger 2008; Wittig et al. 2007; Wittig et al. 2007). This approach has a separation resolution as high as BN-PAGE, uses non-colored mixed micelles to induce a net negative charge on the proteins, and is compatible with fluorimetric and catalytic assays. Nevertheless, hrCN-PAGE favors the dissociation of labile proteins from protein complexes (Braun et al. 2007). Another variation of BN-PAGE is the Native DIGE technique (BN-DIGE) (Dani and Dencher 2008), which couples the fluorescent dyes labeling technique to the previously described BN-PAGE. BN-DIGE facilitates the (i) systematic and quantitative comparison of protein complexes of related protein fractions, (ii) structural investigation of protein complexes, (iii) assignment of protein complexes to subcellular fractions like organelles and (iv) electrophoretic mapping of isoforms of subunits from protein complexes with respect to a larger proteome (Dani and Dencher 2008; Heinemeyer et al. 2009; Wittig and Schagger 2009).

Zymography is a simple, sensitive, quantifiable, and functional approach for the analysis of proteolytic activity in cell and tissue extracts (Heussen and Dowdle 1980). The standard method is based on the use of SDS-PAGE co-polymerized with a protein substrate (e.g. gelatin, casein, or fibrin) of a protease (Wilkesman and Kurz 2009). Using non-reducing conditions (i.e. in the absence of heating and reducing agent), proteases activity is preserved and might be detected as white bands on a dark blue background resultant of coomassie blue staining (Wilkesman and Kurz 2009).

Zymography was already used to study mitochondrial proteolytic activity (Padrao et al. 2012), contributing to a better understanding of mitochondrial proteolysis in various pathophysiological conditions.

2.2.2. Gel-Free Approaches

Nowadays, gel-free proteomic techniques (Abdallah et al. 2012; Lefort et al. 2009; Roe and Griffin 2006) are considered an attractive alternative to 2-DE since they allow to overcome the disadvantages of gel-based approaches such as the laborious procedure involved, the large amount of samples required, the limited dynamic range, the difficulty in resolving low abundance proteins and the ones with extreme p*I*, MW and hydrophobicity (Tan et al. 2008). In fact, in the last years, a series of gel-free methods have provided complementary information to 2-DE, driving mitochondrial molecular investigation to a higher level of data production and accuracy.

Gel-free methods are based on the separation of complex protein samples by liquid chromatography (e.g. reversed-phase, strong cationic exchange) followed by direct MS analysis (Nagele et al. 2004; Gilmore and Washburn 2010). This separation strategy might involve more than one LC column, being referred as multidimensional protein identification technology (MudPIT) (Link et al. 1999; Washburn et al. 2001; Wolters et al. 2001; Yates et al. 1999; Yates et al. 2000). MudPIT has been recognized as a high throughput method with enhanced ability to identify thousands of proteins within a single experiment (Motoyama and Yates 2008). For some time, gel-free approaches have suffered from the disadvantage of being only qualitative, hence not useful for differential display analyses. In addition, most of these approaches fall short of the resolution achieved with 2-DE gels and are still biased with respect to p*I* and molecular weight. This is because very acidic proteins will be underrepresented in the mixture due to fewer tryptic cleavage sites, and low molecular weight proteins will be underrepresented due to the production of fewer peptides (Washburn et al. 2001). A clear advantage is that most of these methods are very easily automated (Lopez and Melov 2002).

In recent years, approaches in shotgun proteomics have been developed, and are being increasingly used (Gilmore and Washburn 2010). Gel-free strategies have also being enriched by new, parallel developments in mass spectrometry, HPLC systems [i.e., Ultra Performance Liquid Chromatography (UPLC) technologies] as well as by peptide fragmentation techniques (i.e., ETD), which increased the number of proteins identified by MS (Silvestri et al. 2010). Moreover, the combination of SDS-PAGE with HPLC-ESI-MS/ MS allowed the identification of 823 unique proteins in mitochondria isolated from human *vastus lateralis* biopsies, 487 of which were assigned to mitochondrion (Lefort et al. 2009).

2.2.3. Mitochondrial Protein Microarrays

A promising technique for proteome analysis is the surface-enhanced laser desorption (SELDI) (Kiehntopf et al. 2007; Tang et al. 2004), which is available for the high throughput analysis of complex protein samples. SELDI interfaces coupled to time-of-flight mass spectrometry (SELDI-TOF-MS) consists of binding proteins to a chip with selective surface chemistries followed by TOF analysis of the native proteins in order to obtain a protein profile of a proteome subset (Cadieux et al. 2004). This strategy significantly reduces the complexity of the analyzed samples because it selects specific proteins according to their biochemical properties (Seibert et al. 2004).

SELDI is widely used in biomedical studies to perform, above all, biomarker analysis, and it has also been applied to mitochondrial proteomics research (Nyblom et al. 2006).

2.3. Mitochondrial Protein Identification and Quantification

Most of the studies on mitochondrial proteomics relies on the gel-based separation of proteins, mainly by 2-DE, followed by the excision of a selected protein spot, in-gel digestion with trypsin and identification by MS (Aebersold and Mann 2003). In gel-free approaches, identification readily follows LC separation of digested peptides, being the separation step directly coupled to the mass spectrometer (D'Hertog et al. 2006). Regardless of the strategy used, one of the major problems in the analysis of mitochondrial plasticity is the proteome comparison of different samples towards the detection of expression differences related with the pathophysiological condition in study.

In gel-based assays, quantitative analysis relies on band/spot staining intensity and so, imaging software is required for (i) image alignment and spot matching across the gels, (ii) normalization, background adjustment and noise removal, (iii) spot detection, (iv) calculation of the spot volumes and (v) statistical analysis to highlight differentially present proteins. The software uses multivariate statistical packages, such as ANOVA (analysis of variance), apply FDR (false discovery rates) or *q*-values to avoid the wrongful assignment of significant changes and PCA (Principle Component Analysis) is also often carried out. However, some challenges are associated with computational 2-DE analysis such as experimental variation between gels and the high probability of piling several proteins under one spot (Abdallah et al. 2012).

To overcome these limitations, gel-free based quantitative strategies have been favored to compare differentially expressed mitochondrial proteins. The two main approaches include stable isotope-labeling and label-free for the comparison of LC-MS/MS data.

In stable isotope-labeling quantification two or more distinct protein samples are first differentially labeled, one with an isotopically "light" tag and the other with an isotopically "heavy" tag. After labeling, the samples are combined and the resulting pooled peptides are separated by LC, either in a single dimension or using multidimensional strategies, depending on the complexity of the mixture (Roe and Griffin 2006). Peptides common to both samples, although differentially isotopically labeled, retain the same chemical properties and behave similar during the purification and separation steps. As result, such peptides are detected as peak pairs, differing in mass determined by the isotope label used, and the mass spectral peak heights, or the peak areas, are compared to calculate relative abundance levels of peptides between samples. Proteins or peptides in different samples can be metabolically labeled with stable isotope labeling amino acids in cell culture (SILAC) (Ong et al. 2002), chemically with isotope-coded affinity tag (ICAT) (Gygi et al. 1999), labeled with isobaric tag for relative and absolute quantification (iTRAQ) (Ross et al. 2004) or enzymatically with ^{18}O during proteolytic digestion (Miyagi and Rao 2007). Each of these labeling techniques has its own peculiarities.

SILAC is based on the incorporation of "light" or "heavy" isotope agents (^{2}H, ^{13}C, ^{15}N) in arginine and lysine within distinct cell cultures, which will further synthetize labeled proteins for proteomic comparisons. It is also known as metabolic stable isotope labeling and has been used to investigate the mitochondrial proteome in distinct pathophysiological

conditions, such as Parkinson's treatment (Jin et al. 2007), human cytomegalovirus infection (Zhang et al. 2011) and diabetic sensory neuropathy (Akude et al. 2011). The principal advantage of SILAC is its simplicity, because no *a posteriori* labeling is necessary to carry out the analysis; however, its application is limited to cell cultures (Ong et al. 2003). An alternative strategy assigned as SILAM (Stable Isotope Labeling of Mammals) was developed to metabolically label an entire mammal for quantitative MS analysis, being appropriate for animal models of disease (Geiger et al. 2013). However, no studies are known of its application to mitochondrial proteome analysis.

ICAT technique entails three functional elements: a specific chemical reactive group that binds to sulfhydryl groups of cysteinyl residues, an isotopicaly coded linker with light or heavy isotopes, and a biotin tag for affinity purification. The proteins containing cysteine residues are labeled either with light or heavy isotopes, where the latter form has eight ^{13}C atoms. Afterwards, light- and heavy-labeled samples are pooled and proteolytically cleaved. The complexity of the sample is reduced prior to MS analysis through the purification of tagged cysteine-containing peptides by affinity chromatography using biotin-avidin affinity columns. This technique was already applied to the study of mitochondrial proteome from primary neuron cultures (Lovell et al. 2005) but ICAT fails to identify non-cysteine containing proteins, being a major technical limitation. Moreover, ICAT has obviously limited use for the analysis of PTMs and splice isoforms (Bantscheff et al. 2007).

Another isotopic labeling approach involves the use of a protease (e.g. trypsin) and ^{18}O-enriched water (Yao et al. 2001), being the oxygen enzymatically incorporated in the C-terminal end of the peptide during the digestion procedure. Chromatographic and MS analyses are then performed to identify and quantify (relatively) the proteins from which the peptides were originated. This technique determines the ratio of individual protein expression levels between two samples, and can be used to quantitatively examine protein expression and PTMs, and to study protein-protein interactions (Miyagi and Rao 2007; Stewart et al. 2001; Mirgorodskaya et al. 2000). This quantitation method was used to evaluate the differential expression of cardiac mitochondrial proteins related with heart failure (Smith et al. 2008). Stable isotope-labeling experiments have great advantages in quantitative proteomics considering its accuracy and reproducibility in the study of complex samples. However, most of these stable isotope-labeling methods suffer potential limitations, including limited linear dynamic range, increased time and complexity of sample preparation and high cost of the labeling reagents (Chen et al. 2010). To overcome these limitations, a new amine reactive, isobaric tag named iTRAQ was developed (Ross et al. 2004). Within this method, proteins from different samples are digested and the resultant peptides are separately labeled with different isotopic variants of iTRAQ reagents, and then combined for LC-MS/MS analysis. A major improvement brought by this method is the ability to analyze up to eight different samples in the same experiment (Ross et al. 2004). iTRAQ is one of the most popular quantitation tools in mitochondrial proteome research (Baseler et al. 2011; Jullig et al. 2007; Kavazis et al. 2009; Glancy and Balaban 2011; Meany et al. 2007; Jullig et al. 2008).

Label-free LC-MS represents an attractive approach for quantitative mitochondrial proteomics (Lundgren et al. 2010; Lai et al. 2013; Zhu et al. 2010; Old et al. 2005) since it is simple, reproducible, cost effective, and less prone to errors and side reactions related to the labeling process. Protein quantification is generally based on two categories of measurements: i) ion intensity such as peptide peak areas or peak heights in chromatography (Old et al. 2005; Ono et al. 2006); ii) spectral counting of identified proteins after MS/MS analysis (Lundgren

et al. 2010; Old et al. 2005; Gilchrist et al. 2006). Peptide peak intensity or spectral count is measured in individual LC-MS/MS or LC/LC-MS/MS runs and changes in protein abundance are calculated via a direct comparison between different analyses (Zhu et al. 2010). Though straightforward, this method has the disadvantage of include the variation related with all preparation steps as well as those due to variations in the performance of LC-MS/MS unit. Nevertheless, label-free quantitative proteomics was already successfully applied to the systematic analysis of tissue-specific mitochondrial proteome changes related with diabetes mellitus (Bugger et al. 2009) and cardiovascular diseases (Smith et al. 2008; Bugger et al. 2010).

2.3.1. Mitochondrial Protein Posttranslational Modifications

PTMs of mitochondrial proteins have been reported to regulate mitochondrial functions and so, numerous studies have been conducted using MS-based approaches. Phosphorylation is an important PTM that was reported to regulate mitochondrial dynamics (Koc and Koc 2012; Zhao et al. 2011). The identification of phosphorylated proteins and its specific phosphosites has been performed by MS-based strategies in combination with phospho-specific enrichment methods, such as immobilized metal ion affinity chromatography (IMAC) and titanium dioxide (TiO_2) chromatography (Eyrich et al. 2011). Besides phosphorylation, other PTMs in mitochondrial proteins, such as acetylation and oxidative modifications have been studied. Protein tyrosine nitration is a common modification that occurs in mitochondria under conditions of oxidative stress (Greenacre and Ischiropoulos 2001), being classically analyzed by 2-DE in combination with western blotting and MS (Turko et al. 2003). Protein oxidation has been detected by western blotting analysis of carbonylated proteins with an anti-DNP antibody followed by MS identification of the oxidized proteins (Padrao et al. 2012). Acetylation is another modification found in mitochondrial proteins, mainly in the ones involved in metabolic pathways (Kim et al. 2006). Its analysis usually involves immunoenrichment procedures with an acetyl lysine antibody. Despite all the achievements observed in the last years, many challenges remain in the PTMs characterization of mitochondrial proteins, but it is clear that MS-based approaches can make a unique contribution on how these modifications are modulated by distinct stimuli and what are their functional repercussions.

2.4. Mitochondrial Proteins Database

The need of cataloguing and archiving mitochondrial proteomic data already resulted in the development of several mitochondrial proteome databases that combine information on genetic, functional and pathogenic aspects of nuclear-encoded mitochondrial proteins and include MitoP2 (Elstner et al. 2009; Elstner et al. 2008), Mitoproteome (Cotter et al. 2004), Mito-Carta (Pagliarini et al. 2008), Human mitochondrial Protein database and MitoMiner (Smith and Robinson 2009), as well as the CardiacOrganellar Protein Atlas Knowledgebase (COPaKB) (table 1).

Table 2.

Proteomic approaches						Proteins differentially expressed		
Mitochondrial purification methods	Analytic method	Condition	Specie	Sample	Alterations of mitochondrial physiology	Up-regulated	Down-regulated	References
Type 1 Diabetes								
Differential centrifugation Percoll-density centrifugation	Isotopic labeling, 2-DE, MALDI-TOF	STZ-induced diabetes rats	Rat	Heart mitochondria	-	FAO	ETC; CK; VDAC1, Hsp60, Grp75	(Turko and Murad 2003)
Differential centrifugation	iTRAQ, MudPIT MS/MS	STZ-induced diabetes rats	Rat	Heart mitochondria	-	FAO (particularly long-chain fatty acids);	ETC; amino acid catabolism; biosynthesis and HSPs/chaperones	(Jullig, Hickey et al. 2007)
Differential centrifugation, density centrifugation	iTRAQ, DIGE; LC-MALDI-TOF/TOF	STZ-induced diabetic mice	Mice	Heart SS and IMF	-	FAO in IMF;	ETC in IMF; Protein import and substrate transport (mtHsp70, ANT1, mitochondrial phosphate carrier)	(Baseler, Dabkowski et al. 2011)
Differential centrifugation Percoll-density centrifugation	Label free	Akita diabetic mice	Mice	Heart mitochondria	↓State 3 respiration, ATP synthesis, mitochondrial cristae density in cardiac mitochondria	FAO	TCA	(Bugger, Chen et al. 2009)
Differential centrifugation Percoll-density centrifugation	BN-PAGE, zymography/LC-MALDI-TOF/TOF, Western blotting	STZ-induced diabetic rats	Rat	IMF gastrocnemius mitochondria	↓ complex V respiratory complex activity ↑ oxidative damage	-	Lon, paraplegin, MMP-9	(Padrao, Carvalho et al. 2012)

Table 2. (Continued)

Proteomic approaches						Proteins differentially expressed		
Mitochondrial purification methods	Analytic method	Condition	Specie	Sample	Alterations of mitochondrial physiology	Up-regulated	Down-regulated	References
Type 1 Diabetes (Continued)								
Differential centrifugation	2DE, Western blotting; MALDI-TOF	ALS and ALR mice	mice	Heart mitochondria	# protein nitration levels	Nitrated SCOT, CK, peroxiredoxin 3, VDAC1	-	(Turko, Li et al. 2003)
Type 2 diabetes								
Differential centrifugation	2DE, LC-ESI-MS/MS; western-blotting	db/db mice	Mice	Heart mitochondria	# protein nitration levels	Nitrated SCOT, NADH dehydrogenase (ubiquinone) Fe-S protein 1, Trifunctional enzyme subunit alpha, dihydrolipoamide dehydrogenase, ATP synthase subunit alpha isoform 1, Aldehyde dehydrogenase family 6, Glutamate dehydrogenase 1, fumarate hydratase 1, Dihydrolipoamide succinyltransferase component of 2-oxoglutarate dehydrogenase complex, short-chain acyl-CoA dehydrogenase, Pyruvate hydrogenase E1 alpha, Isovaleryl-CoA dehydrogenase, mitochondrial, acetyl-Coenzyme A dehydrogenase medium chain, CK, glutamate oxaloacetate transaminase 2, Trifunctional enzyme subunit alpha (HADHB), 3-ketoacyl-CoA thiolase, isocitrate dehydrogenase 3 beta subunit	-	(Wang, Peng et al. 2010)

Proteomic approaches						Proteins differentially expressed		
Mitochondrial purification methods	Analytic method	Condition	Specie	Sample	Alterations of mitochondrial physiology	Up-regulated	Down-regulated	References
Type 2 Diabetes (Continued)								
Differential centrifugation density centrifugation	iTRAQ; MudPIT	db/db mice	Mice	Heart SSM and IFM	↓Size and internal complexity of SS ↓State 3 respiration rates, ETC activities, and membrane potential of SS ↑oxidative damage in SS	FAO in both SSM and IMF of db/db hearts	ETC, ATP synthesis, and protein import machinery in SS	(Dabkowski, Baseler et al. 2010)
Differential centrifugation	2-DE; ESI-Q-TOF	Obese db/db mouse	Mice	Heart mitochondria	-	ATP synthase D chain; electron transfer flavoprotein subunit alpha	ubiquinol cytochrome-C reductase core protein 1	(Essop, Chan et al. 2011)
Cardiovascular diseases								
Gradient centrifugation	2-DE, MALDI-TOF	Chronic stress	Rat	Heart mitochondria	Mitochondrial swelling with vacuoles, ↓ ATP synthase activity, ↓ ATP content, ↓ respiratory control rate, ↓ oxidative phosphorylation	CK, prohibitin	TCA, FAO	(Liu, Qian et al. 2004)
Differential centrifugation	2-DE, MALDI-TOF	Desmin null	Mouse	Heart mitochondria	-	Ketone and acetate catabolism, ETC (complex I), VDCA2, mtHsp70, ubiquitin-like 1	Malate/aspartate shuttle, ketone utilization, PDH	(Fountoulakis, Soumaka et al. 2005)

Table 2. (Continued)

Proteomic approaches						Proteins differentially expressed		
Mitochondrial purification methods	Analytic method	Condition	Specie	Sample	Alterations of mitochondrial physiology	Up-regulated	Down-regulated	References
Cardiovascular diseases (continued)								
Differential centrifugation and Percoll-density centrifugation	2-DE, MALDI-TOF	Ischemia-reperfusion	Rabbit	Heart mitochondria	-	PDH, ETC (complex I), FAO long-chain acyl-CoA dehydrogenase and 3-hydroxybutyrate dehydrogenase, mitofillin and translation elongation factor	TCA, ETC (complex III), VDCA2, enoyl-CoA hydratase, prohibitin	(Kim, Lee et al. 2006)
Differential centrifugation	2-DE, MALDI-TOF	Left anterior descending coronary artery ligation	Rat	Heart mitochondria	Small mitochondria with scattered abnormal vacuoles in failing hearts	TCA, PDH, glycolysis	FAO, ETC (complex I, III, IV, V)	(Wang, Bai et al. 2009)
Differential centrifugation	2-DE, ESI-MS/MS, BN-PAGE	Dyssynchronous or resynchronized heart failure	Dog	Heart mitochondria	↑ complex V activity, ↑ efficiency of oxidative phosphorylation in cardiac resynchronization	ETC (complexes I, II, III, V), PDH, VDAC3, protein synthesis and import, ROS scavenging enzymes	cytochrome c, VDAC2	(Agnetti, Kaludercic et al. 2010)
Differential centrifugation	iTRAQ, MudPIT MS/MS	Spontaneously hypertensive	Rat	Heart mitochondria	Enlarged mitochondria with irregularities of the cristae, ↓ respiratory capacity on succinate	Hsp60, Hsp10, mtHsp70, PDH, proapoptotic factors, cytochrome c, cyclophilin D, GPx1, MAO A, ETC (complexes I, III, IV)	ETC (complexes II, V), CK, FAO	(Jüllig, Hickey et al. 2008)

Proteomic approaches						Proteins differentially expressed		
Mitochondrial purification methods	Analytic method	Condition	Specie	Sample	Alterations of mitochondrial physiology	Up-regulated	Down-regulated	References
Cardiovascular diseases (continued)								
Differential centrifugation and density gradient centrifugation	2D-DIGE, MALDI-TOF/TOF	Spontaneously hypertensive	Rat	Heart mitochondria	-	TCA, ETC (complexes I, II)	FAO, PDH, ETC (complex V), VDAC1	(Meng, Jin et al. 2009)
Differential centrifugation	LC-MS/MS, ^{18}O labeling	Dahl salt sensitive	Rat	Heart mitochondria	-	3-hydroxyacyl-CoA dehydrogenase type II, short-chain 3-hydroxyacyl-CoA dehydrogenase	Succinate dehydrogenase, fumarate hydratase, electron transfer flavoprotein alpha	(Smith, Matus et al. 2008)
Differential centrifugation	LC-MS/MS, Label-free	Transverse aortic constriction	Rat	Heart mitochondria	Mitochondria with disorganized cristae and/or reduced cristae density, ↓ mitochondrial volume density, ↓ State 3 respiration	TCA, PDH, ETC (complex I, II, V)	FAO, ECT (complex I, III, IV, V)	(Bugger, Schwarzer et al. 2010)
Differential centrifugation	2-DE, liquid chromatography, ESI-MS/MS	Intermittent hypoxia	Rat	Heart mitochondria	↓ ATP content in intermittent hypoxia at ischemia compared with pro-ischemia and reperfusion	Aldehyde dehydrogenase, aconitase, malate dehydrogenase, ATP synthase β chain, electron transfer flavoprotein α subunit, sirtuin 5, methylmalonate-semialdehyde dehydrogenase	Ubiquinol-cytochrome c reductase iron-sulfur subunit, aspartate aminotransferase	(Zhu, Wu et al. 2012)

Table 2. (Continued)

Proteomic approaches						Proteins differentially expressed		
Mitochondrial purification methods	Analytic method	Condition	Specie	Sample	Alterations of mitochondrial physiology	Up-regulated	Down-regulated	References
Aging								
Differential centrifugation	DIGE, LC-MS, Imunoblotting	Sarcopenia model	Rat	Skeletal muscle mitochondria	# activity of respiratory chain complexes	NADH dehydrogenase, prohibitin, VDAC2, Succinate dehydrogenase, Fis1, acyl-coA dehydrogenase, PRX-III, ubiquinol-cytochrome c reductase core I protein, Succinate CoA ligase, F1-ATPase	-	(O'Connell and Ohlendieck 2009)
Differential centrifugation	2-DE, MALDI-TOF, MALDI-TOF/TOF,HPLC-ESI/MS	24-25 months rats	Rat	Heart Mitochondria, Skeletal muscle mitochondria	-	Isocitrate dehydrogenase, malate dehydrogenase	-	(Chang et al. 2007)
Differential centrifugation	2-DE, Western blotting, MALDI-TOF, ESI-MS/MS, NSI-MS/MS	24-34 months rats	Rat	Skeletal muscle	# protein nitration levels	nitrated succinate dehydrogenase	-	(Kanski et al. 2003)
Differential centrifugation	2-DE, MALDI-TOF	30 months rats	Rat	Skeletal muscle	i protein phosphorylation levels	-	phosphorylated cytochrome c oxidase and aconitase	(Gannon et al. 2008)
Differential centrifugation	SDS-PAGE, LC-MALDI-TOF/TOF, Western blotting	25 months mice	Mice	Heart mitochondria	# protein carbonylation and nitration	carbonylated and nitrated ATP synthase and cytochrome *b-c1* complexes subunits; carbonylated NADH dehydrogenase [ubiquinone] iron-sulfur protein 2,	-	(Padrao et al. 2012)

Proteomic approaches						Proteins differentially expressed		
Mitochondrial purification methods	Analytic method	Condition	Specie	Sample	Alterations of mitochondrial physiology	Up-regulated	Down-regulated	References
Aging (Continued)								
Differential centrifugation	SDS-PAGE, LC-MALDI-TOF/TOF, Western blotting	25 months mice	Mice	Heart mitochondria	# protein carbonylation and nitration	NADH dehydrogenase [ubiquinone] 1 alpha subcomplex subunit 10, ATP synthase subunits d and O,malate dehydrogenase, VDAC1, MnSOD	-	(Padrao et al. 2012)

Legend: FAO: Fatty acid oxidation, SCOT: succinyl-CoA:3-oxoacid CoA transferase, CK: creatine kinase, TCA: tricarboxylic acid cycle, ETC: electron transport chain, OXPHOS: oxidative phosphorylation, PDH: pyruvate dehydrogenase, VDAC: voltage dependent anion channel, ALS: alloxan-susceptible, ALR: alloxanresistant.

Table 1.

Database	Web link	Species	Information given
MitoP2	http://www.mitop.de:8080/mitop2/	yeast, mouse, human, Arabidopsis thaliana, and Neurospora crassa	Computational predictions of signalling sequences and summarize results from proteome mapping, mutant screening, expression profiling, protein-protein interaction and cellular sublocalization studies
Mitoproteome	http://www.mitoproteome.org/	human	Comprehensive curation of public databases and direct experimental evidence; contains both mitochondrial- and nuclear-encoded protein sequences.
MitoCarta	http://www.broadinstitute.org/pubs/MitoCarta/	mouse, human	Inventory of 1098 mouse genes encoding proteins with MS analysis of mitochondria isolated from fourteen tissues, protein localization through large-scale GFP tagging/microscopy, and integration with six other genome-scale datasets of mitochondrial localization, using a Bayesian approach. Inventory of 1013 human HomoloGene homologs to the mouse MitoCarta collection.

Table 1. (Continued)

Database	Web link	Species	Information given
Human mitochondrial Protein database	http://bioinfo.nist.gov/	human	Inventory of proteins involved in mitochondrial biogenesis and function; consolidates information from SwissProt, LocusLink, Protein Data Bank, GenBank, Genome Database, Online Mendelian Inheritance in Man, Human Mitochondrial Genome Database, MITOMAP, Neuromuscular Disease Center and Human 2-D PAGE Databases. Tool to aid in the study of mitochondria-associated diseases.
MitoMiner	http://mitominer.mrc-mbu.cam.ac.uk/release-2.1/begin.do	not defined dataset but allows the analysis of rat, mouse, human, A. thaliana, B. taurus, D. melanogaster, G. lamblia ATCC50803, N. crassa OR74A, P. falciparum 3D7, S. cerevisiae S288c, S. pombae 972h-, T. thermophila SB210.	Integrates mitochondrial proteomics data for a range of organisms.
CardiacOrganellar Protein Atlas Knowledgebase	http://www.heartproteome.org/copa/default.aspx	human, mouse	Provides annotated peptide spectra, their association knowledge on proteome properties, cardiovascular biology, as well as tools to access this resource.

These databases list mitochondrial proteins identified via multiple approaches, including MS/MS analyses, literature references and bioinformatic evaluations. Among these, MitoP2 is one of the most comprehensive database, providing a list of mitochondrial proteins from yeast, mouse, human, *Arabidopsis thaliana*, and *Neurospora crassa*. It gives information about the functional annotation of proteins, as well as their subcellular location, their homologs, along with literature references.

MitoMiner is another mitochondrial protein database that integrates sets of proteomic data from several species (e.g. human, rat, mouse, *Drosophila melanogaster*, *Caenorhabditis elegans,* and *Saccharomyces cerevisiae*), thereby representing the most complete mitochondrial database known to date. It is based on MS experiments together with protein annotation data from Uniprot, metabolic pathway data from Kyoto Encyclopedia of Genes and Genomes (KEGG), protein homology from HomoloGene and disease information from Online Mendelian Inheritance in Man (OMIM).

Importantly, these data-sets have revealed that the number of mammalian mitochondrial proteins is much greater (> 3000) than the early studies have estimated (Meisinger et al. 2008; McDonald and Van Eyk 2003). COPaKB is an integrated resource of proteome biology configured to specifically focus on cardiovascular biology and medicine. It includes proteomic data from large-scale proteomic surveys of cardiac mitochondria (Wilkins 2009). Despite the advances achieved in mitochondrial proteomics research, data quality is still a major challenge in proteomics.

3. Mitochondrial Proteome Plasticity in Pathophysiological Conditions

Several inter-connected metabolic pathways are harbored in mitochondria, which themselves are connected to other important cellular functions. So, any local mitochondrial dysfunction can potentially lead to very complex cellular adaptations, which might be studied using comparative proteomic techniques.

Mitochondrial proteomics of tissues highly reliant on oxidative metabolism as striated muscles have been considered appropriate to increase the understanding of the molecular mechanisms underlying pathophysiological conditions related to heart or skeletal muscle dysfunction, and to find targets for novel therapies. So, in this section, the main findings on mitochondrial proteome alterations in cardiac and skeletal muscles are explored in cardiovascular diseases, diabetes mellitus, cancer and aging (summarized in table 2).

3.1. Cardiovascular Diseases

Mitochondrial proteomics have been applied to the study of cardiovascular diseases, the main "killer" in human beings (Jiang and Wang 2012). Most of the studies in this field aim to characterize heart mitochondrial dysfunction in order to give new insights into an early diagnosis and in the discovery of novel therapeutic targets (Hollander et al. 2011; McGregor and Dunn 2003; McGregor and Dunn 2006; Pieczenik and Neustadt 2007). For that, mitochondria isolated from heart or ventricles from different animal models of heart failure

have been studied either with gel-based or gel-free approaches for protein separation, and mass spectrometry for protein identification (table 2).

For instance, using gel-based approaches (2-DE-MALDI-TOF), five proteins involved in tricarboxylic acid (TCA) cycle and lipid metabolism were found decreased and creatine kinase (CK) and prohibitin increased in the ventricles of stressed rats (Liu et al. 2004). More differentially expressed proteins were recognized in the analysis of heart from desmin null mice with proteins involved in the malate/aspartate shuttle, ketone utilization, and pyruvate dehydrogenase (PDH) subunits found down-regulated, and the electron transport chain (ETC) subunits, voltage dependent anion channel 2 (VDCA2), mtHsp70 and ubiquitin-like 1 were reported in significant higher levels (Fountoulakis et al. 2005). Changes in the abundance of metabolic proteins were also observed in ischemia-reperfusion (IR) and ischemia preconditioned (IPC) rabbit hearts (Kim et al. 2006). Whereas the expression of TCA cycle proteins decreased in IR hearts compared with control and IPC hearts, PDH increased. Respiratory chain proteins showed a variable pattern. The fatty acid oxidation (FAO) enzymes long-chain acyl-CoA dehydrogenase and 3-hydroxybutyrate dehydrogenase expression increased with ischemia, but enoyl-CoA hydratase decreased. Besides metabolism, alterations in the levels of proteins involved in transport and translation were also related with cardiac dysfunction. The mitochondrial proteome profiling of the left ventricle in a canine model of dyssynchronous or resynchronized heart failure performed with 2-DE-MS/MS, and BN-PAGE retrieved an overexpression of OXPHOS subunits (from complexes I, II, III and V), PDH complex proteins, VDAC3, proteins involved in protein synthesis and import and reactive oxygen species (ROS) scavenging enzymes. In contrast, cytochrome c and VDAC2 were down-regulated in cardiac resynchronization therapy, which was related with improved cardiac chamber mechanoenergetics, and decreased morbidity and mortality in patients with ventricular dyssynchrony (Agnetti et al. 2010).

MudPIT MS/MS analysis, combined with iTRAQ labeling, of mitochondria isolated from 20 month old spontaneously hypertensive rats evidenced the down-expression of several proteins from OXPHOS complexes II and V, CK, and proteins involved in FAO, and the overexpression of mitochondrial HSPs, PDH complex subunits, proapoptotic factors, proteins involved in permeability transition pore, ROS production and scavenging (Jüllig et al. 2008). Using LC-MS/MS with ^{18}O labeling for the analysis of heart mitochondrial proteome in a rat model of hypertension, cardiac hypertrophy and heart failure, the Dahl salt sensitive rat model, FAO dehydrogenases were found over-expressed whereas succinate dehydrogenase, fumarate hydratase and electron transfer flavoprotein alpha were down-regulated (Smith et al. 2008). LC-MS/MS with label-free quantitation also allowed the association of down-regulated FAO proteins, and over-expressed proteins from the PDH complex and TCA cycle with heart failure induced by transverse aortic constriction (Bugger et al. 2010).

There are no known studies that characterized the heart mitochondrial proteome in humans with cardiovascular diseases. However, to gain insight into mitochondrial proteome changes associated with these diseases, the analysis of the total heart tissue instead of isolated mitochondria was performed for the study of dilated cardiomyopathy (Knecht et al. 1994; Knecht et al. 1994) and of chronic reversibly and irreversibly dysfunctional myocardium, as well as in end-stage failing myocardium (Urbonavicius et al. 2009). The down-regulation of PDH, VDAC1, MnSOD, TCA cycle and ETC complex I subunits was verified by 2-DE and LC-MS/MS in irreversibly dysfunction and end-stage failing heart (Urbonavicius et al. 2009).

3.2. Diabetes Mellitus

Given their essential role in fatty acid and glucose metabolism (Baker and Haynes 2011; Duncan 2011), mitochondria from cardiac and skeletal muscles are likely to be impacted by diabetes mellitus (DM) and related complications (Baseler et al. 2011; Padrao et al. 2012; Jullig et al. 2007; Bugger et al. 2009; Duncan 2011; Romanello and Sandri 2010; Sivitz and Yorek 2010; Turko and Murad 2003; Dabkowski et al. 2010; Dabkowski et al. 2009; Essop et al. 2011). There are more studies in cardiac then in skeletal muscle mitochondria, focused on the understanding of the early events in DM-related cardiomyopathy. The majority of the mitochondrial proteome research has been conducted in animal models exhibiting T2DM (db/db mouse model) and T1DM, including streptozotocin (STZ)-induced T1DM mice/rats and diabetic Akita mouse.

Among the mitochondrial proteins modulated by STZ-induced T1DM, it was found by 2DE-MALDI-TOF/TOF an overexpression of FAO proteins and a selective down-regulation of OXPHOS and other mitochondrial proteins, such as CK, VDAC1, Hsp60, and Grp75 (Turko and Murad 2003). Employing iTRAQ labeling coupled with MudPIT, 65 proteins were identified in significantly different levels in cardiac mitochondria from STZ rats compared with control ones. Enzymes involved in long-chain fatty acids oxidation were found in increased amounts, further confirmed by enzyme assays, whereas multiple proteins involved in OXPHOS and catabolism of short-chain fatty acids and branched-chain amino acids were detected in decreased levels. Altered levels of several enzymes linked to oxidative stress were also observed (Jullig et al. 2007). Label-free proteome expression analyses of several tissues from wild-type and T1DM Akita mice (kidney, liver, brain, and heart) evidenced tissue-specific remodeling of the mitochondrial proteome, which in the case of the dysfunctional heart was manifested by an increase of FAO enzymes (Bugger et al. 2009).

Focusing on the role of mitochondrial protein quality control systems, zymography-LC-MALDI-MS/MS analysis was performed in order to identify the effect of T1DM on the expression and activity of mitochondrial proteases in *gastrocnemius* muscle. The AAA Lon protease, the metalloproteases PreP, LAP-3 and MIP, and cathepsin D were identified in muscle mitochondria and the content and activity of Lon protease was lower in the STZ animals and related with the accumulation of oxidized proteins (Padrao et al. 2012).

Besides changes in mitochondrial protein expression, PTMs seem to play an important role in DM-related mitochondria functionality. Protein tyrosine nitration was reported in the mitochondrial proteome from diabetic mouse heart (Turko and Murad 2003; Wang et al. 2010) and seems to affect energy production, antioxidant defense and apoptosis (Turko et al. 2003). Hollander's research group investigated thoroughly the differential response of the two populations of heart mitochondria in both T1DM and T2DM, using proteomic tools (Baseler et al. 2011; Dabkowski et al. 2010; Dabkowski et al. 2009). Based on iTRAQ and DIGE data, SS and IMF were analyzed to determine whether T1DM influenced their proteomic makeup in the heart. The decreased abundance of FAO and ETC proteins, of mitochondrial protein import and substrate transport (Hsp70, ANT1, and mitochondrial phosphate carrier) was more notorious in IMF mitochondria from diabetic subjects. Besides alterations in protein levels, PTMs including oxidations and deamidations were most prevalent in diabetic IMF mitochondria (Baseler et al. 2011). Using iTRAQ with MudPIT-based mass spectral analyses, proteins from FAO were found increased in both SS and IMF mitochondria of db/db hearts, though more pronounced in SS. Inner mitochondrial membrane proteins, including ETC, ATP

synthase, and mitochondrial protein import machinery, were predominantly decreased in SS and related with impaired activity of this organelle (Dabkowski et al. 2010).

3.3. Cancer

Proteomic studies focused on mitochondria from striated muscle of individuals with cancer are scarce and mainly target cancer cachexia. Though recently emphasis has been given to mitochondrial dysfunction in cancer cachexia (Julienne et al. 2012; Lokireddy et al. 2012; White et al. 2012), no studies are known that performed protein profiling of mitochondria isolated from skeletal or cardiac muscles. Nevertheless, cancer-related muscle wasting was associated with altered expression of mitochondrial proteins measured by western blotting. For instance, cancer-related activation of TNF-alpha –induced NFκB was shown to decrease the expression of regulatory factors involved in mitochondrial biogenesis and consequently to disturb muscle oxidative capacity (Julienne et al. 2012; Wang et al. 2012). Moreover, the proteome analysis of whole *gastrocnemius*, *tibialis anterior*, *extensor digitorum longus* and *soleus,* and heart from rats inoculated with Yoshida AH-130 ascites hepatoma cells using 2-DE coupled to MALDI-TOF evidenced a higher susceptibility of proteins involved in ATP production and mitochondrial metabolism to oxidative damage (Marin-Corral et al. 2010).

3.4. Aging

The knowledge of mitochondrial proteome plasticity in skeletal and cardiac muscles of aged individuals have given new insights on the molecular mechanisms underlying this pathophysiological condition, which is characterized by a progressive, irreparable and time dependent deterioration of overall body functions (Figueiredo et al. 2008; Lenaz et al. 2000; Ventura et al. 2002). Proteomic profiling of mitochondria-enriched fractions from different animal's skeletal muscles has revealed a shift to a more aerobic oxidative metabolism in slower-twitching fibre populations during age-related muscle degeneration (O'Connell and Ohlendieck 2009; Ohlendieck 2011). Using DIGE with MS for protein identification, 11 mitochondrial proteins were found differentially expressed, with an aged-dependent elevation of ETC complexes I and III, mitofilin, peroxiredoxin isoform PRX-III, F1-ATPase, succinate dehydrogenase, fission protein Fis 1, succinate-coenzyme A ligase, acyl-coenzyme A dehydrogenase, VDAC2 and prohibitin (O'Connell and Ohlendieck 2009). The effect of aging was studied in mitochondria from 25-month-old rats and compared with 6-month-old ones using 2-DE coupled to MALDI-TOF-MS, MALDI-TOF/TOF-MS/MS and HPLC-ESI-MS and 3 heart proteins and 5 skeletal muscle proteins were found altered in an age dependent way, namely the metabolic enzymes isocitrate dehydrogenase and malate dehydrogenase (Chang et al. 2007).

Besides protein profiling, abnormal PTMs have been studied in aged skeletal and cardiac muscles' mitochondria (Schoneich 2006). For instance, higher levels of carbonylated ATP synthase, NADH dehydrogenase, pyruvate dehydrogenase and isocitrate dehydrogenase were reported in mitochondria from aged skeletal muscle based on data obtained from LC-ESI-MS/MS analysis with iTRAQ (Feng et al. 2008). Moreover, fast-twitch muscles seem to

contain twice as many carbonylated mitochondrial proteins than slow-twitch muscles and 22 proteins showed significant changes in the carbonylation state with age, as for example trifunctional enzyme subunits α and β, acetyl-CoA acetyltransferase, NADH dehydrogenase (ubiquinone) Fe-S protein 1, Stress-70 protein, Hsp60, among others (Feng et al. 2008). The decreased capacity of aged mitochondria for ATP production was related with the increased carbonylation of specific proteins, mostly from TCA and OXPHOS (Alves et al. 2010). Using SDS-PAGE coupled to LC-MALDI-TOF/TOF and western blotting to identify the mitochondrial proteins more susceptibility to oxidation in mice cardiac muscle, it was verified an aged-related accumulation of oxidized OXPHOS subunits, some metabolic enzymes, transport proteins and antioxidant enzymes as MnSOD (Padrao et al. 2012).

3.5. Integrated Analysis of Mitochondrial Proteome Dynamics in Striated Muscle

Regardless the insult that triggers mitochondrial dysfunction, there are some similarities in the pattern of disease-related protein expression. Metabolic proteins, OXPHOS subunits, chaperones like HSPs and transport proteins as VDACs were found altered in all the pathophysiological conditions analyzed. Concerning metabolism, in diabetes mellitus, either type 1 or type 2, proteins from FAO were found up-regulated in cardiac mitochondria while ETC subunits were identified in significantly lower levels. Indeed, the metabolic phenotype of the diabetic heart is characterized by raises in fatty acid uptake and oxidation, a pattern largely mediated by competition between glucose and fatty acid metabolism (reviewed by Isfort et al. 2013). An opposite tendency was verified in distinct models of cardiovascular diseases, with FAO enzymes in lower levels in heart mitochondria. Though alterations in the expression of TCA and ETC proteins were also observed, distinct metabolic profiles were reported depending on the animal model studied. In contrast to the normal adult heart, the non-ischemic failing heart generally uses relatively more glucose at the expense of FAO. However, not all heart failure is metabolically the same. Comorbid conditions, degree of ischemia, degree of FAO metabolism machinery dysfunction, and plasma substrate levels also appear to modulate myocardial metabolism (reviewed by Kadkhodayan et al. 2012).

Besides metabolic proteins, the expression of heat shock proteins and VDACs was found to be modulated by these pathologies. The up-regulation of VDAC1 in T1DM and the altered expression of VDAC1-3 in cardiovascular diseases may result in disturbed energy production, metabolite cross-talk between cytosol and mitochondria, or apoptosis regulation (Shoshan-Barmatz and Ben-Hail 2012). The enhanced expression of HSPs might protect mitochondrial energetics, contributing to the recovery of myocardial function in ischaemia-reperfusion (Sammut and Harrison 2003).

More than protein profiling, several studies targeted the proteins more susceptible to PTMs in pathophysiological conditions, particularly in aging. Metabolic proteins are particularly prone to oxidative modifications in aged heart and skeletal muscle mitochondria. Indeed, increased carbonylated and nitrated TCA enzymes as aconitate hydratase and OXPHOS proteins like ATP synthase subunits α and β were previously reported (Turko et al. 2003; Alves et al. 2010). Because proteins that undergo oxidation are involved in major

mitochondrial functions, such as energy production and antioxidant defense, increased levels of oxidized proteins have been associated with disease-related dysfunctional mitochondria.

4. Future Perspectives

The mitochondrion, as the biochemical nexus of the cell, is a critical consideration in the proteomics era. Great progress has already been made in mitochondrial proteomics to elucidate the role of mitochondria from striated muscles in the pathogenesis of diseases like diabetes mellitus or heart failure. However, mitochondria harbor a multitude of proteins and despite technical and methodological advances in mitochondrial protein profiling, there are many proteins yet to be characterized and their biological functions better understood. Standardizing experiments in terms of sample preparation, protein separation and identification as well as data analysis with bioinformatic tools is necessary for unbiased proteomic studies. Considering the increasingly recognized role of PTMs in the regulation of protein's function, further studies focused on the functional consequences of mitochondrial protein specific posttranslational modifications would provide a better understanding of the biological significance of signaling pathways centered on mitochondria.

Acknowledgments

This work was supported by Fundação para a Ciência e a Tecnologia (FCT, Portugal), European Union, QREN, FEDER and COMPETE for funding the QOPNA research unit (project PEst-C/QUI/UI0062/2011), research projects (PTDC/DES/114122/2009 and PTDC/DES/104567/2008) and post-graduation students (grant numbers SFRH/BD/66642/2009 to A.I.P, SFRH/BD/91067/2012 to R.N.F).

References

Abdallah, C., Dumas-Gaudot, E., Renaut, J., Sergeant, K. (2012) Gel-based and gel-free quantitative proteomics approaches at a glance. *International journal of plant genomics* 2012494572

Aebersold, R., Mann, M. (2003) Mass spectrometry-based proteomics. *Nature* 422(6928): 198-207

Agnetti, G., Kaludercic, N., Kane, L. A., Elliott, S. T., Guo, Y., Chakir, K., Samantapudi, D., Paolocci, N., Tomaselli, G. F., Kass, D. A., Van Eyk, J. E. (2010) Modulation of Mitochondrial Proteome and Improved Mitochondrial Function by Biventricular Pacing of Dyssynchronous Failing Hearts. *Circulation: Cardiovascular Genetics* 3(1):78-87

Akude, E., Zherebitskaya, E., Chowdhury, S. K., Smith, D. R., Dobrowsky, R. T., Fernyhough, P. (2011) Diminished superoxide generation is associated with respiratory chain dysfunction and changes in the mitochondrial proteome of sensory neurons from diabetic rats. *Diabetes* 60(1):288-297

Alves, R. M., Vitorino, R., Figueiredo, P., Duarte, J. A., Ferreira, R., Amado, F. (2010) Lifelong physical activity modulation of the skeletal muscle mitochondrial proteome in mice. *J. Gerontol. A Biol. Sci. Med. Sci*. 65(8):832-842

Baker, B. M., Haynes, C. M. (2011) Mitochondrial protein quality control during biogenesis and aging. *Trends in biochemical sciences* 36(5):254-261

Balaban, R. S. (2010) The mitochondrial proteome: a dynamic functional program in tissues and disease states. *Environmental and molecular mutagenesis* 51(5):352-359

Bantscheff, M., Schirle, M., Sweetman, G., Rick, J., Kuster, B. (2007) Quantitative mass spectrometry in proteomics: a critical review. *Anal. Bioanal. Chem*. 389(4):1017-1031

Baseler, W. A., Dabkowski, E. R., Williamson, C. L., Croston, T. L., Thapa, D., Powell, M. J., Razunguzwa, T. T., Hollander, J. M. (2011) Proteomic alterations of distinct mitochondrial subpopulations in the type 1 diabetic heart: contribution of protein import dysfunction. *Am. J. Physiol. Regul. Integr. Comp. Physiol*. 300(2):R186-200

Benard, G., Faustin, B., Passerieux, E., Galinier, A., Rocher, C., Bellance, N., Delage, J. P., Casteilla, L., Letellier, T., Rossignol, R. (2006) Physiological diversity of mitochondrial oxidative phosphorylation. *American journal of physiology Cell physiology* 291(6):C11 72-1182

Benard, G., Rossignol, R. (2008) Ultrastructure of the mitochondrion and its bearing on function and bioenergetics. *Antioxid. Redox. Signal* 10(8):1313-1342

Braun, R. J., Kinkl, N., Beer, M., Ueffing, M. (2007) Two-dimensional electrophoresis of membrane proteins. *Analytical and bioanalytical chemistry* 389(4):1033-1045

Brookes, P. S., Pinner, A., Ramachandran, A., Coward, L., Barnes, S., Kim, H., Darley-Usmar, V. M. (2002) High throughput two-dimensional blue-native electrophoresis: a tool for functional proteomics of mitochondria and signaling complexes. *Proteomics* 2 (8):969-977

Bugger, H., Chen, D., Riehle, C., Soto, J., Theobald, H. A., Hu, X. X., Ganesan, B., Weimer, B. C., Abel, E. D. (2009) Tissue-specific remodeling of the mitochondrial proteome in type 1 diabetic akita mice. *Diabetes* 58(9):1986-1997

Bugger, H., Schwarzer, M., Chen, D., Schrepper, A., Amorim, P. A., Schoepe, M., Nguyen, T. D., Mohr, F. W., Khalimonchuk, O., Weimer, B. C., Doenst, T. (2010) Proteomic remodelling of mitochondrial oxidative pathways in pressure overload-induced heart failure. *Cardiovasc. Res*. 85(2):376-384

Cadieux, P. A., Beiko, D. T., Watterson, J. D., Burton, J. P., Howard, J. C., Knudsen, B. E., Gan, B. S., McCormick, J. K., Chambers, A. F., Denstedt, J. D., Reid, G. (2004) Surface-enhanced laser desorption/ionization-time of flight-mass spectrometry (SELDI-TOF-MS): a new proteomic urinary test for patients with urolithiasis. *Journal of clinical laboratory analysis* 18(3):170-175

Chacinska, A., Koehler, C. M., Milenkovic, D., Lithgow, T., Pfanner, N. (2009) Importing mitochondrial proteins: machineries and mechanisms. *Cell* 138(4):628-644

Chang, J., Cornell, J. E., Van Remmen, H., Hakala, K., Ward, W. F., Richardson, A. (2007) Effect of aging and caloric restriction on the mitochondrial proteome. The journals of gerontology Series A, *Biological sciences and medical sciences* 62(3):223-234

Chen, X., Li, J., Hou, J., Xie, Z., Yang, F. (2010) Mammalian mitochondrial proteomics: insights into mitochondrial functions and mitochondria-related diseases. *Expert review of proteomics* 7(3):333-345

Cotter, D., Guda, P., Fahy, E., Subramaniam, S. (2004) MitoProteome: mitochondrial protein sequence database and annotation system. *Nucleic acids research* 32(Database issue): D4 63-467

Dabkowski, E. R., Baseler, W. A., Williamson, C. L., Powell, M., Razunguzwa, T. T., Frisbee, J. C., Hollander, J. M. (2009) Mitochondrial dysfunction in the type 2 diabetic heart is associated with alterations in spatially distinct mitochondrial proteomes. *American journal of physiology Heart and circulatory physiology* 299(2):H529-540

Dabkowski, E. R., Baseler, W. A., Williamson, C. L., Powell, M., Razunguzwa, T. T., Frisbee, J. C., Hollander, J. M. (2010) Mitochondrial dysfunction in the type 2 diabetic heart is associated with alterations in spatially distinct mitochondrial proteomes. *American journal of physiology Heart and circulatory physiology* 299(2):H529-540

Dabkowski, E. R., Williamson, C. L., Bukowski, V. C., Chapman, R. S., Leonard, S. S., Peer, C. J., Callery, P. S., Hollander, J. M. (2009) Diabetic cardiomyopathy-associated dysfunction in spatially distinct mitochondrial subpopulations. *American journal of physiology Heart and circulatory physiology* 296(2):H359-369

Dani, D., Dencher, N. A. (2008) Native-DIGE: a new look at the mitochondrial membrane proteome. *Biotechnology journal* 3(6):817-822

Devreese, B., Vanrobaeys, F., Smet, J., Van Beeumen, J., Van Coster, R. (2002) Mass spectrometric identification of mitochondrial oxidative phosphorylation subunits separated by two-dimensional blue-native polyacrylamide gel electrophoresis. *Electrophoresis* 23(15):2525-2533

D'Hertog, W., Mathieu, C., Overbergh, L. (2006) Type 1 diabetes: entering the proteomic era. *Expert review of proteomics* 3(2):223-236

Dimmer, K. S., Rapaport, D. (2008) Proteomic view of mitochondrial function. *Genome biology* 9(2):209

Dorn, G. W., 2nd (2013) Mitochondrial dynamics in heart disease. *Biochimica et biophysica acta* 1833(1):233-241

Duchen, M. R. (2004) Mitochondria in health and disease: perspectives on a new mitochondrial biology. *Molecular aspects of medicine* 25(4):365-451

Duncan, J. G. (2011) Mitochondrial dysfunction in diabetic cardiomyopathy. *Biochim. Biophys. Acta* 1813(7):1351-1359

Egan, B., Dowling, P., O'Connor, P. L., Henry, M., Meleady, P., Zierath, J. R., O'Gorman, D. J. (2011) 2-D DIGE analysis of the mitochondrial proteome from human skeletal muscle reveals time course-dependent remodelling in response to 14 consecutive days of endurance exercise training. *Proteomics* 11(8):1413-1428

Elstner, M., Andreoli, C., Ahting, U., Tetko, I., Klopstock, T., Meitinger, T., Prokisch, H. (2008) MitoP2: an integrative tool for the analysis of the mitochondrial proteome. *Molecular biotechnology* 40(3):306-315

Elstner, M., Andreoli, C., Klopstock, T., Meitinger, T., Prokisch, H. (2009) The mitochondrial proteome database: MitoP2. *Methods in enzymology* 4573-20

Essop, M. F., Chan, W. A., Hattingh, S. (2011) Proteomic analysis of mitochondrial proteins in a mouse model of type 2 diabetes. *Cardiovascular journal of Africa* 22(4):175-178

Eyrich, B., Sickmann, A., Zahedi, R. P. (2011) Catch me if you can: mass spectrometry-based phosphoproteomics and quantification strategies. *Proteomics* 11(4):554-570

Feng, J., Xie, H. W., Meany, D. L., Thompson, L. V., Arriaga, E. A., Griffin, T. J. (2008) Quantitative Proteomic Profiling of Muscle Type-Dependent and Age-Dependent Protein

Carbonylation in Rat Skeletal Muscle Mitochondria. *J. Gerontol. a-Biol.* 63(11):1137-1152

Ferreira, R., Vitorino, R., Alves, R. M., Appell, H. J., Powers, S. K., Duarte, J. A., Amado, F. (2010) Subsarcolemmal and intermyofibrillar mitochondria proteome differences disclose functional specializations in skeletal muscle. *Proteomics* 10(17):3142-3154

Figueiredo, P. A., Mota, M. P., Appell, H. J., Duarte, J. A. (2008) The role of mitochondria in aging of skeletal muscle. *Biogerontology* 9(2):67-84

Flatmark, T. (1966) On the heterogeneity of beef heart cytochrome c. II. Some physico-chemical properties of the main subfractions (Cy I-Cy 3). *Acta chemica Scandinavica* 20 (6):1476-1486

Forner, F., Arriaga, E. A., Mann, M. (2006) Mild protease treatment as a small-scale biochemical method for mitochondria purification and proteomic mapping of cytoplasm-exposed mitochondrial proteins. *Journal of proteome research* 5(12):3277-3287

Fountoulakis, M., Schlaeger, E. J. (2003) The mitochondrial proteins of the neuroblastoma cell line IMR-32. *Electrophoresis* 24(1-2):260-275

Fountoulakis, M., Soumaka, E., Rapti, K., Mavroidis, M., Tsangaris, G., Maris, A., Weisleder, N., Capetanaki, Y. (2005) Alterations in the heart mitochondrial proteome in a desmin null heart failure model. *J. Mol. Cell. Cardiol.* 38(3):461-474

Fukada, K., Zhang, F., Vien, A., Cashman, N. R., Zhu, H. (2004) Mitochondrial proteomic analysis of a cell line model of familial amyotrophic lateral sclerosis. *Molecular and cellular proteomics : MCP* 3(12):1211-1223

Geiger, T., Velic, A., Macek, B., Lundberg, E., Kampf, C., Nagaraj, N., Uhlen, M., Cox, J., Mann, M. (2013) Initial quantitative proteomic map of twenty-eight mouse tissues using the SILAC mouse. *Molecular and cellular proteomics : MCP*

Gilchrist, A., Au, C. E., Hiding, J., Bell, A. W., Fernandez-Rodriguez, J., Lesimple, S., Nagaya, H., Roy, L., Gosline, S. J., Hallett, M., Paiement, J., Kearney, R. E., Nilsson, T., Bergeron, J. J. (2006) Quantitative proteomics analysis of the secretory pathway. *Cell* 127(6):1265-1281

Gilmore, J. M., Washburn, M. P. (2010) Advances in shotgun proteomics and the analysis of membrane proteomes. *Journal of proteomics* 73(11):2078-2091

Glancy, B., Balaban, R. S. (2011) Protein composition and function of red and white skeletal muscle mitochondria. *American journal of physiology Cell physiology* 300(6):C1280-1290

Graham, J. M. (1993) Isolation of mitochondria, mitochondrial membranes, lysosomes, peroxisomes, and Golgi membranes from rat liver. *Methods Mol. Biol.* 1929-40

Greenacre, S. A., Ischiropoulos, H. (2001) Tyrosine nitration: localisation, quantification, consequences for protein function and signal transduction. *Free radical research* 34(6): 541-581

Gorg, A., Obermaier, C., Boguth, G., Csordas, A., Diaz, J. J., Madjar, J. J. (1997) Very alkaline immobilized pH gradients for two-dimensional electrophoresis of ribosomal and nuclear proteins. *Electrophoresis* 18(3-4):328-337

Gygi, S. P., Corthals, G. L., Zhang, Y., Rochon, Y., Aebersold, R. (2000) Evaluation of two-dimensional gel electrophoresis-based proteome analysis technology. *Proceedings of the National Academy of Sciences of the US* 97(17):9390-9395

Gygi, S. P., Rist, B., Gerber, S. A., Turecek, F., Gelb, M. H., Aebersold, R. (1999) Quantitative analysis of complex protein mixtures using isotope-coded affinity tags. *Nature biotechnology* 17(10):994-999

Hanson, B. J., Schulenberg, B., Patton, W. F., Capaldi, R. A. (2001) A novel subfractionation approach for mitochondrial proteins: a three-dimensional mitochondrial proteome map. *Electrophoresis* 22(5):950-959

Hartwig, S., Feckler, C., Lehr, S., Wallbrecht, K., Wolgast, H., Muller-Wieland, D., Kotzka, J. (2009) A critical comparison between two classical and a kit-based method for mitochondria isolation. *Proteomics* 9(11):3209-3214

Heinemeyer, J., Scheibe, B., Schmitz, U. K., Braun, H. P. (2009) Blue native DIGE as a tool for comparative analyses of protein complexes. *Journal of proteomics* 72(3):539-544

Herrnstadt, C., Clevenger, W., Ghosh, S. S., Anderson, C., Fahy, E., Miller, S., Howell, N., Davis, R. E. (1999) A novel mitochondrial DNA-like sequence in the human nuclear genome. *Genomics* 60(1):67-77

Heussen, C., Dowdle, E. B. (1980) Electrophoretic analysis of plasminogen activators in polyacrylamide gels containing sodium dodecyl sulfate and copolymerized substrates. *Analytical biochemistry* 102(1):196-202

Hogeboom, G. H., Schneider, W. C., Pallade, G. E. (1948) Cytochemical studies of mammalian tissues; isolation of intact mitochondria from rat liver; some biochemical properties of mitochondria and submicroscopic particulate material. *The Journal of biological chemistry* 172(2):619-635

Hollander, J. M., Baseler, W. A., Dabkowski, E. R. (2011) Proteomic remodeling of mitochondria in heart failure. *Congest. Heart Fail.* 17(6):262-268

Hoppel, C. L., Tandler, B., Fujioka, H., Riva, A. (2009) Dynamic organization of mitochondria in human heart and in myocardial disease. *Int. J. Biochem. Cell. Biol.* 41 (10):1949-1956

Hoppeler, H. (1986) Exercise-induced ultrastructural changes in skeletal muscle. *International journal of sports medicine* 7(4):187-204

Hoppeler, H., Fluck, M. (2003) Plasticity of skeletal muscle mitochondria: structure and function. *Medicine and science in sports and exercise* 35(1):95-104

Huber, L. A., Pfaller, K., Vietor, I. (2003) Organelle proteomics: implications for subcellular fractionation in proteomics. *Circulation research* 92(9):962-968

Isfort, M., Stevens, S. C., Schaffer, S., Jong, C. J., Wold, L. E. (2013) Metabolic dysfunction in diabetic cardiomyopathy. *Heart failure reviews*

Jiang, X. S., Zhou, H., Zhang, L., Sheng, Q. H., Li, S. J., Li, L., Hao, P., Li, Y. X., Xia, Q. C., Wu, J. R., Zeng, R. (2004) A high-throughput approach for subcellular proteome: identification of rat liver proteins using subcellular fractionation coupled with two-dimensional liquid chromatography tandem mass spectrometry and bioinformatic analysis. *Molecular and cellular proteomics : MCP* 3(5):441-455

Jiang, Y., Wang, X. (2012) Comparative mitochondrial proteomics: perspective in human diseases. *Journal of hematology and oncology* 511

Jin, J., Davis, J., Zhu, D., Kashima, D. T., Leroueil, M., Pan, C., Montine, K. S., Zhang, J. (2007) Identification of novel proteins affected by rotenone in mitochondria of dopaminergic cells. *BMC neuroscience* 867

Julienne, C. M., Dumas, J. F., Goupille, C., Pinault, M., Berri, C., Collin, A., Tesseraud, S., Couet, C., Servais, S. (2012) Cancer cachexia is associated with a decrease in skeletal

muscle mitochondrial oxidative capacities without alteration of ATP production efficiency. *Journal of cachexia, sarcopenia and muscle*

Jüllig, M., Hickey, A. J. R., Chai, C. C., Skea, G. L., Middleditch, M. J., Costa, S., Choong, S. Y., Philips, A. R. J., Cooper, G. J. S. (2008) Is the failing heart out of fuel or a worn engine running rich? A study of mitochondria in old spontaneously hypertensive rats. *Proteomics* 8(12):2556-2572

Jullig, M., Hickey, A. J., Chai, C. C., Skea, G. L., Middleditch, M. J., Costa, S., Choong, S. Y., Philips, A. R., Cooper, G. J. (2008) Is the failing heart out of fuel or a worn engine running rich? A study of mitochondria in old spontaneously hypertensive rats. *Proteomics* 8(12):2556-2572

Jullig, M., Hickey, A. J., Middleditch, M. J., Crossman, D. J., Lee, S. C., Cooper, G. J. (2007) Characterization of proteomic changes in cardiac mitochondria in streptozotocin-diabetic rats using iTRAQ isobaric tags. *Proteomics Clinical applications* 1(6):565-576

Johnson, D. T., Harris, R. A., Blair, P. V., Balaban, R. S. (2007) Functional consequences of mitochondrial proteome heterogeneity. *American journal of physiology Cell physiology* 292 (2):C698-707

Jung, E., Heller, M., Sanchez, J. C., Hochstrasser, D. F. (2000) Proteomics meets cell biology: the establishment of subcellular proteomes. *Electrophoresis* 21(16):3369-3377

Kadkhodayan, A., Coggan, A. R., Peterson, L. R. (2012) A "PET" area of interest: myocardial metabolism in human systolic heart failure. *Heart failure reviews*

Kane, L. A., Yung, C. K., Agnetti, G., Neverova, I., Van Eyk, J. E. (2006) Optimization of paper bridge loading for 2-DE analysis in the basic pH region: application to the mitochondrial subproteome. *Proteomics* 6(21):5683-5687

Kang, D., Oh, S., Reschiglian, P., Moon, M. H. (2008) Separation of mitochondria by flow field-flow fractionation for proteomic analysis. *The Analyst* 133(4):505-515

Kavazis, A. N., Alvarez, S., Talbert, E., Lee, Y., Powers, S. K. (2009) Exercise training induces a cardioprotective phenotype and alterations in cardiac subsarcolemmal and intermyofibrillar mitochondrial proteins. *American journal of physiology Heart and circulatory physiology* 297(1):H144-152

Kerner, J., Lee, K., Hoppel, C. L. (2011) Post-translational modifications of mitochondrial outer membrane proteins. *Free radical research* 45(1):16-28

Kiehntopf, M., Siegmund, R., Deufel, T. (2007) Use of SELDI-TOF mass spectrometry for identification of new biomarkers: potential and limitations. *Clinical chemistry and laboratory medicine : CCLM / FESCC* 45(11):1435-1449

Kim, N., Lee, Y., Kim, H., Joo, H., Youm, J. B., Park, W. S., Warda, M., Cuong, D. V., Han, J. (2006) Potential biomarkers for ischemic heart damage identified in mitochondrial proteins by comparative proteomics. *Proteomics* 6(4):1237-1249

Kim, S. C., Sprung, R., Chen, Y., Xu, Y., Ball, H., Pei, J., Cheng, T., Kho, Y., Xiao, H., Xiao, L., Grishin, N. V., White, M., Yang, X. J., Zhao, Y. (2006) Substrate and functional diversity of lysine acetylation revealed by a proteomics survey. *Molecular cell* 23(4):607-618

Knecht, M., Regitz-Zagrosek, V., Pleissner, K. P., Emig, S., Jungblut, P., Hildebrandt, A., Fleck, E. (1994) Dilated cardiomyopathy: computer-assisted analysis of endomyocardial biopsy protein patterns by two-dimensional gel electrophoresis. *Eur. J. Clin. Chem. Clin. Biochem*. 32(8):615-624

Knecht, M., Regitz-Zagrosek, V., Pleissner, K. P., Jungblut, P., Steffen, C., Hildebrandt, A., Fleck, E. (1994) Characterization of myocardial protein composition in dilated cardiomyopathy by two-dimensional gel electrophoresis. *Eur. Heart J.* 15 Suppl. D37-44

Koc, E. C., Koc, H. (2012) Regulation of mammalian mitochondrial translation by post-translational modifications. *Biochim. Biophys. Acta* 1819(9-10):1055-1066

Koehler, C. M. (2000) Protein translocation pathways of the mitochondrion. *FEBS letters* 476 (1-2):27-31

Lai, X., Wang, L., Witzmann, F. A. (2013) Issues and applications in label-free quantitative mass spectrometry. *International journal of proteomics* 2013756039

Lee, Y. H., Tan, H. T., Chung, M. C. (2010) Subcellular fractionation methods and strategies for proteomics. *Proteomics* 10(22):3935-3956

Lefort, N., Yi, Z., Bowen, B., Glancy, B., De Filippis, E. A., Mapes, R., Hwang, H., Flynn, C. R., Willis, W. T., Civitarese, A., Hojlund, K., Mandarino, L. J. (2009) Proteome profile of functional mitochondria from human skeletal muscle using one-dimensional gel electrophoresis and HPLC-ESI-MS/MS. *J. Proteomics* 72(6):1046-1060

Lenaz, G., D'Aurelio, M., Merlo Pich, M., Genova, M. L., Ventura, B., Bovina, C., Formiggini, G., Parenti Castelli, G. (2000) Mitochondrial bioenergetics in aging. *Biochimica et biophysica acta* 1459(2-3):397-404

Li, J., Cai, T., Wu, P., Cui, Z., Chen, X., Hou, J., Xie, Z., Xue, P., Shi, L., Liu, P., Yates, J. R., 3rd, Yang, F. (2009) *Proteomic analysis of mitochondria from Caenorhabditis elegans*. *Proteomics* 9(19):4539-4553

Lilley, K. S., Friedman, D. B. (2004) All about DIGE: quantification technology for differential-display 2D-gel proteomics. *Expert review of proteomics* 1(4):401-409

Lilley, K. S., Razzaq, A., Dupree, P. (2002) Two-dimensional gel electrophoresis: recent advances in sample preparation, detection and quantitation. *Current opinion in chemical biology* 6(1):46-50

Link, A. J., Eng, J., Schieltz, D. M., Carmack, E., Mize, G. J., Morris, D. R., Garvik, B. M., Yates, J. R., 3rd (1999) Direct analysis of protein complexes using mass spectrometry. *Nature biotechnology* 17(7):676-682

Liu, X. H., Qian, L. J., Gong, J. B., Shen, J., Zhang, X. M., Qian, X. H. (2004) Proteomic analysis of mitochondrial proteins in cardiomyocytes from chronic stressed rat. *Proteomics* 4(10):3167-3176

Lokireddy, S., Wijesoma, I. W., Bonala, S., Wei, M., Sze, S. K., McFarlane, C., Kambadur, R., Sharma, M. (2012) Myostatin is a novel tumoral factor that induces cancer cachexia. *The Biochemical journal*

Lopez, M. F., Melov, S. (2002) Applied proteomics: mitochondrial proteins and effect on function. *Circ. Res.* 90(4):380-389

Lovell, M. A., Xiong, S., Markesbery, W. R., Lynn, B. C. (2005) Quantitative proteomic analysis of mitochondria from primary neuron cultures treated with amyloid beta peptide. *Neurochemical research* 30(1):113-122

Lowell, B. B., Shulman, G. I. (2005) Mitochondrial dysfunction and type 2 diabetes. *Science* 307 (5708):384-387

Lundgren, D. H., Hwang, S. I., Wu, L., Han, D. K. (2010) Role of spectral counting in quantitative proteomics. *Expert review of proteomics* 7(1):39-53

Marin-Corral, J., Fontes, C. C., Pascual-Guardia, S., Sanchez, F., Olivan, M., Argiles, J. M., Busquets, S., Lopez-Soriano, F. J., Barreiro, E. (2010) Redox balance and carbonylated

proteins in limb and heart muscles of cachectic rats. *Antioxid. Redox. Signal* 12(3):365-380

Marouga, R., David, S., Hawkins, E. (2005) The development of the DIGE system: 2D fluorescence difference gel analysis technology. *Analytical and bioanalytical chemistry* 382(3):669-678

Mathy, G., Sluse, F. E. (2008) Mitochondrial comparative proteomics: strengths and pitfalls. *Biochim. Biophys. Acta* 1777(7-8):1072-1077

McBride, H. M., Neuspiel, M., Wasiak, S. (2006) Mitochondria: more than just a powerhouse. *Curr. Biol.* 16(14):R551-560

McDonald, T. G., Van Eyk, J. E. (2003) Mitochondrial proteomics. Undercover in the lipid bilayer. *Basic research in cardiology* 98(4):219-227

McGregor, E., Dunn, M. J. (2003) Proteomics of heart disease. *Human Molecular Genetics* 12(suppl. 2):R135-R144

McGregor, E., Dunn, M. J. (2006) Proteomics of the Heart: Unraveling Disease. *Circulation Research* 98(3):309-321

Meany, D. L., Xie, H., Thompson, L. V., Arriaga, E. A., Griffin, T. J. (2007) Identification of carbonylated proteins from enriched rat skeletal muscle mitochondria using affinity chromatography-stable isotope labeling and tandem mass spectrometry. *Proteomics* 7 (7): 1150-1163

Meisinger, C., Sickmann, A., Pfanner, N. (2008) The mitochondrial proteome: from inventory to function. *Cell* 134(1):22-24

Meisinger, C., Sommer, T., Pfanner, N. (2000) Purification of Saccharomcyes cerevisiae mitochondria devoid of microsomal and cytosolic contaminations. *Analytical biochemistry* 287(2):339-342

Meng, C., Jin, X., Xia, L., Shen, S.-M., Wang, X.-L., Cai, J., Chen, G.-Q., Wang, L.-S., Fang, N.-Y. (2009) Alterations of Mitochondrial Enzymes Contribute to Cardiac Hypertrophy before Hypertension Development in Spontaneously Hypertensive Rats. *Journal of Proteome Research* 8(5):2463-2475

Minden, J. (2007) Comparative proteomics and difference gel electrophoresis. *BioTechniques* 43(6):739, 741, 743 passim

Millar, A. H., Sweetlove, L. J., Giege, P., Leaver, C. J. (2001) Analysis of the Arabidopsis mitochondrial proteome. *Plant physiology* 127(4):1711-1727

Mirgorodskaya, O. A., Kozmin, Y. P., Titov, M. I., Korner, R., Sonksen, C. P., Roepstorff, P. (2000) Quantitation of peptides and proteins by matrix-assisted laser desorption/ ionization mass spectrometry using (18)O-labeled internal standards. *Rapid communications in mass spectrometry : RCM* 14(14):1226-1232

Miyagi, M., Rao, K. C. (2007) Proteolytic 18O-labeling strategies for quantitative proteomics. *Mass spectrometry reviews* 26(1):121-136

Mootha, V. K., Bunkenborg, J., Olsen, J. V., Hjerrild, M., Wisniewski, J. R., Stahl, E., Bolouri, M. S., Ray, H. N., Sihag, S., Kamal, M., Patterson, N., Lander, E. S., Mann, M. (2003) Integrated analysis of protein composition, tissue diversity, and gene regulation in mouse mitochondria. *Cell* 115(5):629-640

Motoyama, A., Yates, J. R., 3rd (2008) Multidimensional LC separations in shotgun proteomics. *Analytical chemistry* 80(19):7187-7193

Nagele, E., Vollmer, M., Horth, P., Vad, C. (2004) 2D-LC/MS techniques for the identification of proteins in highly complex mixtures. *Expert Rev. Proteomics* 1(1):37-46

Neupert, W., Herrmann, J. M. (2007) Translocation of proteins into mitochondria. *Annual review of biochemistry* 76723-749

Nijtmans, L. G., Henderson, N. S., Holt, I. J. (2002) Blue Native electrophoresis to study mitochondrial and other protein complexes. *Methods* 26(4):327-334

Nyblom, H. K., Thorn, K., Ahmed, M., Bergsten, P. (2006) Mitochondrial protein patterns correlating with impaired insulin secretion from INS-1E cells exposed to elevated glucose concentrations. *Proteomics* 6(19):5193-5198

O'Connell, K., Ohlendieck, K. (2009) Proteomic DIGE analysis of the mitochondria-enriched fraction from aged rat skeletal muscle. *Proteomics* 9(24):5509-5524

O'Farrell, P. H. (1975) High resolution two-dimensional electrophoresis of proteins. *The Journal of biological chemistry* 250(10):4007-4021

Ohlendieck, K. (2011) Skeletal muscle proteomics: current approaches, technical challenges and emerging techniques. *Skeletal muscle* 1(1):6

Old, W. M., Meyer-Arendt, K., Aveline-Wolf, L., Pierce, K. G., Mendoza, A., Sevinsky, J. R., Resing, K. A., Ahn, N. G. (2005) Comparison of label-free methods for quantifying human proteins by shotgun proteomics. *Molecular and cellular proteomics : MCP* 4(10): 1487-1502

Ong, S. E., Blagoev, B., Kratchmarova, I., Kristensen, D. B., Steen, H., Pandey, A., Mann, M. (2002) Stable isotope labeling by amino acids in cell culture, SILAC, as a simple and accurate approach to expression proteomics. *Molecular and cellular proteomics: MCP* 1 (5): 376-386

Ong, S. E., Foster, L. J., Mann, M. (2003) Mass spectrometric-based approaches in quantitative proteomics. *Methods* 29(2):124-130

Ong, S. E., Pandey, A. (2001) An evaluation of the use of two-dimensional gel electrophoresis in proteomics. *Biomolecular engineering* 18(5):195-205

Ono, M., Shitashige, M., Honda, K., Isobe, T., Kuwabara, H., Matsuzuki, H., Hirohashi, S., Yamada, T. (2006) Label-free quantitative proteomics using large peptide data sets generated by nanoflow liquid chromatography and mass spectrometry. *Molecular and cellular proteomics : MCP* 5(7):1338-1347

Padrao, A. I., Carvalho, T., Vitorino, R., Alves, R. M., Caseiro, A., Duarte, J. A., Ferreira, R., Amado, F. (2012) Impaired protein quality control system underlies mitochondrial dysfunction in skeletal muscle of streptozotocin-induced diabetic rats. *Biochim. Biophys. Acta* 1822(8):1189-1197

Padrao, A. I., Ferreira, R., Vitorino, R., Alves, R. M., Figueiredo, P., Duarte, J. A., Amado, F. (2012) Effect of lifestyle on age-related mitochondrial protein oxidation in mice cardiac muscle. *Eur. J. Appl. Physiol.* 112(4):1467-1474

Padrao, A. I., Ferreira, R. M., Vitorino, R., Alves, R. M., Neuparth, M. J., Duarte, J. A., Amado, F. (2011) OXPHOS susceptibility to oxidative modifications: the role of heart mitochondrial subcellular location. *Biochimica et biophysica acta* 1807(9):1106-1113

Pagliarini, D. J., Calvo, S. E., Chang, B., Sheth, S. A., Vafai, S. B., Ong, S. E., Walford, G. A., Sugiana, C., Boneh, A., Chen, W. K., Hill, D. E., Vidal, M., Evans, J. G., Thorburn, D. R., Carr, S. A., Mootha, V. K. (2008) A mitochondrial protein compendium elucidates complex I disease biology. *Cell* 134(1):112-123

Palmer, J. W., Tandler, B., Hoppel, C. L. (1977) Biochemical properties of subsarcolemmal and interfibrillar mitochondria isolated from rat cardiac muscle. *The Journal of biological chemistry* 252(23):8731-8739

Perocchi, F., Jensen, L. J., Gagneur, J., Ahting, U., von Mering, C., Bork, P., Prokisch, H., Steinmetz, L. M. (2006) Assessing systems properties of yeast mitochondria through an interaction map of the organelle. *PLoS genetics* 2(10):e170

Pieczenik, S. R., Neustadt, J. (2007) Mitochondrial dysfunction and molecular pathways of disease. *Experimental and Molecular Pathology* 83(1):84-92

Reinders, J., Zahedi, R. P., Pfanner, N., Meisinger, C., Sickmann, A. (2006) Toward the complete yeast mitochondrial proteome: multidimensional separation techniques for mitochondrial proteomics. *J. Proteome. Res*. 5(7):1543-1554

Rezaul, K., Wu, L., Mayya, V., Hwang, S. I., Han, D. (2005) A systematic characterization of mitochondrial proteome from human T leukemia cells. *Molecular and cellular proteomics: MCP* 4(2):169-181

Romanello, V., Sandri, M. (2013) Mitochondrial biogenesis and fragmentation as regulators of protein degradation in striated muscles. *Journal of molecular and cellular cardiology* 5564-72

Riva, A., Tandler, B., Loffredo, F., Vazquez, E., Hoppel, C. (2005) Structural differences in two biochemically defined populations of cardiac mitochondria. *American journal of physiology Heart and circulatory physiology* 289(2):H868-872

Roe, M. R., Griffin, T. J. (2006) Gel-free mass spectrometry-based high throughput proteomics: tools for studying biological response of proteins and proteomes. *Proteomics* 6(17):4678-4687

Roepstorff, P. (2012) Mass spectrometry based proteomics, background, status and future needs. *Protein and cell* 3(9):641-647

Romanello, V., Sandri, M. (2010) Mitochondrial biogenesis and fragmentation as regulators of muscle protein degradation. *Curr. Hypertens. Rep*. 12(6):433-439

Ross, P. L., Huang, Y. N., Marchese, J. N., Williamson, B., Parker, K., Hattan, S., Khainovski, N., Pillai, S., Dey, S., Daniels, S., Purkayastha, S., Juhasz, P., Martin, S., Bartlet-Jones, M., He, F., Jacobson, A., Pappin, D. J. (2004) Multiplexed protein quantitation in Saccharomyces cerevisiae using amine-reactive isobaric tagging reagents. *Molecular and cellular proteomics : MCP* 3(12):1154-1169

Ryan, M. T., Hoogenraad, N. J. (2007) Mitochondrial-nuclear communications. *Annual review of biochemistry* 76701-722

Santoni, V., Molloy, M., Rabilloud, T. (2000) Membrane proteins and proteomics: un amour impossible? *Electrophoresis* 21(6):1054-1070

Schagger, H., von Jagow, G. (1991) Blue native electrophoresis for isolation of membrane protein complexes in enzymatically active form. *Anal. Biochem*. 199(2):223-231

Schoneich, C. (2006) Protein modification in aging: An update. *Exp. Gerontol*. 41(9):807-812

Schulze, W. X., Usadel, B. (2010) Quantitation in mass-spectrometry-based proteomics. *Annual review of plant biology* 61491-516

Schwerzmann, K., Cruz-Orive, L. M., Eggman, R., Sanger, A., Weibel, E. R. (1986) Molecular architecture of the inner membrane of mitochondria from rat liver: a combined biochemical and stereological study. *The Journal of cell biology* 102(1):97-103

Seibert, V., Wiesner, A., Buschmann, T., Meuer, J. (2004) Surface-enhanced laser desorption ionization time-of-flight mass spectrometry (SELDI TOF-MS) and ProteinChip technology in proteomics research. *Pathology, research and practice* 200(2):83-94

Unlu, M., Morgan, M. E., Minden, J. S. (1997) Difference gel electrophoresis: a single gel method for detecting changes in protein extracts. *Electrophoresis* 18(11):2071-2077

Urbonavicius, S., Wiggers, H., Botker, H. E., Nielsen, T. T., Kimose, H. H., Ostergaard, M., Lindholt, J. S., Vorum, H., Honore, B. (2009) Proteomic analysis identifies mitochondrial metabolic enzymes as major discriminators between different stages of the failing human myocardium. *Acta Cardiol*. 64(4):511-522

Van den Bergh, G., Arckens, L. (2004) Fluorescent two-dimensional difference gel electrophoresis unveils the potential of gel-based proteomics. *Current opinion in biotechnology* 15(1):38-43

Ventura, B., Genova, M. L., Bovina, C., Formiggini, G., Lenaz, G. (2002) Control of oxidative phosphorylation by Complex I in rat liver mitochondria: implications for aging. *Biochimica et biophysica acta* 1553(3):249-260

Wallace, D. C. (1999) Mitochondrial diseases in man and mouse. *Science* 283(5407):1482-1488

Wang, X., Pickrell, A. M., Zimmers, T. A., Moraes, C. T. (2012) Increase in muscle mitochondrial biogenesis does not prevent muscle loss but increased tumor size in a mouse model of acute cancer-induced cachexia. *PloS one* 7(3):e33426

Wang, Y., Peng, F., Tong, W., Sun, H., Xu, N., Liu, S. (2010) The nitrated proteome in heart mitochondria of the db/db mouse model: characterization of nitrated tyrosine residues in SCOT. *Journal of proteome research* 9(8):4254-4263

Warda, M., Kim, H. K., Kim, N., Ko, K. S., Rhee, B. D., Han, J. (2013) A matter of life, death and diseases: mitochondria from a proteomic perspective. *Expert Rev. Proteomics* 10(1):97-111

Washburn, M. P., Wolters, D., Yates, J. R., 3rd (2001) Large-scale analysis of the yeast proteome by multidimensional protein identification technology. *Nature biotechnology* 19(3):242-247

Werhahn, W., Niemeyer, A., Jansch, L., Kruft, V., Schmitz, U. K., Braun, H. (2001) Purification and characterization of the preprotein translocase of the outer mitochondrial membrane from Arabidopsis. Identification of multiple forms of TOM20. *Plant physiology* 125(2):943-954

White, J. P., Puppa, M. J., Sato, S., Gao, S., Price, R. L., Baynes, J. W., Kostek, M. C., Matesic, L. E., Carson, J. A. (2012) IL-6 regulation on skeletal muscle mitochondrial remodeling during cancer cachexia in the ApcMin/+ mouse. *Skeletal muscle* 2(1):14

Wilkesman, J., Kurz, L. (2009) Protease analysis by zymography: a review on techniques and patents. *Recent patents on biotechnology* 3(3):175-184

Wilkins, M. (2009) Proteomics data mining. *Expert review of proteomics* 6(6):599-603

Wilkins, M. R., Gasteiger, E., Sanchez, J. C., Bairoch, A., Hochstrasser, D. F. (1998) Two-dimensional gel electrophoresis for proteome projects: the effects of protein hydrophobicity and copy number. *Electrophoresis* 19(8-9):1501-1505

Wittig, I., Carrozzo, R., Santorelli, F. M., Schagger, H. (2007) Functional assays in high-resolution clear native gels to quantify mitochondrial complexes in human biopsies and cell lines. *Electrophoresis* 28(21):3811-3820

Wittig, I., Karas, M., Schagger, H. (2007) High resolution clear native electrophoresis for in-gel functional assays and fluorescence studies of membrane protein complexes. *Molecular and cellular proteomics: MCP* 6(7):1215-1225

Wittig, I., Schagger, H. (2008) Features and applications of blue-native and clear-native electrophoresis. *Proteomics* 8(19):3974-3990

Wittig, I., Schagger, H. (2009) Native electrophoretic techniques to identify protein-protein interactions. *Proteomics* 9(23):5214-5223

Witze, E. S., Old, W. M., Resing, K. A., Ahn, N. G. (2007) Mapping protein post-translational modifications with mass spectrometry. *Nature methods* 4(10):798-806

Wolters, D. A., Washburn, M. P., Yates, J. R., 3rd (2001) An automated multidimensional protein identification technology for shotgun proteomics. *Analytical chemistry* 73(23): 5683-5690

Yao, X., Freas, A., Ramirez, J., Demirev, P. A., Fenselau, C. (2001) Proteolytic 18O labeling for comparative proteomics: model studies with two serotypes of adenovirus. *Analytical chemistry* 73(13):2836-2842

Yates, J. R., 3rd, Carmack, E., Hays, L., Link, A. J., Eng, J. K. (1999) Automated protein identification using microcolumn liquid chromatography-tandem mass spectrometry. *Methods Mol. Biol.* 112553-569

Yates, J. R., 3rd, Link, A. J., Schieltz, D. (2000) Direct analysis of proteins in mixtures. Application to protein complexes. *Methods Mol. Biol.* 14617-26

Zhang, A., Williamson, C. D., Wong, D. S., Bullough, M. D., Brown, K. J., Hathout, Y., Colberg-Poley, A. M. (2011) Quantitative proteomic analyses of human cytomegalovirus-induced restructuring of endoplasmic reticulum-mitochondrial contacts at late times of infection. *Molecular and cellular proteomics : MCP* 10(10):M111 009936

Zhang, J., Lin, A., Powers, J., Lam, M. P., Lotz, C., Liem, D., Lau, E., Wang, D., Deng, N., Korge, P., Zong, N. C., Cai, H., Weiss, J., Ping, P. (2012) Perspectives on: SGP symposium on mitochondrial physiology and medicine: mitochondrial proteome design: from molecular identity to pathophysiological regulation. *The Journal of general physiology* 139(6):395-406

Zhang, J., Li, X., Mueller, M., Wang, Y., Zong, C., Deng, N., Vondriska, T. M., Liem, D. A., Yang, J. I., Korge, P., Honda, H., Weiss, J. N., Apweiler, R., Ping, P. (2008) Systematic characterization of the murine mitochondrial proteome using functionally validated cardiac mitochondria. *Proteomics* 8(8):1564-1575

Zhao, X., Leon, I. R., Bak, S., Mogensen, M., Wrzesinski, K., Hojlund, K., Jensen, O. N. (2011) Phosphoproteome analysis of functional mitochondria isolated from resting human muscle reveals extensive phosphorylation of inner membrane protein complexes and enzymes. *Molecular and cellular proteomics : MCP* 10(1):M110 000299

Zhu, W., Smith, J. W., Huang, C. M. (2010) Mass spectrometry-based label-free quantitative proteomics. *Journal of biomedicine and biotechnology* 2010840518

Zischka, H., Weber, G., Weber, P. J., Posch, A., Braun, R. J., Buhringer, D., Schneider, U., Nissum, M., Meitinger, T., Ueffing, M., Eckerskorn, C. (2003) Improved proteome analysis of Saccharomyces cerevisiae mitochondria by free-flow electrophoresis. *Proteomics* 3(6):906-916

N.G.

CHAPTER III

REVIEW

UNRAVELING THE PHOSPHOPROTEOME DYNAMICS IN MAMMAL MITOCHONDRIAL FROM A NETWORK PERSPECTIVE

Journal of proteome research

Reviews

pubs.acs.org/jpr

Unraveling the Phosphoproteome Dynamics in Mammal Mitochondria from a Network Perspective

Ana Isabel Padrão,[†] Rui Vitorino,[*,†] José Alberto Duarte,[‡] Rita Ferreira,[†] and Francisco Amado[§]

[†]QOPNA, Department of Chemistry, University of Aveiro, 3810-193 Aveiro, Portugal

[‡]CIAFEL, Faculty of Sports, University of Porto, 4200-450 Porto, Portugal

[§]QOPNA, Health School of Sciences, University of Aveiro, 3810-193 Aveiro, Portugal

Supporting Information

ABSTRACT: With mitochondrion garnering more attention for its inextricable involvement in pathophysiological conditions, it seems imperative to understand the means by which the molecular pathways harbored in this organelle are regulated. Protein phosphorylation has been considered a central event in cellular signaling and, more recently, in the modulation of mitochondrial activity. Efforts have been made to understand the molecular mechanisms by which protein phosphorylation regulates mitochondrial signaling. With the advances in mass-spectrometry-based proteomics, there is a substantial hope and expectation in the increased knowledge of protein phosphorylation profile and its mode of regulation. On the basis of phosphorylation profiles, attempts have been made to disclose the kinases involved and how they control the molecular processes in mitochondria and, consequently, the cellular outcomes. Still, few studies have focused on mitochondrial phosphoproteome profiling, particularly in diseases. The present study reviews current data on protein phosphorylation profiling in mitochondria, the potential kinases involved and how pathophysiological conditions modulate the mitochondrial phosphoproteome. To integrate data from distinct research papers, we performed network analysis, with bioinformatic tools like Cytoscape, String, and PANTHER taking into consideration variables such as tissue specificity, biological processes, molecular functions, and pathophysiological conditions. For instance, data retrieved from these analyses evidence some homology in the mitochondrial phosphoproteome among liver and heart, with proteins from transport and oxidative phosphorylation clusters particularly susceptible to phosphorylation. A distinct profile was noticed for adipocytes, with proteins form metabolic processes, namely, triglycerides metabolism, as the main targets of phosphorylation. Regarding disease conditions, more phosphorylated proteins were observed in diabetics with some distinct phosphoproteins identified in type 2 prediabetic states and early type 2 diabetes mellitus. Heart-failure-related phosphorylated proteins are in much lower amount and are mainly involved in transport and metabolism. Nevertheless, technical considerations related to mitochondria isolation and protein separation should be considered in data comparison among different proteomic studies. Data from the present review will certainly open new perspectives of protein phosphorylation in mitochondria and will help to envisage future studies targeting the underlying regulatory mechanisms.

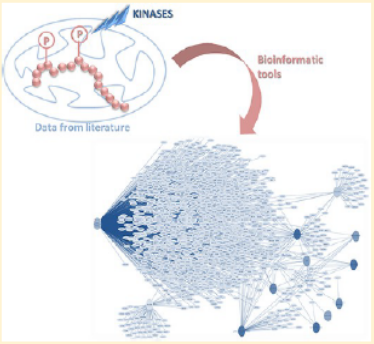

1. INTRODUCTION

Cell survival critically depends on the integrity and functionality of mitochondria, which house biosynthetic pathways and oxidative phosphorylation machinery for ATP production. Besides providing cellular energy, mitochondria are involved in multiple cell-signaling cascades and in the regulation of cellular metabolism, calcium homeostasis and apoptosis.[1,2] In agreement with this multitude of cellular functions, mitochondrial dysfunction is thought to contribute to cellular aging and to a series of diseases, such as diabetes mellitus, cancer, and neurodegenerative disorders.[3−7] The involvement of mitochondria in such a wide range of cellular processes requires an integrated system of signaling to coordinate the various molecular messages that enter or exit the mitochondrion according to the diverse needs of the cells.[8] Growing evidence suggests that mitochondrial plasticity relies on a range of reversible protein post-translational modifications (PTMs),[9] such as phosphorylation, acetylation, or ubiquitination.[10] Protein phosphorylation is the most widespread type of PTM in signal transduction and at present is the most studied PTM.[11−15] The role of mitochondrial phosphorylated proteins in the regulation of cellular and physiological events has been known for decades; however, the extent of this mode of regulation is just beginning to be disclosed. Moreover, abnormal protein phosphorylation is known to cause or be the consequence of many pathophysiological conditions, such as cancer, diabetes mellitus, and neurodegenerative diseases.[16−18]

Proteins of eukaryotic cells are mainly phosphorylated on serine (Ser), threonine (Thr), or tyrosine (Tyr) amino acid residues by the enzymatic activities of protein kinases that

Received: April 26, 2013
Published: August 22, 2013

catalyze the transfer of γ-phosphate group from adenosine 5′-triphosphate (ATP) to side chains of these specific amino acids in proteins.[15] Indeed, the dynamic protein phosphorylation is tightly regulated by kinases and phosphatases systems.[16,19] There are more than 500 kinases encoded from the human genome,[20] and around 700 000 phosphorylated sites are predicted for any given kinase.[15] Phosphorylation also occurs on histidine residues; however, phosphohistidine is highly labile and therefore hardly identified.[21] Protein phosphorylation has the potential to induce functional changes in a protein,[22] through modification of protein's activity, location, or interaction with other cellular components.[23] These functional changes typically occur as a consequence of conformational changes to protein tertiary or quaternary structures.[10] The extent and complex nature of phosphorylation events arise from the possibility of multiple amino acid residues being phosphorylated on a single protein.[24,25] Moreover, it is predicted that more than 30% of cellular proteins are phosphorylated at any given time.[26] While some amino acid residues are always quantitatively phosphorylated, others may only be transiently phosphorylated up to 0.5%. Especially regarding signaling pathways, phosphorylation rates and thereby phosphoprotein abundance are very low (with only 1 to 2% of a given protein present in a phosphorylated form). The analysis of phosphoproteins is also complicated by the complexity of phosphorylation patterns and the sheer number of phosphorylation sites.[11] Nevertheless, one decade after the introduction of proteomics and following the advances in mass spectrometry (MS), there is a substantial hope and expectation in the increasing knowledge of protein profile analysis and in the understanding of the molecular mechanisms by which protein phosphorylation modulates diverse mitochondrial functions.[10,27] Some authors argue that the analysis of mitochondrial phosphoproteome may lead to the identification of novel therapeutic targets and biomarkers.[18,26] Considering the central regulatory role of mitochondrial phosphorylation in the maintenance of living cells' dynamics, here we review the main findings in the characterization of mitochondrial phosphoproteome using mass-spectrometry-based proteomics, the potential kinases involved in its regulation, and the alterations in the phosphorylation pattern related to pathophysiological conditions. To integrate data from distinct studies focused on mitochondrial phosphoproteome profiling, we used the bioinformatic tools Cytoskape (Bingo[28] and ClueGo[29] plugins), PANTHER,[30] and STRING.[31]

2. MITOCHONDRIAL PHOSPHOPROTEOME SURVEY

The importance of phosphorylation/dephosphorylation in the regulation of mitochondrial protein activities is supported by the findings that mitochondria contain protein kinases, phosphatases, and phosphorylated proteins.[32] In mitochondria, more than 50 kinases were already identified[33] within the expected organellar proteome of a few thousand, and the number of identified mitochondrial phosphoproteins is far below the one-third of proteome size.[34] With the development of mass-spectrometry-based approaches, a growing number of studies have provided evidence that phosphorylation of mitochondrial proteins is much more frequent than expected.[9,35,36] Studies focused on mitochondrial protein phosphorylation profiling retrieved more than 3817 distinct phosphoproteins identified in mitochondria (although 72 proteins have no known annotation at Uniprot), considering all tissues/cells from all specie (rat, mouse, cow, bovine, rabbit, and human) and pathophysiological conditions studied. Eighty eight percent of these phosphoproteins were identified in liver mitochondria, but no known study was performed with human liver samples, unlike that observed for skeletal muscle. In heart, 184 distinct phosphoproteins were identified in isolated mitochondria from rodents, and only 8 were reported in human tissue (Table S1 in the Supporting Information). Regarding animal species, most of the phosphorylated proteins identified in mitochondria correspond to mouse (57%) and rat (45%) proteins (Table S2 in the Supporting Information). The orthology prediction analysis of the 3817 proteins reported to be phosphorylated in isolated mitochondria retrieved 3465 ortholog groups (Table S3 in the Supporting Information). This high number suggests that few protein sequences are shared by two or more species/genomes. We evaluated the distribution of phosphoproteins per tissue by performing an integrated analysis of the unique proteins in each tissue with Cytoscape v2.8.3, an open-source software platform for visualizing complex networks. The protein−protein interaction network presented in Figure S1 in the Supporting Information was imported from the databases Intact (http://www.ebi.ac.uk/intact/) and STRING 9.1 (http://string-db.org) and contains 3284 proteins and 3693 protein−protein interactions. These proteins are distributed in nine clusters centered in distinct organs/cells. The highest number of phosphopeptides, phosphorylation sites, and phosphoproteins was observed in liver, followed by heart, without any direct relation to the methodology used (with and without phosphopeptide enrichment). Most of the studies on mitochondrial phosphoproteome profiling were performed with phospho-enriched and non-enriched samples obtained from different species. In brain, only two studies targeting mitochondrial phosphoproteome are known, and both used gel-free approaches without using phosphoenrichment procedures (Table S1 in the Supporting Information), which might justify the considerable lower number of phosphoproteins reported in this tissue in comparison with heart and liver. To the best of our knowledge, only one study performed mitochondrial phosphoprotein profiling in skeletal muscle. The comparison of the mitochondrial phosphoproteome among tissues (Figure 1) revealed only two common phosphoproteins, specifically aconitase and ADP/ATP translocase 1 (ANT1), with no evident tissue-specific phosphosites. Hexokinase protein 2 was

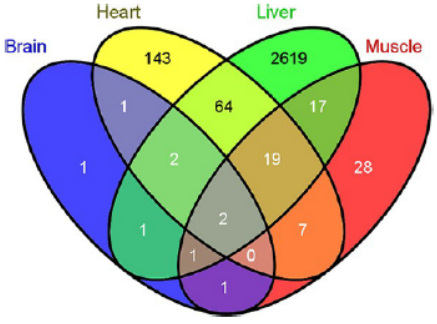

Figure 1. Venn diagram of phosphorylated mitochondrial proteins identified in different tissues (brain, liver, heart, and skeletal muscle) (http://bioinfogp.cnb.csic.es/tools/venny/index.html). Data here analyzed were retrieved from several studies: 2 for brain, 17 for heart, 11 for liver, and 1 for skeletal muscle, independently of the pathophysiological condition and methodology strategy used.

dx.doi.org/10.1021/pr4003917 | J. Proteome Res. 2013, 12, 4257−4267

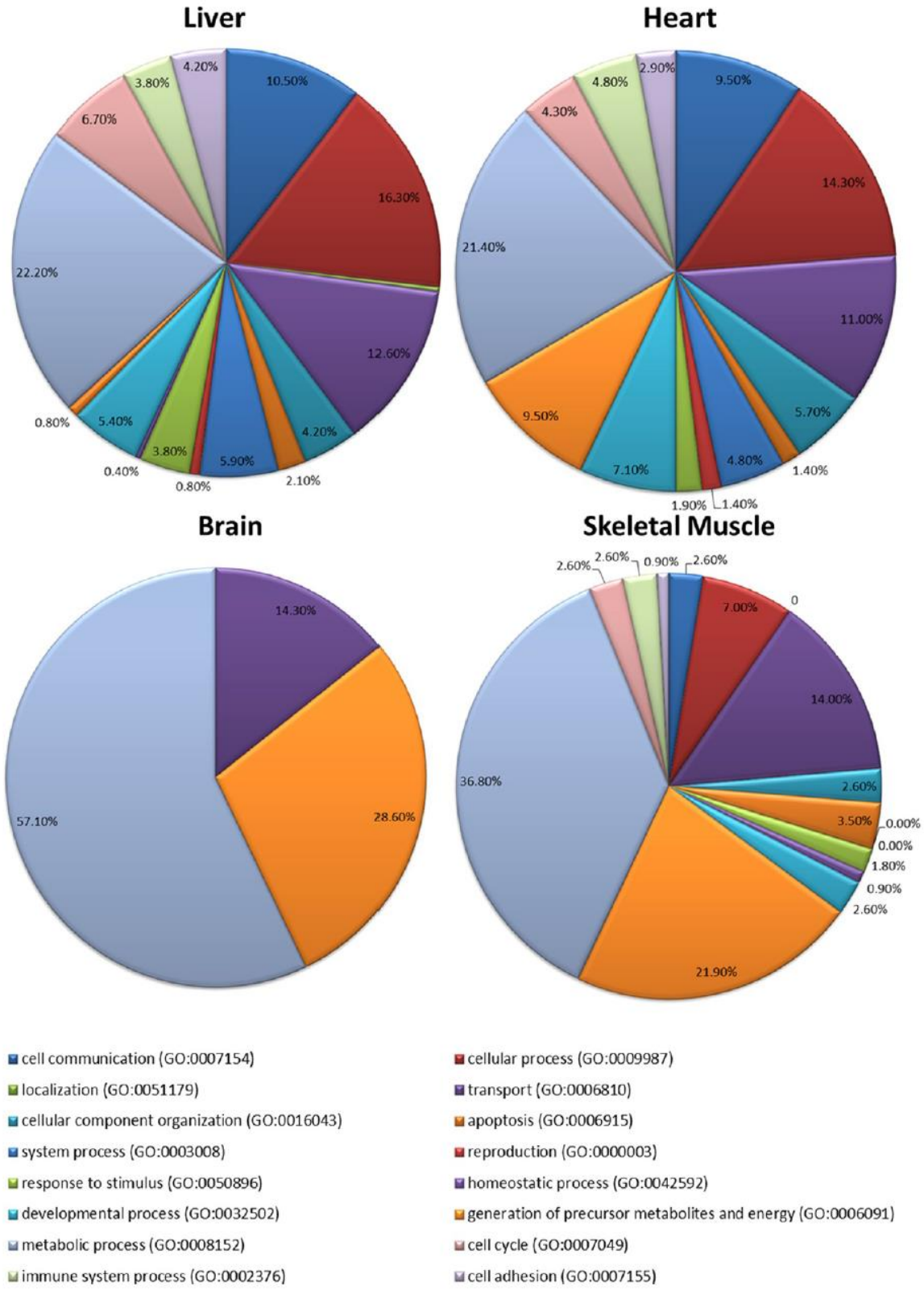

Figure 2. Categorical analysis based on molecular function of phosphorylated proteins in several tissues/organs performed with the Gene Ontology Annotation after Bonferroni correlation.

only found phosphorylated in mitochondria isolated from brain. Sixty-four common phosphorylated mitochondrial proteins were observed when comparing heart with liver, most of which belong to metabolic processes (28%), generation of

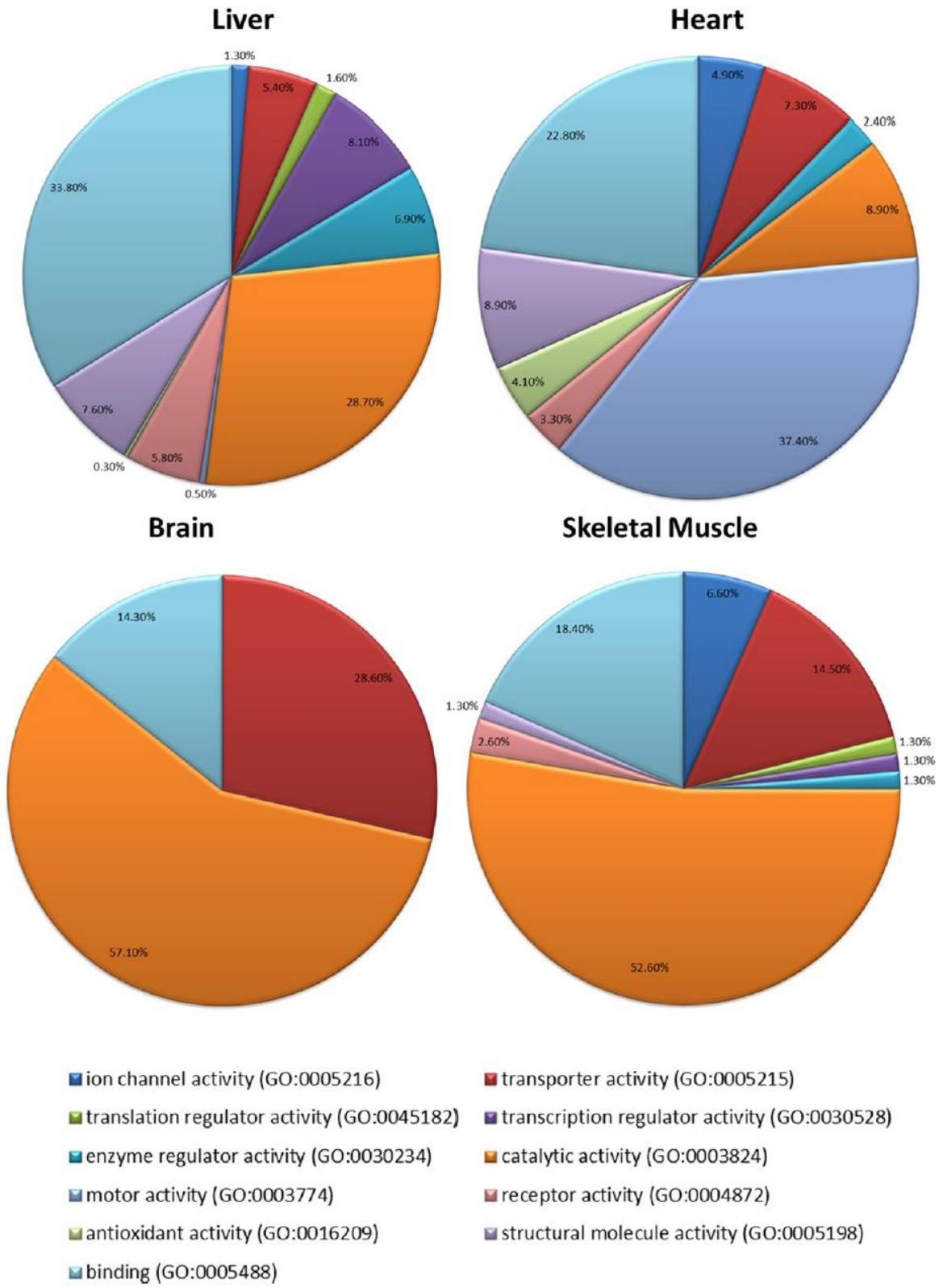

Figure 3. Categorical analysis based on biological process of phosphorylated proteins in different tissues/cells performed with the Gene Ontology Annotation after Bonferroni correlation.

precursor metabolites and energy (14%), and cellular processes (11%) according to PANTHER. Only seven phosphoproteins were identified when comparing skeletal muscle with heart, the majority of which are involved in metabolic processes. Despite

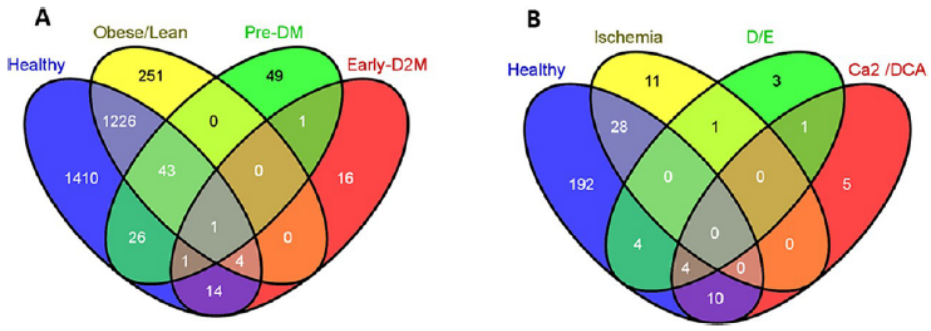

Figure 4. Venn diagram of phosphorylated mitochondrial proteins identified in liver (A) and heart (B) under distinct pathophysiological conditions (http://bioinfogp.cnb.csic.es/tools/venny/index.html). Data related to pathophysiological conditions were retrieved from two studies performed with liver and three with heart mitochondria. Regarding heart mitochondria, one of the studies targeted the inhibition of PDH phosphorylation under energized and de-energized conditions (with DCA), other characterized εPKC targets in ischemia, and the third used tissue from heart failure patients (Obese/lean, obese/lean type 2 diabetes mellitus; DCA, dichloroacetate; D, de-energization; E, energization; Pre-DM, prediabetes mellitus type 2; Early-D2M, early diabetes mellitus type 2).

technical issues underlying tissue-specific proteomic data, this variety seems to reflect differences in complexity and in intracellular signaling within each tissue, possibly involving distinct kinases, to make these biological processes more organ-efficient.[35,37,38]

2.1. Mitochondrial Phosphoproteins Identified by MS-Based Approaches

The analysis of phosphoproteins and phosphopeptides is still one of the most challenging tasks in contemporary proteome research.[39] Phosphoproteomic analyses are more difficult than protein identification for several reasons. First, highly sensitive methods are required for detection due to a low stoichiometry. Because only 5−10% of a protein kinase substrate is phosphorylated, methods that detect the modified protein at very low levels (<5−10 fmol) are needed. Second, because the covalent bond between the PTM and amino acid side chain is typically labile, it is often difficult to maintain the peptide in its modified state during sample preparation and subsequent ionization in the mass spectrometer. Third, phosphoproteins are frequently transient in dynamic homeostasis of nature.[40,41] Therefore, information on the identification and quantification of a given phosphorylated protein is necessary to identify new phosphorylated amino acid residues and their position in the protein.[39] Because not every phosphoprotein is accessible by a certain method and identification of the phosphorylated amino acid residue is required in the majority of cases, various strategies for the detection and localization of the phosphorylation have been developed.[11] Currently, MS-based strategies are the methods of choice for either characterizing single phosphorylated proteins or in performing global phosphoproteome analysis of mitochondrial extracts obtained from cells or tissues, for their speedy and highly sensitive analytical operations, with the ability to analyze thousands of phosphopeptides in a single experiment.[41−46] Protein phosphorylation events are detected by increases of +80 Da in amino acid residue mass, which report the addition of HPO_3.[12,47]

To achieve reliable and reproducible proteomic outputs, the preparation of pure and functionally viable mitochondria is crucial.[48] Most of the proteomic studies here analyzed prepare mitochondrial fractions by the disruption of the cellular organization (tissue homogenization) and differential centrifugation of the homogenate, followed by purification using density gradients (e.g., Percoll, Ficoll, or Nycodenz). Despite yielding highly purified preparations, this approach is expensive and demands a large amount of sample.[49] To overcome this limitation, some authors use pools of tissue from different animals.[34]

Using MS-based approaches, many researchers have studied the mitochondrial phophoproteome profile in heart,[34,38,50−65] liver,[9,36,50,58,65−72] skeletal muscle,[27] adipocytes,[73,74] brain,[75,76] INS-1 β cells,[33] and T98G gliobastoma cells,[77] aiming to understand the molecular and physiological role of phosphorylation in mitochondria biology. Putative mitochondrial phosphoproteins identified by MS are summarized in Table S1 in the Supporting Information.

On the basis of the published studies focused on protein phosphorylation in mitochondria isolated from different organs (specifically liver, heart, brain, and skeletal muscle), we performed categorical analysis based on molecular function and biological processes with the Gene Ontology Annotation after Bonferroni correlation. Regarding molecular function (Figure 2), most of the phosphorylated mitochondrial proteins in liver present binding, catalytic, and transcription activity, whereas in heart the prevalent cluster is motor activity. In skeletal muscle mitochondria, most of the phosphorylated proteins have catalytic, binding, and transport activity, and in the brain all of the identified phosphorylated proteins belong to these three clusters. Considering biological processes (Figure 3), the majority of phosphoproteins are involved in metabolism, cellular processes, and transport, with similar distribution profiles observed for heart, liver, and skeletal muscle mitochondria. In brain, mitochondrial phosphorylated proteins are distributed per three clusters: metabolism, generation of precursor metabolites and energy, and transport. Independently of the tissue/cell used for mitochondria isolation, the most prevalent phosphorylated amino acid residue is serine, with 9416 phosphoserines identified (82%), followed by phosphothreonine (15%) and phosphotyrosine (3%) (Table S1 in the Supporting Information).

2.2. Disease-Related Distribution of Mitochondrial Protein Phosphorylation

The understanding of protein phosphorylation on a molecular level has been of great interest toward the understanding of disease-related cellular states, which eventually may open new avenues for target therapies. Despite its importance, there are

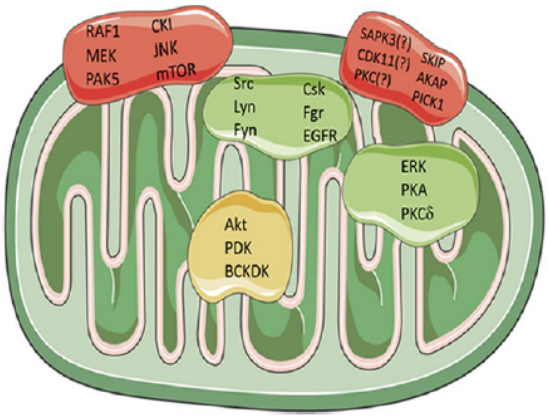

Group or family	Kinases
TK	Src, Lyn, Fyn, Csk, Fgr, Abl, EGRF
TKL	RAF1, RIP3
STE	MEK, PAK5
CKI	CK1
CMGC	GSK3, ERK, CKII, JNK, p38, SAPK3, CDK11
AGC	PKA, PKB/Akt, PKC, DMPK
CAMK	PIMK1
Atypical	mTOR, PDK, BCKDK

Figure 5. Mitochondrial kinases of each principal group or family that have been reported to have mitochondrial localization. Kinases expected to be located at the outer membrane (red boxes), at the intermembrane space/inner membrane (green boxes), or at the matrix (yellow box). Kinases with no known mitochondrial location are signaled with (?). Figure was made based on Servier Medical Art.

few studies that characterized the mitochondrial phosphoproteome profile in pathophysiological conditions, and the existing ones are mainly focused on diabetes mellitus[9,36] and heart failure.[54,55] To disclose the mitochondrial phosphoproteome alterations related to pathophysiological conditions, an integrated perspective was pursued using bioinformatic tools for the analysis of data already published in studies that: (i) analyzed mitochondria isolated from tissues or cells and (ii) used MS-based approaches for proteome profiling. Studies that retrieved mitochondrial phosphoproteome alterations in whole tissue or cell samples were not considered. According to Grimsrud et al.,[9] phosphorylation is a key mechanism involved in the regulation of ketogenesis during the onset of obesity and type 2 diabetes mellitus. Combining BN-PAGE electrophoresis with nanoLC–MS/MS, Fang et al.[54] mapped the possible ischemia-induced phosphorylation sites on particular subunits of cytochrome *c* oxidase from rabbit hearts subjected to ischemia/reperfusion and reported specific phosphosites suggestive of PKA activation. According to O'Rourke et al.,[78] defective mitochondrial function contributes to cardiac decompensation in heart failure, which is underlined by alterations in the phosphorylation of mitochondrial signaling proteins involved in transport, cell death, mitochondrial fission/fusion, free radical balance, respiratory chain activity, and TCA metabolism.

To integrate data from different studies, we performed protein–protein interaction analysis with STRING/Intact databases to create an interaction map of mitochondrial protein phosphorylation under pathophysiological conditions (Figure S2 in the Supporting Information). The higher number of phosphorylated proteins was reported in mitochondria isolated from liver of diabetic rodents with some distinct phosphoproteins identified in type 2 prediabetic states and early type 2 diabetes mellitus. Indeed, from the 1525 proteins identified in liver mitochondria from lean/obese type 2 diabetic mice, 251 were unique to this pathophysiological condition (Figure 4A) and participate in metabolic processes (24%), cellular processes (15%), and transport (11%). Pre-diabetic-related unique proteins are mainly involved in metabolism (26%), transport (12%), and cellular (10%) and developmental (10%) processes. A greater amount of unique metabolic proteins (31%) was observed in mitochondria from early type 2 diabetic rats. In mitochondria of ischemic heart, 30 phosphoproteins were identified, 11 of which were unique to this pathological conditions (Figure 4B), where the majority were involved in metabolism (38%). The reported heart-failure-related 11 phosphorylated proteins are mainly implicated in transport (e.g., tubulin and desmin) and metabolism (e.g., glyceraldehyde-3-phosphate dehydrogenase, electron-transfer flavoprotein-ubiquinone oxidoreductase).

Independently of the tissue/cell, animal species and condition studied, the proteins more susceptible to phosphorylation are the transport proteins voltage-dependent anion channels (VDACs) 1–3, ANT1–2, and metabolic proteins like aconitase, carnitine palmitoyl transferase 1 (CPT1), ATP synthase subunits d, e, alpha, and beta, glutamate dehydrogenase, and pyruvate dehydrogenase (PDH) E1 alpha (Table S1 in the Supporting Information). No association between phosphosites and a given pathophysiological condition was apparent for these proteins, with the exception of PDH E1 alpha. Whereas phosphorylated Ser-293 and Ser-300 were common to PDH E1 alpha of mitochondria isolated from all tissues and conditions studied, phosphorylated Tyr-70, Tyr-139, and Tyr-266 were reported only in ischemic heart (Table S1 in the Supporting Information), suggesting the activation of distinct kinases.

3. PHOSPHOPROTEOME MODULATION: PREDICTED KINASES ACTING IN MITOCHONDRIA

The observation that dynamic phosphorylation is widespread among mitochondrial proteins has motivated the investigation of the kinases responsible for such modifications. More than 52 kinases were suggested to be responsible for the phosphorylation of mitochondrial proteins.[33] These kinases represent nearly every known mammalian kinase subgroups (e.g., TK (tyrosine kinases), STE (homologues of the yeast STE7, STE11, and STE20 genes, which form the MAPK cascade), CKI (casein kinase 1), AGC (named after the protein kinase A, G, and C families), CAMK (calmodulin/calcium regulated kinases), CMGC (named after a set of families, CDK, MAPK, GSK3, and CLK), and atypical (includes the kinases and candidate kinases with no structural similarity to eukaryotic protein kinases (ePKs))) (Figure 5).[35] Curiously, from the 282 kinases reported to be phosphorylated in mitochondria (Table S1 in the Supporting Information), the ones known to be involved in the phosphorylation of mitochondrial proteins (e.g.,

dx.doi.org/10.1021/pr4003917 | J. Proteome Res. 2013, 12, 4257–4267

RAF, Fyn, GRK5, GSK3, PKCbeta, Lyn, Src, STK, Yes) were identified only in liver, from either healthy or diabetic subjects.

There are close links between mitochondrial and cytosol kinases, thus integrating signals from both cell locations.[33] Indeed, numerous kinases that become target to mitochondrion, such as Abl, PKB/Akt, glycogen synthase kinase (GSK) 3β, extracellular-regulated kinases (ERK), and protein kinase C (PKC) δ, seem to do so only in their active state[2] after the activation of different receptors.[79] However, the mechanism involved in this process is poorly understood, but the kinases are present in all compartments of mitochondrion[35,78] (Figure 5). The vast majority of these kinases lack MTS, implying that they are not located in the matrix. So, many of the phosphorylation reactions involving mitochondrial proteins might occur in cytosol before their import.[80] However, the extent of proteins that are transported in a phosphorylated state into the matrix from the cytosol is not comprehended.

According to Zhao et al.[27] around 78% of phosphorylation sites in proteins from skeletal muscle mitochondria are potential substrates of CKII, PKA, PKC, or DNA-dependent protein kinase (DNAPK). These authors used NetworkKIN database, which integrates consensus substrate motifs with context modeling for improved prediction of cellular kinase–substrate relation.[81] Deng et al.[34] obtained for 29 phosphopeptides of murine cardiac mitochondrial proteins a match with the consensus substrate motifs of eight kinases with known mitochondrion residence, according to NetPhosK database.[82] Among these kinases were pyruvate dehydrogenase kinase (PDHK), Src kinase, branched-chain α-ketoacid dehydrogenase (BCKDH), GSK3, epidermal growth factor receptor (EGFR), and PKCε kinases. Grimsrud et al.,[9] performed a quantitative analysis of liver mitochondrial phosphoproteome and searched their data within kinase motifs as defined in the PHOSIDA database,[83] further supported by data analysis with Motif-X algorithm.[84] Among the active kinases in mitochondria they reported PKA and CK2.[9] Cui et al.[33] integrated with Cytoscape the kinase-substrate network of phosphoproteins with the functional interaction proteins of the mitochondrial phosphoproteins from INS-1 β cells and verified numerous associations. For instance, several kinase subgroups, such as CK2 and PKC, seem to regulate the OXPHOS system. Nevertheless, the functional impact of mitochondrial protein phosphorylation is poorly comprehended with few exceptions. Mitochondrial proteins with identified phosphosites related to alterations in protein function are listed in Table 1. All of the proteins listed in this Table are mainly metabolic ones, for example, PDH, cytochrome *c* oxidase, and CPT1. Phosphorylation of PDH at several phosphosites is clearly associated with decreased activity. The same effect was reported for several phosphosites in cytochrome *c* oxidase and for phosphorylation of complex V β subunit at Ser-529 (Table 1).

The regulation of PDH phosphorylation by PDHK and PDHP (pyruvate dehydrogenase phosphatase) system was the first example of metabolic control to be reported.[85] PDH constitutes the major entry point of reducing equivalents from glycolysis to OXPHOS, and its dephosphorylation plays a role in the adaptation of metabolic conversion rates to cardiac workload.[35,80] BCKDH participates in the metabolism of the essential amino acids valine, isoleucine, and leucine in heart and other tissues, where the phosphorylation of E1B$_\alpha$ subunit is related to activity inhibition.[80] Both of these kinases are in the matrix of mitochondrion and present sequence similarities with histidine protein kinases found in prokaryotes, most likely

Table 1. Mitochondrial Proteins with Specific Phosphosites Highlighted and the Associated Repercussions for Protein Function

protein	species	tissue	pathophysiological situation	modified amino acid residue	effect of modification	refs
glycerol-3-phosphate acyltransferase (GPAT1)	rat	adipocytes	healthy	Ser-632, Ser-695	↑ V_{max} and K_M for the substrates glycerol-3-phosphate and palmitoyl-CoA (treatment with insulin)	93
carnitine palmitoyltransferase-Ia	rat	liver	healthy	Ser-741, Ser-749	↑ activity and altered malonyl-CoA inhibition	94
cytochrome *c* oxidase subunit I	rabbit	heart	ischemia/reperfusion	Ser-115, Ser-116	↓ activity	54
cytochrome *c* oxidase subunit IVi1	rabbit	heart	ischemia/reperfusion	Thr-52	↓ activity	54
complex V F1γ subunit	human	heart	healthy	Tyr-52	↓ activity	95
cytochrome *c* oxidase subunit Vb	rabbit	heart	ischemia/reperfusion	Ser-40	↓ activity	54
cytochrome *c* oxidase subunit 1	cow	liver	healthy	Tyr-304	↓ activity	67
pyruvate dehydrogenase E1 alpha 1	rat	liver	pre-D2M/early-D2M	Ser-233, Ser-294, Ser-296, Ser-301, Tyr-290, Tyr-302	↓ activity	36
pyruvate dehydrogenase E1 alpha 1	mouse	liver	healthy	Ser-232, Ser-293, Ser-300	↓ activity potentially reduces ROS production and promotes glycolysis when cellular conditions do not favor glucose oxidation.	68
pyruvate dehydrogenase E1 alpha 1	pig	heart	healthy (CTL/DCA; D/E)	Ser-231, Ser-292, Ser-299	↓ activity	51
UCP 1	rat	adipocytes	healthy (cold-acclimated/room temperature)	Ser-3, Ser-4, Ser-51	↑ activity	74
Hmgcs2 (hydroxymethylglutaryl-CoA synthase)	mouse	liver	healthy obese diabetic/lean diabetic	Ser-456	↑ activity	9
complex V β subunit	mouse	liver	healthy	Ser-529	↓ activity	68

dx.doi.org/10.1021/pr4003917 | J. Proteome Res. 2013, 12, 4257–4267

evolved from genes originally present in respiration-dependent bacteria endocytosed by primitive eukaryotic cells.[86] The mitochondrial location of PKA is not clear, but once it is anchored to an A-kinase anchoring protein (AKAP) on the outer membrane it phosphorylates BAD, a proapoptotic member of the Bcl-2 family, it inactivates it and promotes its dissociation from mitochondria.[35,78] Other mitochondrial targets consistently found to be phosphorylated by PKA are VDAC, mitochondrial import receptor subunit TOM70, and several enzymes involved in fatty acid metabolism as CPT1 and oxidative phosphorylation complexes.[78] Matrix localization of PKA was also reported and implied by cAMP-dependent changes in the phosphorylation status of inner membrane proteins, among which there are subunits of complex I of the respiratory chain.[87] VDAC, a pivotal protein in the regulation of energy (ADP/ATP) exchange, utilization of ATP by hexokinase (HK) and apoptosis,[88] is a target of different kinases in addition to PKA, such as GSK3β, Nek1, PKCε, and p38 MAP kinase.[89,90] VDAC forms a complex with ANT, and the ADP produced as a result of glucose phosphorylation by HK is transported via ANT to the mitochondrial matrix and used for ATP production by ATP synthase.[79] The phosphorylation of VDAC by GSK3 in hepatocytes inhibits the influx of water and calcium into mitochondria, depolarization, and cytochrome *c* release.[91] Sheldon et al.[89] suggested that alterations in VDAC phosphorylation lead to different strength of interaction with cytoskeleton and trigger the consequent modification of mitochondrial potential and respiration. In myocardium, mitochondrial Akt seems to play a protective role through the induction of mitochondrial translocation of HK, a substrate of Akt, and inhibition of mPTP opening after reperfusion.[79] The prevention of tyrosine phosphorylation by the inhibition of p38 MAP kinase was also reported to have a cardioprotection role.[88]

Regarding TKs, the receptor-type EGFR has been reported to translocate to the inner membrane of mitochondria in response to EGF treatment, where it interacts with cytochrome *c* oxidase (COX) subunit II.[78] The non-receptor-type c-Src also phosphorylates this COX subunit, which is required for the activity of the mitochondrial electron transport chain. The phosphorylation of Tyr-304 in COX catalytic subunit I together with the activation of the cAMP-dependent pathway leads to the suppression of enzyme activity (Table 1). In addition, the phosphorylation of NADH dehydrogenase [ubiquinone] flavoprotein 2 (NDUFV2) at Tyr-193 and of succinate dehydrogenase A (SDHA) at Tyr-215 follow-on c-Src activity seems to be essential for mitochondrial functions and cell viability.[77] The role of mitochondria-localized TK-like RAF kinases is not fully understood, although they were suggested to be involved in the regulation of apoptosis. RAF1 might phosphorylate BAD and form a complex with Bcl-2, preventing apoptosis.[92]

4. CONCLUSIONS

Here we have overviewed the mitochondrial phosphoproteins and the kinases involved in their phosphorylation. The number of identified PTMs on mitochondrial proteins has dramatically increased due to novel MS-based approaches, and it is becoming increasingly evident that, as in other cellular compartments, phosphorylation is likely to play a regulatory role. On the basis of phosphorylation profiles, attempts have been made to disclose the kinases involved in mitochondria signaling pathways and how mitochondrial and cytosolic kinases interact in the regulation of metabolic processes and cell fate. Further studies integrating mitochondrial protein phosphorylation profiles with the kinases acting on a given condition will lead to a better understanding of the mitochondrial response pathophysiological phenomena.

■ ASSOCIATED CONTENT

Supporting Information

Distribution of mitochondrial phosphoproteins per tissues/cells and pathophysiological conditions based on Intact and visualized with Cytoscape (v2.8.3), list of all mitochondrial proteins identified in a phosphorylated state by MS approaches, relative contribution of phosphorylated proteins (reported in different studies) to whole mitochondrial proteome according to animal species, and list of ortholog groups related to mitochondrial proteins from Table S1. This material is available free of charge via the Internet at http://pubs.acs.org.

■ AUTHOR INFORMATION

Corresponding Author

*Phone: +351 234370700. Fax: +351 234370084. E-mail: rvitorino@ua.pt.

Notes

The authors declare no competing financial interest.

■ ACKNOWLEDGMENTS

This work was supported by Fundação para a Ciência e a Tecnologia (FCT, Portugal;), European Union, QREN, FEDER and COMPETE for funding the QOPNA research unit (project PEst-C/QUI/UI0062/2011), research projects (PTDC/DES/114122/2009, PTDC/DES/104567/2008 and COMPETE, FCOMP-01-0124-FEDER-014707), postgraduation student (grant number SFRH/BD/66642/2009 to A.I.P) and to CENTRO-07-ST24-FEDER-002034 (cofinanciated by QREN, Mais Centro- Programa Operacional Regional do Centro e União Europeia/Fundo Europeu de Desenvolvimento Regional).

■ ABBREVIATIONS:

AKAP, A-kinase anchoring protein; BCKDH, branched-chain α ketoacid dehydrogenase; CAMK, calmodulin/calcium-regulated kinases; CKI, casein kinase 1; COX, cytochrome *c* oxidase; CPT1, carnitine palmitoyl transferase 1; DNAPK, DNA-dependent protein kinase; EGFR, epidermal growth factor receptor; ePKs, eukaryotic protein kinases; ERK, extracellular-regulated kinases; GSK, glycogen synthase kinase; HK, hexokinase; Hmgcs2, hydroxymethylglutaryl-CoA synthase; mitochondrial; IMAC, immobilized metal affinity chromatography; PDHK, pyruvate dehydrogenase kinase; PDHP, pyruvate dehydrogenase phosphatase; PDH, pyruvate dehydrogenase; PKC, protein kinase C; PTM, post-translational modification; SDHA, succinate dehydrogenase A; TiO_2, titanium dioxide; TK, tyrosine kinases; TOM, translocase of the outer membrane; VDAC, voltage-dependent anion channel

■ REFERENCES

(1) McBride, H. M.; Neuspiel, M.; Wasiak, S. Mitochondria: more than just a powerhouse. *Curr. Biol.* **2006**, *16* (14), R551−60.

(2) Benard, G.; Rossignol, R. Ultrastructure of the mitochondrion and its bearing on function and bioenergetics. *Antioxid. Redox Signaling* **2008**, *10* (8), 1313−42.

(3) Green, D. R.; Kroemer, G. The pathophysiology of mitochondrial cell death. *Science* **2004**, *305* (5684), 626−9.
(4) Duchen, M. R. Mitochondria in health and disease: perspectives on a new mitochondrial biology. *Mol Aspects Med* **2004**, *25* (4), 365−451.
(5) Van Remmen, H.; Richardson, A. Oxidative damage to mitochondria and aging. *Exp Gerontol* **2001**, *36* (7), 957−68.
(6) Kwong, J. Q.; Beal, M. F.; Manfredi, G. The role of mitochondria in inherited neurodegenerative diseases. *J Neurochem* **2006**, *97* (6), 1659−75.
(7) Nunnari, J.; Suomalainen, A. Mitochondria: in sickness and in health. *Cell* **2012**, *148* (6), 1145−59.
(8) Goldenthal, M. J.; Marin-Garcia, J. Mitochondrial signaling pathways: a receiver/integrator organelle. *Mol. Cell. Biochem.* **2004**, *262* (1−2), 1−16.
(9) Grimsrud, P. A.; Carson, J. J.; Hebert, A. S.; Hubler, S. L.; Niemi, N. M.; Bailey, D. J.; Jochem, A.; Stapleton, D. S.; Keller, M. P.; Westphall, M. S.; Yandell, B. S.; Attie, A. D.; Coon, J. J.; Pagliarini, D. J. A quantitative map of the liver mitochondrial phosphoproteome reveals posttranslational control of ketogenesis. *Cell Metab* **2012**, *16* (5), 672−83.
(10) Koc, E. C.; Koc, H. Regulation of mammalian mitochondrial translation by post-translational modifications. *Biochim. Biophys. Acta* **2012**, *1819* (9−10), 1055−66.
(11) Reinders, J.; Sickmann, A. State-of-the-art in phosphoproteomics. *Proteomics* **2005**, *5* (16), 4052−61.
(12) Rogers, L. D.; Foster, L. J. Phosphoproteomics−finally fulfilling the promise? *Mol Biosyst* **2009**, *5* (10), 1122−9.
(13) Kane, L. A.; Van Eyk, J. E. Post-translational modifications of ATP synthase in the heart: biology and function. *J Bioenerg Biomembr* **2009**, *41* (2), 145−50.
(14) Distler, A. M.; Kerner, J.; Hoppel, C. L. Proteomics of mitochondrial inner and outer membranes. *Proteomics* **2008**, *8* (19), 4066−82.
(15) Ubersax, J. A.; Ferrell, J. E., Jr. Mechanisms of specificity in protein phosphorylation. *Nat. Rev. Mol. Cell Biol.* **2007**, *8* (7), 530−41.
(16) Cohen, P. The role of protein phosphorylation in human health and disease. The Sir Hans Krebs Medal Lecture. *Eur. J. Biochem.* **2001**, *268* (19), 5001−10.
(17) Cohen, P. The origins of protein phosphorylation. *Nat. Cell Biol.* **2002**, *4* (5), E127−30.
(18) Johnson, L. N. Protein kinase inhibitors: contributions from structure to clinical compounds. *Q. Rev. Biophys.* **2009**, *42* (1), 1−40.
(19) Sacco, F.; Perfetto, L.; Castagnoli, L.; Cesareni, G. The human phosphatase interactome: An intricate family portrait. *FEBS Lett.* **2012**, *586* (17), 2732−9.
(20) Manning, G.; Whyte, D. B.; Martinez, R.; Hunter, T.; Sudarsanam, S. The protein kinase complement of the human genome. *Science* **2002**, *298* (5600), 1912−34.
(21) Puttick, J.; Baker, E. N.; Delbaere, L. T. Histidine phosphorylation in biological systems. *Biochim. Biophys. Acta* **2008**, *1784* (1), 100−5.
(22) Olsen, J. V.; Blagoev, B.; Gnad, F.; Macek, B.; Kumar, C.; Mortensen, P.; Mann, M. Global, in vivo, and site-specific phosphorylation dynamics in signaling networks. *Cell* **2006**, *127* (3), 635−48.
(23) Greengard, P. Phosphorylated proteins as physiological effectors. *Science* **1978**, *199* (4325), 146−52.
(24) Cohen, P. The regulation of protein function by multisite phosphorylation−a 25 year update. *Trends Biochem. Sci.* **2000**, *25* (12), 596−601.
(25) Gunawardena, J. Multisite protein phosphorylation makes a good threshold but can be a poor switch. *Proc. Natl. Acad. Sci. U. S. A.* **2005**, *102* (41), 14617−22.
(26) Cutillas, P. R.; Jorgensen, C. Biological signalling activity measurements using mass spectrometry. *Biochem. J.* **2011**, *434* (2), 189−99.
(27) Zhao, X.; Leon, I. R.; Bak, S.; Mogensen, M.; Wrzesinski, K.; Hojlund, K.; Jensen, O. N. Phosphoproteome analysis of functional mitochondria isolated from resting human muscle reveals extensive phosphorylation of inner membrane protein complexes and enzymes. *Mol. Cell. Proteomics* **2011**, *10* (1), M110 000299.
(28) Maere, S.; Heymans, K.; Kuiper, M. BiNGO: a Cytoscape plugin to assess overrepresentation of gene ontology categories in biological networks. *Bioinformatics* **2005**, *21* (16), 3448−9.
(29) Bindea, G.; Mlecnik, B.; Hackl, H.; Charoentong, P.; Tosolini, M.; Kirilovsky, A.; Fridman, W. H.; Pages, F.; Trajanoski, Z.; Galon, J. ClueGO: a Cytoscape plug-in to decipher functionally grouped gene ontology and pathway annotation networks. *Bioinformatics* **2009**, *25* (8), 1091−3.
(30) Mi, H.; Guo, N.; Kejariwal, A.; Thomas, P. D. PANTHER version 6: protein sequence and function evolution data with expanded representation of biological pathways. *Nucleic Acids Res.* **2007**, *35* (Database issue), D247−52.
(31) Franceschini, A.; Szklarczyk, D.; Frankild, S.; Kuhn, M.; Simonovic, M.; Roth, A.; Lin, J.; Minguez, P.; Bork, P.; von Mering, C.; Jensen, L. J. STRING v9.1: protein-protein interaction networks, with increased coverage and integration. *Nucleic Acids Res.* **2013**, *41* (Database issue), D808−15.
(32) Salvi, M.; Brunati, A. M.; Toninello, A. Tyrosine phosphorylation in mitochondria: a new frontier in mitochondrial signaling. *Free Radical Biol. Med.* **2005**, *38* (10), 1267−77.
(33) Cui, Z.; Hou, J.; Chen, X.; Li, J.; Xie, Z.; Xue, P.; Cai, T.; Wu, P.; Xu, T.; Yang, F. The profile of mitochondrial proteins and their phosphorylation signaling network in INS-1 beta cells. *J. Proteome Res.* **2010**, *9* (6), 2898−908.
(34) Deng, N.; Zhang, J.; Zong, C.; Wang, Y.; Lu, H.; Yang, P.; Wang, W.; Young, G. W.; Korge, P.; Lotz, C.; Doran, P.; Liem, D. A.; Apweiler, R.; Weiss, J. N.; Duan, H.; Ping, P. Phosphoproteome analysis reveals regulatory sites in major pathways of cardiac mitochondria. *Mol. Cell. Proteomics* **2011**, *10* (2), M110 000117.
(35) Pagliarini, D. J.; Dixon, J. E. Mitochondrial modulation: reversible phosphorylation takes center stage? *Trends Biochem. Sci.* **2006**, *31* (1), 26−34.
(36) Deng, W. J.; Nie, S.; Dai, J.; Wu, J. R.; Zeng, R. Proteome, phosphoproteome, and hydroxyproteome of liver mitochondria in diabetic rats at early pathogenic stages. *Mol. Cell. Proteomics* **2010**, *9* (1), 100−16.
(37) Horbinski, C.; Chu, C. T. Kinase signaling cascades in the mitochondrion: a matter of life or death. *Free Radical Biol. Med.* **2005**, *38* (1), 2−11.
(38) Hopper, R. K.; Carroll, S.; Aponte, A. M.; Johnson, D. T.; French, S.; Shen, R. F.; Witzmann, F. A.; Harris, R. A.; Balaban, R. S. Mitochondrial matrix phosphoproteome: effect of extra mitochondrial calcium. *Biochemistry* **2006**, *45* (8), 2524−36.
(39) Delom, F.; Chevet, E. Phosphoprotein analysis: from proteins to proteomes. *Proteome Sci.* **2006**, *4*, 15.
(40) Seo, J.; Lee, K. J. Post-translational modifications and their biological functions: proteomic analysis and systematic approaches. *J. Biochem. Mol. Biol.* **2004**, *37* (1), 35−44.
(41) Thingholm, T. E.; Jensen, O. N.; Larsen, M. R. Analytical strategies for phosphoproteomics. *Proteomics* **2009**, *9* (6), 1451−68.
(42) Beltran, L.; Cutillas, P. R. Advances in phosphopeptide enrichment techniques for phosphoproteomics. *Amino Acids* **2012**, *43* (3), 1009−24.
(43) Jensen, O. N. Interpreting the protein language using proteomics. *Nat. Rev. Mol. Cell Biol.* **2006**, *7* (6), 391−403.
(44) Grimsrud, P. A.; Swaney, D. L.; Wenger, C. D.; Beauchene, N. A.; Coon, J. J. Phosphoproteomics for the masses. *ACS Chem. Biol.* **2010**, *5* (1), 105−19.
(45) Witze, E. S.; Old, W. M.; Resing, K. A.; Ahn, N. G. Mapping protein post-translational modifications with mass spectrometry. *Nat. Methods* **2007**, *4* (10), 798−806.
(46) Pocsfalvi, G. Selective enrichment in phosphopeptides for the identification of phosphorylated mitochondrial proteins. *Methods Enzymol.* **2009**, *457*, 81−96.
(47) Paradela, A.; Albar, J. P. Advances in the analysis of protein phosphorylation. *J. Proteome Res.* **2008**, *7* (5), 1809−18.

(48) Zhang, J.; Lin, A.; Powers, J.; Lam, M. P.; Lotz, C.; Liem, D.; Lau, E.; Wang, D.; Deng, N.; Korge, P.; Zong, N. C.; Cai, H.; Weiss, J.; Ping, P. Perspectives on: SGP symposium on mitochondrial physiology and medicine: mitochondrial proteome design: from molecular identity to pathophysiological regulation. *J. Gen. Physiol.* **2012**, *139* (6), 395−406.
(49) Hermstadt, C.; Clevenger, W.; Ghosh, S. S.; Anderson, C.; Fahy, E.; Miller, S.; Howell, N.; Davis, R. E. A novel mitochondrial DNA-like sequence in the human nuclear genome. *Genomics* **1999**, *60* (1), 67−77.
(50) Aponte, A. M.; Phillips, D.; Hopper, R. K.; Johnson, D. T.; Harris, R. A.; Blinova, K.; Boja, E. S.; French, S.; Balaban, R. S. Use of (32)P to study dynamics of the mitochondrial phosphoproteome. *J. Proteome Res.* **2009**, *8* (6), 2679−95.
(51) Boja, E. S.; Phillips, D.; French, S. A.; Harris, R. A.; Balaban, R. S. Quantitative mitochondrial phosphoproteomics using iTRAQ on an LTQ-Orbitrap with high energy collision dissociation. *J. Proteome Res.* **2009**, *8* (10), 4665−75.
(52) Budas, G.; Costa, H. M., Jr.; Ferreira, J. C.; Teixeira da Silva Ferreira, A.; Perales, J.; Krieger, J. E.; Mochly-Rosen, D.; Schechtman, D. Identification of epsilonPKC targets during cardiac ischemic injury. *Circ. J.* **2012**, *76* (6), 1476−85.
(53) Distler, A. M.; Kerner, J.; Hoppel, C. L. Mass spectrometric demonstration of the presence of liver carnitine palmitoyltransferase-I (CPT-I) in heart mitochondria of adult rats. *Biochim. Biophys. Acta* **2009**, *1794* (3), 431−7.
(54) Fang, J. K.; Prabu, S. K.; Sepuri, N. B.; Raza, H.; Anandatheerthavarada, H. K.; Galati, D.; Spear, J.; Avadhani, N. G. Site specific phosphorylation of cytochrome *c* oxidase subunits I, IVi1 and Vb in rabbit hearts subjected to ischemia/reperfusion. *FEBS Lett.* **2007**, *581* (7), 1302−10.
(55) Feng, J.; Zhu, M.; Schaub, M. C.; Gehrig, P.; Roschitzki, B.; Lucchinetti, E.; Zaugg, M. Phosphoproteome analysis of isoflurane-protected heart mitochondria: phosphorylation of adenine nucleotide translocator-1 on Tyr194 regulates mitochondrial function. *Cardiovasc. Res.* **2008**, *80* (1), 20−9.
(56) Helling, S.; Huttemann, M.; Ramzan, R.; Kim, S. H.; Lee, I.; Muller, T.; Langenfeld, E.; Meyer, H. E.; Kadenbach, B.; Vogt, S.; Marcus, K. Multiple phosphorylations of cytochrome *c* oxidase and their functions. *Proteomics* **2012**, *12* (7), 950−9.
(57) Helling, S.; Vogt, S.; Rhiel, A.; Ramzan, R.; Wen, L.; Marcus, K.; Kadenbach, B. Phosphorylation and kinetics of mammalian cytochrome *c* oxidase. *Mol. Cell. Proteomics* **2008**, *7* (9), 1714−24.
(58) Lam, M. P.; Lau, E.; Scruggs, S. B.; Wang, D.; Kim, T. Y.; Liem, D. A.; Zhang, J.; Ryan, C. M.; Faull, K. F.; Ping, P. Site-specific quantitative analysis of cardiac mitochondrial protein phosphorylation. *J Proteomics* **2013**, *81*, 15−23.
(59) Lee, I.; Salomon, A. R.; Yu, K.; Doan, J. W.; Grossman, L. I.; Huttemann, M. New prospects for an old enzyme: mammalian cytochrome *c* is tyrosine-phosphorylated in vivo. *Biochemistry* **2006**, *45* (30), 9121−8.
(60) Palmisano, G.; Sardanelli, A. M.; Signorile, A.; Papa, S.; Larsen, M. R. The phosphorylation pattern of bovine heart complex I subunits. *Proteomics* **2007**, *7* (10), 1575−83.
(61) Papa, S.; Sardanelli, A. M.; Cocco, T.; Speranza, F.; Scacco, S. C.; Technikova-Dobrova, Z. The nuclear-encoded 18 kDa (IP) AQDQ subunit of bovine heart complex I is phosphorylated by the mitochondrial cAMP-dependent protein kinase. *FEBS Lett.* **1996**, *379* (3), 299−301.
(62) Pocsfalvi, G.; Cuccurullo, M.; Schlosser, G.; Scacco, S.; Papa, S.; Malorni, A. Phosphorylation of B14.5a subunit from bovine heart complex I identified by titanium dioxide selective enrichment and shotgun proteomics. *Mol. Cell. Proteomics* **2007**, *6* (2), 231−7.
(63) Schilling, B.; Aggeler, R.; Schulenberg, B.; Murray, J.; Row, R. H.; Capaldi, R. A.; Gibson, B. W. Mass spectrometric identification of a novel phosphorylation site in subunit NDUFA10 of bovine mitochondrial complex I. *FEBS Lett.* **2005**, *579* (11), 2485−90.
(64) Chen, R.; Fearnley, I. M.; Peak-Chew, S. Y.; Walker, J. E. The phosphorylation of subunits of complex I from bovine heart mitochondria. *J. Biol. Chem.* **2004**, *279* (25), 26036−45.
(65) Schulenberg, B.; Aggeler, R.; Beechem, J. M.; Capaldi, R. A.; Patton, W. F. Analysis of steady-state protein phosphorylation in mitochondria using a novel fluorescent phosphosensor dye. *J. Biol. Chem.* **2003**, *278* (29), 27251−5.
(66) Distler, A. M.; Kerner, J.; Hoppel, C. L. Post-translational modifications of rat liver mitochondrial outer membrane proteins identified by mass spectrometry. *Biochim. Biophys. Acta* **2007**, *1774* (5), 628−36.
(67) Lee, I.; Salomon, A. R.; Ficarro, S.; Mathes, I.; Lottspeich, F.; Grossman, L. I.; Huttemann, M. cAMP-dependent tyrosine phosphorylation of subunit I inhibits cytochrome *c* oxidase activity. *J. Biol. Chem.* **2005**, *280* (7), 6094−100.
(68) Lee, J.; Xu, Y.; Chen, Y.; Sprung, R.; Kim, S. C.; Xie, S.; Zhao, Y. Mitochondrial phosphoproteome revealed by an improved IMAC method and MS/MS/MS. *Mol. Cell. Proteomics* **2007**, *6* (4), 669−76.
(69) Miller, J. L.; Cimen, H.; Koc, H.; Koc, E. C. Phosphorylated proteins of the mammalian mitochondrial ribosome: implications in protein synthesis. *J. Proteome Res.* **2009**, *8* (10), 4789−98.
(70) Miller, J. L.; Koc, H.; Koc, E. C. Identification of phosphorylation sites in mammalian mitochondrial ribosomal protein DAP3. *Protein Sci.* **2008**, *17* (2), 251−60.
(71) Yu, H.; Lee, I.; Salomon, A. R.; Yu, K.; Huttemann, M. Mammalian liver cytochrome *c* is tyrosine-48 phosphorylated in vivo, inhibiting mitochondrial respiration. *Biochim. Biophys. Acta* **2008**, *1777* (7−8), 1066−71.
(72) Zhang, L.; Liang, Z.; Yang, K.; Xia, S.; Wu, Q.; Zhang, Y. Mesoporous TiO2 aerogel for selective enrichment of phosphopeptides in rat liver mitochondria. *Anal. Chim. Acta* **2012**, *729*, 26−35.
(73) Gnad, F.; Forner, F.; Zielinska, D. F.; Birney, E.; Gunawardena, J.; Mann, M. Evolutionary constraints of phosphorylation in eukaryotes, prokaryotes, and mitochondria. *Mol. Cell. Proteomics* **2010**, *9* (12), 2642−53.
(74) Carroll, A. M.; Porter, R. K.; Morrice, N. A. Identification of serine phosphorylation in mitochondrial uncoupling protein 1. *Biochim. Biophys. Acta* **2008**, *1777* (7−8), 1060−5.
(75) Lewandrowski, U.; Sickmann, A.; Cesaro, L.; Brunati, A. M.; Toninello, A.; Salvi, M. Identification of new tyrosine phosphorylated proteins in rat brain mitochondria. *FEBS Lett.* **2008**, *582* (7), 1104−10.
(76) Salvi, M.; Morrice, N. A.; Brunati, A. M.; Toninello, A. Identification of the flavoprotein of succinate dehydrogenase and aconitase as in vitro mitochondrial substrates of Fgr tyrosine kinase. *FEBS Lett.* **2007**, *581* (29), 5579−85.
(77) Ogura, M.; Yamaki, J.; Homma, M. K.; Homma, Y. Mitochondrial c-Src regulates cell survival through phosphorylation of respiratory chain components. *Biochem. J.* **2012**, *447* (2), 281−9.
(78) O'Rourke, B.; Van Eyk, J. E.; Foster, D. B. Mitochondrial protein phosphorylation as a regulatory modality: implications for mitochondrial dysfunction in heart failure. *Congestive Heart Failure* **2011**, *17* (6), 269−82.
(79) Miura, T.; Tanno, M.; Sato, T. Mitochondrial kinase signalling pathways in myocardial protection from ischaemia/reperfusion-induced necrosis. *Cardiovasc. Res.* **2010**, *88* (1), 7−15.
(80) Covian, R.; Balaban, R. S. Cardiac mitochondrial matrix and respiratory complex protein phosphorylation. *Am. J. Physiol.: Heart Circ. Physiol.* **2012**, *303* (8), H940−66.
(81) Linding, R.; Jensen, L. J.; Pasculescu, A.; Olhovsky, M.; Colwill, K.; Bork, P.; Yaffe, M. B.; Pawson, T. NetworKIN: a resource for exploring cellular phosphorylation networks. *Nucleic Acids Res.* **2008**, *36* (Database issue), D695−9.
(82) Blom, N.; Sicheritz-Ponten, T.; Gupta, R.; Gammeltoft, S.; Brunak, S. Prediction of post-translational glycosylation and phosphorylation of proteins from the amino acid sequence. *Proteomics* **2004**, *4* (6), 1633−49.

(83) Gnad, F.; Gunawardena, J.; Mann, M. PHOSIDA 2011: the posttranslational modification database. *Nucleic Acids Res.* **2011**, *39* (Database issue), D253−60.
(84) Schwartz, D.; Gygi, S. P. An iterative statistical approach to the identification of protein phosphorylation motifs from large-scale data sets. *Nat. Biotechnol.* **2005**, *23* (11), 1391−8.
(85) Linn, T. C.; Pettit, F. H.; Reed, L. J. Alpha-keto acid dehydrogenase complexes. X. Regulation of the activity of the pyruvate dehydrogenase complex from beef kidney mitochondria by phosphorylation and dephosphorylation. *Proc. Natl. Acad. Sci. U. S. A.* **1969**, *62* (1), 234−41.
(86) Harris, R. A.; Popov, K. M.; Zhao, Y.; Kedishvili, N. Y.; Shimomura, Y.; Crabb, D. W. A new family of protein kinases–the mitochondrial protein kinases. *Adv. Enzyme Regul.* **1995**, *35*, 147−62.
(87) Sardanelli, A. M.; Signorile, A.; Nuzzi, R.; Rasmo, D. D.; Technikova-Dobrova, Z.; Drahota, Z.; Occhiello, A.; Pica, A.; Papa, S. Occurrence of A-kinase anchor protein and associated cAMP-dependent protein kinase in the inner compartment of mammalian mitochondria. *FEBS Lett.* **2006**, *580* (24), 5690−6.
(88) Kerner, J.; Lee, K.; Tandler, B.; Hoppel, C. L. VDAC proteomics: Post-translation modifications. *Biochim. Biophys. Acta* **2012**, *1818* (6), 1520−5.
(89) Sheldon, K. L.; Maldonado, E. N.; Lemasters, J. J.; Rostovtseva, T. K.; Bezrukov, S. M. Phosphorylation of voltage-dependent anion channel by serine/threonine kinases governs its interaction with tubulin. *PLoS One* **2011**, *6* (10), e25539.
(90) Schwertz, H.; Carter, J. M.; Abdudureheman, M.; Russ, M.; Buerke, U.; Schlitt, A.; Muller-Werdan, U.; Prondzinsky, R.; Werdan, K.; Buerke, M. Myocardial ischemia/reperfusion causes VDAC phosphorylation which is reduced by cardioprotection with a p38 MAP kinase inhibitor. *Proteomics* **2007**, *7* (24), 4579−88.
(91) Martel, C.; Allouche, M.; Esposti, D. D.; Fanelli, E.; Boursier, C.; Henry, C.; Chopineau, J.; Calamita, G.; Kroemer, G.; Lemoine, A.; Brenner, C. Glycogen synthase kinase 3-mediated voltage-dependent anion channel phosphorylation controls outer mitochondrial membrane permeability during lipid accumulation. *Hepatology* **2013**, *57* (1), 93−102.
(92) Yao, Z.; Seger, R. The ERK signaling cascade–views from different subcellular compartments. *Biofactors* **2009**, *35* (5), 407−16.
(93) Bronnikov, G. E.; Aboulaich, N.; Vener, A. V.; Stralfors, P. Acute effects of insulin on the activity of mitochondrial GPAT1 in primary adipocytes. *Biochem. Biophys. Res. Commun.* **2008**, *367* (1), 201−7.
(94) Kerner, J.; Distler, A. M.; Minkler, P.; Parland, W.; Peterman, S. M.; Hoppel, C. L. Phosphorylation of rat liver mitochondrial carnitine palmitoyltransferase-I: effect on the kinetic properties of the enzyme. *J. Biol. Chem.* **2004**, *279* (39), 41104−13.
(95) Di Pancrazio, F.; Bisetto, E.; Alverdi, V.; Mavelli, I.; Esposito, G.; Lippe, G. Differential steady-state tyrosine phosphorylation of two oligomeric forms of mitochondrial F0F1ATPsynthase: a structural proteomic analysis. *Proteomics* **2006**, *6* (3), 921−6.

CHAPTER IV

EXPERIMENTAL WORK

STUDY I - EFFECT OF LIFESTYLE ON AGE-RELATED MITOCHONDRIAL PROTEIN OXIDATION IN MICE CARDIAC MUSCLE

Eur J Appl Physiol (2012) 112:1467–1474
DOI 10.1007/s00421-011-2100-3

ORIGINAL ARTICLE

Effect of lifestyle on age-related mitochondrial protein oxidation in mice cardiac muscle

Ana Isabel Padrão · Rita Ferreira · Rui Vitorino · Renato M. P. Alves · Pedro Figueiredo · José Alberto Duarte · Francisco Amado

Received: 23 December 2010 / Accepted: 26 July 2011 / Published online: 11 August 2011

Abstract This study investigated the influence of lifestyle on aging-related changes in cardiac proteins' oxidative modifications profile. Thirty C57BL/6 strain mice (2 months) were randomly divided into three groups (young Y, old sedentary S, and old active A). The S and A mice were individually placed into standard cages and in cages with running wheels, respectively, for 23 months. Upon killing, heart mitochondrial fractions were obtained for the evaluation of general proteins oxidative modifications profile, the identification of preferential protein targets, and oxidative phosphorylation (OXPHOS) activity. We observed age-related cardiac muscle impairment, evidenced by decreased OXPHOS activity, paralleled by an increased protein susceptibility to carbonylation and nitration. Among the main targets to these posttranslational modifications we found mitochondrial proteins, mainly from OXPHOS complexes, MnSOD and enzymes from lipid metabolism. Lifelong sedentary behavior exacerbated the nitrative damage of mitochondrial proteins, paralleled by a statistically significant decrease of respiratory chain complexes II and III activities. In overall, our results highlight the determinant role of aging in cardiac muscle impairment, which is worsened by a sedentary lifestyle.

Keywords Carbonylation · Nitration · Oxidative phosphorylation · Mitochondria · Wheel running

Communicated by Keith Phillip George.

Electronic supplementary material The online version of this article (doi:10.1007/s00421-011-2100-3) contains supplementary material, which is available to authorized users.

A. I. Padrão · R. Ferreira (✉) · R. Vitorino · R. M. P. Alves · F. Amado
QOPNA, Chemistry Department, University of Aveiro, Campus de Santiago, 3810-193 Aveiro, Portugal
e-mail: ritaferreira@ua.pt

P. Figueiredo · J. A. Duarte
CIAFEL, Faculty of Sport, University of Porto, Porto, Portugal

Introduction

Mitochondria are severely affected by age, being proposed that mitochondrial dysfunction plays a major role in the aging process (Figueiredo et al. 2008; Prokai et al. 2007). Several evidences have shown that cumulative oxidative damage to mitochondrial DNA (Judge et al. 2005; Judge and Leeuwenburgh 2007; Nair 2005; Petrosillo et al. 2009), mitochondrial protein synthesis, permeability of the inner membrane (Nair 2005), and activity of electron chain complexes (ETC) (Choksi and Papaconstantinou 2008) leads to a decline in mitochondrial bioenergetics and, subsequently, to its dysfunction (Petrosillo et al. 2009). Mechanisms underlying age-induced mitochondrial changes are usually related with a misbalance between the levels of reactive oxygen/nitrogen species (RONS) and antioxidant systems—oxidative stress (Kanski et al. 2005; Sohal 2002), since these organelles are considered the main source and, simultaneously, the main target of endogenously generated RONS (Benard and Rossignol 2008). Because the heart is a vital organ with high-metabolic demand and rich in mitochondria, it is particularly vulnerable to oxidative damage (Benard and Rossignol 2008; Dai and Rabinovitch 2009). Hence, a decline in cardiac mitochondrial function coupled with the accumulation of oxidative/nitrative damage to macromolecules may be linked to the decline in cardiac performance with age (Dai and Rabinovitch 2009; Judge and Leeuwenburgh 2007).

A prospective strategy to minimize or retard the deleterious effect of aging is to take advantage of the beneficial effects of a proper lifelong physical activity (Judge and Leeuwenburgh 2007). In wheel running old animals it was observed the off set of many age-related gene expression changes associated with inflammatory and stress response, signal transduction and energy metabolism (Bronikowski et al. 2003). Moreover, several experimental works with laboratory animals have shown that lifelong voluntary wheel running reduces the oxidative damage levels (Navarro et al. 2004; Rosa et al. 2005) with a consequent diminishing of mitochondrial oxidative damage and increased mitochondrial functionality in heart muscle (Allen et al. 2001; Navarro and Boveris 2007; Navarro et al. 2004; Rosa et al. 2005). However, to the best of our knowledge, there are no studies that analyzed the effect of lifelong lifestyle in the cardiac mitochondrial plasticity and protein susceptibility to oxidative and nitrative damage.

In the present study, we focused on the analysis of cardiac mitochondrial protein targets to oxidation and nitration in young, old active and old sedentary mice, relating it with the mitochondrial respiratory chain activity. We hypothesized that animals' age plays a determinant role in oxidized protein profile with functional consequences, which are modulated by lifestyle.

Methods

Animals and experimental protocol

Male C57BL/6 strain mice aged 2 months were randomly divided into three groups (young Y, old sedentary S, old active A). After one week of quarantine, animals from Y group ($n = 10$) were killed, whereas animals from S ($n = 10$) and A ($n = 10$) groups were individually placed into standard cages 355 × 235 × 190 mm (Ref. 2150E, Tecniplast, Italy) and in cages equipped with running wheels (25 cm in diameter) with 364 × 258 × 350 mm (Ref. 1284L0106, Tecniplast, Italy), respectively, until killing at 25 months old. Active mice performed an average of 7 km per day during the experimental period, with a peak of activity of 13.0 ± 2.5 km per day noticed between the fourth and fifth week of the experiment. Then the animals' activity progressively declined until the 15th week of the experiment, reaching a steady state of approximately 5.0 ± 2.0 km per day, which was maintained till the end of the protocol. At the time of killing, there were only eight animals in the S group since two animals died during the experimental protocol (with 20 and 22 months of age, respectively). Animals from both groups were housed at constant temperature (21°–24°C) on a daily light schedule of 12 h of light versus dark until killing. All animals were provided with food and water ad libitum. Housing and experimental treatment of animals were in accordance with the Guide for the Care and Use of Laboratory Animals from the Institute for Laboratory Animal Research (ILAR 1996). The experiments were complied with the current national laws.

Cardiac muscle mitochondria isolation

At the end of the experimental protocol, mice were killed by cervical dislocation followed by thoracotomy with heart extraction. Mitochondria isolation was performed using the conventional methods of differential centrifugation, as previously described by Ascensao et al. (2005). All procedures were performed at 0–4°C. In brief, after excised the hearts were immediately minced in an ice-cold isolation medium containing 250 mM sucrose, 0.5 mM EGTA, 10 mM HEPES–KOH (pH 7.4), and 0.1% defatted BSA (Catalog. No A6003, Sigma). The minced blood-free tissue was resuspended in isolation medium containing protease subtilopeptidase A type VIII (Catalog No. P5380, Sigma; 1 mg/g tissue) and homogenized with tightly fitted Potter–Elvehjen homogenizer and Teflon pestle. The suspension was incubated for 1 min (4°C), rehomogenized and centrifuged at 14,500*g* during 10 min. The supernatant fluid was decanted, and the pellet, essentially devoid of protease, was gently resuspended in isolation medium. The suspension was centrifuged at 750*g* for 10 min, and the resulting supernatant was centrifuged at 12,000*g* for 10 min. The pellet was resuspended and repelleted at 12,000*g* for 10 min. The final pellet, containing the mitochondrial fraction, was gently resuspended in a washing medium containing 250 mM sucrose, 10 mM HEPES–KOH, pH 7.4.

Mitochondrial protein concentration was spectrophotometrically estimated with the colorimetric method "RC DC protein assay" (Bio-Rad, Hercules, CA, USA), using bovine serum albumin (BSA) as standard. This assay is based on a modification of the Lowry et al. (1951) protocol, allowing the quantification of the protein in the presence of reducing agents and detergents.

Determination of respiratory chain complexes activity

For spectrophotometric determination of respiratory chain complexes activity (I, II, III, IV, V), mitochondrial fractions were disrupted by a combination of freeze–thawing cycles in hypotonic media (25 mM potassium phosphate, pH 7.2) to allow free access to substrates for all assays (Taylor et al. 1994). All assays were performed at 30°C. Complex I activity was measured by following the reduction of 2,6-dichlorophenolindophenol (DCIP) at 600 nm for 4 min, after which rotenone was added and the

absorbance was measured again for 4 min (Janssen et al. 2007). Complex II activity was determined according to Birch-Machin et al. (1994). In brief, the enzyme catalyzed reduction of DCIP was followed at 600 nm for 3 min after addition of 65 μM ubiquinone. The antimycin A-sensitive complex III activity was assayed at 550 nm as previously described (Choksi and Papaconstantinou 2008). The specific activity of cytochrome *c* oxidase was measured by following the oxidation of cytochrome *c* (II) at 550 nm (Birch-Machin et al. 1994). ATP synthase activity was measured according to Simon et al. (2003). The phosphate produced by hydrolysis of ATP reacts with ammonium molybdate in the presence of reducing agents to form a blue-color complex, the intensity of which is proportional to the concentration of phosphate in solution. Oligomycin was used as an inhibitor of mitochondrial ATPase activity.

Separation of mitochondrial proteins by SDS–PAGE and Western blotting analysis

Equivalent amounts of mitochondrial proteins from each group were electrophoresed on a 12.5% SDS–PAGE as described by Laemmli (1970). Gels were stained with Colloidal Coomassie Blue or were blotted onto a nitrocellulose membrane (Whatman®, Protan®) and nonspecific binding was blocked with 5% (w/v) dry non–fat milk in TBS-T (100 mM Tris, 1.5 mM NaCl, pH 8.0 and 0.5% Tween 20). The membrane was then incubated with anti-3-nitrotyrosine primary antibody solution (1:1,000 dilution, mouse monoclonal IgG, Chemicon). After 2 h incubation, the membrane was washed with TBS-T and incubated with anti-mouse IgG peroxidase secondary antibody (1:1000 dilution, Amersham Pharmacia Biotech).

Carbonylated proteins were assayed according to Robinson et al. (1999) with some modifications. Briefly, a given volume (1 V) of sample containing 20 μg of protein was derivatized with 2,4-dinitrophenylhydrazine (DNPH). The sample was mixed with 1 V of 12% SDS plus 2 V of 20 mM DNPH/10% TFA, followed by 30 min incubation in dark, after which 1.5 V of 2 M Tris–base/18% of *β*-mercaptoethanol was added for neutralization. Then, derivatized proteins were subjected to 12.5% SDS–PAGE gel and electrotransferred to nitrocellulose membrane blots as described. Immunodetection of carbonylated proteins was performed using rabbit anti-DNP (DakoCytomation, Hamburg, Germany) as primary antibody.

Immunoreactive bands were detected with enhanced chemiluminescence reagents (ECL, Amersham Pharmacia Biotech) according to the manufacturer's procedure and images were recorded using X-ray films (Kodak Biomax light Film, Sigma). The films and the gels were scanned in Molecular Imager Gel Doc XR + System (Bio-Rad) and analyzed with Quantity One software version 4.6.3 (Bio-Rad, Hercules, CA).

Protein and PTMs identification by nLC-MALDI-Tof/Tof

Protein bands corresponding to the ones identified in western blot maps were excised manually from SDS–PAGE gel. To ensure PTMs identification, pools of four bands with the same MW were made for each experimental group. These bands were destained with 25 mM ammonium bicarbonate/50% acetonitrile and dried under vacuum (SpeedVac®, Thermo Savant, USA). The dried gel pieces were rehydrated with 25 μL of 10 μg/mL trypsin in 50 mM ammonium bicarbonate and digested overnight at 37°C. Tryptic peptides were extracted from the gel with formic acid and were then dried in a vacuum concentrator and resuspended in 10 μL of a 50% acetonitrile/0.1% formic acid solution. Separation of tryptic peptides by nano-HPLC was performed on the module separation Ultimate 3000 (LC Packings) using a capillary column (Pepmap100 C18; 3 μm particle size; 0.75 μm internal diameter, 15 cm in length). A gradient of solvent A (water/acetonitrile/trifluoroacetic acid (98:2:0.05, v/v/v)) to solvent B (water/acetonitrile/trifluoroacetic acid (10:90:0.045, v/v/v)) was used. The separation of 2 μg/μL sample was performed using a linear gradient (5–55% B for 30 min, 55–80% B for 10 min and 70–5% A for 5 min) with a flow rate of 0.3 μL/min. The eluted peptides were applied directly on a MALDI plate in 7 s fractions using an automatic fraction collector Probot (Dionex, Amsterdam).

Mass spectra were obtained on a matrix-assisted laser desorption/ionization-time-of-flight MALDI-TOF/TOF mass spectrometer (4800 Proteomics Analyzer, Applied Biosystems, Foster City, CA, USA) in the positive ion reflector mode and obtained in the mass range from 700 to 4,500 Da with 1,000 laser shots. A data-dependent acquisition method was created to select the 16 most intense peaks in each sample spot for subsequent tandem mass spectrometry (MS/MS) data acquisition, excluding those from the matrix, due to trypsin autolysis or acrylamide peaks. Trypsin autolysis peaks (*m/z* 842.5 and *m/z* 2211.1) were used for internal calibration of the mass spectra. MS/MS data was searched against the Swissprot nonredundant protein database (peptide fragment fingerprinting) (mus musculus 18012011) with paragon algorithm from ProteinPilot™ software (version 4.0, Applied Biosystems, USA). For Protein Pilot, the search parameters were the following: enzyme (trypsin), special factor (gel-based ID), species (mus musculus), ID focus (biological modification, amino acid substitution), detected protein threshold: more than 1 (90%) and running the FDR. Detected PTMs were manually inspected and cross-validated using de novo

sequencing data analysis software (GPS, Applied Biosystems). Spectra for all validated PTMs are presented as Supplementary data (Figure S1).

Data analysis

The results are presented as mean ± SD for each group experimental. The Kolmogorov–Smirnov test was used to test normality of distribution for all data. Since all variable were normal distributed, significant differences between groups were evaluated using one-way ANOVA followed by the Tukey–Kramer multiple comparisons test. Statistical Package for the Social Science (version 15.0) was used for all analysis. The significance level was set at 5%.

Results

Characterization of animals' response

Body weight, heart muscle wet weight and heart/body weight ratio for the three animals groups are shown in Table 1. A significant enhancement of the heart/body weight ratio in aged compared with young mice is noticed, more evident in old active animals (38% higher than in young mice). In this group, there was a lower body weight, but a higher heart weight than in old sedentary mice, which was statistically significant.

Assessment of mitochondrial respiratory chain activity

To evaluate the effect of aging and lifestyle on heart mitochondrial functionality, the activity of the respiratory chain complexes I, II, III, IV and V was spectrophotometrically measured in the mitochondrial fractions. As can be depicted from Table 2, oxidative phosphorylation (OXPHOS) activity decreased with age, although only statistically significant for complexes II, III and V. There was an age-related decrease of succinate:ubiquinone reductase activity of 45%, being this reduction more pronounced in S mice (69%). Moreover, when comparing both old animal groups, the activity of this respiratory complex was significantly lower (44%) in S mice. A similar profile was noticed for cytochrome c reductase activity, with a 34% diminishing of activity with aging, being this impairment more noticeable (51%) in S animals. Regarding the activity of ATP synthase, a significant decrease was observed with age, with a reduction of 54 and 59% for A and S groups, respectively. No significant differences were noticed among old mice groups.

Protein susceptibility to carbonylation

To assess the levels of cardiac muscle protein oxidation in the three groups, we measured the total carbonyl content in mitochondria by western blotting with an anti-DNPH antibody. A quantitative comparison of carbonylation levels between groups evidenced a reproducible age-dependent increase (Fig. 1). However, no significant differences were observed between the two aged groups. A more detailed analysis of Fig. 1 evidenced the presence of bands 3 and 4 only in aged mice. No significant differences in the DNP signal of these bands were observed between A and S groups.

LC–MS/MS analysis of tryptic digests from DNP-reactive bands allowed the identification of an average of 70 distinct proteins per band, corresponding to different functional clusters, most of which belonging to "metabolism" and "OXPHOS" (Table S1 of Supplementary material). To discriminate the modified proteins, the oxidation of amino acid side chains (namely on Thr, Lys, Glu, Pro, Arg and Asp) that result in the formation of carbonyl groups was searched by mass spectrometry. Indeed, though the large number of identified proteins per gel band, the presence of PTMs was only confirmed in 14, 17, 16 and 28 proteins in the carbonylated bands analyzed, bands 1–4, respectively. Oxidative modifications in ATP synthase subunits alpha and beta and cytochrome *c*–bc1 complex subunits 1 and 2 were identified in all the four bands analyzed, which evidence the high susceptibility of this OXPHOS subunits to oxidative damage with consequent protein fragmentation. In ATP synthase subunit beta only Met oxidation was observed whereas in subunit alpha pyro-Glu was also identified. Creatine kinase S-type, aspartate

Table 1 Physiological parameters from young (Y), old active (A), old sedentary (S) mice

	Groups		
	Y	A	S
Body weight (g)	27.1 ± 1.1	33.3 ± 2.2***,#	36.3 ± 4.1**
Heart weight (mg)	121.1 ± 7.9	210.0 ± 12.8***,#	187.7 ± 18.1***
Heart/body weight (mg/g)	4.5 ± 0.2	6.2 ± 0.3***,#	5.2 ± 0.7*

Values are presented as mean ± standard deviation of eight separate experiments in each group (*$p < 0.05$ vs. Y mice, **$p < 0.01$ vs. Y mice, ***$p < 0.001$ vs. Y mice, #$p < 0.05$ vs. S mice)

Eur J Appl Physiol (2012) 112:1467–1474

Table 2 Respiratory chain complexes activity in young (Y), old active (A) and old sedentary (S) mice

	Groups		
	Y	A	S
NADH:ubiquinone oxidoreductase (U/g)	140.5 ± 18.8	84.7 ± 21.2	94.6 ± 15.9
Succinate:ubiquinone reductase (μmol/min/g)	235.4 ± 23.6	130.3 ± 48.9***,##	72.6 ± 13.4***
Cytochrome *c* reductase (μmol/min/g)	23.0 ± 3.8	15.1 ± 4.7***,#	11.2 ± 2.4**
Cytochrome *c* oxidase (nmol/min/mg)	67.6 ± 22.5	61.9 ± 32.6	63.3 ± 19.8
ATP synthase (μmol Pi/min/mg)	69.8 ± 13.4	32.3 ± 14.4***	28.8 ± 14.4**

Values are presented as mean ± standard deviation of eight separate experiments in each group (**$p < 0.01$ vs. Y mice, ***$p < 0.001$ vs. Y mice, #$p < 0.05$ vs. S mice, ##$p < 0.01$ vs. S mice)

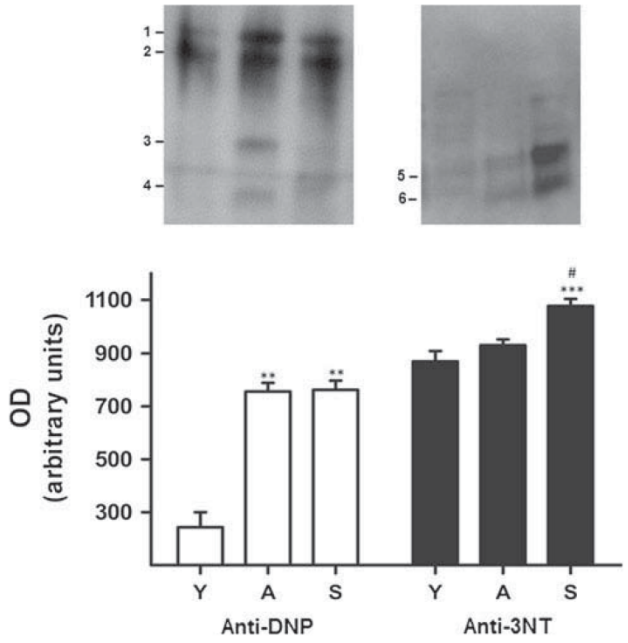

Fig. 1 Effect of lifelong physical activity on carbonyl and 3-nitrotyrosine content in mitochondria. Representative image of immunoblot of carbonyl (*left*) and nitration content (*right*) in young (Y), old active (A) and old sedentary (S) mice, using anti-DNP and anti-nitrotyrosine (3-NT) antibodies, are presented above their corresponding *densitometric graph*. Values are mean ± standard deviation. Protein bands are numbered according to the identification in Table S1 of Supplementary material (*$p < 0.01$ vs. Y mice, ***$p < 0.001$ vs. Y mice, ###$p < 0.001$ vs. S mice)

aminotransferase, VDAC1, ADP/ATP translocase 1, isocitrate dehydrogenase [NADP] mitochondrial and enzymes involved in lipid metabolism were also found as preferential targets to oxidation (Table S1 of Supplementary material). However, the oxidative modification of malate dehydrogenase, mtDNA-encoded cytochrome *c* oxidase subunit 2, NADH dehydrogenase [ubiquinone] flavoprotein 2, NADH dehydrogenase [ubiquinone] iron-sulfur protein, NADH dehydrogenase [ubiquinone] 1 beta subcomplex, cytochrome *b*–*c*1 complex subunit Rieske, ATP synthase subunits d and O and MnSOD, seem to be age dependent. Among the modifications more prevalent and with biological relevance, we found pyro-Glu, Trp dioxidation, kynurenin, Cys oxidation and aminoadipic semialdehyde (Table S1 of Supplementary material).

Protein susceptibility to nitration

To assess the nitration protein levels, we measured the 3-nitrotyrosine content in mitochondria by western blotting. As depicted in Fig. 1, the levels of 3-nitrotyrosine significantly increased in old sedentary mice when compared with young and old active mice. No significant differences between young and old active animals were noticed. Only two anti-3-nitrotyrosine reactive bands were detected, although being present in all groups. The differences between groups (Fig. 1) were observed in band 5, which presented a fourfold increase in S comparing to Y, but without significant differences between A and Y, and in band 6 that presented a 4.5-fold increase in S compared with Y and a twofold increase in A compared with Y.

To identify the proteins more susceptible to nitration, LC–MS/MS analysis of tryptic digests from gel bands was performed and the results obtained are listed in Table S1 of Supplementary material. An average of 42 distinct proteins per band was identified in 3-nitrotyrosine-reactive bands (Fig. 1), most of which OXPHOS subunits (16 from NADH dehydrogenase, 1 from succinate dehydrogenase, 5 from cytochrome *b*–*c*1 complex, 7 from cytochrome *c* oxidase and 7 from ATP synthase). Although some of these subunits were also identified in DNP-reactive bands, others like ATP synthase subunits delta, g and e or NADH dehydrogenase [ubiquinone] 1 subunit C2 and alpha subcomplex 12 were only observed in band 6. We also screened the potential 3-nitrotyrosine-containing peptides; however, MS/MS analysis did not allow its identification.

Discussion

The results from our study corroborate previous findings (Kanski et al. 2005; Murray et al. 2008) that point to an

age-related accumulation of damaged proteins, associated with a decrease in OXPHOS activity (Tables 2, 3 of Supplementary material; Fig. 1). Posttranslational oxidative modifications of proteins, manifested as carbonylation and nitration, appear to be a key mechanism of protein impaired functional and/or structural integrity underlying mitochondrial dysfunction (Choksi and Papaconstantinou 2008; Kanski et al. 2005). Given the increased levels of carbonylation and nitration observed in aged cardiac mitochondria (Fig. 1), we have searched for proteins more prone to these modifications. As preferential targets of carbonylation we identified some proteins of respiratory chain complexes, particularly ATP synthase and cytochrome *b*–*c*1 complex subunits. The higher susceptibility of OXPHOS proteins to oxidation has been reported by several authors in different tissues (Alves et al. 2010; Meany et al. 2007; Prokai et al. 2007), namely in heart (Choksi and Papaconstantinou 2008; Padrao et al. 2011). Complex III is one of the RONS generating sites in mitochondria, and therefore is not surprising that subunits 1 and 2 of this complex (Table S1 of Supplementary material) are preferential targets of oxidative damage. Given its location and abundance in mitochondria, complex V also represents a favored target of oxidative damage (Choksi and Papaconstantinou 2008). Creatine kinase, an important enzyme in energy transduction in tissues with high energy demands such as heart, was also identified in more than one DNP-reactive bands, suggesting a high susceptibility to oxidation with consequent fragmentation, which is in agreement with a previous study of aged mice skeletal muscle (Alves et al. 2010). The aging effect was noticed in the carbonylation of other OXPHOS subunits like NADH dehydrogenase [ubiquinone] iron-sulfur protein 2, NADH dehydrogenase [ubiquinone] 1 alpha subcomplex subunit 10, ATP synthase subunits d and O, some metabolic enzymes as malate dehydrogenase, transport proteins like VDAC1 and antioxidant enzymes as MnSOD (Table S1 of Supplementary material). PTMs with known biological relevance and usually related with protein dysfunction like N-formylkynurenine, a product of double tryptophan oxidation (Taylor et al. 2003) were identified in some of these proteins, namely in some subunits of respiratory chain complexes, ANT1 and MnSOD. Aminoadipic semialdehyde, a carbonyl product of metal-catalyzed oxidation of proteins (Requena et al. 2001), was also identified in some proteins like cytochrome *b*–*c*1 complex subunit 1, specifically in the metal-binding domain. The increased damage of these proteins that play relevant roles in mitochondria justifies, at least partially, the aging cardiomyocyte phenotype.

Several authors suggest that lifestyle factors, including physical activity, modulate the physiological and pathophysiological consequences of aging (Nair 2005; Rosa et al. 2005). Herein, we studied the effect of lifelong sedentary behavior on cardiac mitochondria functionality and susceptibility to oxidative damage. We select an animal model where mice have free access to running wheel once it better mimics the normal intermittent exercise routine of animals in the wilderness (Eisele et al. 2008; Figueiredo et al. 2009). Its effectiveness was confirmed by the cardiac hypertrophy observed in A mice, assessed through the heart/body weight ratio (Table 1), which is generally seen as a sign of cardiac adaptation to meet higher energy demands (Eisele et al. 2008; Rosa et al. 2005). Although the well understood age-related hypertrophy was noticed (27.4% in A compared to Y), this effect was attenuated with sedentary lifestyle (13.5% higher in S compared to Y). In this context mitochondria assume a relevant role and it has been suggested that regular physical exercise increases its biogenesis as well as the synthesis of respiratory chain subunits to meet energy demands, and delay the oxidative damage resultant from the aging process (Judge et al. 2005; Navarro and Boveris 2007). Although we observed an age-related activity decline of respiratory chain complexes (Table 2), which is in agreement with previous studies (Choksi and Papaconstantinou 2008; Nair 2005), only succinate-ubiquinone reductase and cytochrome c reductase presented lifestyle-associated differences, with a significant decrease in activity in S mice (Table 2). The notion that a sedentary behavior results in a general impairment of cardiac mitochondrial functionality was not as evident as in other tissues like skeletal muscle (Alves et al. 2010; Figueiredo et al. 2009), which might be explained by the permanent heart contractile activity.

Intriguingly, no differences of protein carbonylation between A and S mice were observed in mitochondrial fractions (Fig. 1). In opposition, lifestyle seems to modulate mitochondrial proteins susceptibility to nitration (Fig. 1). This posttranslational modification is particularly relevant in cardiac muscle since its proteins are exposed to periodic fluxes of endogenous nitric oxide (NO), which plays an important regulatory role in heart function; this cellular messenger reacts with superoxide to produce the highly reactive peroxynitrite anion that reacts with proteins generating nitrotyrosine (Kanski et al. 2005). Few studies have been successful in the identification of nitrated proteins and the specific modified tyrosine residue within the protein (reviewed in Bailey et al. 2005). Although no amino acid residues were unequivocally found nitrated with the methodological approach used in the present work, some of the proteins identified in 3-nitrotyrosine-reactive bands were already reported as particularly susceptible to this modification (Table S1 of Supplementary material). For instance, the nitration of cytochrome b-c1 complex proteins, ATP synthase subunits, MnSOD, VDAC1 and cytochrome c was previously identified by several authors

in vivo (Bailey et al. 2005; Liu et al. 2009; Peluffo and Radi 2007). The nitrative damage of these proteins seems to be exacerbated by lifelong sedentary behavior with potential negative consequences to the energetic and redox balance of the aging heart.

In summary, our data evidenced the age-related cardiac muscle impairment, evidenced by decreased OXPHOS activity, partially justified by the increased mitochondrial protein susceptibility to oxidative modifications. Moreover, the sedentary lifestyle worsens the functional consequences of aging, although not as evident as in other tissues.

Acknowledgments The authors would like to thank Celeste Resende for her assistance in animal care. This work was funded by the Portuguese Foundation for Science and Technology (FCT) [Grant numbers PTDC/DES/70757/2006, SFRH/BD/66642/2009 (to A.I.P.), SFRH/BPD/24158/2005 (to R.F.) and SFRH/BD/46829/2008 (to R.A.)].

Conflict of interest The authors have declared no conflict of interest.

References

Allen DL, Harrison BC, Maass A, Bell ML, Byrnes WC, Leinwand LA (2001) Cardiac and skeletal muscle adaptations to voluntary wheel running in the mouse. J Appl Physiol 90:1900–1908

Alves RM, Vitorino R, Figueiredo P, Duarte JA, Ferreira R, Amado F (2010) Lifelong physical activity modulation of the skeletal muscle mitochondrial proteome in mice. J Gerontol A Biol Sci Med Sci 65:832–842

Ascensao A, Magalhaes J, Soares JM, Ferreira R, Neuparth MJ, Marques F, Oliveira PJ, Duarte JA (2005) Moderate endurance training prevents doxorubicin-induced in vivo mitochondriopathy and reduces the development of cardiac apoptosis. Am J Physiol Heart Circ Physiol 289:H722–H731

Bailey SM, Landar A, Darley-Usmar V (2005) Mitochondrial proteomics in free radical research. Free Radic Biol Med 38:175–188

Benard G, Rossignol R (2008) Ultrastructure of the mitochondrion and its bearing on function and bioenergetics. Antioxid Redox Signal 10:1313–1342

Birch-Machin MA, Briggs HL, Saborido AA, Bindoff LA, Turnbull DM (1994) An evaluation of the measurement of the activities of complexes I–IV in the respiratory chain of human skeletal muscle mitochondria. Biochem Med Metab Biol 51:35–42

Bronikowski AM, Carter PA, Morgan TJ, Garland T Jr, Ung N, Pugh TD, Weindruch R, Prolla TA (2003) Lifelong voluntary exercise in the mouse prevents age-related alterations in gene expression in the heart. Physiol Genomic 12:129–138

Choksi KB, Papaconstantinou J (2008) Age-related alterations in oxidatively damaged proteins of mouse heart mitochondrial electron transport chain complexes. Free Radic Biol Med 44:1795–1805

Dai DF, Rabinovitch PS (2009) Cardiac aging in mice and humans: the role of mitochondrial oxidative stress. Trends Cardiovasc Med 19:213–220

Eisele JC, Schaefer IM, Randel Nyengaard J, Post H, Liebetanz D, Bruel A, Muhlfeld C (2008) Effect of voluntary exercise on number and volume of cardiomyocytes and their mitochondria in the mouse left ventricle. Basic Res Cardiol 103:12–21

Figueiredo PA, Mota MP, Appell HJ, Duarte JA (2008) The role of mitochondria in aging of skeletal muscle. Biogerontology 9:67–84

Figueiredo PA, Powers SK, Ferreira RM, Appell HJ, Duarte JA (2009) Aging impairs skeletal muscle mitochondrial bioenergetic function. J Gerontol A Biol Sci Med Sci 64:21–33

Guide for the Care and Use of Laboratory Animals (1996) Institute for Laboratory Animal Research. The National Academies Press, Washington

Janssen AJ, Trijbels FJ, Sengers RC, Smeitink JA, van den Heuvel LP, Wintjes LT, Stoltenborg-Hogenkamp BJ, Rodenburg RJ (2007) Spectrophotometric assay for complex I of the respiratory chain in tissue samples and cultured fibroblasts. Clin Chem 53:729–734

Judge S, Leeuwenburgh C (2007) Cardiac mitochondrial bioenergetics, oxidative stress, and aging. Am J Physiol Cell Physiol 292:C1983–C1992

Judge S, Jang YM, Smith A, Hagen T, Leeuwenburgh C (2005) Age-associated increases in oxidative stress and antioxidant enzyme activities in cardiac interfibrillar mitochondria: implications for the mitochondrial theory of aging. FASEB J 19:419–421

Kanski J, Behring A, Pelling J, Schoneich C (2005) Proteomic identification of 3-nitrotyrosine-containing rat cardiac proteins: effects of biological aging. Am J Physiol Heart Circ Physiol 288:H371–H381

Laemmli UK (1970) Cleavage of structural proteins during the assembly of the head of bacteriophage T4. Nature 227:680–685

Liu B, Tewari AK, Zhang L, Green-Church KB, Zweier JL, Chen YR, He G (2009) Proteomic analysis of protein tyrosine nitration after ischemia reperfusion injury: mitochondria as the major target. Biochim Biophys Acta 1794:476–485

Lowry OH, Rosebrough NJ, Farr AL, Randall RJ (1951) Protein measurement with the Folin phenol reagent. J Biol Chem 193:265–275

Meany DL, Xie H, Thompson LV, Arriaga EA, Griffin TJ (2007) Identification of carbonylated proteins from enriched rat skeletal muscle mitochondria using affinity chromatography-stable isotope labeling and tandem mass spectrometry. Proteomics 7:1150–1163

Murray J, Oquendo CE, Willis JH, Marusich MF, Capaldi RA (2008) Monitoring oxidative and nitrative modification of cellular proteins; a paradigm for identifying key disease related markers of oxidative stress. Adv Drug Deliv Rev 60:1497–1503

Nair KS (2005) Aging muscle. Am J Clin Nutr 81:953–963

Navarro A, Boveris A (2007) The mitochondrial energy transduction system and the aging process. Am J Physiol Cell Physiol 292:C670–C686

Navarro A, Gomez C, Lopez-Cepero JM, Boveris A (2004) Beneficial effects of moderate exercise on mice aging: survival, behavior, oxidative stress, and mitochondrial electron transfer. Am J Physiol Regul Integr Comp Physiol 286:R505–R511

Padrao AI, Ferreira RM, Vitorino R, Alves RM, Neuparth MJ, Duarte JA, Amado F (2011) OXPHOS susceptibility to oxidative modifications: the role of heart mitochondrial subcellular location. Biochim Biophys Acta 1807(9):1106–1113

Peluffo G, Radi R (2007) Biochemistry of protein tyrosine nitration in cardiovascular pathology. Cardiovasc Res 75:291–302

Petrosillo G, Matera M, Moro N, Ruggiero FM, Paradies G (2009) Mitochondrial complex I dysfunction in rat heart with aging: critical role of reactive oxygen species and cardiolipin. Free Radic Biol Med 46:88–94

Prokai L, Yan LJ, Vera-Serrano JL, Stevens SM Jr, Forster MJ (2007) Mass spectrometry-based survey of age-associated protein carbonylation in rat brain mitochondria. J Mass Spectrom 42:1583–1589

Requena JR, Chao CC, Levine RL, Stadtman ER (2001) Glutamic and aminoadipic semialdehydes are the main carbonyl products of metal-catalyzed oxidation of proteins. Proc Natl Acad Sci USA 98:69–74

Robinson CE, Keshavarzian A, Pasco DS, Frommel TO, Winship DH, Holmes EW (1999) Determination of protein carbonyl groups by immunoblotting. Anal Biochem 266:48–57

Rosa EF, Silva AC, Ihara SS, Mora OA, Aboulafia J, Nouailhetas VL (2005) Habitual exercise program protects murine intestinal, skeletal, and cardiac muscles against aging. J Appl Physiol 99:1569–1575

Simon N, Papa K, Vidal J, Boulamery A, Bruguerolle B (2003) Circadian rhythms of oxidative phosphorylation: effects of rotenone and melatonin on isolated rat brain mitochondria. Chronobiol Int 20:451–461

Sohal RS (2002) Role of oxidative stress and protein oxidation in the aging process. Free Radic Biol Med 33:37–44

Taylor RW, Birch-Machin MA, Bartlett K, Lowerson SA, Turnbull DM (1994) The control of mitochondrial oxidations by complex III in rat muscle and liver mitochondria. Implications for our understanding of mitochondrial cytopathies in man. J Biol Chem 269:3523–3528

Taylor SW, Fahy E, Murray J, Capaldi RA, Ghosh SS (2003) Oxidative post-translational modification of tryptophan residues in cardiac mitochondrial proteins. J Biol Chem 278:19587–19590

STUDY II - OXPHOS SUSCEPTIBILITY TO OXIDATIVE MODIFICATIONS: THE ROLE OF HEART MITOCHONDRIAL SUBCELLULAR LOCATION

Biochimica et Biophysica Acta 1807 (2011) 1106–1113

Contents lists available at ScienceDirect

Biochimica et Biophysica Acta

journal homepage: www.elsevier.com/locate/bbabio

OXPHOS susceptibility to oxidative modifications: The role of heart mitochondrial subcellular location

Ana Isabel Padrão [a], Rita M.P. Ferreira [a], Rui Vitorino [a], Renato M.P. Alves [a], Maria João Neuparth [b,c], José Alberto Duarte [b], Francisco Amado [a,*]

[a] QOPNA, Chemistry Department, University of Aveiro, Aveiro, Portugal
[b] CIAFEL, Faculty of Sport, University of Porto, Porto, Portugal
[c] CITS, IPSN, CESPU, Famalicão, Portugal

ARTICLE INFO

Article history:
Received 19 February 2011
Received in revised form 11 April 2011
Accepted 13 April 2011
Available online 1 May 2011

Keywords:
Intermyofibrillar mitochondria
Subsarcolemmal mitochondria
2-D BN-PAGE/MS/MS
3-Nitrotyrosine
Carbonylation
Respiratory chain complexes

ABSTRACT

In cardiac tissue two mitochondria subpopulations, the subsarcolemmal and the intermyofibrillar mitochondria, present different functional emphasis, although limited information exists about the underlying molecular mechanisms. Our study evidenced higher OXPHOS activity of intermyofibrillar compared to subsarcolemmal mitochondria, paralleled by distinct membrane proteins susceptibility to oxidative damage and not to quantitative differences of OXPHOS composition. Indeed, subsarcolemmal subunits of respiratory chain complexes were more prone to carbonylation while intermyofibrillar mitochondria were more susceptible to nitration. Among membrane protein targets to posttranslational modifications, ATP synthase subunits alpha and beta were notoriously more carbonylated in both subpopulations, although more intensely in subsarcolemmal mitochondria. Our data highlight a localization dependence of cardiac mitochondria OXPHOS activity and susceptibility to posttranslational modifications.

1. Introduction

Essential mechanisms of energy production, signaling, biosynthesis and apoptosis are contained within mitochondria, and their orchestration plays a determinant role in cell physiology [1,2]. Since mitochondria generate between 80% and 90% of all ATP produced in the cell, it is understandable that in tissues like the cardiac muscle these organelles occupy 20–30% of the cell volume, having mitochondrial function, or dysfunction, a critical role in the performance of this tissue [3]. In cardiomyocytes, like in skeletal muscle fibers, there is the added dimension of two mitochondria subpopulations located in different regions of the cell: one abuts the sarcolemma (subsarcolemmal mitochondria, SS), and the other is trapped within the contractile apparatus (intermyofibrillar mitochondria, IMF) [4–6]. These mitochondrial subpopulations possess different properties, which may contribute to their distinct capacities for adaptation to different stimuli [4,6–10]. For instance, previous studies have reported higher respiratory rates in IMF compared to SS in cardiac tissue [6,7,11], which might be related with the levels of the unwanted by-products of inefficient electron transfer within mitochondria [10,12]. As major sources of reactive oxygen and nitrogen species (RONS), mitochondria themselves, and particularly oxidative phosphorylation (OXPHOS) complexes, are especially susceptible to oxidative and nitrative damage [2,10,12]. Protein carbonylation is considered to be a major form of protein oxidation, being widely detected namely by Western blot immunoassay [13]. Among the main carbonyl products of metal-catalyzed oxidation of proteins are glutamic and aminoadipic semialdehydes [15]. The assay of these compounds involves derivatization of the carbonyl group with 2,4-dinitrophenylhydrazine (DNPH), with formation of dinitrophenyl (DNP) hydrazone product. DNPH also reacts with sulfenic acid, resultant from cysteine oxidation, a modification that regulates protein function [13]. Western blot is also used for the search of 3-nitrotyrosine modification, a hallmark of reactive nitrogen species (RNS), generally associated with impaired functional and/or structural integrity of target proteins [14]. With the advancements in proteomics technology it is now possible to identify relevant protein targets of such posttranslational modifications (PTMs) in pathophysiological conditions like aging [16,17] or diabetes [7].

Although it has been verified that mitochondria subpopulations have different functional emphases [6,10,11,18], the molecular mechanisms underlying their discrete properties in cardiac tissue are still poorly understood. As mitochondria comprise a primary locus for the formation and reactions of RONS [10,12], functional differences

Abbreviations: 2D-BN-PAGE, two-dimensional blue native polyacrylamide gel electrophoresis; Anti-DNP, anti-2,4-dinitrophenylhydrazone; Anti-3-NT, anti-3-nitrotyrosine; OXPHOS, oxidative phosphorylation; ETC, electron transport chain; IMF, intermyofibrillar mitochondria; SS, subsarcolemmal mitochondria

* Corresponding author at: Chemistry Department, University of Aveiro, Campus de Santiago, 3810-193 Aveiro, Portugal. Tel.: +351 234370700; fax: +351 234370084.
E-mail address: famado@ua.pt (F. Amado).

0005-2728/$ – see front matter © 2011 Elsevier B.V. All rights reserved.
doi:10.1016/j.bbabio.2011.04.002

among heart mitochondrial subpopulations' properties should be, at least partially, a consequence of the distinct susceptibility of IMF and SS mitochondrial proteins to oxidative modifications. In order to verify our assumption, fractions of SS and IMF mitochondria were isolated from heart tissue from Wistar rats following a methodological procedure recently described for skeletal muscle [18], which guarantees the high purity of mitochondrial subpopulations obtained.

2. Materials and methods

2.1. Chemicals

All reagents were obtained from Sigma-Aldrich (St. Louis, USA), unless otherwise specified. Mouse monoclonal anti-3-nitrotyrosine antibody was obtained from Chemicon (Temecula, CA, USA), rabbit polyclonal anti-DNP antibody was obtained from DakoCytomation (Hamburg, Germany), anti-ATPB antibody (cat. no. ab14730) was obtained from Abcam (Cambridge, UK) and secondary peroxidase-conjugated antibodies (anti-mouse IgG and anti-rabbit IgG) were obtained from GE Healthcare (Buckinghamshire, UK).

2.2. Animals

Adult male Wistar rats (Charles River Laboratories, Barcelona, Spain) with an age of 12–16 weeks were used in these experiments. All procedures were performed in accordance with the *Guide for the Care and Use of Laboratory Animals*. Twenty-five rats weighing approximately 300 g were housed in collective cages before use. Out of these 25 animals, groups of 5 rats were sacrificed at different points of time within 2 weeks to have their heart muscle pooled for further analysis. All samples were used to separate their mitochondria subpopulations.

2.3. SS and IMF mitochondria isolation

Mitochondrial populations were purified from heart muscle following the protocol described by our group for skeletal muscle [18], which is based on tissue mechanical treatment and enzymatic digestion as previously reported by Palmer et al. [11]. In brief, cardiac tissue was minced with scissors in homogenization buffer (250 mM sucrose, 10 mM Tris–HCl, 0.1 mM EGTA (pH 7.4)), supplemented with 2 mM PMSF and 0.25 mg/ml trypsin (Promega, Wisconsin, USA). Following 10 minof incubation on ice, albumin fat-free was added to a final concentration of 10 mg/ml. The tissue was subsequently rinsed three times with buffer and then homogenized with a Potter homogenizer (Teflon pestle). Large cellular debris and nuclei were pelleted by centrifuging for 5 min at 1000×*g*. A mitochondria enriched fraction was obtained by centrifuging the supernatant for 20 min at 16,000×*g* and ressuspending the pellet in a small volume of homogenization buffer. Pure mitochondrial subpopulations were then obtained by ultracentrifugation at 95,000×*g* for 30 min on a density-gradient with 50% (v/v) Percoll. Two brown bands were observed; the lower band corresponded to IMF mitochondria while the upper band corresponded to SS mitochondria [18]. The mitochondrial fractions were then washed twice and were aliquoted for subsequent biochemical analysis. Protein content was determined with RC DC Protein Assay kit (Bio-Rad, Hercules, CA, USA).

2.4. Respiratory chain complexes activity

Mitochondrial fractions were disrupted by a combination of freeze–thawing in hypotonic media (25 mM potassium phosphate, pH 7.2) to allow free access to substrates for all assays [19]. Complex I activity was measured by following the reduction of 2,6-dichlorophenolindophenol (DCIP) at 600 nm for 4 min, after which rotenone was added and the absorbance was measured again for 4 min[20]. Complex II activity was determined according to Birch-Machin et al. [21]. In brief, the enzyme catalyzed reduction of DCIP was followed at 600 nm for 3 min after addition of 65 μM ubiquinone. The antimycin A-sensitive complex III activity was assayed at 550 nm as described [16]. The specific activity of cytochrome *c* oxidase was measured by following the oxidation of cytochrome *c* (II) at 550 nm [21]. ATP synthase activity was measured according to Simon et al. [22]. The phosphate produced by hydrolysis of ATP reacts with ammonium molybdate in the presence of reducing agents to form a blue-colour complex, the intensity of which is proportional to the concentration of phosphate in solution. Oligomycin was used as an inhibitor of mitochondrial ATPase activity.

2.5. Blue-native PAGE separation of mitochondria membrane complexes

BN-PAGE was performed using the method described by Schagger and von Jagow [23] with minor modifications. Mitochondria (400 μg of protein) from each subpopulation were pelleted by centrifugation at 20,000×*g* for 10 min and then resuspended in solubilization buffer (50 mM NaCl, 50 mM Imidazole, 2 mM ε-amino n-caproic acid, 1 mM EDTA pH 7.0) with 1% (w/v) digitonin. After 10 min on ice, insoluble material was removed by centrifugation at 20,000×*g* for 30 min at 4 °C. Soluble components were combined with 0.5% (w/v) Coomassie Blue G250, 50 mM ε-amino n-caproic acid, 4% (w/v) glycerol and separated on a 4–13% gradient acrylamide gradient gel with 3.5% sample gel on top. Anode buffer contained 25 mM Imidazole pH 7.0. Cathode buffer (50 mM tricine and 7.5 mM Imidazole pH 7.0) containing 0.02% (w/v) Coomassie Blue G250 was used during 1 h at 70 V, the time needed for the dye front reach approximately one-third of the gel. Cathode buffer was then replaced with one containing only 0.002% (w/v) Coomassie Blue G250 and the native complexes were separated at 200 V for 4 h at 4 °C. A native protein standard HMW-native marker (GE Healthcare, Buckinghamshire, UK) was used. The gels were stained with Coomassie Colloidal for protein visualization and scanned with Gel Doc XR System (Bio-Rad, Hercules, CA, USA). Band detection, quantification and matching were performed using QuantityOne Imaging software (v4.6.3, Bio-Rad).

2.6. In-gel activity of complexes IV and V

The in-gel activity and histochemical staining assays of complexes IV and V were determined using the methods described by Zerbetto et al. [24] with minor modifications. Complex IV-specific heme stain in BN-PAGE gels was determined using 10 μl horse heart cytochrome *c* (5 mM) and 0.5 mg diaminobenzidine (DAB) dissolved in 1 ml 50 mM sodium-phosphate, pH 7.2. The reaction was stopped by 50% (v/v) methanol, 10% (v/v) acetic acid, and the gels were then transferred to water. ATP hydrolysis activity of complex V was analyzed by incubating the native gels with 35 mM Tris, 270 mM glycine buffer, pH 8.3 at 37 °C, that had been supplemented with 14 mM $MgSO_4$, 0.2% (w/v) $Pb(NO_3)_2$, and 8 mM ATP. Lead phosphate precipitation that is proportional to the enzymatic ATP hydrolysis activity was stopped by 50% (v/v) methanol (30 min), and the gels were then transferred to water.

2.7. 2-D BN-PAGE separation of respiratory complexes subunits

Each lane of the first dimension gel was excised and was subsequently incubated in equilibration buffer (2% (w/v) SDS, 6 M urea, 30% glycerol, 0.05 M Tris–HCl pH 8,8 and 20 mg/ml DTT) for 30 min at room temperature to induce dissociation of the protein complexes. Next, the lanes were placed on top of a 4% stacking SDS gel polymerized over a 5–20% gradient SDS-PAGE (18×16 cm) and this gel was run at 100 V during 1 h and then at 200 V during 3–4 h. Gel was stained with Coomassie Colloidal for protein visualization or was blotted onto a nitrocellulose membrane (Whatman®, Protan®) for subsequent 3-nitrotyrosine and carbonyl groups detection by

Western blotting. Stained gel was scanned with Gel Doc XR System (Bio-Rad, Hercules, CA, USA). Spot detection, quantification and matching were performed using PDQuest software (v8.0.1, Bio-Rad).

2.8. Western blotting analysis

Mitochondrial proteins separated by 2-D BN-PAGE were blotted on a nitrocellulose membrane (Whatman®, Protan) in transfer buffer (25 mM Tris, 192 mM glycine, pH 8.3 and 20% methanol) during 2 h (200 mA). Then, nonspecific binding was blocked with 5% (w/v) dry non fat milk in TBS-T (100 mM Tris, 1.5 mM NaCl, pH 8.0 and 0.5% Tween 20) and the membrane was incubated with anti-3-nitrotyrosine primary antibody solution (1:1000 dilution). After 2-h incubation, the membrane was washed with TBS-T and incubated with anti-mouse IgG peroxidase-conjugated secondary antibody (1:1000 dilution).

Carbonylated proteins were assayed as previously described [25,26], with some modifications. Briefly, each lane of BN-PAGE was incubated with 12% SDS by 30 min at room temperature. Then, the lanes were derivatized with 20 mM DNPH/10% TFA. After 30 min in the dark, the reaction was stopped with equilibration buffer (2% (w/v) SDS, 6 M urea, 30% glycerol, 0.05 M Tris–HCl pH 8,8 and 20 mg/ml DTT) for 30 min at room temperature. The second dimension was obtained as described in 2D-BN-PAGE section and proteins were blotted onto a nitrocellulose membrane. Immunodetection of carbonylated proteins was performed using rabbit anti-DNP as primary antibody.

In order to validate gel data, the expression levels of ATPB were also evaluated by Western blotting analysis. In brief, mitochondrial proteins were separated by 12.5% SDS-PAGE, electrotransfered to a nitrocellulose membrane and immunodetection was carried for ATPB.

Immunoreactive bands were detected by enhanced chemiluminescence ECL (Amersham Pharmacia Biotech) according to the manufacturer's procedure and images were recorded using X-ray films (Kodak Biomax light Film, Sigma). The films and the gels were scanned in Molecular Imager Gel Doc XR + System (Bio-Rad) and analyzed with QuantityOne software (v 4.6.3 Bio-Rad). 2D-BN-PAGE blot images were analyzed with the PDQuest software (version 8.0.1; Bio-Rad). A matchset from 3 biological replicates was performed with correlation coefficient values of at least 0.8. To simplify the experiment, blots images were cropped and fitted to the same dimension (65 × 58mm) for further analyses. Following automatic spot detection, matching was performed. The image with the highest number of spots was selected as the master gel. The spot boundary tool was applied to detect large spots. The patterns in sections of the blots in appropriate magnification were checked and spots were added manually to the master image to allow matching unique spots present in the individual blots. The spot quantity table containing all matched spots was generated based on normalization of spot intensity (density) per total intensity of all valid spots in each blot image. In the case of carbonyl blot, the normalization was performed taken in consideration the total background intensity. The quantity table was exported to a spreadsheet .xls file and submitted to statistical analyses.

2.9. Protein identification by MALDI-TOF/TOF analysis

Spots from 2-D BN-PAGE were excised manually and in-gel tryptic digestion was performed. In brief, the gel pieces were washed twice with 25 mM ammonium bicarbonate/50% acetonitrile, followed by a wash with 100% acetonitrile. They were then dried under vacuum in a concentrator (SpeedVac® Plus SC 210A, Thermo Savant, NY, USA) and 21 µl of 10 µg/ml sequence-grade modified porcine trypsin in 25 mM ammonium bicarbonate was added to the dried residues and incubated overnight at 37 °C. The tryptic peptides were extracted from the gel with formic acid and were then dried under vacuum and re-suspended in 10 µl of a 50% acetonitrile/0.1% formic acid solution. Mass spectra was obtained on a matrix-assisted laser desorption/ionization–time of flight MALDI-TOF/TOF mass spectrometer (4800 Proteomics Analyzer, Applied Biosystems, Foster City, CA, USA) in the positive ion reflector mode and obtained in the mass range from 700 to 4500 Da with 1000 laser shots. A data-dependent acquisition method was created to select the ten most intense peaks in each sample spot for subsequent tandem mass spectrometry (MS/MS) data acquisition, excluding those from the matrix, due to trypsin autolysis or acrylamide peaks. Trypsin autolysis peaks (m/z 842.5 and m/z 2211.1) were used for internal calibration of the mass spectra. Spectra were processed and analyzed by the Global Protein Server Workstation (Applied Biosystems, Foster City, CA, USA), which uses internal Mascot software (Matrix Science, London, UK) on searching the peptide mass fingerprinting (PMF) and MS/MS data. Searches were performed against the Swiss-Prot nonredundant protein database (peptide fragment fingerprinting; rodents 18012009), allowing oxidation of methionine and acrylamide adducts (propionamide) of the cysteine residues as variable modifications. The peptide mass tolerance was 30 ppm and fragment ion mass tolerance was 0.3 Da. Protein identifications were considered as reliable when the MASCOT score was > 70 (MASCOT score was calculated as $-10 \times \log P$, where P is the probability that the observed match is a random event). This is the lowest confidence score for protein identification indicated by the program as significant ($p < 0.05$) and indicated by the probability of incorrect protein identification.

2.10. Posttranslational modifications identification by nLC-MALDI-MS/MS

The protein digests corresponding to the spots identified in the 2D Western blot maps were diluted to a final concentration of 5% acetonitrile and separated using an Ultimate 3000 (LCPackings) nano-HPLC. Briefly, the sample was washed over a C18 trapping column (Zorbax 300SB-C18, 5 µm particle size, 5 × 0.3 mm, Agilent Technologies) for 5 min with 95% buffer A (water, 0.1% TFA), 5% Buffer B (acetonitrile, 0.05% TFA) at a flow rate of 300 nl/min. Flow was then reversed over the trapping column, and sample was eluted onto a 150 mm × 75 µm Zorbax 300SB capillary analytical C18 column with 3.5 µm particle size (Agilent Technologies) at a flow rate of 300 nl/min. A linear gradient of 5% Buffer B to 50% Buffer B was run over a period of 35 min. The column was washed with a 5 min gradient from 50% to 85% Buffer B, followed by a 5-min hold at 85% Buffer B. The column was re-equilibrated in 5% Buffer B prior to further analyses. Using the micro-collector Probot (Dionex/LC Packings) and, after a lag time of 5 min, peptides eluting from the capillary column were mixed with a continuous flow of α-CHCA matrix solution (270 nl/min, 2 mg/ml in 70% ACN/0.3% TFA and internal standard Glu-Fib at 15 ftmol) were directly deposited onto the LC-MALDI plates at 20-second intervals for each spot (100 nl/fraction). For every separation run, 156 fractions were collected. The MS analysis was performed using a MALDI-TOF/TOF instrument. An S/N threshold of 50 was used to select peaks for MS/MS analyses. A fragmentation voltage of 2 kV was used throughout the automated runs.

Mass spectra were acquired and processed as described above. Mascot has the limitation of allowing only 9 modifications per search. Therefore, 6 independent searches were performed with a maximum of 9 modifications each, in a total of 26 variable different modifications. The following modifications targeted were oxidation (C, H, W, D, K, N, P, F, Y, R, M), dioxidation (W, M, F, Y, C, P, R, K, N), nitration (Y, W), nitrosilation (Y), nitrene insertion (Y), arginine oxidation to glutamic semialdehyde and lysine oxidation to aminoadipic semialdehyde. When a peptide presented different modifications in different searches, it was submitted to a new search using the combination of all the modifications identified for that same peptide, to eliminate false positives.

In order to estimate the false discovery rate (FDR) a random decoy database was created for all SwissProt in 8% of FDR (false positive peptides/(false positive peptides + total peptides))*100. Unique peptides retrieved from FDR search were considered for PTM characterization. Searched PTMs were considered as reliable when the program indicated the MASCOT score as significant ($p<0.05$) and the individual ion score for each MS/MS spectra (calculated as described above for protein search) was higher than 30. Further validation of peptide modifications found was conducted using the Paragon algorithm and the ProteinPilot 4.0 software (Applied Biosystems, Foster City, CA, USA) to perform a new search. For Paragon, PTMs were searched with a 95% confidence interval for protein identifications including two missed cleavages, biological modifications and FDR. Proteins were identified based on the presence of at least two unmodified peptides from the same protein by the Pro Group algorithm at the 99% confidence level. For PTM analysis of each protein, modified peptide confidence score cut-off >2 and 99 was used prior to manual inspection, if other peptides from presented confidence scores greater than 99. For Paragon searching algorithm, the peptide identification false positive rates were estimated at less than 3% based on the number of forward to reversed peptide hits.

Each PTM confirmed by both searching procedures was further manually validated.

2.11. Statistical analysis

Optical densities of differentially expressed protein spots in Western blots were exported from QuantityOne to SPSS (v15.0). The Kolmogorov–Smirnov test was used to test normality of distribution for all data (i.e., OXPHOS activity, gel and Western blotting analysis). Since all variables were normally distributed, significant differences between the two mitochondrial subpopulations were evaluated with the unpaired Student's *t*-test. A p value <0.05 was considered significant.

3. Results

3.1. Respiratory chain complexes organization and activity

To evaluate the effect of mitochondrial cell location on respiratory chain complexes' organization, digitonin-solubilized membrane proteins from SS and IMF fractions were resolved by BN-PAGE. As can be depicted in Fig. 1A, the pattern of the five respiratory chain complexes is consistent with the molecular weight described in the literature [23]. No qualitative or quantitative differences of the overall band pattern were observed among isolated IMF and SS mitochondria. Western blotting analysis of ATP synthase subunit beta was performed in order to validate the protein expression profile observed and no differences were observed among mitochondrial populations (Fig. S1). Interestingly, the analysis of the in-gel activity of complexes IV and V revealed higher activity levels in IMF mitochondria (Fig. 1). Spectrophotometric quantification of all respiratory chain complexes supports this tendency (Table 2). Indeed, higher activity levels of respiratory chain complexes II and IV were observed for IMF mitochondria, with uppermost values noticed for cytochrome *c* oxidase (1.6 fold, $p<0.05$). A tendency for increased activity in IMF mitochondria was observed for complexes I, III (Table 2) and V (Fig. 1 and Table 2).

3.2. Protein susceptibility to nitration and carbonylation

The mitochondrial membrane proteins' susceptibility to carbonylation and nitration was assessed by 2D-BN-PAGE followed by Western blotting with anti-DNP or anti-3-nitrotyrosine antibodies, respectively. A semi-quantitative comparative analysis of Western blots obtained with both antibodies was performed using the volume contour tool from the PDQuest software (Bio-Rad). As can be seen in Fig. 2–D, IMF mitochondria were more susceptible to membrane proteins nitration than SS whereas higher carbonylation levels were observed in this subpopulation. The proteins in the spots corresponding to carbonylated and/or nitrated proteins were further identified

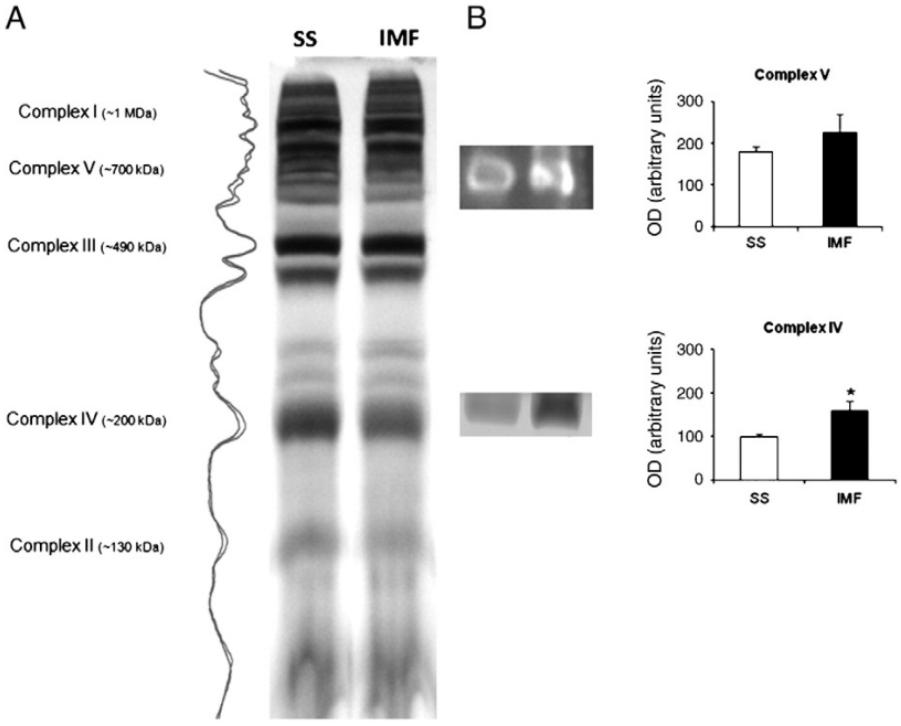

Fig. 1. (A) BN-PAGE profile of SS and IMF mitochondria. An overlap of the density variation for both lanes is presented on the right. (B) Representative image of histochemical staining of in-gel activity of complexes IV and V. On the right side is presented a semi-quantitative analysis of in-gel activity of both complexes. *$p<0.05$.

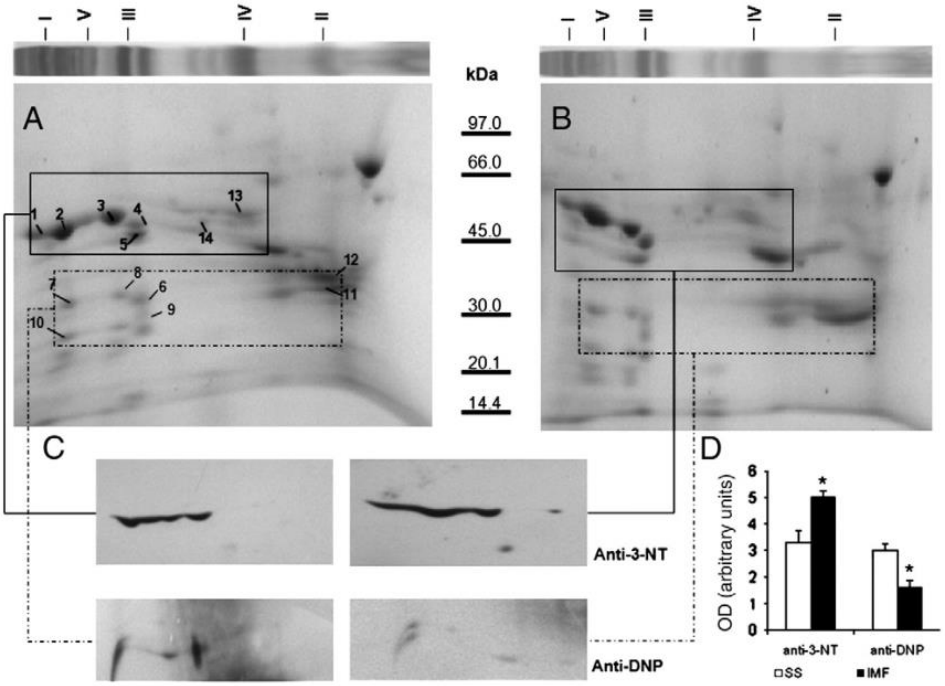

Fig. 2. Representative 2D maps for heart SS (A) and IMF (B) mitochondria are presented. A magnified comparison of 2D Western blot for nitrated and carbonylated proteins is presented in panel (C). Whole blot signal intensity was compared between mitochondrial subpopulations and significant differences ($p<0.05$) were found (D). For numbering refer to Table 1.

by MS/MS. In overall, 18 distinct proteins were detected as preferential targets of these modifications (7 nitrated and 15 carbonylated). From these, 8 proteins were observed in 2D-BN-PAGE spots corresponding to the predicted molecular weight.

Among the proteins with nitrated tyrosines were cytochrome *b–c*1 complex subunits 1 and 2 from complex III, ATP synthase subunits alpha and beta from complex V (spots 1, 2, 3, 4 and 5; Fig. 2 and Table 1), the tricarboxylic acid cycle enzymes, malate dehydrogenase and isocitrate dehydrogenase [NAD] subunit alpha, and dihydrolipoyl dehydrogenase, an enzyme of the pyruvate dehydrogenase complex (spots 13 and 14). The core proteins of complex III (spots 4 and 5) and the metabolic enzymes from the TCA cycle and pyruvate dehydrogenase complex presented higher nitration levels in IMF (1.6 ± 0.3-, 35.1 ± 11.2-, 23.6 ± 9.8-fold, respectively; $p<0.05$) (Fig. 1 and Table 1).

NADH dehydrogenase 1 alpha subcomplex subunit 9 (spot 7), succinate dehydrogenase flavoprotein and iron-sulfur subunits (spot 11), cytochrome *c* oxidase subunit 4 (spot 9) and ATP synthase subunits alpha and beta, gamma and f (spots 6, 7, 8 and 12) were found carbonylated in both mitochondrial subpopulations. A PDQuest evaluation of blotting data demonstrates the higher susceptibility ($p<0.05$) of ATP synthase subunit beta, cytochrome *c* oxidase polypeptide VIc-2 (spot 8) and ATP synthase subunit alpha (spot 9) to carbonylation in SS mitochondria (24.3 ± 5.1-, 32.2 ± 8.3-fold, respectively). Some of the detected proteins, particularly ATP synthase subunits alpha and beta, were identified in several different spots, with lower molecular weight than the intact proteins in both subpopulations, suggesting a higher turnover of these complex V subunits.

Complementary analysis of trypsin digests from gel spots corresponding to nitrated and carbonylated proteins was performed by nano-LC/MS/MS. With this approach, in both subpopulations we found oxidatively modified amino acid residues in NADH dehydrogenase 1 alpha subcomplex subunit 9, succinate dehydrogenase flavoprotein and iron-sulfur subunits, cytochrome *b–c*1 complex subunit 2, cytochrome *c* oxidase polypeptide VIc, and in ATP synthase subunits alpha and beta (Table 1). Among the modifications more prevalent we found pyro-Glu and Met oxidation (Table 1). Some of these pyro-Glu modifications were located in particular domains of respiratory chain complexes subunits. For instance, in cytochrome *c* oxidase polypeptide VIc, the pyro-Glu observed was in the topological domain of the mitochondrial intermembrane space, whereas in ATP synthase subunit alpha was in the nucleotide-binding domain. Fig. 3 shows a representative MS/MS spectrum of the precursor ion at *m/z* 1399 attributed to the modified peptide ^{157}FIHVSHLNASMK^{168} from NADH dehydrogenase [ubiquinone] 1 alpha subcomplex subunit 9. The hydroxylation at Lys168 (located in the Rossmann fold domain) was confirmed by the ions belonging to the a, b and y fragmentation series, where there are no modification for b series (until b11), but y1, y7 and y8 present a 16-Da mass shift due to the conversion of C-terminal lysine residue to hydoxylysine.

Regarding nitration, we screened the potential 3-nitrotyrosine-containing peptides; however, no satisfactory MS/MS spectra were obtained.

4. Discussion

When analyzing the impact of the mitochondria subcellular location on membrane proteins' susceptibility to oxidative modifications, overall our data showed higher levels of carbonylation in SS, whereas mitochondria trapped within the contractile apparatus seem more prone to nitration. Concomitantly, higher OXPHOS activity levels were detected in IMF compared to SS mitochondria. Since no significant differences on OXPHOS complexes composition were detected among subpopulations by PDQuest analysis of protein spots' intensity in 2D-BN-PAGE gels (further confirmed by Western blotting of ATPB), distinct OXPHOS activity seems to reflect membrane complexes' susceptibility to oxidative modifications. These results are consistent with the idea that mitochondrial dysfunction may be due to the higher susceptibility and/or accumulation of oxidatively modified proteins [2,16,17]. Moreover, our results are in agreement with the previous findings of Adhihetty et al. [10], that reported, in skeletal muscle, higher ROS production and damage in SS compared to IMF mitochondria. Indeed, though a natural consequence

Table 1
Nitrated (white lines) and carbonylated (grey lines) proteins identified in Western blots in cardiac SS and IMF mitochondria. Proteins for which modified peptides were found by nLC-MS/MS are signaled in bold.

Spot #	Protein name	UNIPROT Accession n°.	Protein MW	Protein pI	Peptide count	% coverage	Sequence	Modification	dMass (ppm)	Prec MW	Theor MW	Conf %	OD ratio 2D BN Page (IMF/SS)	OD ratio blot (IMF/SS)
1	ATP synthase subunit beta	ATPB_RAT	56318.5	5.19	21	47							1.3 ± 0.4	1.56 ± 0.4
	ATP synthase subunit alpha	ATPA_RAT	59716.6	9.22	19	45								
2	ATP synthase subunit beta	ATPB_RAT	56318.5	5.19	21	48							1.4 ± 0.3	1.56 ± 0.4
	ATP synthase subunit alpha	ATPA_RAT	59716.6	9.22	19	45								
3	ATP synthase subunit beta	ATPB_RAT	56318.5	5.19	21	48							−1.3 ± 0.4	1.56 ± 0.4
	ATP synthase subunit alpha	ATPA_RAT	59716.6	9.22	19	45								
4	Cytochrome b-c1 complex subunit 1	QCR1_RAT	52815.4	5.57	12	34							−1.4 ± 0.4	1.6 ± 0.3*
	Cytochrome b-c1 complex subunit 2	QCR2_RAT	48366.2	9.16	8	23								
5	Cytochrome b-c1 complex subunit 2	QCR2_RAT	48366.2	9.16	8	23							−1.5 ± 0.3	1.6 ± 0.3*
6	ATP synthase subunit beta	ATPB_RAT	56318.5	5.19	2	8							−1.9 ± 1.2	− 32.2 ± 8.3*
	Cytochrome b-c1 complex subunit 8	QCR8_MOUSE	9762.1	10.26	13	39								
	ATP synthase subunit alpha	ATPA_RAT	59716.6	9.22	2	5								
7	ATP synthase subunit gamma	ATPG_RAT	30171.7	8.87	4	12							−1.2 ± 0.5	−1.6 ± 0.2*
	NADH dehydrogenase [ubiquinone] 1 alpha subcomplex subunit 9	NDUA9_RAT	41785.9	9.77	16	41	FIHVSHLNASMK	Oxidation(K)@[12]	6	1399.72	1399.72	99		
							FIHVSHLNASMK	Oxidation(M)@[11]	−5	1399.72	1399.73	99		
							QPVYVADVSK	Gln->pyro-Glu@N-term	−7	1088.56	1088.56	99		
							WLSSEIEETKPAK	FormaldehydeAdduct(W)@1	−5	1529.77	1529.78	99		
	Dihydrolipoyllysine-residue succinyltransferase component of 2-oxoglutarate dehydrogenase complex	ODO2_RAT	48894.4	8.89	1	3								
8	ATP synthase subunit beta	ATPB_RAT	56318.5	5.19	10	18	IMNVIGEPIDER	Oxidation(M)@[2]	−5	1401.70	1401.71	99	− 1.91 ± 0.8	− 24.3 ± 5.1*
	ATP synthase subunit f	ATPK_MOUSE	10337.4	9.95	1	3								
	Cytochrome c oxidase polypeptide VIc-2	COX6C2_RAT	8455.0	10.07	6	21	QAGVFQSAK	Gln->pyro-Glu@N-term	−8	918.45	918.46	99		
9	Cytochrome c oxidase subunit 4 isoform 1	COX41_RAT	19502.1	9.45	9	24							1.6 ± 0.5	− 32.2 ± 8.3*
	ATP synthase subunit alpha	ATPA_RAT	59716.6	9.22	11	12	EAYPGDVFYLHSR	Glu->pyro-Glu@N-term	−5	1535.72	1535.72	99		
	ATP synthase subunit beta	ATPB_RAT	56318.5	5.19	12	27								
10	NADH dehydrogenase [ubiquinone] 1 alpha subcomplex subunit 10	NDUAA_RAT	40467.6	7.64	14	36							1.3 ± 0.4	−1.6 ± 0.2*
	ATP synthase subunit beta	ATPB_RAT	56318.5	5.19	11	25								
	Cytochrome b-c1 complex subunit 8	QCR8_RAT	9843.2	10.52	5	15								
	Cytochrome b-c1 complex subunit 2	QCR2_RAT	48366.2	9.16	15	33	EVAEQFLNIR	Glu->pyro-Glu@N-term	−6	1200.63	1200.64	99		
							MALVGLGVSHSILK	Oxidation(M)@[1]	−5	1440.82	1440.83	99		
							NALANPLYCPDYR	Carbamyl(C)@9; Dimethyl(R)@13	−5	1580.74	1580.75	99		
							QHLLGAGPHIK	Gln->pyro-Glu@N-term	−6	1153.64	1153.64	99		
							QPQELEFTK	Gln->pyro-Glu@N-term	−7	1102.53	1102.54	99		
							VAEQFLNIR	Lys-add@N-term	−6	1217.61	1217.62	99		
	ATP synthase subunit beta	ATPB_RAT	56318.5	5.19	9	36								
	NADH dehydrogenase [ubiquinone] iron-sulfur protein 3	NDUS3_MOUSE	30130.5	6.67	13	33								
11	Succinate dehydrogenase [ubiquinone] flavoprotein subunit	DHSA_RAT	71569.7	6.75	12	22	VSQLYGDLQHLK	Gln->Lys@[9]	−13	1399.76	1399.78	99	1.7 ± 0.8	−1.4 ± 0.6
	Succinate dehydrogenase [ubiquinone] iron-sulfur subunit	DHSB_RAT	31808.9	8.96	14	42	DLVPDLSNFYAQYK	Oxidation (P)@[4]; Asp->Val@[5]	−22	1671.81	1671.85	99		
							IYPLPHMYVIK	Oxidation(M)@[7]	−3	1388.75	1388.75	99		
							QQYLQSIEDR	Gln->pyro-Glu@N-term	1	1261.59	1261.59	99		
							QQYLQSIEDREK	Gln->pyro-Glu@N-term	0	1518.73	1518.73	99		
							YLGPAVLMQAYR	Dethiomethyl(M)@[8]	−20	1332.69	1332.72	99		
	Dihydrolipoyl dehydrogenase	DLDH_RAT	54004.1	7.96	9	29								
12	ATP synthase subunit beta	ATPB_RAT	56318.5	5.19	15	33							− 1.9 ± 0.6	− 2.9 ± 1.4*
13	Malate dehydrogenase	MDHM_RAT	35660.8	8.93	14	37							− 1.8 ± 1.3	35.1 ± 11.2*
	Dihydrolipoyl dehydrogenase	DLDH_RAT	54004.1	7.96	9	15								
14	Isocitrate dehydrogenase [NAD] subunit alpha	IDH3A_RAT	39588.0	6.47	10	16							3.2 ± 1.3*	23.6 ± 9.8*

*$p < 0.05$.

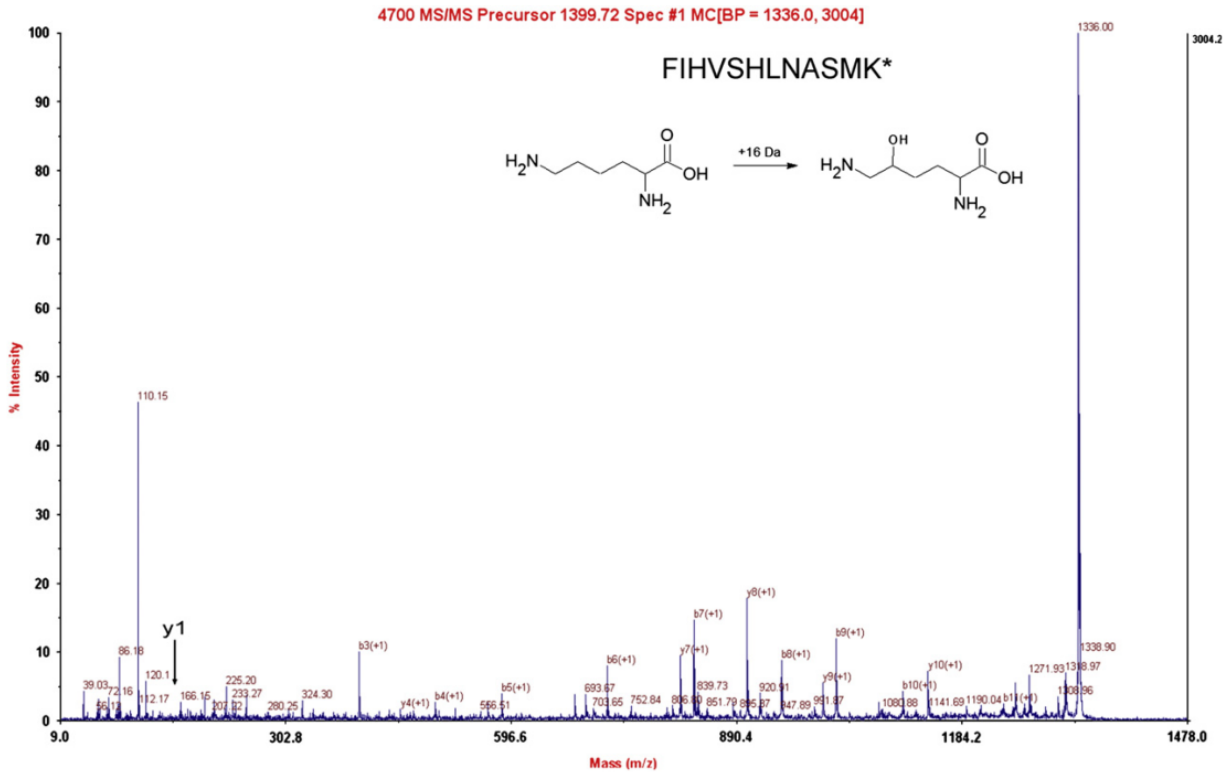

Fig. 3. MS/MS spectrum of the peptide ^{157}FIHVSHLNASMK^{168} derived from tryptic digestion of NADH dehydrogenase [ubiquinone] 1 alpha subcomplex subunit 9 (accession # NDUA9_RAT) which contains an oxidation (+16 Da mass shift) at the terminal lysine (indicated as *K**). The b and y ion series are annotated.

of aerobic life, the accumulation of carbonylated mitochondrial proteins is undoubtedly associated with impaired respiratory function, playing a crucial role in the cellular response to physiopathological stimuli [12,16,17]. The comparative analysis of nitrotyrosine levels (Table 1 and Figs. 1 and 2) suggests that the nitration of mitochondrial complexes, particularly of complex III, did not affect their function, since higher 3-NT levels were paralleled with an increased OXPHOS efficiency noticed in IMF mitochondria. If these modifications caused structural change(s), this did not affect their function. Unlike carbonylation, the role of protein nitration in cell physiology is unclear [27]. This posttranslational modification occurs as a consequence of the reaction of superoxide with NO, a cellular messenger found in cardiac tissue, to produce the highly reactive peroxynitrite anion that reacts with proteins generating nitrotyrosine [12,14]. According to some authors [27,28], tyrosine nitration can be selective, dynamic and reversible, leaving open the possibility of being beneficial as well as detrimental. For instance, protein nitration might regulate electron transport chain (ETC) activity such that excessive superoxide generation is blocked, buffering changes in oxygen concentration [27]. Looking specifically to the protein targets of nitration, the results do not support the deleterious effect of this modification on OXPHOS efficiency (Tables 1 and 2). This was particularly evident for complex III, being core protein 1 and 2 preferential targets of RONS-induced posttranslational modifications due to its location in the ETC process [16]. The metabolic enzymes malate dehydrogenase, dihydrolipoyl dehydrogenase and isocitrate dehydrogenase subunit alpha were found to be significantly more nitrated in IMF (Table 1), attenuating the deleterious effect of increased superoxide anion produced [12,14] as a consequence of the higher metabolic activity reported in this mitochondrial subpopulation [11,18,29].

Among the other 12 distinct OXPHOS proteins identified as more prone to carbonylation and/or nitration, the high susceptibility of F1F0-ATP synthase stands out. Although not part of the ETC, its location, as well as its abundance, makes it a prime candidate for oxidative modification [14,16]. During enzyme turnover, ATP synthase goes through a sequence of coordinated conformational changes of its major subunits [14]. The high susceptibility of ATP synthase subunits alpha and beta to oxidation, together with the high number of its fragments observed in 2D-BN-PAGE gels (Fig. 2 and Table 1), supports the notion of an elevated turnover of complex V. According to Choksi et al. [16], oxidative modifications of the alpha and beta chains may alter their binding affinity for complex V and dissociation of both modified proteins from complex V may be a protective function. The more than 20-fold increase in the carbonylation of ATP synthase subunits alpha and beta observed in SS mitochondria is paralleled by lower activity in this subpopulation (Table 2). The main carbonyl products of metal-catalyzed oxidation of

Table 2
Respiratory chain complexes activity in SS and IMF mitochondria, measured spectrophotometrically.

Mitochondrial subpopulation	NADH:ubiquinone oxidoreductase (U/g)	Succinate:ubiquinone reductase (μmol/min/g)	Cytochrome *c* reductase activity (μmol/min/g)	Cytochrome *c* oxidase (nmol/min/mg)	ATP synthase (μmolPi/min/mg)
SS	56.7 ± 7.6	186.2 ± 23.4	82.3 ± 11.2	61.7 ± 11.0	15.9 ± 6.0
IMF	68.5 ± 10.4	222.8 ± 10.1*	107.7 ± 13.4	101.8 ± 20.7 *	21.9 ± 2.3

* $p<0.05$.

proteins, glutamic and aminoadipic semialdehydes usually related to protein dysfunction [15], were not identified in the present study. Apart from the amino acid residue found modified (pyro-Glu) in the nucleotide binding domain of ATP synthase subunit alpha, no evidence of oxidative modifications-induced structural changes was noticed and warranted further investigation. Nevertheless, an association between protein susceptibility to carbonylation and decreased activity was noticed for the ETC complexes, whose subunits were found more carbonylated in SS mitochondria.

In conclusion, our results show evidence of higher OXPHOS activity in IMF compared to SS mitochondria; moreover, unlike nitration, the overall effect of increased carbonylation of OXPHOS complexes subunits may be an underlying mechanism of cardiac mitochondria decreased functionality.

Supplementary materials related to this article can be found online at doi:10.1016/j.bbabio.2011.04.002.

Acknowledgments

This work was supported by the Portuguese Foundation for Science and Technology (FCT) [grant numbers PTDC/QUI/72683/2006, REDE/1505/REM/2005, SFRH/BD/66642/2009 (to A.I.P.), SFRH/BPD/24158/2005 (to R.F.) and SFRH/BD/46829/2008 (to R.A.)]. The authors would like to thank Celeste Resende for her assistance in animal care.

References

[1] G. Benard, B. Faustin, E. Passerieux, A. Galinier, C. Rocher, N. Bellance, J.P. Delage, L. Casteilla, T. Letellier, R. Rossignol, Physiological diversity of mitochondrial oxidative phosphorylation, Am. J. Physiol. Cell Physiol. 291 (2006) C1172–C1182.
[2] S.M. Bailey, A. Landar, V. Darley-Usmar, Mitochondrial proteomics in free radical research, Free Radic. Biol. Med. 38 (2005) 175–188.
[3] J.R. Smith, I.R. Matus, D.A. Beard, A.S. Greene, Differential expression of cardiac mitochondrial proteins, Proteomics 8 (2008) 446–462.
[4] A. Riva, B. Tandler, F. Loffredo, E. Vazquez, C. Hoppel, Structural differences in two biochemically defined populations of cardiac mitochondria, Am. J. Physiol. Heart Circ. Physiol. 289 (2005) H868–H872.
[5] C.L. Hoppel, B. Tandler, H. Fujioka, A. Riva, Dynamic organization of mitochondria in human heart and in myocardial disease, Int. J. Biochem. Cell Biol. 41 (2009) 1949–1956.
[6] L. Manneschi, A. Federico, Polarographic analyses of subsarcolemmal and intermyofibrillar mitochondria from rat skeletal and cardiac muscle, J. Neurol. Sci. 128 (1995) 151–156.
[7] E.R. Dabkowski, W.A. Baseler, C.L. Williamson, M. Powell, T.T. Razunguzwa, J.C. Frisbee, J.M. Hollander, Mitochondrial dysfunction in the type 2 diabetic heart is associated with alterations in spatially distinct mitochondrial proteomes, Am. J. Physiol. Heart Circ. Physiol. 299 (2009) H529–H540.
[8] D.A. Hood, Invited review: contractile activity-induced mitochondrial biogenesis in skeletal muscle, J. Appl. Physiol. 90 (2001) 1137–1157.
[9] M. Takahashi, D.A. Hood, Protein import into subsarcolemmal and intermyofibrillar skeletal muscle mitochondria. Differential import regulation in distinct subcellular regions, J. Biol. Chem. 271 (1996) 27285–27291.
[10] P.J. Adhihetty, V. Ljubicic, K.J. Menzies, D.A. Hood, Differential susceptibility of subsarcolemmal and intermyofibrillar mitochondria to apoptotic stimuli, Am. J. Physiol. Cell Physiol. 289 (2005) C994–C1001.
[11] J.W. Palmer, B. Tandler, C.L. Hoppel, Biochemical properties of subsarcolemmal and interfibrillar mitochondria isolated from rat cardiac muscle, J. Biol. Chem. 252 (1977) 8731–8739.
[12] J. Murray, C.E. Oquendo, J.H. Willis, M.F. Marusich, R.A. Capaldi, Monitoring oxidative and nitrative modification of cellular proteins; a paradigm for identifying key disease related markers of oxidative stress, Adv. Drug Deliv. Rev. 60 (2008) 1497–1503.
[13] I. Dalle-Donne, M. Carini, M. Orioli, G. Vistoli, L. Regazzoni, G. Colombo, R. Rossi, A. Milzani, G. Aldini, Protein carbonylation: 2,4-dinitrophenylhydrazine reacts with both aldehydes/ketones and sulfenic acids, Free Radic. Biol. Med. 46 (2009) 1411–1419.
[14] J. Kanski, A. Behring, J. Pelling, C. Schoneich, Proteomic identification of 3-nitrotyrosine-containing rat cardiac proteins: effects of biological aging, Am. J. Physiol. Heart Circ. Physiol. 288 (2005) H371–H381.
[15] J.R. Requena, C.C. Chao, R.L. Levine, E.R. Stadtman, Glutamic and aminoadipic semialdehydes are the main carbonyl products of metal-catalyzed oxidation of proteins, Proc. Natl. Acad. Sci. U. S. A. 98 (2001) 69–74.
[16] K.B. Choksi, J. Papaconstantinou, Age-related alterations in oxidatively damaged proteins of mouse heart mitochondrial electron transport chain complexes, Free Radic. Biol. Med. 44 (2008) 1795–1805.
[17] R.M. Alves, R. Vitorino, P. Figueiredo, J.A. Duarte, R. Ferreira, F. Amado, Lifelong physical activity modulation of the skeletal muscle mitochondrial proteome in mice, J. Gerontol. A. Biol. Sci. Med. Sci. 65 (2010) 832–842.
[18] R. Ferreira, R. Vitorino, R.M. Alves, H.J. Appell, S.K. Powers, J.A. Duarte, F. Amado, Subsarcolemmal and intermyofibrillar mitochondria proteome differences disclose functional specializations in skeletal muscle, Proteomics 10 (2010) 3142–3154.
[19] R.W. Taylor, M.A. Birch-Machin, K. Bartlett, S.A. Lowerson, D.M. Turnbull, The control of mitochondrial oxidations by complex III in rat muscle and liver mitochondria. Implications for our understanding of mitochondrial cytopathies in man, J. Biol. Chem. 269 (1994) 3523–3528.
[20] A.J. Janssen, F.J. Trijbels, R.C. Sengers, J.A. Smeitink, L.P. van den Heuvel, L.T. Wintjes, B.J. Stoltenborg-Hogenkamp, R.J. Rodenburg, Spectrophotometric assay for complex I of the respiratory chain in tissue samples and cultured fibroblasts, Clin. Chem. 53 (2007) 729–734.
[21] M.A. Birch-Machin, H.L. Briggs, A.A. Saborido, L.A. Bindoff, D.M. Turnbull, An evaluation of the measurement of the activities of complexes I–IV in the respiratory chain of human skeletal muscle mitochondria, Biochem. Med. Metab. Biol. 51 (1994) 35–42.
[22] N. Simon, C. Morin, S. Urien, J.P. Tillement, B. Bruguerolle, Tacrolimus and sirolimus decrease oxidative phosphorylation of isolated rat kidney mitochondria, Br. J. Pharmacol. 138 (2003) 369–376.
[23] H. Schagger, G. von Jagow, Blue native electrophoresis for isolation of membrane protein complexes in enzymatically active form, Anal. Biochem. 199 (1991) 223–231.
[24] E. Zerbetto, L. Vergani, F. Dabbeni-Sala, Quantification of muscle mitochondrial oxidative phosphorylation enzymes via histochemical staining of blue native polyacrylamide gels, Electrophoresis 18 (1997) 2059–2064.
[25] C.C. Conrad, J. Choi, C.A. Malakowsky, J.M. Talent, R. Dai, P. Marshall, R.W. Gracy, Identification of protein carbonyls after two-dimensional electrophoresis, Proteomics 1 (2001) 829–834.
[26] C.E. Robinson, A. Keshavarzian, D.S. Pasco, T.O. Frommel, D.H. Winship, E.W. Holmes, Determination of protein carbonyl groups by immunoblotting, Anal. Biochem. 266 (1999) 48–57.
[27] K.S. Aulak, T. Koeck, J.W. Crabb, D.J. Stuehr, Dynamics of protein nitration in cells and mitochondria, Am. J. Physiol. Heart Circ. Physiol. 286 (2004) H30–H38.
[28] A.J. Gow, C.R. Farkouh, D.A. Munson, M.A. Posencheg, H. Ischiropoulos, Biological significance of nitric oxide-mediated protein modifications, Am. J. Physiol. Lung Cell. Mol. Physiol. 287 (2004) L262–L268.
[29] A.M. Cogswell, R.J. Stevens, D.A. Hood, Properties of skeletal muscle mitochondria isolated from subsarcolemmal and intermyofibrillar regions, Am. J. Physiol. 264 (1993) C383–C389.

STUDY III - IMPAIRED PROTEIN QUALITY CONTROL SYSTEM UNDERLIES MITOCHONDRIAL DYSFUNCTION IN SKELETAL MUSCLE OF STREPTOZOTOCIN-INDUCED DIABETIC RATS

Biochimica et Biophysica Acta 1822 (2012) 1189–1197

Contents lists available at SciVerse ScienceDirect

Biochimica et Biophysica Acta

journal homepage: www.elsevier.com/locate/bbadis

Impaired protein quality control system underlies mitochondrial dysfunction in skeletal muscle of streptozotocin-induced diabetic rats

Ana Isabel Padrão [a], Tiago Carvalho [a], Rui Vitorino [a], Renato M.P. Alves [a], Armando Caseiro [a], José Alberto Duarte [b], Rita Ferreira [a], Francisco Amado [a,c,*]

[a] QOPNA, Chemistry Department, University of Aveiro, Aveiro, Portugal
[b] CIAFEL, Faculty of Sport, University of Porto, Porto, Portugal
[c] School of Health Sciences, University of Aveiro, Aveiro, Portugal

ARTICLE INFO

Article history:
Received 9 December 2011
Received in revised form 6 April 2012
Accepted 13 April 2012
Available online 21 April 2012

Keywords:
Intermyofibrillar mitochondria
Mitochondrial proteolysis
Protein quality control
Gastrocnemius
Type 1 diabetes mellitus

ABSTRACT

Hyperglycaemia-related mitochondrial impairment is suggested as a contributor to skeletal muscle dysfunction. Aiming a better understanding of the molecular mechanisms that underlie mitochondrial dysfunction in type 1 diabetic skeletal muscle, the role of the protein quality control system in mitochondria functionality was studied in intermyofibrillar mitochondria that were isolated from *gastrocnemius* muscle of streptozotocin (STZ)-induced diabetic rats. Hyperglycaemic rats showed more mitochondria but with lower ATP production ability, which was related with increased carbonylated protein levels and lower mitochondrial proteolytic activity assessed by zymography. LC-MS/MS analysis of the zymogram bands with proteolytic activity allowed the identification of an AAA protease, Lon protease; the metalloproteases PreP, LAP-3 and MIP; and cathepsin D. The content and activity of the Lon protease was lower in the STZ animals, as well as the expression of the m-AAA protease paraplegin, evaluated by western blotting. Data indicated that in muscle from diabetic rats the mitochondrial protein quality control system was compromised, which was evidenced by the decreased activity of AAA proteases, and was accompanied by the accumulation of oxidatively modified proteins, thereby causing adverse effects on mitochondrial functionality.

1. Introduction

Mitochondria are the center of fatty acid and glucose metabolism [1,2] and thus are likely to be impacted by the impaired metabolism related with diabetes mellitus [2–5], particularly evident in skeletal muscle because of its high metabolic rate [4]. Indeed, skeletal muscle mitochondrial dysfunction has already been linked with insulin deprivation and/or resistance [6]. Dysfunctional mitochondria carry a greater risk of futile ATP hydrolysis and enhanced reactive oxygen species (ROS) generation [2,3,7], being mitochondrial respiratory chain one of its main sources and mitochondrial proteins especially susceptible to oxidative modification [3,8]. When this damage cannot be repaired by chaperones, defective proteins are targeted for degradation [7,9]. Selective proteolysis occurs in mitochondria in order to remove short-lived regulatory proteins and to prevent the harmful accumulation of non-native polypeptides. By degrading misfolded and non-assembled polypeptides, mitochondrial proteases perform quality control surveillance in the organelle [1,7,9]. Among the mitochondrial proteolytic systems are the membrane-bound ATP-dependent proteases, namely m-AAA proteases composed of Afg312 and paraplegin subunits, which mediate the breakdown of membrane proteins, Clp-like and Lon proteases that are present in the matrix and HtrA2/Omi in the intermembrane space [1,7,10–12]. Given the protective role of these mitochondrial proteases, interest is unsurprisingly increasing in the literature aiming the understanding of the quality control surveillance mechanisms involved in pathophysiological conditions, like neurodegenerative diseases, aging [7], and cancer [13]. For instance, a correlation between decreased Lon protein levels and increased ROS concentration was observed with increasing age [14]. Although a clear association between defective mitochondrial oxidative phosphorylation (OXPHOS) and diabetes has already been reported [2,3,5,6], the contribution of mitochondrial proteases to the organelle's dysfunction secondary to this disease is far from being understood.

The mitochondria's ability to adapt to hyperglycaemia depends on cell type. Within myofibers, mitochondria exist in two spatial distinct populations according to their subcellular spatial arrangement. Subsarcolemmal (SS) mitochondria are found beneath the sarcolemma, and intermyofibrillar (IMF) mitochondria are intermingled within the myofibrils [4,15,16]. Although similar in their central role in cellular function, mitochondrial subpopulations demonstrate unique adaptative capacities according to their different functional, compositional, and

Abbreviations: BN-PAGE, blue native polyacrylamide gel electrophoresis; Anti-DNP, anti-2,4-dinitrophenylhydrazone; OXPHOS, oxidative phosphorylation; IMF, intermyofibrillar mitochondria; STZ, streptozotocin; T1DM, type 1 diabetes mellitus

* Corresponding author at: School of Health Sciences, University of Aveiro, Campus de Santiago, 3810-193 Aveiro, Portugal. Tel.: +351 234370700; fax: +351 234370084.
E-mail address: famado@ua.pt (F. Amado).

0925-4439/$ – see front matter © 2012 Elsevier B.V. All rights reserved.
doi:10.1016/j.bbadis.2012.04.009

biochemical properties [17]. For instance, in obese-insulin-resistant subjects, skeletal muscle IMF content was lower and correlated with abnormal fuel utilization patterns [18]. Adhihetty et al. [19] reported a greater rate of mtPTP opening within the IMF subpopulation in response to ROS. A similar effect was observed by Williamson et al. [20] in the cardiac mitochondria of streptozotocin (STZ) rats and was accomplished by significant changes in the levels of apoptotic proteins, which is suggestive of an association between diabetes-related mitochondrial dysfunction and an enhanced apoptotic propensity of IMF mitochondria. These findings suggest a greater susceptibility of IMF to hyperglycaemia, and the need for a deeper examination of the molecular mechanisms that underlie the spatial influence of the diabetic phenotype on mitochondrial dysfunction. Thus, the goal of our study was to determine whether IMF mitochondrial protein quality control systems are affected by STZ-induced hyperglycaemia and how they relate to mitochondrial dysfunction in skeletal muscle.

2. Materials and methods

2.1. Chemicals

Streptozotocin [N-(Methylnitrosocarbamoyl)-a-D-glucosamine] was obtained from Sigma Chemical Co. (St Louis, MO, USA), and prepared prior to use in 100 mM citrate, pH 4.5. All other reagents and chemicals used were of highest grade of purity commercially available. Rabbit polyclonal anti-paraplegin antibody (cat. no. sc-135026) was obtained from Santa Cruz Biotechnology, INC. (CA, USA). Rabbit polyclonal anti-mtTFA antibody (cat. no. ab47548), rabbit polyclonal anti-mitofilin antibody (cat. no. ab48139), rabbit polyclonal anti-LONP1 (ab103809) and mouse monoclonal anti-ATPB antibody (cat. no. ab14730) were obtained from Abcam (Cambridge, UK). Rabbit polyclonal anti-DNP antibody was obtained from DakoCytomation (Hamburg; Germany). Mouse monoclonal MMP-9 (Clone 36020; cat.no.MAB936) was acquired from R&D systems (Minneapolis, USA) and rabbit polyclonal anti-UCP3 (U7757) was obtained from Sigma. Secondary peroxidase-conjugated antibodies (anti-mouse IgG and anti-rabbit IgG) were obtained from GE Healthcare (Buckinghamshire, UK).

2.2. Animals

Twenty Wistar male rats (aged 6–8 weeks, weighing 200 g at the beginning of the experiments) were used. During the experimental protocol, the animals were housed in collective cages (4 rats per cage) and were maintained in a room at normal environment (21–24 °C; ~50–60% humidity) receiving food and water *ad libitum* in 12 h light/dark cycles. The animals were randomly divided into two groups ($n = 10$ *per* group): type 1 diabetic group (T1DM) and control group (CONT). Housing and experimental treatment were in accordance with *Guide for the Care and Use of Laboratory Animals* from the Institute for Laboratory Animal Research (ILAR, 1996). The local Ethics Committee had approved the study and the experimental procedures were complied with the current national laws.

2.3. Induction and characterization of STZ-induced hyperglycemia

In order to induce hyperglycemia, one group of animals (T1DM) was treated with a single intraperitoneal injection of Streptozotocin (STZ; 60 mg/kg), after a 16-h fasting period. Control animals were injected with citrate solution. During the experimental period, weight was measured and glucose concentration was determined in blood samples collected from the tail vein with Glucocard (A. Menarini diagnostic). Values were taken just before STZ administration and in the weeks after until the end of the protocol. Animals were considered hyperglycemic when, after feeding, blood glucose exceeded 250 mg/dl. After 4r months, animals were sacrificed and gastrocnemius muscle was dissected out. Small muscle portions were kept for TEM analysis with the remaining tissue used for the isolation of mitochondrial populations. Three pools of muscles from 3 or 4 rats were performed for each experimental group.

2.4. IMF mitochondria isolation

The IMF mitochondria were purified from gastrocnemius muscle following the protocol described by Ferreira et al. [15], which is based on tissue mechanical treatment and enzymatic digestion as previously reported by Palmer et al. [21]. Muscle pools from each group were simultaneously processed to avoid potential methodological bias. All the procedures were performed on ice or below 4 °C. The muscle tissue was washed three times with 20 mM MOPS, 110 mM KCl, 1 mM EGTA (pH 7.5), minced with scissors and then incubated in the aforementioned buffer with 0.25 mg/mL trypsin (Promega, Wisconsin, USA). After 25 min on ice, albumin fat-free (Sigma, St. Louis, MO, USA) was added to a final concentration of 10 mg/mL. The tissue was subsequently rinsed three times with buffer and then homogenized with a Potter homogenizer (Teflon pestle). An aliquot of whole homogenate was separated for CS activity assay. Large cellular debris and nuclei were pelleted by centrifuging for 5 min at 1000 ×*g*. A mitochondria enriched fraction was obtained by centrifuging the supernatant for 20 min at 16,000 ×*g* and re-suspending the pellet in a small volume of buffer (250 mM sucrose, 10 mM Tris–HCl, 0.1 mM EGTA (pH 7.4)). Pure IMF mitochondria were then obtained by ultracentrifugation at 95,000 ×*g* for 30 min on a density-gradient with 50% (v/v) Percoll. Two brown bands were observed; the lower band corresponded to IMF mitochondria while the upper band corresponded to SS mitochondria [15]. The IMF mitochondrial fraction was then washed twice and aliquoted for TEM analysis, BN-PAGE, in-gel activity of complexes IV and V, spectrophotometric assay of complexes III and V activities, immunoblot detection of paraplegin, Lon, ATP synthase subunit β, mtTFA, UCP-3, mitofilin, slot–blot of carbonyl content and MMP-9 and zymography/nLC-Maldi-MS/MS analysis of mitochondrial proteases. Protein content was determined with RC DC Protein Assay kit (Bio-Rad, Hercules, CA, USA) and mtDNA content was quantified with Qubit™ fluorometer (Invitrogen, Carlsbad, CA, USA).

2.5. Electron microscopic analysis

For morphological characterization, 75 μL of mitochondrial suspension of IMF mitochondria of each group was centrifuged at 7000 ×*g* for 10 min and the resulting pellet was processed as previously described [15]. Ultra-thin (100 nm) sections were contrasted with uranyl acetate and lead citrate for TEM analysis (Zeiss EM 10A).

2.6. Citrate synthase (CS) activity

The CS activity was measured in muscle homogenate and in IMF mitochondria using the method proposed by Coore et al. [22]. In brief, the CoASH released from the reaction of acetyl-CoA with oxaloacetate was measured by its reaction with 5,5′-dithiobis-(2-nitrobenzoic acid) (DTNB) at 412 nm (molar extinction coefficient $\varepsilon = 13.6\ mM^{-1}\ cm^{-1}$).

2.7. Respiratory chain complexes activities

For spectrophotometric determination of respiratory chain complexes activity (III and V), the mitochondrial fractions were disrupted by a combination of freeze–thawing cycles in hypotonic media (25 mM potassium phosphate, pH 7.2) to allow free access to substrates for all assays [23]. CIII activity was measured at 550 nm ($\varepsilon = 19\ mM^{-1}\ cm^{-1}$) in a reaction mixture containing reaction buffer (50 mM potassium phosphate, pH 7.4, 5 mM $MgCl_2$, and 1 mg/ml BSA), 1 μg of sonicated mitochondria, 20 μM rotenone, 2 mM KCN, 0.2 mM ATP, and 40 μM cytochrome *c*. The reaction was initiated by the addition of 100 μM decyl benzoquinol with or without 7.4 μM antimycin A. The final rate was measured by subtracting the antimycin A-insensitive rate from the rate without the addition of the

inhibitor [24]. ATP synthase activity was measured according to Simon et al. [25]. The phosphate produced by hydrolysis of ATP reacts with ammonium molybdate in the presence of reducing agents to form a blue-color complex, the intensity of which is proportional to the concentration of phosphate in solution. Oligomycin was used as an inhibitor of mitochondrial ATPase activity.

A Multiskan GO Microplate Spectrophotometer (Thermo Scientific) was used for respiratory chain complexes activities measurement, which was performed at 30 °C.

2.8. Blue-native PAGE separation of mitochondria membrane complexes

BN-PAGE was performed using the method described by Schägger and von Jagow [26] with minor modifications. IMF mitochondria (400 μg of protein) from each group (duplicate of $n=3$) were pelleted by centrifugation at 20,000 ×*g* for 10 min and then resuspended in solubilization buffer (50 mM NaCl, 50 mM Imidazole, 2 mM α-amino n-caproic acid, 1 mM EDTA pH 7.0) with 1% (w/v) digitonin. After 10 min on ice, insoluble material was removed by centrifugation at 20,000 ×*g* for 30 min at 4 °C. Soluble components were combined with 0.5% (w/v) Coomassie Blue G250, 50 mM α-amino n-caproic acid, 4% (w/v) glycerol and separated on a 4–13% gradient acrylamide gradient gel with 3.5% sample gel on top. Anode buffer contained 25 mM Imidazole pH 7.0. Cathode buffer (50 mM Tricine and 7.5 mM Imidazole pH 7.0) containing 0.02% (w/v) Coomassie Blue G250 was used during 1 h at 70 V, the time needed for the dye front reach approximately one-third of the gel. Cathode buffer was then replaced with one containing only 0.002% (w/v) Coomassie Blue G250 and the native complexes were separated at 200 V for 4 h at 4 °C. A native protein standard HMW-native marker (GE Healthcare, Buckinghamshire, UK) was used. The gels were stained with Coomassie Colloidal (0.12% (w/v) Coomassie Blue G250 prepared in 20% methanol) after 1 h fixation in a solution of 10% acetic acid and 40% methanol. Gels were then destained with 25% methanol and scanned with Gel Doc XR System (Bio-Rad, Hercules, CA, USA). Band detection, quantification and matching were performed using QuantityOne Imaging software (v4.6.3, Bio-Rad).

2.9. In-gel activity of complexes IV and V

The histochemical staining assays of complexes IV and V were determined using the methods described by Zerbetto et al. [27] with minor modifications. Complex IV-specific heme stain in BN-PAGE gels was determined using 10 μL horse heart cytochrome *c* (5 mM) and 0.5 mg diaminobenzidine (DAB) dissolved in 1 mL 50 mM sodium-phosphate, pH 7.2. The reaction was stopped by 50% (v/v) methanol, 10% (v/v) acetic acid, and the gels were then transferred to water. ATP hydrolysis activity of complex V was analyzed by incubating the native gels with 35 mM Tris, 270 mM glycine buffer, pH 8.3 at 37 °C, that had been supplemented with 14 mM $MgSO_4$, 0.2% (w/v) $Pb(NO_3)_2$, and 8 mM ATP. Lead phosphate precipitation that is proportional to the enzymatic ATP hydrolysis activity was stopped by 50% (v/v) methanol (after 30 min), and the gels were then transferred to water.

2.10. Analysis of mitochondrial proteolytic activity analysis through gelatine zymography

Zymography assays were performed according to Vitorino et al. [28] with minor alterations. Briefly, the zymography was performed using a 10% SDS-PAGE separation gel with 0.1% of gelatin. Forty micrograms of IMF mitochondria from each group was incubated on charging buffer (100 mM Tris pH 6.8, 5% SDS, 20% glycerol, 0.1% bromophenol blue) for 10 min on ice, in a proportion of 1:1 (v/v). After the run, the gels were incubated in renaturation buffer (2.5% Triton X-100) for 30 min, with soft agitation. Then, the zymogram gels were changed to a development buffer (50 mM Tris, 5 mM NaCl, 10 mM $CaCl_2$, 1 μm $ZnCl_2$, 0.02% (v/v) Triton X-100, pH 7.4) for more 30 min, also with soft agitation. Finally, the gels were changed to a new development buffer, and incubated overnight at 37 °C. For specific inhibition studies zymograms were incubated in the presence of 10 mM EDTA or 1 mM PMSF. The zymography gels were stained with 0.12% (w/v) Coomassie Blue G250 prepared in 20% methanol, after 1 h fixation in a solution of 10% acetic acid and 40% methanol. Gels were then destained with 25% methanol and scanned with Gel Doc XR System (Bio-Rad).

2.11. Proteases identification by nLC-MALDI-MS/MS analysis

The zymography bands that showed proteolytic activity were excised manually from the gel and washed with 25 mM of ammonium bicarbonate/50% acetonitrile and dried under vacuum (SpeedVac® Plus SC 210 A, Thermo Savant, USA). The dried gel pieces were rehydrated with 25 μL of 10 μg/mL trypsin in 50 mM ammonium bicarbonate and digested overnight at 37 °C. Tryptic peptides were extracted from the gel with formic acid and were then dried in a vacuum concentrator and re-suspended in a 10 μL of a 50% acetonitrile/0.1% formic acid solution.

Separation of tryptic peptides by nano-HPLC was performed on the module separation Ultimate 3000 (Dionex, Amsterdam), using a capillary column (Pepmap 100, 3 μm particle size; 0.75 μm internal diameter; 15 cm length). A gradient was used from the A solvent–H_2O/acetonitrile/trifluoracetic acid (95:5:0.045 v/v/v)—to the B solvent—H_2O/acetonitrile/trifluoracetic acid (20/80/0.04 v/v/v). The separation was performed using a linear gradient (5–55% B solution, for 30 min, 55–80% B solution for 10 min and 80–5% B solution for 5 min), each one with a flow of 0.3 μL/min. The eluted fractions were applied directly on a MALDI plate using an automatic fraction collector Probot (LcPackings).

The mass spectra of the peptides resulted from the proteins tryptic digestion and separated through HPLC, were obtained with a mass spectrometer MALDI-TOF/TOF (4800 Proteomics Analyzer, Applied Biosystems, Foster City, CA, USA), in reflectron positive mode and obtained in the mass interval between 700 and 4500 Da, with 850 laser shots. A data-dependent acquisition method was created to select the 16 most intense peaks in each sample spot for subsequent tandem mass spectrometry (MS/MS) data acquisition, excluding those from matrix, due trypsin autolysis or acrylamide peaks. The internal standard Glu-Fib peak (m/z 1570.68 Da) was used as internal calibration. Spectra were processed and analyzed by Global Protein Server (GPS) Workstation (Applied Biosystems, Foster City, CA, USA), which uses internal Mascot software (v2.1.0, Matrix Science, London, UK). Searches were done against the UniProtKB/Swiss-Prot (UniProt release 2011_01) *rodentia* protein database with trypsin specificity (two missed cleavages allowed), carboxyamidomethylation and oxidized methionine as variable modifications. Precursor ion and fragment ion mass tolerances were 20 ppm and 0.3 Da, respectively.

2.12. Western blotting analysis

Equivalent amounts of mitochondrial protein of each group were electrophoresed on a 12.5% SDS-PAGE as described by Laemmli [29]. Gels were blotted onto a nitrocellulose membrane (Whatman®, Protan) in transfer buffer (25 mM Tris, 192 mM glycine, pH 8.3 and 20% methanol) for 2 h (200 mA). Then, nonspecific binding was blocked with 5% (w/v) dry nonfat milk in TBS-T (100 mM Tris, 1.5 mM NaCl, pH 8.0 and 0.5% Tween 20) and the membrane was incubated with primary antibody diluted 1:1000 in 5% w/v nonfat dry milk in TBS-T (anti-paraplegin, anti-Lon, anti-ATPB, anti-UCP3, anti-mitofilin or anti-mtTFA) for 2 h at room temperature, washed and incubated with secondary with horseradish peroxidase-conjugated anti-mouse or anti-rabbit (GE Healthcare), respectively. Immunoreactive bands were detected by enhanced chemiluminescence ECL (Amersham Pharmacia Biotech) according to the manufacturer's procedure and images were recorded using X-ray films (Kodak Biomax Light Film, Sigma, St. Louis, MO, USA). The films were scanned in Molecular Imager Gel Doc XR + System (Bio-Rad) and analyzed with QuantityOne software (v 4.6.3 Bio-Rad). Protein loading was

controlled by Ponceau S staining since no ideal mitochondrial protein target has been described so far. A representative stained western blot is presented as supplementary data (Fig. S2A).

2.13. Slot blot analysis

For the protein carbonyl derivates assay, a given volume (V) of the sample containing 20 μg of protein was derivatized with 2,4-dinitrophenylhydrazine (DNPH). Briefly, the sample was mixed with 1 V of 12% sodium dodecyl sulphate, 2 V of 2 mM DNPH/10% trifluoroacetic acid, followed by 30 min of incubation in the dark, after which 1.5 V of 2 M Tris-base/18.3% of β-mercaptoethanol was added for neutralization. After diluting the derivatized proteins in Tris buffered saline to obtain a final concentration of 0.001 μg/μL, a 100 μL volume was slot-blotted into a nitrocellulose membrane.

For MMP-9 expression evaluation, whole IMF mitochondria samples were diluted in Tris buffered saline (TBS) to obtain a final protein concentration of 0.001 μg/μL and a volume of 100 μL was slot-blotted into a nitrocellulose membrane (Whatman®, Protan ®).

The slot-blot membranes were blocked with 5% (w/v) dry nonfat milk in TBS-T for 30 min and then incubated for 30 min with primary antibody (anti-MMP-9 or anti-DNP antibody) diluted 1:1000 in 5% w/v nonfat dry milk in TBS-T. The membranes were washed three times (10 min each) with TBS-T and incubated for 30 min with a solution of horseradish-conjugated anti-mouse or anti-rabbit antibody (GE Healthcare), respectively, in a dilution of 1:1.000. Detection was carried out with enhanced chemiluminescence (Amersham Pharmacia Biotech) according to the manufacturer's procedure and images were recorded using X-ray films (Kodak Biomax Light Film, Sigma, St. Louis, MO, USA). The films were scanned in Molecular Imager Gel Doc XR + System (Bio-Rad) and analyzed with QuantityOne software (v 4.6.3 Bio-Rad). Protein loading was controlled by Ponceau S staining. A representative stained slot blot is presented as supplementary data (Fig. S2B).

2.14. Statistical analysis

The results are presented as mean ± SD for each group experimental. The Kolmogorov–Smirnov test was used to test normality of distribution for all data. Since all variable were normal distributed, significant differences between the two groups were evaluated with the unpaired Student's *t*-test. Statistical Package for the Social Sciences (SPSS Inc, Chicago, IL, USA, version 12.0) was used for all analyses. A p value <0.05 was considered significant.

3. Results

Four months after STZ administration, body and gastrocnemius muscle weights declined significantly by 43% and 30% ($p<0.0001$; Table 1), respectively. Blood glucose concentration levels were remarkably higher in T1DM than in the control rats ($p<0.01$), which is indicative of pancreatic β-cell destruction. The high blood HbA1c content observed in STZ-treated rats ($p<0.01$; Table 1) corroborated the hyperglycemia profile. During the experimental protocol, polyuria and polydipsia were noticed in the T1DM rats, thereby emphasizing the diabetic condition.

IMF mitochondria were obtained from the gastrocnemius via a differential centrifugation protocol followed by Percoll centrifugation for mitochondria purification, as confirmed by TEM (Fig. S1). No fragmented membranes or any kind of debris was observed. Larger amplitude of mitochondria size was noticed in T1DM group. A significantly higher mtDNA-to-muscle mass ratio and mitochondrial protein-to-muscle mass ratio was also observed in the diabetic rats ($p<0.05$; Table 2), suggestive of an increased IMF mitochondrial content in the T1DM rats. Although in higher amount, IMF mitochondria seem less functional in the gastrocnemius of diabetic animals considering the significant decrease in CS activity (by 42%). Lower CS activity was also detected in the whole muscle homogenate (Table 2).

The analysis of the overall BN-PAGE band pattern revealed no qualitative differences of OXPHOS complexes organization among groups (Fig. 1). However, the OD quantitative profile of the BN-PAGE revealed a 15% decreased in the amount of complex III in T1DM as compared to the control group. No significant differences in the other OXPHOS complexes' levels were observed (Fig. 1D). Western blotting analysis of the ATP synthase subunit beta was performed in order to validate the OXPHOS proteins' expression profile observed and no differences were noticed between CONT and T1DM groups (Fig. 1E). In order to evaluate the OXPHOS functionality, the in-gel activity of complexes IV and V was determined. This analysis showed a decreased activity of these OXPHOS complexes in the T1DM group, which was significant for ATP synthase ($p<0.01$; Fig. 1A). The respiratory chain functionality was also spectrophotometrically assessed by determining the activity of respiratory complexes III and V. The results revealed a significant decrease in ATP synthase activity in T1DM rats ($p<0.0001$; Table 3), which supports the in-gel activity data. The activity of ubiquinol-cytochrome c reductase was also decreased, though with no statistical significance. Zymography analysis of IMF mitochondria revealed an overall decrease in proteolytic activity in the T1DM group. The densitometric evaluation (Fig. 2B) displayed six common bands in the zymograms for the control and diabetic animals. Two of these bands, i.e., one with approximately 15 kDa (band 6) and other with approximately 40 kDa (band 5), showed higher activities. To determine the protease classes present in each band, zymo gels were incubated with different inhibitors (i.e., EDTA—metalloproteinase inhibitor and PMSF—serine protease inhibitor) at their maximum effective concentration. The most outstanding observation from the comparison of zymo gels C, D, and E (Fig. 2) was the predominance of serine proteases. However, PMSF only moderately inhibited the protease activity observed in band 6 (approximately 55%), thereby suggesting the presence of other protease classes in the same band. Using LC-MS/MS for the identification of the mitochondrial proteases in each band, the predominance of serine proteases was confirmed; more specifically the Lon protease was identified in bands 1, 5, and 6 (Table 4). The intact protease was recognized in band 1, which corresponds to the molecular weight of this AAA protease, with the nine peptides identified distributed for the protein sequence, namely in the AAA^+ module (residues 515–681; involved in ATP hydrolysis and in protein substrate remodeling), and in the proteolytic domain (residues 705–959) (based on *MEROPS*). Fragments of this protease were identified in bands 5 and 6, with a predominance of the N-terminus from the main sequence. One of the peptides from the Lon protease fragment identified in band 5 is located in the AAA^+ module whereas the two peptides from the fragment identified in band 6 do not correspond to the AAA^+ module neither to the proteolytic domain (Fig. S3), despite the high proteolytic activity observed in the zymo gels. Presequence protease (PreP), an ATP-independent protease involved in the removal of free targeting peptides [30], was also identified by nanoLC-MS/MS in band 1. The identified 18 peptides of this clearing protease are distributed all over the protein

Table 1
Characterization of animals' response to STZ administration.

Experimental group	Body weight (g)	Muscle weight (g)	Muscle/body weight ratio (mg g^{-1})	Glycemia (mg dL^{-1})	HbA1c (% total Hb)
CONT	437.1 ± 58.4	5.69 ± 0.04	13.03 ± 0.001	66.3 ± 15.0	3.96 ± 0.80
T1DM	251.0 ± 43.1***	3.99 ± 0.88**	15.90 ± 0.006	577.1 ± 234.0***	6.28 ± 1.12***

Values are expressed as mean ± standard deviation. ***$p<0.0001$ vs. Control; ** $p<0.01$ vs CONT.

Table 2
Effects of STZ administration in mitochondrial protein content, mtDNA concentration and citrate synthase (CS) activity in *gastrocnemius* muscle and in IMF mitochondria.

Experimental group	Protein/mtDNA ($\mu g\ g^{-1}$)	mtDNA/muscle weight ($\mu g\ g^{-1}$)	Protein/muscle weight ($mg\ g^{-1}$)	Whole muscle CS ($nmol\ mg^{-1}\ min^{-1}$)	Mitochondria CS ($nmol\ mg^{-1}\ min^{-1}$)
CONT	0.52 ± 0.552	0.55 ± 0.056	0.28 ± 0.006	93.2 ± 18.9	139.7 ± 43.7
T1DM	0.66 ± 0.079	0.941 ± 0.371*	0.63 ± 0.293*	79.4 ± 3.5*	81.4 ± 18,2**

Values are expressed as mean ± standard deviation. * $p<0.05$ vs CONT; ** $p<0.01$ vs CONT

sequence (Table 4). The intact mitochondrial intermediate peptidase (MIP) was detected in band 2 of the zymo gel and the metallopeptidase cytosol aminopeptidase, also called leucine aminopeptidase (LAP-3), was identified in band 3. Typically associated with lysosomes, cathepsin D was also detected in the IMF mitochondria by zymography/LC-MS/MS (band 4; Fig. 2 and Table 4).

Based on OD density analysis and considering bands 5 and 6, the ones with higher proteolytic activity, a decrease of 28% and 47%, respectively, was observed in the T1DM zymo gels. The overall analysis of the mitochondrial proteolytic activity suggests an impairment of Lon protease activity in diabetic animals. To support these data, the Lon expression was assessed by western blotting, and a significant down-regulation was observed in diabetic animals (Fig. 3A). The expression of other AAA proteases, specifically m-AAA paraplegin, was also evaluated (Fig. 3B). The western blot analysis of this protease showed a 2.5 fold decrease in the IMF of T1DM rats, as compared to the CONT group ($p<0.0001$). Considering the moderated inhibitory effect of EDTA on the proteases' activity observed by zymography and previous studies that identified MMP-9 in mitochondria [31], the expression of this MMP was assessed by slot-blot (Fig. 3C). Significantly lower expression values were observed in the IMF mitochondria of diabetic rats (69%; $p<0.01$).

The expression of other mitochondrial proteins was also analyzed. The western blot analysis of the membrane protein mitofilin revealed two distinct bands corresponding to the described mitofilin isoforms (with ~87 kDa and ~89 kDa). For the present study, only the overall OD value was considered, which corresponds to the sum of the OD values of the individual bands. The expression levels of this mitochondrial protein, which is involved in organelle structure maintenance, significantly decreased in T1DM rats ($p<0.01$; Fig. 4A). Long-term hyperglycemia also induced a significant decrease of 20% in the expression of the mitochondrial transcriptional factor mtTFA (Fig. 4B), which indicates the impaired regulation of mtDNA gene expression in IMF mitochondria. Concomitantly, a significant increase of the uncoupling protein UCP3 was observed in T1DM mitochondria ($p<0.01$; Fig. 4C).

To evaluate the effect of T1DM on mitochondrial proteins susceptibility to oxidative damage, the total carbonyl content was measured by slot blot after derivatization with dinitrophenylhydrazine. A significant increase of 21% ($p<0.05$) in the total carbonyl levels was noted in the T1DM group as compared with CONT group (Fig. 4D). Being aconitase particularly susceptible to oxidation under pathophysiological conditions [32,33] and a known substrate of Lon protease [34], oxidatively modified amino acid residues were searched by SDS-PAGE followed by nano-LC-MS/MS analysis. Among the more prevalent oxidative modifications, we found pyro-Glu (Fig. S4), thereby further supporting the T1DM-related higher susceptibility of mitochondrial proteins to oxidative damage.

4. Discussion

The aim of the present study was to gain more insight into the role of the mitochondrial protein quality control (PQC) system to diabetic myopathy by studying skeletal muscle mitochondria from STZ rats, an animal model of type 1 diabetes. T1DM rats exhibited a remarkable hyperglycemia throughout the 4 months of the experimental period due to insulin

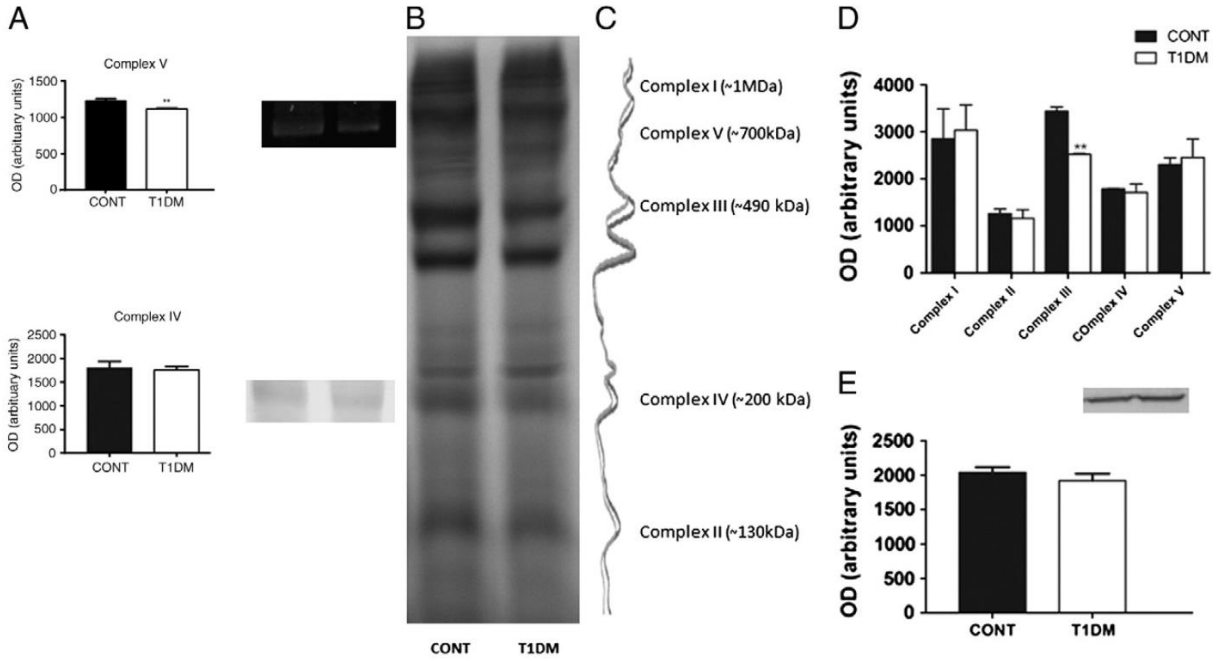

Fig. 1. Evaluation of the respiratory chain structural organization. (A) Representative image of histochemical staining of in-gel activity of complexes IV and V. On the left side is presented a semi-quantitative analysis of in-gel activity of both complexes. (B) Representative image of supramolecular architecture of mitochondrial membrane complexes resolved by Blue Native Polyacrylamide Gel Electrophoresis for type 1 diabetic group (T1DM) and control group (CONT). (C) An overlap of the density variation for both lanes is present on the right. (D) Densitometric analysis of BN-PAGE showing a significant decrease in complex III content in T1DM. (E) ATP synthase beta expression evaluated by western blotting. A representative immunoblot is presented above the graph. Values are expressed as mean ± standard deviation. (** $p<0.01$ vs CONT).

Table 3
Effects of STZ administration in OXPHOS complexes III and V activities of IMF mitochondria.

Experimental group	Ubiquinol cytochrome c reductase (μmol/mg/min)	ATP synthase (μmol Pi/min/mg)
CONT	3.72 ± 1.24	14.36 ± 1.80
T1DM	3.02 ± 0.52	6.04 ± 2.40***

Values are expressed as mean ± standard deviation. ***$p<0.0001$ vs CONT.

deprivation prompted by STZ-induced pancreatic β-cell destruction. This long-term hyperglycemia (Table 1) was associated with reduced IMF mitochondrial ability to produce ATP (Table 3 and Fig. 1) in a similar way as previously reported [5,6,35,36], and with high levels of UCP3 (Fig. 4C), which seems to be involved in mitochondrial membrane potential dissipation to protect against ROS production [37]. UCP3 overexpression was already reported in cardiac mitochondria from type 1 diabetic Akita mice [38]. Being around 80% of the total mitochondrial muscle content [19] and specialized toward energy production for contractile activity [15], focus was given to the IMF subpopulation driven muscle adaptation to type 1 diabetes.

As a source for the formation of ROS, mitochondria themselves are a prime target of oxidative modifications. ROS can directly perturb protein folding by modifying amino acids, or indirectly by introducing mutations in genes encoded by mitochondrial or nuclear DNA [1]. The resulting accumulation of orphaned mitochondrial complex subunits or toxic protein aggregates can generate an overwhelming load of misfolded mitochondrial proteins [1,7], which compromises the signalling networks in this organelle and consequently in the whole cell [7]. The increased amount of carbonylated proteins observed in diabetic mitochondria (Fig. 4D) reflects a disease-related higher susceptibility of mitochondrial proteins to oxidative damage as previously reported [39]. Due to the covalent nature of the protein modifications generated by ROS, the proteolytic removal of damaged peptides is a major protective process of the PQC system under oxidative stress [40]. The typical effector enzymes of protein homeostasis are molecular chaperones and proteases [40]. To evaluate the T1DM effect on mitochondrial proteolysis, gelatin zymography of pure IMF fractions was performed (Fig. 2). The inhibitory effect of PMSF in the protease activities observed in zymo gels highlights the involvement of mitochondrial serine proteases in the mitochondrial PQC. In the zymogram bands with higher proteolytic activity we identified by LC-MS/MS the Lon protease, a serine protease with a recognized critical role in the removal of oxidized protein [1,7,13]. This AAA protease exists in the matrix with the function of degrading misfolded and non-assembled proteins and peptides, including denatured and carbonylated proteins, being aconitase as a good example [41]. In addition to Lon, other ATP-dependent serine proteases play a crucial role in the mitochondrial PQC. For instance, the breakdown of mitochondrial membrane proteins is mediated by membrane-bound AAA proteases [1,42]. The lower expression levels of the paraplegin observed in T1DM mitochondria (i.e., 63%) suggest that the decreased activity of m-AAA may also contribute to the accumulation of oxidatively damaged proteins and might compromise the biogenesis of some nuclear-encoded mitochondrial proteins [5]. Defects in PQC systems have been implicated in certain pathological conditions [7]. Nevertheless, to date, no previous studies have evaluated the involvement of AAA proteases in diabetes-related mitochondrial dysfunction in striated muscle.

Although no notorious inhibitory effect of EDTA was observed in zymograms, three metalloproteases were identified by LC-MS/MS. The diminished activity of the mitochondrial PreP with the consequent accumulation of toxic free presequences that are a result of the action of mitochondrial processing peptidase over precursor proteins was previously reported in Alzheimer disease. If not removed, these free presequences penetrate the mitochondrial inner membrane, dissipate membrane potential and uncouple respiration, thereby compromising mitochondrial functionality [30]. Another mitochondrial metalloproteinase identified by zymography-LC/MS/MS was MIP, a matrix peptidase involved in the proteolytic processing of specific subsets of nuclearly and mitochondrialy encoded precursor polypeptides [43]; however, no activity variations were noticed. The metalloprotease LAP-3 was also identified, but no T1DM-induced activity alterations were observed. To the best of our knowledge, this is the first study where a LAP member was identified in mitochondria. Based on the broader specificity of LAPs, it seems difficult to predict its role in mitochondrial structure or functionality. The identification of traditionally extracellular or cytoplasmic metalloproteases in mitochondria is not original, being MMPs good examples. Indeed, the notion of the intracellular location of MMPs has already been suggested [44] and the presence of MMP-2 and MMP-9 in cardiac mitochondria was reported by others [31]. Although not identified by zymography, MMP-9 was detected by slot-blot analysis and a T1DM-related modulation of its expression levels was identified (Fig. 3C). The MMP active site is bound with nitric oxide, and once activated, a decrease in eNO bioavailability with an increased generation of peroxynitrite occurs [31]. No association between MMP-9 activation and ROS production was observed in the present study considering the observed T1DM-related decrease of MMP-9 and the increased carbonyl group content. Nevertheless, the mechanisms involved in mtMMP activation and its physiological consequences are currently not clearly understood.

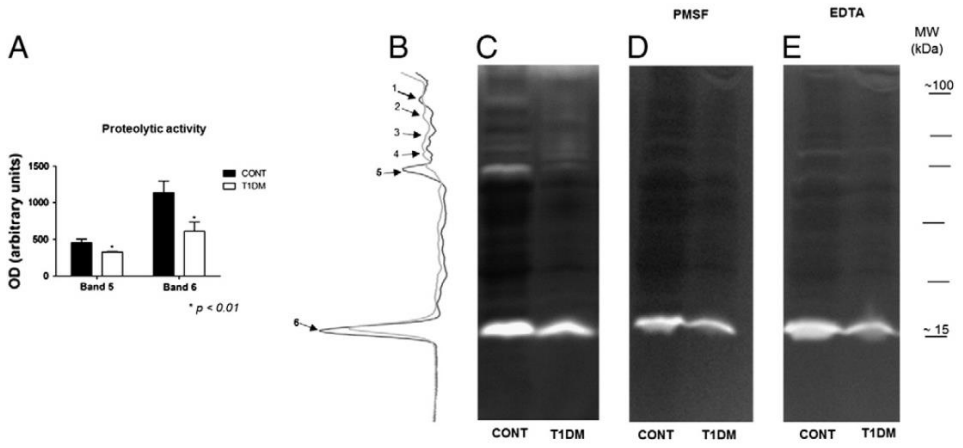

Fig. 2. Effect of 4 months of STZ administration in the mitochondrial proteolytic activity of *gastrocnemius* muscle. (C) Representative image of the zymography evidencing two bands with noticeable proteolytic activity (bands 5 and 6). An overlap of densitometric variation for CONT and T1DM lanes is presented in (B). Semi-quantitative analysis of proteolytic activity of bands 5 and 6 is presented in (A). Representative image of the zymo gels in the presence of inhibitors for (D) serine proteases (PMSF) and for (E) metalloproteinases (EDTA). Values are expressed as mean ± standard deviation. (*$p<0.01$ vs CONT).

Table 4
List of proteases identified by zymography-LC-MS/MS. The information regarding protein accession number and name, protein molecular weight (M.W.), isoelectric point (pI) of the protein, peptide count, protein score, % coverage and peptide sequence is presented.

Band no.	Protein name	Accession number	Total ion score	Total ion score C.I. %	Protein MW	Protein PI	Peptide count	% coverage	Best peptide sequence	Start sequence position	End sequence position	Ion score	Ion score C.I. %	Ion score C.I. %	Calculated mass	Observed mass
1									NPVFPR	120	125	40,54	99,51		729,40	729,43
									IAYTFAR	806	812	38,14	99,15		841,46	841,47
									YLVPQAR	663	669	35,65	98,48		846,48	846,50
									LAQPYVGVFLK	147	157	55,88	99,99		1234,72	1234,72
	Lon protease homolog, mitochondrial	LONM_RAT	470,77	100	105726,25	6,17	9	11,00	VLEFIAVSQLR	491	501	79,10	100,00	100,00	1274,75	1274,75
									NLQKQVEKVLR	701	711	8,40	0,00		1354,82	1354,74
									LALLDNHSSEFNVTR	435	449	81,45	100,00		1715,87	1715,86
									TENPLVLIDEVDKIGR	572	587	115,85	100,00		1810,99	1810,98
									IVSGEAQTVHVTPENLQDFVGKPVFTVER	717	745	16,94	0,00		3196,66	3196,68
									NPVFPR	120	125	40,54	99,51		729,40	729,43
									IAYTFAR	806	812	38,14	99,15		841,46	841,47
									YLVPQAR	663	669	35,65	98,48		846,48	846,50
									LAQPYVGVFLK	147	157	55,88	99,99		1234,72	1234,72
									VLEFIAVSQLR	491	501	79,10	100,00		1274,75	1274,75
									NLQKQVEKVLR	701	711	8,40	0,00		1354,82	1354,74
									LALLDNHSSEFNVTR	435	449	81,45	100,00		1715,87	1715,86
									TENPLVLIDEVDKIGR	572	587	115,85	100,00		1810,99	1810,98
	Presequence protease, mitochondrial	PREP_MOUSE	256,72	100	117297,23	6,76	18	17,95	IVSGEAQTVHVTPENLQDFVGKPVFTVER	717	745	16,94	0,00	99,99	3196,66	3196,68
									YLHLAR	76	81	26,26	86,83		772,45	772,47
									FLHTEIR	893	899	29,49	93,74		915,50	915,53
									IFSQHLQNK	216	224	39,76	99,41		1114,60	1114,61
									NNLFSVQFR	85	93	0,58	0,00		1124,58	1124,51
									ELDFWQEGWR	174	183	58,25	99,99		1365,62	1365,62
									TVPYADPDHASLK	871	883	48,95	99,93		1413,70	1413,70
									LVTDPTFKPCQMK	841	853	3,37	0,00		1507,76	1507,81
									KLVTDPTFKPCQMK	840	853	2,93	0,00		1635,86	1635,80
									ALIESGLGTDFSPDVGYNGYTR	364	385	47,13	99,89		2332,11	2332,10
									IGHPEQAFR	125	133	37,23	98,96	99,99	1054,54	1054,56
									HLLPEHIQHHFAR	230	242	55,83	99,99		1634,87	1634,86
									SAGVDDQENWHEGKENIR	105	122	129,69	100,00	100,00	2083,94	2083,92
									DKDDDVPQFTSAGENFNK	44	61	108,81	100,00		2026,90	2026,88
									TLIEFLLR	506	513	59,95	100,00		1004,61	1004,64
									NIFSFYLNR	222	230	37,40	99,02	100,00	1173,53	1173,52
2	Mitochondrial intermediate peptidase	MIPEP_RAT	93,06	100	80621,32	6,06	2	2,82	LGGQNYELHPEK	337	348	62,07	100,00		1384,69	1384,69
3	Cytosol aminopeptidase	AMPL_RAT	298,56	100	56114,68	6,77	3	7,90	NLQKQVEKVLR	701	711	7,32	0,00	100,00	1354,82	1354,75
4	Cathepsin D	CATD_RAT	99,47	100	44651,89	6,66	2	4,70	TENPLVLIDEVDKIGR	572	587	65,56	100,00		1810,99	1810,98
5	Lon protease homolog, mitochondrial	LONM_RAT	71,70	100	105726,25	6,17	2	2,63	NPVFPR	120	125	38,90	99,28	99,28	729,40	729,43
6	Lon protease homolog, mitochondrial	LONM_RAT	90,46	100	105726,25	6,17	2	1,05	RIHISR	201	206	31,72	96,26	96,26	781,48	781,50

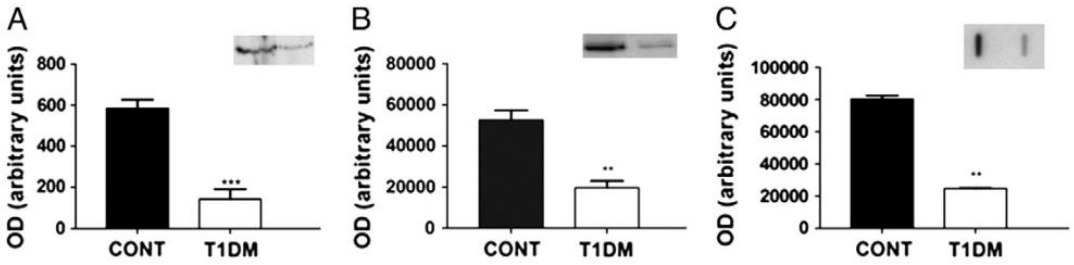

Fig. 3. Effect of 4 months of STZ administration in the AAA proteases Lon (A) and paraplegin (B) expression evaluated by western blotting and in the MMP-9 expression evaluated by slot-blot (C). Representative immunoblots are presented above the respective graph. Values are expressed as mean ± standard deviation. (**$p<0.01$vs CONT; ***$p<0.001$vs CONT).

Besides serine and metalloproteases, cathepsin D was also identified by zymography/LC-MS/MS. This lysosomal protease was already detected by 2DE-MS/MS in the matrix of pure IMF fractions isolated from gastrocnemius [15]. Though its role in mitochondria homeostasis is still to be addressed, cathepsin D seems to trigger a mitochondrial apoptotic cascade [45]. Regarding its contribution to diabetes complications, a decreased activity of cathepsin D in the whole heart tissue of STZ animals was previously reported [46]. In the present study, no T1DM-related alteration in the mitochondrial activity of this aspartyl protease was observed.

The limited capacity of the PQC system observed in diabetic mitochondria might explain the disease-induced alterations in mitochondrial biogenesis, which controls the number, mass and function of this organelle [1]. Unlike previous studies that reported a diabetes-related decrease of mitochondrial mass [39,47], we observed an increase in IMF mitochondria based on mtDNA-to-muscle mass ratio (Table 2), a rough marker of mitochondrial content [15]. Though present in apparently higher number, IMF mitochondria showed a lower citrate synthase activity, thereby corroborating previous studies that identified compromised activity of the Krebs cycle enzymes in diabetes [39,47]. Mitochondrial biogenesis requires a coordinated control of nuclear and mitochondrial genes encoding mitochondrial proteins. Tfam plays a critical role in nuclear-mitochondrial interactions [48], and we found that it was down-regulated in diabetic muscle (Fig. 4B). This nuclear encoded transcription factor is one of the most important proteins that controls mtDNA replication and transcription [49], thereby regulating the expression of mitochondrial proteins required for ATP synthesis [4], which was impaired in diabetic animals. Kanazawa et al. [50] did not detect differences in the expression levels of Tfam in control and diabetic rat hearts, but they observed a decreased binding activity related with insufficient RNA polymerase access to the initiation site of the transcription. Concomitant with lower Tfam levels in T1DM mitochondria, alterations of mitofilin content were also observed (Fig. 4A). The inner mitochondrial membrane protein mitofilin has been suggested to control mitochondrial cristae organization, and its down-regulation was previously related to a drastic change in the organization of the inner membrane [51]. So, the T1DM-related mitochondrial impairment might be at least partially related to the destabilization of the inner membrane organization, where OXPHOS complexes are harbored. Several studies reported morphological disturbances in STZ rats, including an increased number of disarrayed cristae and mitochondrial swelling [39,47]. Nevertheless, besides changes in the levels of mitofilin, no notorious ultrastructural evidence of T1DM-induced cristae disorganization was observed (Fig. S1).

In conclusion, data from our study indicate that in an animal model for prolonged severe hyperglycaemia that mimics uncontrolled type 1 diabetes in humans, the impaired IMF mitochondria functionality observed in *gastrocnemius* is associated with decreased mitochondrial

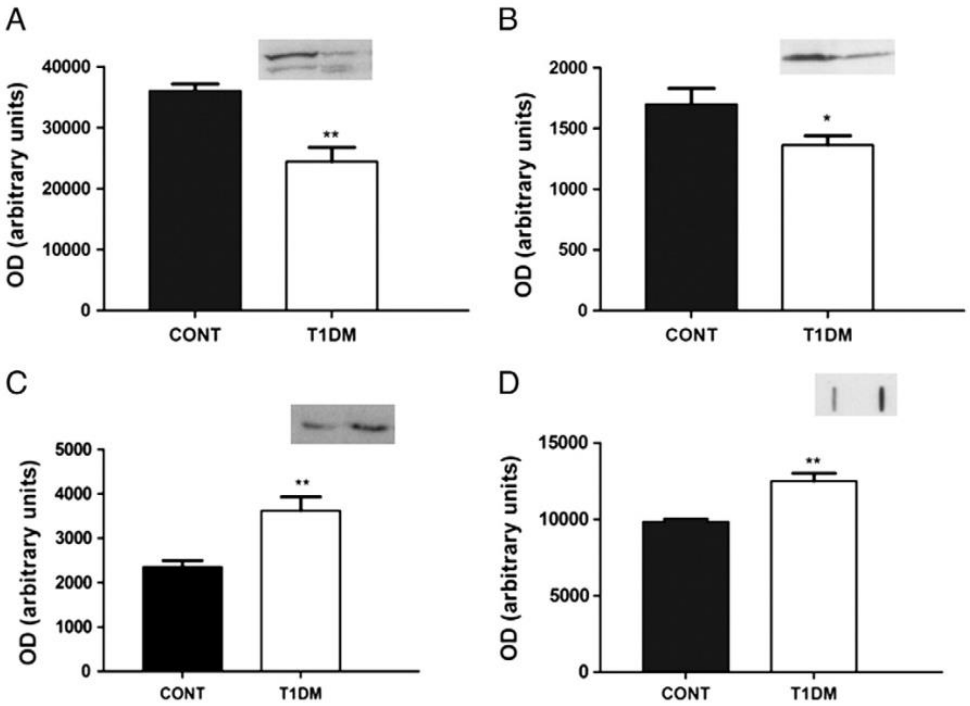

Fig. 4. Effect of 4 months of STZ administration in mitofilin (A), mtTFA (B), UCP3 (C) expression and in the mitochondrial protein carbonylation levels (D). Representative immunoblots are presented above the corresponding graph. Values are expressed as mean ± standard deviation. (*$p<0.05$vs CONT; **$p<0.01$vs CONT).

PQC activity and the subsequent accumulation of damaged proteins. For the first time, our data highlighted the T1DM-related down-regulation of AAA proteases, namely the membranar paraplegin and the matrix Lon protease. A deeper understanding of the involvement of these AAA proteases in the PQC regulation of mitochondrial biogenesis would possibly contribute to a better design of preventive and/or therapeutic countermeasures against type 1 diabetes-related muscular complications.

Supplementary data related to this article can be found online at http://dx.doi.org/10.1016/j.bbadis.2012.04.009.

Acknowledgments

This work was supported by Portuguese Foundation for Science and Technology (FCT) [grant numbers SFRH/BD/66642/2009 (to A.I.P), PTDC/QUI/72683/2006, PEst-C/QUI/UI0062/2011]. The authors would like to thank Celeste Resende for her assistance in animal care and sample preparation for TEM analysis.

References

[1] B.M. Baker, C.M. Haynes, Mitochondrial protein quality control during biogenesis and aging, Trends Biochem. Sci. 36 (2011) 254–261.
[2] J.G. Duncan, Mitochondrial dysfunction in diabetic cardiomyopathy, Biochim. Biophys. Acta 1813 (2011) 1351–1359.
[3] E.R. Dabkowski, W.A. Baseler, C.L. Williamson, M. Powell, T.T. Razunguzwa, J.C. Frisbee, J.M. Hollander, Mitochondrial dysfunction in the type 2 diabetic heart is associated with alterations in spatially distinct mitochondrial proteomes, Am. J. Physiol. Heart Circ. Physiol. 299 (2009) H529–H540.
[4] V. Romanello, M. Sandri, Mitochondrial biogenesis and fragmentation as regulators of muscle protein degradation, Curr. Hypertens. Rep. 12 (2010) 433–439.
[5] W.A. Baseler, E.R. Dabkowski, C.L. Williamson, T.L. Croston, D. Thapa, M.J. Powell, T.T. Razunguzwa, J.M. Hollander, Proteomic alterations of distinct mitochondrial subpopulations in the type 1 diabetic heart: contribution of protein import dysfunction, Am. J. Physiol. Regul. Integr. Comp. Physiol. 300 (2011) R186–R200.
[6] H. Karakelides, Y.W. Asmann, M.L. Bigelow, K.R. Short, K. Dhatariya, J. Coenen-Schimke, J. Kahl, D. Mukhopadhyay, K.S. Nair, Effect of insulin deprivation on muscle mitochondrial ATP production and gene transcript levels in type 1 diabetic subjects, Diabetes 56 (2007) 2683–2689.
[7] T. Tatsuta, T. Langer, Quality control of mitochondria: protection against neurodegeneration and ageing, EMBO J. 27 (2008) 306–314.
[8] A.I. Padrao, R.M.P. Ferreira, R. Vitorino, R.M.P. Alves, M.J. Neuparth, J.A. Duarte, F. Amado, OXPHOS susceptibility to oxidative modifications: the role of heart mitochondrial subcellular location, Biochim. Biophys. Acta, Bioenerg. 1807 (2011) 1106–1113.
[9] M. Escobar-Henriques, T. Langer, Mitochondrial shaping cuts, Biochim. Biophys. Acta 1763 (2006) 422–429.
[10] L. Vande Walle, M. Lamkanfi, P. Vandenabeele, The mitochondrial serine protease HtrA2/Omi: an overview, Cell Death Differ. 15 (2008) 453–460.
[11] D.A. Bota, H. Van Remmen, K.J. Davies, Modulation of Lon protease activity and aconitase turnover during aging and oxidative stress, FEBS Lett. 532 (2002) 103–106.
[12] D. Korbel, S. Wurth, M. Kaser, T. Langer, Membrane protein turnover by the m-AAA protease in mitochondria depends on the transmembrane domains of its subunits, EMBO Rep. 5 (2004) 698–703.
[13] A.L. Bulteau, A. Bayot, Mitochondrial proteases and cancer, Biochim. Biophys. Acta, Bioenerg. 1807 (2011) 595–601.
[14] B. Friguet, A.L. Bulteau, I. Petropoulos, Mitochondrial protein quality control: implications in ageing, Biotechnol. J. 3 (2008) 757–764.
[15] R. Ferreira, R. Vitorino, R.M. Alves, H.J. Appell, S.K. Powers, J.A. Duarte, F. Amado, Subsarcolemmal and intermyofibrillar mitochondria proteome differences disclose functional specializations in skeletal muscle, Proteomics 10 (2010) 3142–3154.
[16] T.R. Koves, R.C. Noland, A.L. Bates, S.T. Henes, D.M. Muoio, R.N. Cortright, Subsarcolemmal and intermyofibrillar mitochondria play distinct roles in regulating skeletal muscle fatty acid metabolism, Am. J. Physiol. Cell Physiol. 288 (2005) C1074–C1082.
[17] D.A. Hood, Invited Review: contractile activity-induced mitochondrial biogenesis in skeletal muscle, J. Appl. Physiol. 90 (2001) 1137–1157.
[18] P. Chomentowski, P.M. Coen, Z. Radikova, B.H. Goodpaster, F.G. Toledo, Skeletal muscle mitochondria in insulin resistance: differences in intermyofibrillar versus subsarcolemmal subpopulations and relationship to metabolic flexibility, J. Clin. Endocrinol. Metab. 96 (2011) 494–503.
[19] P.J. Adhihetty, V. Ljubicic, K.J. Menzies, D.A. Hood, Differential susceptibility of subsarcolemmal and intermyofibrillar mitochondria to apoptotic stimuli, Am. J. Physiol. Cell Physiol. 289 (2005) C994–C1001.
[20] C.L. Williamson, E.R. Dabkowski, W.A. Baseler, T.L. Croston, S.E. Alway, J.M. Hollander, Enhanced apoptotic propensity in diabetic cardiac mitochondria: influence of subcellular spatial location, Am. J. Physiol. Heart Circ. Physiol. 298 (2010) H633–H642.
[21] J.W. Palmer, B. Tandler, C.L. Hoppel, Biochemical properties of subsarcolemmal and interfibrillar mitochondria isolated from rat cardiac muscle, J. Biol. Chem. 252 (1977) 8731–8739.
[22] H.G. Coore, R.M. Denton, B.R. Martin, P.J. Randle, Regulation of adipose tissue pyruvate dehydrogenase by insulin and other hormones, Biochem. J. 125 (1971) 115–127.
[23] R.W. Taylor, M.A. Birch-Machin, K. Bartlett, S.A. Lowerson, D.M. Turnbull, The control of mitochondrial oxidations by complex III in rat muscle and liver mitochondria. Implications for our understanding of mitochondrial cytopathies in man, J. Biol. Chem. 269 (1994) 3523–3528.
[24] K.B. Choksi, J. Papaconstantinou, Age-related alterations in oxidatively damaged proteins of mouse heart mitochondrial electron transport chain complexes, Free Radic. Biol. Med. 44 (2008) 1795–1805.
[25] N. Simon, K. Papa, J. Vidal, A. Boulamery, B. Bruguerolle, Circadian rhythms of oxidative phosphorylation: effects of rotenone and melatonin on isolated rat brain mitochondria, Chronobiol. Int. 20 (2003) 451–461.
[26] H. Schagger, G. von Jagow, Blue native electrophoresis for isolation of membrane protein complexes in enzymatically active form, Anal. Biochem. 199 (1991) 223–231.
[27] E. Zerbetto, L. Vergani, F. Dabbeni-Sala, Quantification of muscle mitochondrial oxidative phosphorylation enzymes via histochemical staining of blue native polyacrylamide gels, Electrophoresis 18 (1997) 2059–2064.
[28] R. Vitorino, A. Barros, A. Caseiro, P. Domingues, J.A. Duarte, F. Amado, Towards defining the whole salivary peptidome, Proteomics Clin. Appl. 3 (2009) 528–540.
[29] U.K. Laemmli, Cleavage of structural proteins during the assembly of the head of bacteriophage T4, Nature 227 (1970) 680–685.
[30] E. Glaser, N. Alikhani, The organellar peptidasome, PreP: a journey from *Arabidopsis* to Alzheimer's disease, Biochim. Biophys. Acta 1797 (2010) 1076–1080.
[31] S.C. Tyagi, N. Tyagi, J.C. Vacek, S. Givvimani, U. Sen, Cardiac specific deletion of *N*-methyl-D-aspartate receptor 1 ameliorates mtMMP-9 mediated autophagy/mitophagy in hyperhomocysteinemia, J. Recept. Signal Transduction 30 (2010) 78–87.
[32] R.M.P. Alves, R. Vitorino, P. Figueiredo, J.A. Duarte, R. Ferreira, F. Amado, Lifelong physical activity modulation of the skeletal muscle mitochondrial proteome in mice, J. Gerontol. A Biol. Sci. Med. Sci. 65 A (2010) 832–842.
[33] A.I. Padrao, R. Ferreira, R. Vitorino, R.M. Alves, P. Figueiredo, J.A. Duarte, F. Amado, Effect of lifestyle on age-related mitochondrial protein oxidation in mice cardiac muscle, Eur. J. Appl. Physiol. 112 (2011) 1467–1474.
[34] E. Gur, R.T. Sauer, Recognition of misfolded proteins by Lon, a AAA(+) protease, Genes Dev. 22 (2008) 2267–2277.
[35] J. Lumini-Oliveira, A. Ascensao, C.V. Pereira, S. Magalhaes, F. Marques, P.J. Oliveira, J. Magalhaes, Long-term hyperglycaemia decreases gastrocnemius susceptibility to permeability transition, Eur. J. Clin. Invest. 40 (2010) 319–329.
[36] J. Lumini-Oliveira, J. Magalhaes, C.V. Pereira, A.C. Moreira, P.J. Oliveira, A. Ascensao, Endurance training reverts heart mitochondrial dysfunction, permeability transition and apoptotic signaling in long-term severe hyperglycemia, Mitochondrion 11 (2011) 54–63.
[37] V. Azzu, M. Jastroch, A.S. Divakaruni, M.D. Brand, The regulation and turnover of mitochondrial uncoupling proteins, Biochim. Biophys. Acta 1797 (2010) 785–791.
[38] H. Bugger, S. Boudina, X.X. Hu, J. Tuinei, V.G. Zaha, H.A. Theobald, U.J. Yun, A.P. McQueen, B. Wayment, S.E. Litwin, E.D. Abel, Type 1 diabetic akita mouse hearts are insulin sensitive but manifest structurally abnormal mitochondria that remain coupled despite increased uncoupling protein 3, Diabetes 57 (2008) 2924–2932.
[39] C. Bonnard, A. Durand, S. Peyrol, E. Chanseaume, M.A. Chauvin, B. Morio, H. Vidal, J. Rieusset, Mitochondrial dysfunction results from oxidative stress in the skeletal muscle of diet-induced insulin-resistant mice, J. Clin. Invest. 118 (2008) 789–800.
[40] T. Bender, C. Leidhold, T. Ruppert, S. Franken, W. Voos, The role of protein quality control in mitochondrial protein homeostasis under oxidative stress, Proteomics 10 (2010) 1426–1443.
[41] E. Gur, R.T. Sauer, Recognition of misfolded proteins by Lon, a AAA(+) protease, Genes Dev. 22 (2008) 2267–2277.
[42] M. Kaser, T. Langer, Protein degradation in mitochondria, Semin. Cell Dev. Biol. 11 (2000) 181–190.
[43] O. Gakh, P. Cavadini, G. Isaya, Mitochondrial processing peptidases, Biochim. Biophys. Acta 1592 (2002) 63–77.
[44] L.J. McCawley, L.M. Matrisian, Matrix metalloproteinases: they're not just for matrix anymore! Curr. Opin. Cell Biol. 13 (2001) 534–540.
[45] U. Repnik, B. Turk, Lysosomal–mitochondrial cross-talk during cell death, Mitochondrion 10 (2010) 662–669.
[46] M.A. Nerurkar, J.G. Satav, S.S. Katyare, Insulin-dependent changes in lysosomal cathepsin D activity in rat liver, kidney, brain and heart, Diabetologia 31 (1988) 119–122.
[47] V. Chen, C.D. Ianuzzo, Metabolic alterations in skeletal muscle of chronically streptozotocin-diabetic rats, Arch. Biochem. Biophys. 217 (1982) 131–138.
[48] X. Shen, S. Zheng, V. Thongboonkerd, M. Xu, W.M. Pierce Jr., J.B. Klein, P.N. Epstein, Cardiac mitochondrial damage and biogenesis in a chronic model of type 1 diabetes, Am. J. Physiol. Endocrinol. Metab. 287 (2004) E896–E905.
[49] D.A. Clayton, Transcription and replication of mitochondrial DNA, Hum. Reprod. 15 (Suppl. 2) (2000) 11–17.
[50] A. Kanazawa, Y. Nishio, A. Kashiwagi, H. Inagaki, R. Kikkawa, K. Horiike, Reduced activity of mtTFA decreases the transcription in mitochondria isolated from diabetic rat heart, Am. J. Physiol. Endocrinol. Metab. 282 (2002) E778–E785.
[51] G.B. John, Y. Shang, L. Li, C. Renken, C.A. Mannella, J.M. Selker, L. Rangell, M.J. Bennett, J. Zha, The mitochondrial inner membrane protein mitofilin controls cristae morphology, Mol. Biol. Cell 16 (2005) 1543–1554.

STUDY IV - BLADDER CANCER-INDUCED CACHEXIA: DISCLOSING THE ROLE OF MITOCHONDRIA PLASTICITY IN SKELETAL MUSCLE WASTING

The International Journal of Biochemistry & Cell Biology 45 (2013) 1399–1409

Contents lists available at SciVerse ScienceDirect

The International Journal of Biochemistry & Cell Biology

journal homepage: www.elsevier.com/locate/biocel

Bladder cancer-induced skeletal muscle wasting: Disclosing the role of mitochondria plasticity

Ana Isabel Padrão[a], Paula Oliveira[b], Rui Vitorino[a], Bruno Colaço[b], Maria João Pires[b], Marcela Márquez[c], Enrique Castellanos[c], Maria João Neuparth[d], Catarina Teixeira[a,b], Céu Costa[e], Daniel Moreira-Gonçalves[f], Sónia Cabral[g], José Alberto Duarte[f], Lúcio Lara Santos[e,g], Francisco Amado[a,h], Rita Ferreira[a,*]

[a] QOPNA, Chemistry Department, University of Aveiro, Aveiro, Portugal
[b] CECAV, Department of Veterinary Sciences, University of Trás-os-Montes e Alto Douro, Vila Real, Portugal
[c] Department of Oncology and Pathology, Karolinska Institutet, Stockholm, Sweden
[d] CITS, IPSN, CESPU CRL, Famalicão, Portugal
[e] Health Faculty, Fernando Pessoa University, Porto, Portugal
[f] CIAFEL, Faculty of Sport, University of Porto, Porto, Portugal
[g] Experimental Pathology and Therapeutics Group, Portuguese Institute of Oncology, Porto, Portugal
[h] Health School of Sciences, University of Aveiro, Aveiro, Portugal

ARTICLE INFO

Article history:
Received 18 October 2012
Received in revised form 15 March 2013
Accepted 14 April 2013
Available online xxx

Keywords:
Urothelial carcinoma
Gastrocnemius wasting
Mitochondrial proteolysis
Protein quality control system

ABSTRACT

Loss of skeletal muscle is a serious consequence of cancer as it leads to weakness and increased risk of death. To better understand the interplay between urothelial carcinoma and skeletal muscle wasting, cancer-induced catabolic profile and its relationship with muscle mitochondria dynamics were evaluated using a rat model of chemically induced urothelial carcinogenesis by the administration of N-butyl-N-(4-hydroxybutyl)-nitrosamine (BBN). The histologic signs of non-muscle-invasive bladder tumors observed in BBN animals were related to 17% loss of body weight and high serum levels of IL-1β, TNF-α, TWEAK, C-reactive protein, myostatin and lactate and high urinary MMPs activities, suggesting a catabolic phenotype underlying urothelial carcinoma. The 12% loss of *gastrocnemius* mass was related to mitochondrial dysfunction, manifested by decreased activity of respiratory chain complexes due to, at least partially, the impairment of protein quality control (PQC) systems involving the mitochondrial proteases paraplegin and Lon. This was paralleled by the accumulation of oxidatively modified mitochondrial proteins. In overall, our data emphasize the relevance of studying the regulation of PQC systems in cancer cachexia aiming to identify therapeutic targets to counteract muscle wasting.

1. Introduction

The majority of patients with advanced cancer experience involuntary weight loss (Blum et al., 2011; Tisdale, 2009), which by itself is responsible for 25–30% of cancer-related deaths (Bonetto et al., 2011). Patients with pancreatic or gastric cancer have the highest frequency of weight loss (Tisdale, 2009) while urological cancer is not usually associated with significant cachexia (Buskermolen et al., 2012). Nevertheless, in a population of around 200 patients with bladder cancer we verified (data not published) that 48% were at risk of undernutrition and 23% showed clear signs of cancer-related body wasting, according to the Buzby's Prognostic Nutritional Index (Dempsey et al., 1983). Though over the last two decades trends in urologic cancer mortality have been favourable, it stills the 9th leading cause of death from cancer in men (Mistry et al., 2011; Jacobs et al., 2012).

The presence of muscle wasting is usually associated with intolerance to treatment, poor quality of life and high mortality in patients (Wang et al., 2012). So, a better understanding of the molecular processes underlying cancer-induced skeletal muscle wasting is critical in planning therapeutic strategies focused on both quality and longevity of patients. In this context, well characterized animal models that mimic human clinical conditions are crucial. Nitrosamine-induced tumorigenesis in rat bladder is a valuable animal model for the study of urothelial carcinoma and related complications (Palmeira et al., 2010).

Among the molecular mechanisms underlying cancer-induced muscle wasting, it has been suggested that tumor and host-derived cytokines affect normal homeostasis and energy metabolism,

* Corresponding author at: Chemistry Department, University of Aveiro, Campus de Santiago, 3810-193 Aveiro, Portugal. Tel.: +351 234370700; fax: +351 234370084.
E-mail address: ritaferreira@ua.pt (R. Ferreira).

1357-2725/$ – see front matter © 2013 Elsevier Ltd. All rights reserved.
http://dx.doi.org/10.1016/j.biocel.2013.04.014

resulting in altered muscle respiration, muscle fatigue and degradation (Shum et al., 2012). A complex network of cytokine signaling encompassing raised levels of tumor-derived IL-1β, IL-6, TNF-alpha has been implicated in the pathogenesis of cancer cachexia (Shum et al., 2012). TGF-β ligands like myostatin, which function through ActRIIB-mediated signaling are also associated with the development of skeletal muscle wasting (Lokireddy et al., 2012; Zhou et al., 2010), which was related to the disruption of the delicate balance between the rates of muscle protein synthesis and degradation (White et al., 2011). The involvement of mitochondrial dysfunction in skeletal muscle wasting was recently reported (Wang et al., 2012; White et al., 2011, 2012; Julienne et al., 2012). The activation of TNF-alpha-induced NFκB was shown to decrease the expression of regulatory factors involved in mitochondrial biogenesis and affect downstream oxidative proteins and consequently disturb muscle oxidative capacity (Wang et al., 2012; Julienne et al., 2012). Morphological changes such as the presence of electron-lucent areas and swelling were also reported in muscle mitochondria of C26-bearing mice (Shum et al., 2012). However, the underlying mechanisms are not known.

Using a rat model of N-butyl-N-(4-hydroxybutyl)-nitrosamine (BBN)-induced urothelial carcinogenesis, we investigated the interplay between urothelial carcinoma-induced catabolic profile and skeletal muscle phenotype focusing on muscle mitochondrial plasticity. Data obtained highlight an association between mitochondrial dysfunction and the accumulation of oxidized proteins in *gastrocnemius* muscle from BBN animals due to the impairment of protein quality control (PQC) systems.

2. Materials and methods

2.1. Chemicals

N-butyl-N-(4-hydroxybutyl)-nitrosamine (BBN) was purchased from Tokyo Kasey Kogyo (Japan). All other reagents and chemicals used were of highest grade of purity commercially available. Rabbit polyclonal anti-paraplegin antibody (sc-135026) was obtained from Santa Cruz Biotechnology, Inc. (CA, USA). Rabbit polyclonal anti-mtTFA antibody (ab47548), mouse monoclonal anti-ATPB antibody (ab14730), rabbit monoclonal anti-CRP antibody (C reactive protein; ab32412), rabbit polyclonal anti-GDF8 antibody (myostatin; ab996), rabbit polyclonal anti-LONP1 antibody (ab103809), rabbit monoclonal anti-TRAF6 (ab33915), rabbit polyclonal anti-TWEAK (ab37170), rabbit polyclonal anti-MURF1 (ab77577), rabbit polyclonal anti-phospho Smad3 (S423 and S425; ab51451) and rabbit polyclonal anti-IL-6 (ab6672) were acquired from Abcam (Cambridge, UK). Rabbit polyclonal anti-DNP antibody was obtained from DakoCytomation (Hamburg; Germany). Mouse monoclonal anti-3-nitrotyrosine antibody (#06-284; Millipore) was obtained from Chemicon (CA, USA). Mouse monoclonal MMP-9 (Clone 36020; MAB936) was acquired from R&D systems (Minneapolis, USA). Rabbit polyclonal atrogin-1 antibody (AP2041) was obtained from ECM BioAciences (KY, USA). Rabbit polyclonal antibodies for *p*-mTOR (#2971) and *p*-Akt (#4058), and rabbit monoclonal *p*-4E-BP1 (#2855) and *p*-p70S6K (#9234) were acquired from Cell Signalling Technology (MA, USA). Secondary peroxidase-conjugated antibodies (anti-mouse IgG and anti-rabbit IgG) were obtained from GE Healthcare (UK). ELISA kit for the determination of IL-1β was acquired from R&D (cat. no RLB00). Colorimetric kit from RANDOX (LC2389; UK) was used to measure serum lactate.

2.2. Animals

Twenty three female Wistar rats were obtained at the age of 5 weeks from Harlan (Barcelona, Spain). During the experimental protocol, animals were housed in groups of 4 rats/cage, in a controlled environment at 22 ± 3 °C and 60 ± 10% of relative humidity with 12:12 h light-dark cycle, with free access to food and water. After a week of acclimatization, the animals were randomly divided into two groups: control (CONT; $n = 10$) and urothelial carcinogenesis (BBN; $n = 13$). The following protocol was approved by the Portuguese Ethics Committee for Animal Experimentation.

2.3. Induction and characterization of BBN-induced urothelial carcinogenesis

In order to induce urothelial carcinogenesis, one group of animals was treated with N-butyl-N-(4-hydroxybutyl)-nitrosamine (BBN group), which was administered in the drinking water, in light impermeable bottles, at a concentration of 0.05%. No chemical supplementation was added to the drinking water of control animals. The urothelial carcinogenesis group was exposed to BBN for 20 weeks and was maintained with normal tap water until the end of the experiment. After 28 weeks, all animals were sacrificed with 0.4% sodium pentobarbital (1 mL/kg, intraperitoneal) and blood was collected from heart. The urinary bladders were inflated in situ by injection of 10% phosphate-buffered formalin (300 μL), ligated around the neck to maintain proper distension and then were immersed in the same solution for 12 h. After fixation, the formalin was removed; the urinary bladder was cut into strips and was routinely processed for haematoxylin and eosin staining. Urine was collected one week before the end of the experimental protocol with the use of metabolic cages (after a 48 h adaptation period).

2.4. Histopathological analysis

All sections were reviewed by two researchers and the urothelial lesions staged by the World Health Organization/International Society of Urological Pathology consensus classification of urothelial (transitional cell) neoplasms of the urinary bladder (Epstein et al., 1998). The urothelial lesions were categorized as simple hyperplasia, nodular hyperplasia, papillary hyperplasia, dysplasia, carcinoma *in situ* (CIS), papilloma, papillary neoplasm of low malignant potential, low-level papillary carcinoma, high-level papillary carcinoma, invasive carcinoma and epidermoid metaplasia.

2.5. Blood tests

Serum albumin, total protein, cholesterol, HDL-cholesterol and triglycerides were measured in duplicate on an AutoAnalyzer (PRESTIGE 24i, Cormay PZ). IL-1β serum levels were detected by an ELISA kit used according to the manufacturer instructions (R&D). Serum from each animal was assayed in triplicate. Serum lactate was measured with a commercial kit (RANDOX). Serum C-reactive protein, IL-6, TNF-a, TWEAK and myostatin levels were assayed by immunoblotting as described below.

2.6. Mitochondria isolation from gastrocnemius muscle

The *gastrocnemius* muscles were extracted during animals' sacrifice for the preparation of isolated mitochondria, as previously described (Tonkonogi and Sahlin, 1997). All the procedures were performed on ice or below 4 °C. Briefly, muscles were immediately excised and minced in ice-cold isolation medium containing 100 mM sucrose, 0.1 mM ethylene glycol tetraacetic acid, 50 mM Tris–HCl, 100 mM KCl, 1 mM KH_2PO_4, and 0.2% free fatty acid bovine serum albumin (BSA), pH 7.4. Minced blood-free tissue was rinsed and suspended in 10 mL of fresh medium containing 0.2 mg/mL bacterial proteinase (Nagarse E.C.3.4.21.62, type XXVII; Sigma, MO) and stirred for 2 min. The sample was then carefully homogenized

with a tightly fitted Potter–Elvehjem homogenizer and a Teflon pestle. An aliquot of whole homogenate was reserved for biochemical analysis. After homogenization, three volumes of Nagarse-free isolation medium were added to the homogenate, which was then centrifuged at 700 *g* for 10 min. The resulting supernatant suspension was centrifuged at 10,000 *g* for 10 min. The pellet was gently resuspended in the isolation medium (1.3 mL/100 mg initial tissue) and centrifuged at 7000 *g* for 3 min. The final pellet, containing the mitochondrial fraction, was gently resuspended (0.4 mL/mg initial tissue) in a medium containing 225 mM mannitol, 75 mM sucrose, 10 mM Tris, and 0.1 mM EDTA, pH 7.4.

Mitochondrial fraction was aliquoted for subsequent biochemical analysis. Protein content was determinate with RD DC Protein Assay Kit (Bio-Rad, CA, USA) and mtDNA content was quantified with Qubit™ fluorometer (Invitrogen, CA, USA).

2.7. Blue-native PAGE separation of mitochondrial membrane complexes and in-gel activity of complexes IV and V

BN-PAGE was performed using the method described by Schagger and von Jagow (Taylor et al., 1994) with minor modifications. Muscle mitochondria (400 μg of protein) from each animal were pelleted by centrifugation at 20,000 *g* for 10 min and then resuspended in solubilization buffer (50 mM NaCl, 50 mM imidazole, 2 mM ε-amino n-caproic acid, 1 mM EDTA pH 7.0) with 1% (w/v) digitonin. After 10 min on ice, insoluble material was removed by centrifugation at 20,000 *g* for 30 min at 4 °C. Soluble components were combined with 0.5% (w/v) Coomassie Blue G250, 50 mM ε-amino n-caproic acid, 4% (w/v) glycerol and separated on a 4–13% gradient acrylamide gradient gel with 3.5% sample gel on top. Anode buffer contained 25 mM imidazole pH 7.0. Cathode buffer (50 mM tricine and 7.5 mM imidazole pH 7.0) containing 0.02% (w/v) Coomassie Blue G250 was used during 1 h at 70 V, the time needed for the dye front reach approximately one-third of the gel. Cathode buffer was then replaced with one containing only 0.002% (w/v) Coomassie Blue G250 and the native complexes were separated at 200 V for 4 h at 4 °C. Gels were stained with Coomassie Colloidal for protein visualization and scanned with Molecular Imager Gel Doc XR+ System (Bio-Rad).

The in-gel activity and histochemical staining assays of complexes IV and V were determined using the methods described by Zerbetto et al. (Simon et al., 2003). Complex IV-specific heme stain in BN-PAGE gels was determined using 10 μL horse heart cytochrome c (5 mM) and 0.5 mg diaminobenzidine (DAB) dissolved in 1 mL 50 mM sodium-phosphate, pH 7.2. The reaction was stopped by 50% (v/v) methanol, 10% (v/v) acetic acid, and the gels were then transferred to water. ATP hydrolysis activity of complex V was analyzed by incubating the native gels with 35 mM Tris, 270 mM glycine buffer, pH 8.3 at 37 °C, that had been supplemented with 14 mM $MgSO_4$, 0.2% (w/v) $Pb(NO_3)_2$, and 8 mM ATP. Lead phosphate precipitation that is proportional to the enzymatic ATP hydrolysis activity, was stopped by 50% (v/v) methanol, and the gels were then transferred to water. Band detection and activity quantification were performed using QuantityOne Imaging software (v4.6.3, Bio-Rad).

2.8. Spectrophotometric assay of ATP synthase activity

For spectrophotometric determination of complex V respiratory chain activity mitochondrial fractions and whole *gastrocnemius* muscle were disrupted by a combination of freeze–thawing cycles in hypotonic media (25 mM potassium phosphate, pH 7.2) to allow free access to substrates for all assays (Taylor et al., 1994). ATP synthase activity was measured according to Simon et al. (2003). The phosphate produced by hydrolysis of ATP reacts with ammonium molybdate in the presence of reducing agents to form a blue-color complex, the intensity of which is proportional to the concentration of phosphate in solution. Oligomycin was used as an inhibitor of mitochondrial ATPase activity. A Multiskan GO Microplate Spectrophotometer (Thermo Scientific) was used for respiratory chain complexes activities measurement, which was performed at 30 °C.

2.9. Analysis of proteolytic activity through gelatine zymography

Zymography assays were performed according to Caseiro et al. (2012) with minor modifications. Briefly, a 10% SDS-PAGE separation gel with 0.1% of gelatin was used. Fifteen micrograms of protein from whole *gastrocnemius* muscle or urine samples were incubated on charging buffer (100 mM Tris pH 6.8, 5% SDS, 20% glycerol, 0.1% bromophenol blue) for 10 min on ice, in a proportion of 1:1 (v/v). After the run, gels were incubated in renaturation buffer (2.5% Triton X-100) for 30 min, with agitation. The zymo gels were changed to a development buffer (50 mM Tris, 5 mM NaCl, 10 mM $CaCl_2$, 1 μm $ZnCl_2$, 0.02% (v/v) Triton X-100, pH 7.4) for more 30 min, followed by an overnight incubation at 37 °C in a new development buffer. For specific inhibition studies zymograms were incubated in a solution containing 10 mM EDTA or 1 mM PMSF. The zymo gels were stained with 0.12% (w/v) Coomassie Blue G250 prepared in 20% methanol, after 1 h fixation in a solution of 10% acetic acid and 40% methanol. Gels were then destained with 25% methanol and scanned with Molecular Imager Gel Doc XR+ System.

2.10. Immunoblotting analysis

Equivalent amounts of serum, mitochondrial or whole *gastrocnemius* muscle proteins of each group were electrophoresed on a 12.5% SDS-PAGE as described by Laemmli (1970). Gels were blotted onto a nitrocellulose membrane (Whatman®, Protan) in transfer buffer (25 mM Tris, 192 mM glycine, pH 8.3 and 20% methanol) during 2 h (200 mA). Then, nonspecific binding was blocked with 5% (w/v) dry nonfat milk in TBS-T (100 mM Tris, 1.5 mM NaCl, pH 8.0 and 0.5% Tween 20). Membranes with serum samples were incubated with primary antibody diluted 1:1000 5% (w/v) nonfat dry milk in TBS-T (anti-CRP, anti-GDF8, anti-IL-6, anti-TNF-α or anti-TWEAK) for 2 h at room temperature, washed and incubated with secondary horseradish peroxidase-conjugated anti-rabbit (1:1000; GE Healthcare). Membranes with mitochondria fractions were incubated with primary antibody diluted 1:1000 in 5% (w/v) nonfat dry milk in TBS-T (anti-paraplegin, anti-ATPB, anti-LONP1 or anti-mtTFA) for 2 h at room temperature, washed and incubated with secondary horseradish peroxidase-conjugated anti-mouse or anti-rabbit (GE Healthcare), respectively. Whole *gastrocnemius* muscle membranes were incubated with primary antibody diluted 1:1000 in 5% (w/v) BSA in TBS-T (anti-phospho-Akt, anti-atrogin-1, anti-GDF8, anti-TWEAK, anti-MuRF1, anti-TRAF6, anti-phospho-mTOR, anti-phospho-p70S6K, anti-phospho-4E-BP1 or anti-phospho-Smad3) for 2 h at room temperature, washed and incubated with secondary horseradish peroxidase-conjugated anti-rabbit (GE Healthcare). Immunoreactive bands were detected by enhanced chemiluminescence ECL (Amersham Pharmacia Biotech) according to the manufacturer's procedure and images were recorded using X-ray films (Kodak Biomax Light Film, Sigma, MO, USA). The films were scanned in Molecular Imager Gel Doc XR+ System and analyzed with QuantityOne software. Control for protein loading was confirmed by Ponceau S staining.

For the protein carbonyl derivates assay, a given volume (V) of sample containing 20 μg of protein was derivatized with 2,4-dinitrophenylhydrazine (DNPH). Briefly, the sample was mixed with 1 V of 12% sodium dodecyl sulfate, 2 V of 2 mM DNPH/10% trifluoroacetic acid, followed by 30 min of incubation in the dark, after which 1.5 V of 2 M Tris-base/18.3% of β-mercaptoethanol was added for neutralization. After diluting the derivatized proteins

Table 1
Characterization of the animals used in the study regarding body weight, muscle mass and muscle-to-body weight.

Experimental groups	Body weight (g)	Muscle weight (g)	Muscle/body weight ratio (mg g^{-1})
CONT	309.0 ± 21.1	3.3 ± 0.3	10.5 ± 0.5
BBN	256.6 ± 4.1***	2.9 ± 0.1*	11.2 ± 1.5

Values are expressed as mean ± standard deviation.
* $p < 0.05$ vs CONT.
*** $p < 0.001$ vs CONT.

in TBS to obtain a final concentration of 0.001 μg/μL, a 100 μL volume was slot-blotted into a nitrocellulose membrane. For 3-nitrotyrosine, mitochondria and whole *gastrocnemius* muscles samples were diluted in TBS to obtain a final protein concentration of 0.001 μg/μL and a volume of 100 μL was slot-blotted into a nitrocellulose membrane. For MMP-9, whole *gastrocnemius* muscle samples were diluted in TBS to obtain a final protein concentration of 0.001 μg/μL and a volume of 100 μL was slot-blotted into a nitrocellulose membrane.

The slot-blot membranes were blocked with 5% (w/v) dry nonfat milk in TBS-T for 30 min and then incubated for 30 min with primary antibody (anti-MMP-9, anti-3-nitrotyrosine or anti-DNP) diluted 1:1000 in 5% (w/v) nonfat dry milk in TBS-T. The membranes were washed three times (10 min each) with TBS-T and incubated for 30 min with a solution of horseradish-conjugated anti-mouse or anti-rabbit antibody, respectively, in a dilution of 1:1000. Detection was carried out with enhanced chemiluminescence and images were recorded using X-ray films. The films were scanned in Molecular Imager Gel Doc XR+ System and analyzed with QuantityOne software. Control for protein loading was confirmed by Ponceau S staining.

2.11. Statistical analysis

The results are presented as mean ± SD for each experimental group. The Kolmogorov–Smirnov test was used to test normality of distribution for all data. Since all variable were normally distributed, significant differences between the two groups were evaluated with the unpaired Student's *t*-test. Statistical Package for the Social Sciences (SPSS Inc., Chicago, IL, USA, version 12.0) was used for all analyses. A p value <0.05 was considered significant.

3. Results

3.1. Characterization of rat's response to BBN administration

Body and *gastrocnemius* muscle weight and *gastrocnemius* muscle-to-body weight ratio for the animal groups studied are reported in Table 1. Significant 17% loss of body weight was observed in BBN-treated rats ($p < 0.001$) when compared with control ones, highlighting the cachexia condition. This body weight decrease was accompanied by a 12% reduction in *gastrocnemius* muscle mass ($p < 0.05$ vs CONT). No significant differences of muscle-to-body weight ratio were observed between groups. Moreover, no significant differences in food intake were associated to urothelial carcinoma (Fig. S1).

Supplementary material related to this article found, in the online version, at http://dx.doi.org/10.1016/j.biocel.2013.04.014.

3.2. Serum catabolic drive

As can be observed in Table 2, serum markers of inflammation and catabolism presented significant alterations in BBN-treated rats, with a decrease of serum albumin and total protein levels ($p < 0.05$), as well as triglycerides and increase in serum lactate ($p < 0.0001$). Total cholesterol and HDL-cholesterol were not affected by BBN treatment.

These alterations were paralleled by an increase in the levels of the pro-inflammatory cytokines TNF-α ($p < 0.05$), TWEAK and IL-1β ($p < 0.01$), of the acute reaction phase protein CRP ($p < 0.001$) and of the TGF-β member myostatin ($p < 0.01$), assessed by immunoblotting and ELISA (for IL-1β) (Fig. 1). No BBN-related differences of IL-6 were noticed (Fig. 1C). Altogether, data highlight the catabolic profile underlying BBN chemically-induced urothelial carcinoma.

3.3. Urine proteolytic profile

The effect of BBN treatment on urine proteolytic profile was evaluated by zymography with gelatin as substrate. As can be seen in Fig. 2, no differences were observed in the profile of zymo bands but BBN-related alterations in the proteolytic activity were noticed, which were higher for bands 4 and 6. The inhibitory effect of EDTA on zymo proteolytic activity suggests a high contribution of MMPs to the urine proteolytic activity. Considering the molecular weight of the bands with proteolytic activity (according to Uniprot (http://www.uniprot.org/) and Brenda (http://www.brenda-enzymes.info/)) we might suspect of the presence of MMP-2 (72 kDa) and MMP-7 (30 kDa). Since several MMPs present a molecular weight of approximately 50 kDa (e.g. MMP-8, MMP-12 or MMP-16), no association with a specific MMP can be established for band 2.

3.4. Macroscopic and microscopic evaluation of urothelial lesions

The incidence of histopathological lesions in each group is shown in Table 3. No histopathological changes in the urothelium were observed in control rats. Nodular hyperplasia was detected in all bladders of BBN-treated rats whereas simple hyperplasia and dysplasia were observed in more than 75% of the animals. Besides benign lesions, BBN administration induced malignant injury in different areas of the urothelium, which occurred simultaneously in most cases. Signs of invasive carcinoma were only observed in

Table 2
Effect of BBN administration in serum biochemical profile.

Experimental groups	Albumin (g L^{-1})	Protein (g L^{-1})	Lactate (mg dL^{-1})	Cholesterol (mg dL^{-1})	HDL-c (mg dL^{-1})	Triglycerides (mg dL^{-1})
CONT	40.3 ± 3.2	66.5 ± 4.8	49.7 ± 6.45	42.4 ± 16.5	15.3 ± 3.7	94.0 ± 20.0
BBN	36.7 ± 3.0*	62.6 ± 3.6*	92.6 ± 22.4***	30.9 ± 12.2	12.8 ± 2.6	50.0 ± 15.8***

Values are expressed as mean ± standard deviation.
* $p < 0.05$ vs CONT.
*** $p < 0.0001$ vs CONT.

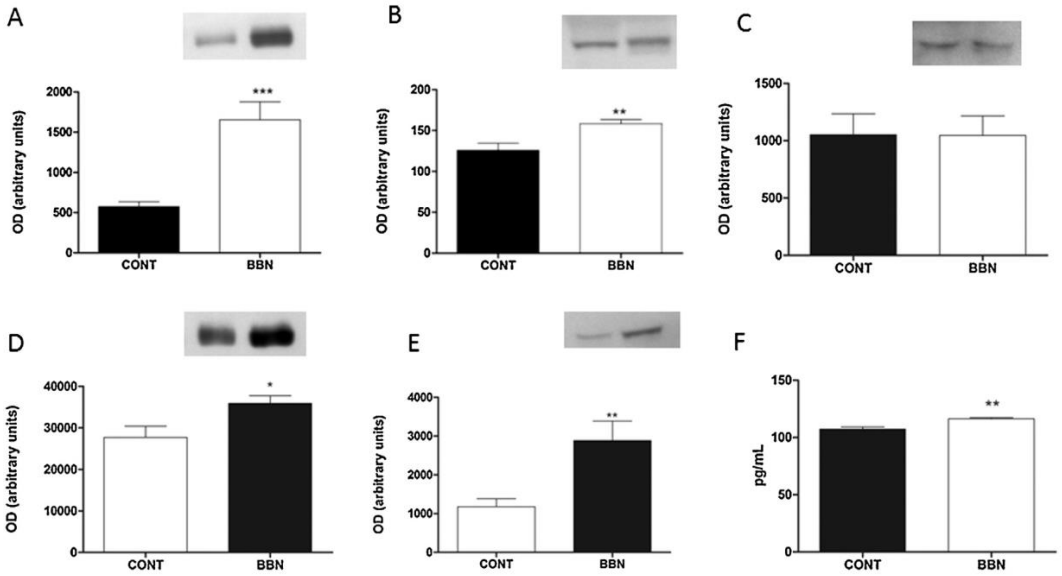

Fig. 1. Serum CRP (A), myostatin (B), IL-6 (C), TNF-α (D) and TWEAK (E) expression evaluated by western blotting, and IL-1β (F) determined by ELISA from BBN and control animals. Representative immunoblots are presented above the corresponding graph. Values are expressed as mean ± standard deviation (*$p < 0.05$ vs CONT, **$p < 0.01$ vs CONT, ***$p < 0.001$ vs CONT).

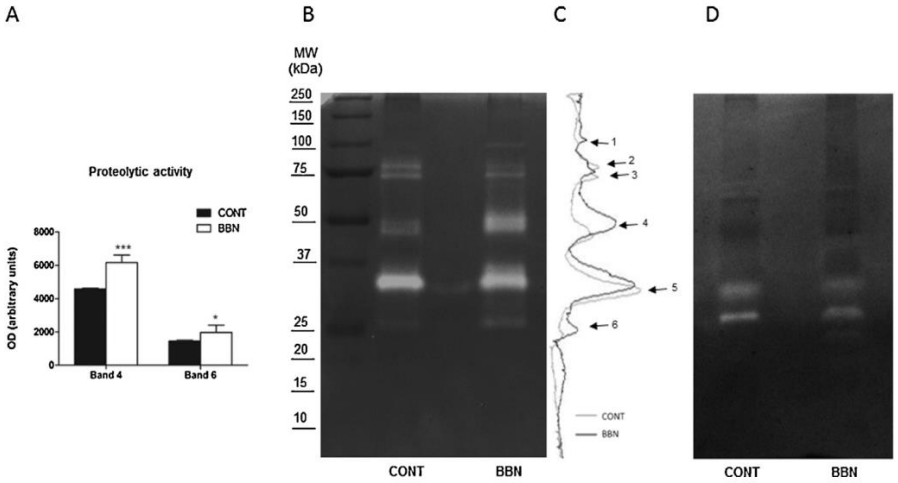

Fig. 2. Effect of BBN administration on urinary proteolytic activity. (B) Representative image of the zymo gel evidencing six bands with proteolytic activity. An overlap of densitometric variation for CONT and BBN lanes is presented in the left side of zymo gel (C). The semi-quantitative analysis of bands 4 and 6′ proteolytic activities for each group is presented in (A). Representative image of the zymo gels in the presence of the metalloproteases inhibitor EDTA (D).

Table 3
Incidence of urothelial lesions in Wistar rats exposed to BBN.

Histological lesion	Experimental groups	
	CONT	BBN
Normal urothelium	10/10 (100%)	0 (0%)
Simple hyperplasia	0 (0%)	11/13 (85%)
Nodular hyperplasia	0 (0%)	13/13 (100)
Papillary hyperplasia	0 (0%)	9/13 (70%)
Dysplasia	0 (0%)	10/13 (76.9%)
CIS	0 (0%)	0 (0%)
Papilloma	0 (0%)	3/13 (23%)
Papillary neoplasm of low malignant potential	0 (0%)	8/13 (61.5%)
Low-level papillary carcinoma	0 (0%)	11/13 (84.6%)
High-level papillary carcinoma	0 (0%)	10/13 (76.9%)
Invasive carcinoma	0 (0%)	5/13 (38.5%)
Epidermoid metaplasia	0 (0%)	9/13 (70%)

39% of BBN animals, suggesting a predominance of non-muscle-invasive bladder tumors.

3.5. Analysis of the anabolic/catabolic balance in gastrocnemius muscle

To determine the effect of BBN administration in activated Akt, phopho-Akt levels were evaluated by western blotting. As can be seen in Fig. 3A, a statistically significant decrease in the expression levels of Akt Ser^{473} phosphorylation were noticed in *gastrocnemius* muscle from BBN-treated rats compared to control ones ($p < 0.05$). The expression of mTOR phosphorylated form was also analyzed and a significant decrease ($p < 0.05$) was found on phosphorylated Ser^{2448} mTOR in BBN group (Fig. 3B). The downstream targets of mTOR were also analyzed and lower levels of phosphorylated

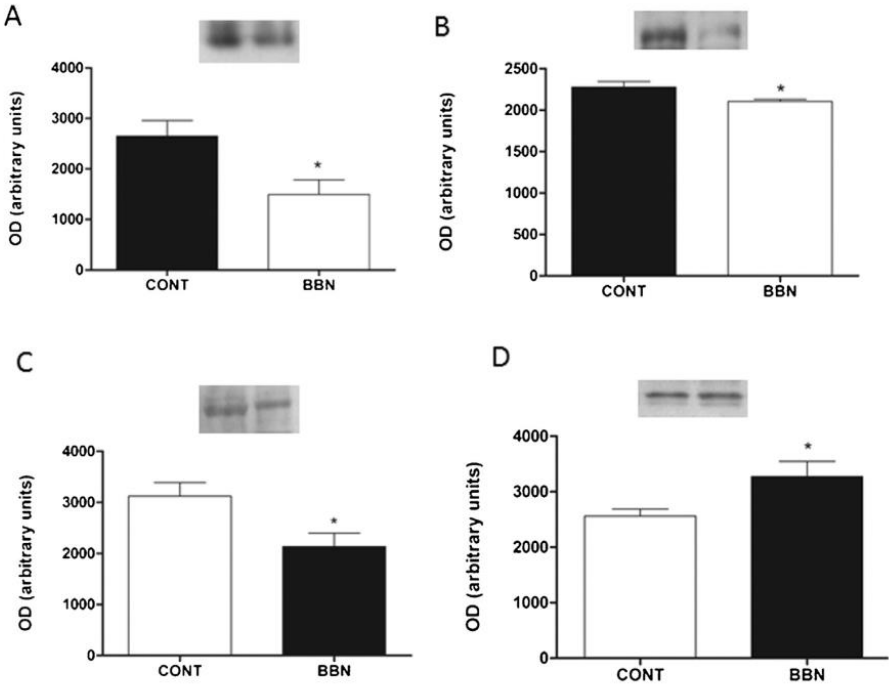

Fig. 3. *p*-Akt (A), *p*-mTOR (B), *p*-S6K1 (C) and *p*-4EBP1 (D) expression evaluated by western blotting in whole *gastrocnemius* muscle from BBN and control animals. Representative immunoblots are presented above the corresponding graph. Values are expressed as mean ± standard deviation (*$p < 0.05$ vs CONT).

Thr^{389} 70S6K1 were detected but an unexpected higher content of $Thr^{37/46}$ 4E-BP1 was observed in the *gastrocnemius* from rats with urothelial carcinoma (Fig. 3C and D, respectively).

The contribution of the ubiquitin–proteasome system to bladder cancer-induced muscle wasting was evaluated by western blotting analysis of MAFbx/atrogin-1, MuRF-1 and TRAF6 (Fig. 4). Data evidences a statistically significant increase of the E3 ligases atrogin-1 (approximately 11%) and TRAF6 (41%) in the *gastrocnemius* muscle from BBN-treated rats ($p < 0.01$). No differences were noticed for MuRF1 (Fig. 4E). The levels of phosphorylated Ser^{423}/Ser^{425} Smad3 increased in the skeletal muscle of BBN animals, as well as the TGF-β superfamily member myostatin (Fig. 4F and A, respectively; $p < 0.01$). Western blotting analysis of TWEAK expression in whole muscle (Fig. 4B) also evidenced a significant increased content of

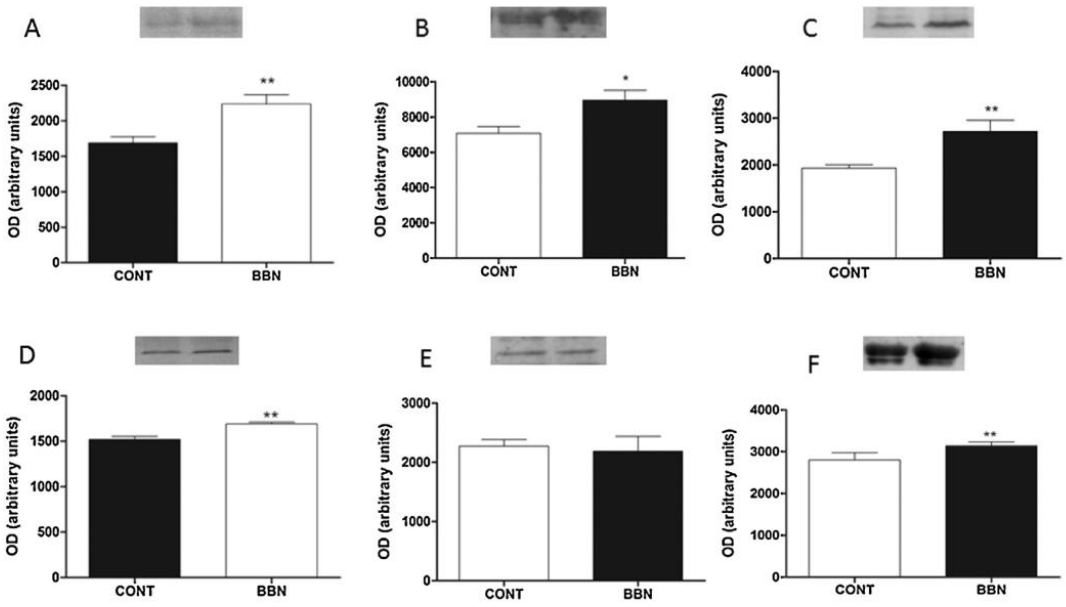

Fig. 4. Myostatin (A), TWEAK (B), TRAF6 (C), atrogin-1 (D), MuRF-1 (E) and *p*-Smad3 (F) expression evaluated by western blotting in whole *gastrocnemius* muscle from BBN and control animals. Representative immunoblots are presented above the corresponding graph. Values are expressed as mean ± standard deviation (*$p < 0.05$ vs CONT; **$p < 0.01$ vs CONT).

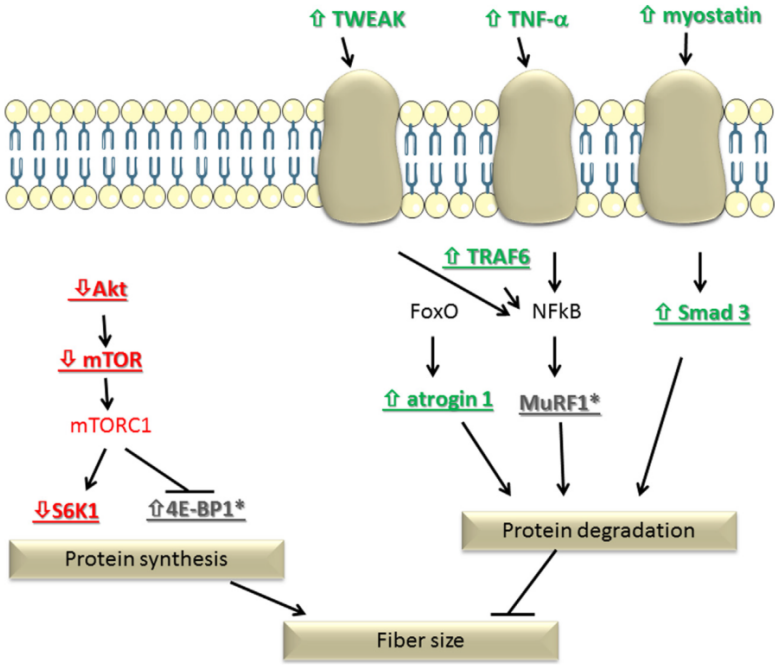

Fig. 5. Integrated perspective of signaling pathways modulated by urothelial carcinoma in *gastrocnemius* muscle. The proteins analyzed in the present study are highlighted (bold and underlined) with the up-regulated ones presented in green and the down-regulated in red. Proteins with unexpected expression variation are presented in grey and marked with an *.

Figure was produced using Servier Medical Art.

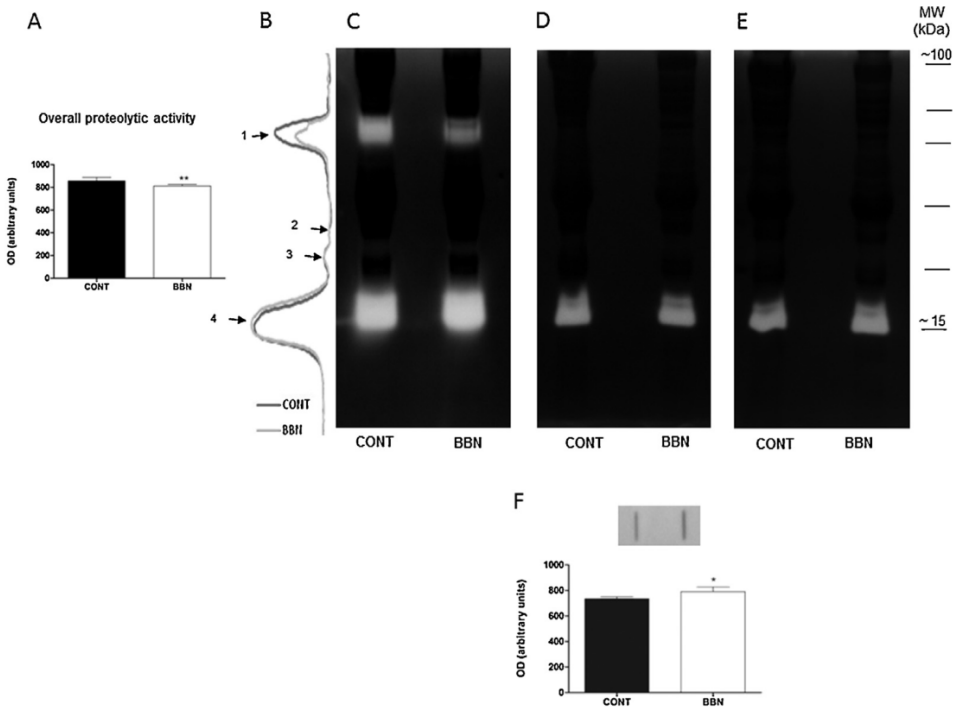

Fig. 6. Effect of BBN administration on whole *gastrocnemius* muscle proteolytic activity. (C) Representative image of the zymography evidencing two bands with noticeable proteolytic activity (bands 1 and 4). An overlap of densitometric variation for CONT and BBN lanes is presented in the left side of zymo gel (B). Semi-quantitative analysis of overall proteolytic activity for each group is presented in (A). Representative images of the zymo gels in the presence of inhibitors for (D) serine protease (PMSF) and for (E) metalloproteases (EDTA). Comparative analysis of MMP-9 expression between groups is presented in (F). A representative immunoblot is presented above the graph. Values are expressed as mean ± standard deviation (*$p < 0.05$ vs CONT; **$p < 0.01$ vs CONT).

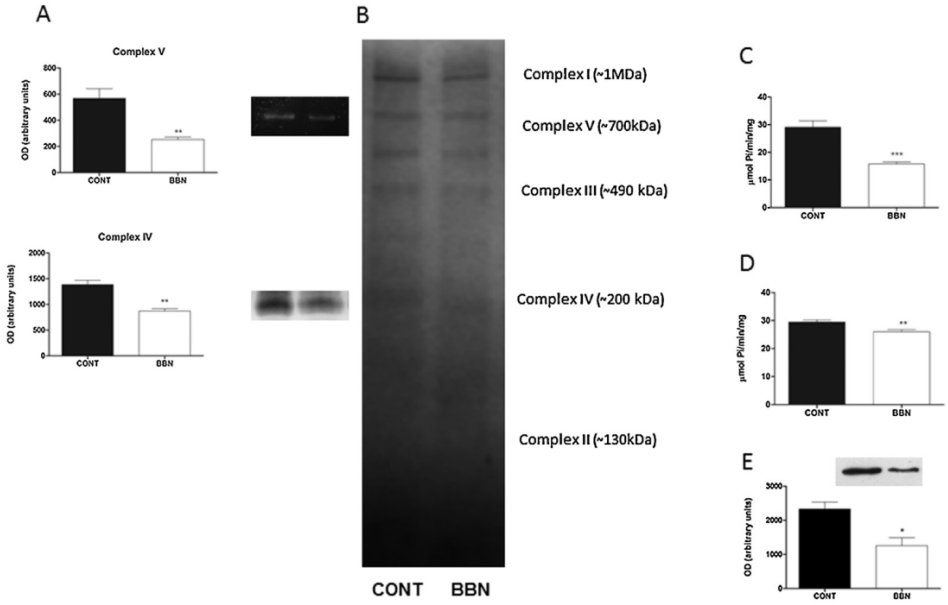

Fig. 7. Evaluation of respiratory chain structural organization and activity. (A) Representative image of histochemical staining of in-gel activity of complexes IV and V. On the left side is presented a semi-quantitative analysis of in-gel activity of both complexes. (B) Representative image of supramolecular architecture of mitochondrial membrane complexes resolved by BN-PAGE for BBN and CONT groups. ATP synthase activity on mitochondria (C) and on whole muscle (D) spectrophotometrically assessed and ATP synthase β (E) expression evaluated by western blotting. Representative immunoblot is presented above the graph. Values are expressed as mean ± standard deviation (*$p < 0.05$ vs CONT; **$p < 0.01$ vs CONT; ***$p < 0.001$ vs CONT).

this pro-inflammatory cytokine in BBN-treated animal ($p < 0.01$). To better visualize all these data, an integrative picture is presented in Fig. 5.

The analysis of muscle proteolysis performed by gelatin zymography evidenced an overall 5% decrease in BBN-treated rats ($p < 0.01$; Fig. 6A). The densitometric evaluation of the zymogram profile (Fig. 6B) displayed four common bands in the muscle of all animals. Two of these bands showed higher activity, one with approximately 80 kDa (band 1) and other with approximately 15 kDa (band 4). Band 1 activity was the most affected by BBN-related urothelial carcinoma. To have a general idea of protease classes present in each band, zymo gels were incubated with different inhibitors at their maximum effective concentration: PMSF (serine protease inhibitor) and EDTA (metalloproteinase inhibitor). Data obtained (Fig. 6D and E) suggest the involvement of both serine- and metalloproteases. The slot blot analysis of MMP-9 showed a significantly higher expression of this metalloprotease in BBN-treated rats (7.5% ($p < 0.05$); Fig. 6F).

3.6. Analysis of mitochondrial functionality, proteolysis and protein susceptibility to oxidation

The levels of mtDNA and mitochondrial protein were quantified in mitochondria isolated from *gastrocnemius* muscle. As can be depicted from Table 4, a higher concentration of muscle mtDNA and protein-to-muscle mass ratio were noticed in BBN-treated rats ($p < 0.05$); however, no significant differences in the ratio mtDNA-to-nDNA and on the SDS-PAGE quantitative profile (Fig. S2) were noticed among groups. Taken together, data suggest the occurrence of muscle atrophy in the animals with urothelial carcinoma. Moreover, these mitochondria showed lower ability to produce ATP in view of lower cytochrome c oxidase and ATP synthase in-gel activities, further corroborated by the spectrophotometric determination of complex V activity and ATP synthase beta expression (Fig. 7A and C). Though lower ATP synthase activities were observed either in isolated mitochondria (Fig. 7C) as in whole muscle (Fig. 7D) of BBN animals, a higher BBN-related decrease was noticed in isolated mitochondria. Lower mtTFA expression levels were also observed in the skeletal muscle mitochondria from these animals (Fig. 8C).

Supplementary material related to this article found, in the online version, at http://dx.doi.org/10.1016/j.biocel.2013.04.014.

To evaluate the involvement of the proteases known to be implicated in mitochondrial protein quality control (PQC), we analyzed the expression of the specific m-AAA protease paraplegin and of the matrix Lon protease (Fig. 8A and B). Lower expression values of these serine proteases (75% for paraplegin ($p < 0.05$; Fig. 8A) and 40% for Lon ($p < 0.001$; Fig. 8B)) were observed in BBN-treated animals.

Taken in consideration the involvement of PQC proteases in the elimination of damaged proteins and their impairment in BBN

Table 4
Effect of BBN administration in mitochondrial protein and mtDNA content, and in the ratio mtDNA-to-nDNA in *gastrocnemius* muscle.

Experimental groups	Protein/mtDNA ($\mu g\,g^{-1}$)	mtDNA/muscle weight ($\mu g\,g^{-1}$)	Protein/muscle weight ($mg\,g^{-1}$)	mtDNA/nDNA (%)
CONT	1.8 ± 0.8	1.1 ± 0.2	1995.9 ± 672.3	21.6 ± 5.6
BBN	0.8 ± 0.3*	4.3 ± 2.8*	2875.1 ± 759.3*	18.7 ± 5.7

Values are expressed as mean ± standard deviation.
* $p < 0.05$ vs CONT.

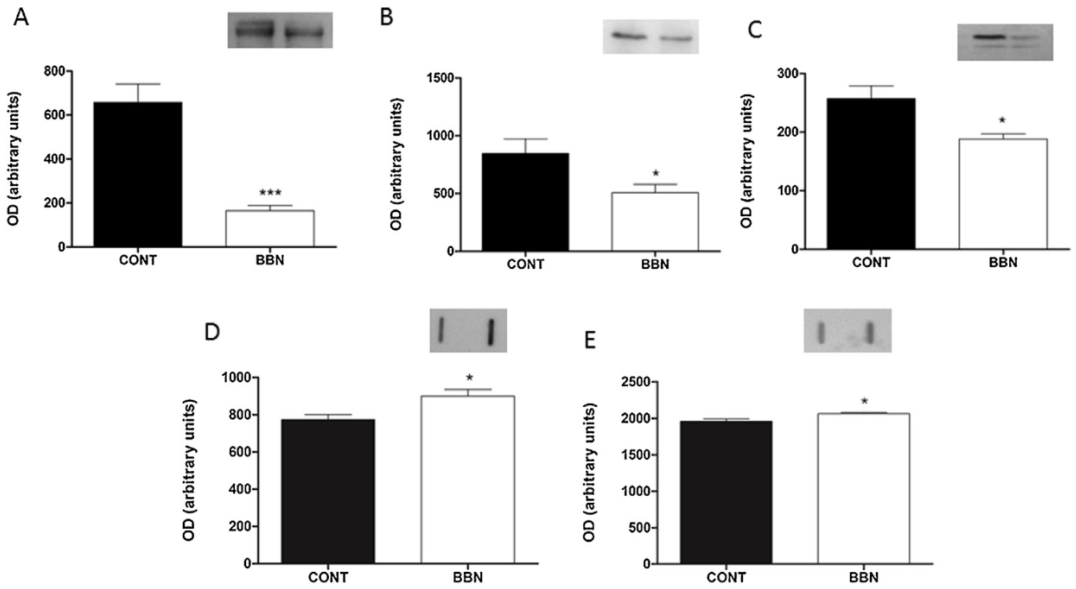

Fig. 8. Effect of BBN administration on m-AAA paraplegin (A) and LonP1 (B), and mtTFA (C) expression evaluated by western blotting in mitochondrial fractions. Protein carbonyl (D) and 3-nitrotyrosine (E) content evaluated by slot blot in isolated mitochondria from BBN and CONT animals. Representative immunoblots are presented above the corresponding graph. Values are expressed as mean ± standard deviation (*$p < 0.05$ vs CONT; ***$p < 0.001$ vs CONT)

mitochondria, the levels of carbonylated proteins were measured by slot blot after derivatization with dinitrophenylhydrazine. A significant increase of 16% ($p < 0.05$) was observed in mitochondria from BBN animals' skeletal muscle when compared with controls (Fig. 8D). In order to assess the protein nitration levels, we measured 3-nitrotyrosine content and, as can be seen in Fig. 8E, higher levels of nitrated proteins were observed in mitochondria from BBN-treated rats (5% ($p < 0.05$)).

4. Discussion

4.1. Overall findings

In the present study, we utilized an animal model of urothelial carcinogenesis chemically induced by the administration of N-butyl-N-(4-hydroxybutyl)-nitrosamine (BBN), a genotoxic compound known to induce cancer (Oliveira et al., 2006). After administration of BBN in the drinking water, bladder tumors formed within 20 weeks. These tumors in rats are equivalent to the non-muscle-invasive urothelial carcinoma clinically observed in humans (Palmeira et al., 2009, 2010; Oliveira et al., 2007). This well-established model reflects one of the most commonly occurring malignant tumors of the urinary tract, associated with chemical risk factors as smoking and aromatic amines (Oliveira et al., 2007; Roupret et al., 2011). Though it is recognized that carcinogen-induced tumors resemble human cancer since they arise spontaneously and reproduce tumor–host interactions, they are not generally used for the study of cancer-induced muscle wasting since the experiments tend to be lengthy and costly (Bennani-Baiti and Walsh, 2011). At the end of the protocol, most of the animals showed histologic signs of non-muscle-invasive carcinoma (Table 3) and evidenced 17% loss of body weight, a value that in humans is seen as a sign of moderate cachexia according to the cachexia score (CASCO) (Argiles et al., 2011). This body weight decrease was paralleled by a 12% loss of *gastrocnemius* mass (Table 1), suggestive of altered muscle properties such as weakness and fatigue (Shum et al., 2012; Argiles et al., 2011).

4.2. Catabolic profile associated with carcinoma-induced muscle wasting

The significantly high serum levels of the pro-inflammatory cytokines IL-1β, TNF-α and TWEAK, and of the acute phase protein CRP observed in BBN animals, supports the catabolic profile noticed in this group. Despite evidences of systemic inflammation, no significant effects on animals' appetite were noticed. No differences of serum IL-6 levels were observed; however, the association between serum levels of this cytokine and weight loss is not straightforward and in studies performed with mice bearing clones of the colon-26 tumor or with patients with non-small-cell-lung cancer no relation between serum IL-6 and cachexia was observed (Patra and Arora, 2012). Myostatin and related ligands have also been suggested as the main responsible for weight loss in patients afflicted by various forms of cancer (Lokireddy et al., 2012). The levels of this member from the transforming growth factor-β superfamily known to be a negative regulator of muscle bulk (Springer et al., 2010) was found in significantly higher levels in the serum of BBN rats (Fig. 1B). Though expressed almost exclusively in skeletal muscle (Springer et al., 2010), myostatin was recently proposed as a novel tumoral factor that might initiate the pathogenesis of cancer cachexia (Lokireddy et al., 2012). Our data suggest that the raise of this TGF-β ligand is due, at least partially, to an increase of its expression in the *gastrocnemius* muscle (Fig. 4A).

BBN administration also induced metabolic disturbances including hypoalbuminaemia and high levels of serum lactate. The diminishing of serum triglycerides does not support the usually described cancer cachexia-related lipolysis (Tisdale, 2009). Nevertheless, bladder cancer-related catabolic phenotype is not always accompanied by altered lipolysis (Lattermann et al., 2003). The higher activity of MMPs in the urine of BBN rats (Fig. 2) further supports the catabolic profile related to urothelial carcinoma. The release of MMP-1, MMP-2 and MMP-9 by rat bladder tumorigenic/invasive cell lines was previously reported (Kawamata et al., 1993). Our data suggest the contribution of MMP-2 and MMP-7 in the extracellular matrix remodeling of urothelium carcinoma. Other MMPs seem involved but further analysis should be

performed to investigate their association with bladder cancer-related muscle wasting. Though interest has been noticed in the monitoring of MMPs in the clinical setting as diagnostic or prognostic biomarkers of bladder cancer (Szarvas et al., 2011), few studies have analyzed the association of these proteases with cancer-induced muscle wasting (Camargo et al., 2011; Peluffo et al., 2004).

Once established the urothelial carcinoma-induced catabolic phenotype, the molecular mechanisms underlying bladder cancer-induced muscle wasting were searched. Myostatin together with cytokines like IL-1β, TNF-α and TWEAK elicits catabolism on skeletal muscle by elevating the levels of muscle-specific E3 ligases and increasing the intracellular protein degradation through the ubiquitin–proteasome pathway (Tisdale, 2009; Lokireddy et al., 2012; Skipworth et al., 2007). Myostatin was reported to block IGF1-PI3K-Akt pathway and to activate FoxO1, promoting the increased expression of atrogin-1, in an NFkB-independent manner. NFkB activation is usually induced by TNF-α and TNF-like weak inducer of apoptosis (TWEAK) leading to muscle wasting mediated by MuRF-1 (Bonaldo and Sandri, 2013; Fearon et al., 2012; Romanello and Sandri, 2013), which levels were unaltered in BBN *gastrocnemius* (Fig. 4E). Another key player in NFkB signaling upregulated in an urothelial carcinoma-dependent way was the ubiquitin ligase TRAF6 that is required not only for the induction of ubiquitin–proteasome system but also of autophagy–lysosome pathway (Bonaldo and Sandri, 2013). Other proteases, namely MMP-9, were found to contribute to muscle proteolysis in BBN-treated rats (Fig. 6). Concomitantly, reduced levels of phosphorylated Akt, mTOR and p70S6K were observed (Fig. 3) suggesting reduced ribosome formation and protein synthesis in *gastrocnemius*, a muscle with a mixed metabolic phenotype. The magnitude of this unbalance between protein synthesis and degradation might differ according to muscle phenotype, as previously suggested for atrophic conditions (Fanzani et al., 2012).

4.3. Mitochondrial-related mechanisms on bladder cancer-induced muscle wasting

Along with muscle catabolism induced by the neoplastic growth-induced systemic disturbance, we detected alterations in mitochondria, a critical regulator of muscle protein turnover (White et al., 2012; Romanello and Sandri, 2010). As hypothesized by Julienne et al. (2012), mitochondria could be the place of energy wasting in situations of high muscle proteolysis as in cancer cachexia. Indeed, data from the present study supports the lower ability to produce ATP in the *gastrocnemius* of BBN-treated animals, taken in consideration the lower cytochrome c oxidase and ATP synthase activities (Fig. 7). These functional alterations were previously related to changes in the normal appearance of mitochondria, namely the presence of electron-lucent areas and swelling, which are indicative of cristae loss and ATP depletion, respectively (Shum et al., 2012). The lower levels of the transcriptional factor mtTFA observed in BBN group (Fig. 8C) might be associated with impaired mitochondria transcription, an important step in mitochondrial biogenesis (Maniura-Weber et al., 2004). These results are in agreement with the previous findings of White et al. (2012), who reported the diminishing of PGC-1α, a marker of mitochondrial biogenesis, and a shift towards smaller mitochondria with the progression of body loss. PGC-1α has been related to mTOR signaling and its reduction in BBN animals points to the repression of the transcription of genes involved in oxidative metabolism (Cunningham et al., 2007). Mitochondrial alterations in skeletal muscle might contribute to the increase in serum lactate concentration associated to bladder cancer supplying whole body energy needs (Julienne et al., 2012). Mitochondrial dysfunction has been related to increased ROS production (Lokireddy et al., 2012). Our data highlight the accumulation of oxidatively modified proteins, either carbonylated or nitrated (Fig. 8), that were not cleared out from BBN mitochondria by the PQC systems. Indeed, mitochondria function depends on the mitochondrial PQC that includes the mitochondrial proteases and the mitochondrial-shaping machinery (Romanello and Sandri, 2013). Mitochondrial proteases are regulators of organelle health, by removing misfolded or oxidatively damaged proteins, maintaining the cellular redox homeostasis (Venkatesh et al., 2012; Bulteau and Bayot, 2011). Data here presented evidence lower levels of the AAA protease paraplegin and the matrix Lon protease in the skeletal muscle mitochondria from BBN-treated rats (Fig. 8). Paraplegin coassembles with a homologous protein, AFG3L2, in the mitochondrial inner membrane and when this complex is lost occurs a decrease of OXPHOS complex I activity and an increased sensitivity to oxidative stress (Atorino et al., 2003). The matrix Lon protease has been suggested to have a similar role to the proteasome in cytosol in eliminating oxidatively modified mitochondrial proteins. This protease also displays chaperone properties and its loss of function was previously related to massive apoptosis, with the classical hallmark of caspase-3 activation, and deregulation of mtDNA replication (Bulteau and Bayot, 2011). Lon-mediated degradation of mtTFA was also reported and seems a PQC mechanism for eliminating misfolded or damaged mtTFA, and/or a regulatory mechanism for controlling mtDNA metabolism (Venkatesh et al., 2012). The severe mitochondrial dysfunction might lead to the activation of mitophagy in order to enable organelle replacement with new, more efficient ones. Recently, Lokireddy et al. (2012), reported a reduction of mtDNA copy number *per* nuDNA in the skeletal muscle from C26-tumor bearing mice and associated it with mitophagy, a process that seems to be mediated by mTOR (Romanello and Sandri, 2013).

In summary, using an animal model of urothelial carcinoma we observed that tumor–host interaction results in increased levels of pro-inflammatory mediators and myostatin, and in higher levels of urinary MMPs, which highlight the catabolic profile underlying body weight loss. Concomitantly with the imbalance between protein synthesis and degradation due to the activation of the ubiquitin–proteasome and suppression of PI3K/Akt/mTOR pathway, we noticed a decrease of the oxidative metabolism in wasted muscle. Focusing on mitochondria isolated from *gastrocnemius* muscle, our data showed that the impairment of mitochondrial PQC systems involving mitochondrial proteases seems to be linked to an increased generation of ROS and with the consequent accumulation of oxidatively modified proteins, which ultimately leads to lower mitochondrial ability to generate ATP. The dynamics and functional versatility of mitochondrial PQC systems need to be further explored aiming to define therapeutic targets to counteract cancer-related muscle wasting.

Conflict of interest

The authors have declared no conflict of interest.

Acknowledgments

This work was supported by Portuguese Foundation for Science and Technology (FCT), European Union, QREN, FEDER and COMPETE for funding the QOPNA research unit (project PEst-C/QUI/UI0062/2011), the research project (PTDC/DES/114122/2009; COMPETE, FCOMP-01-0124-FEDER-014707) and post-graduation students [grant numbers SFRH/BD/66642/2009 (to A.I.P.), SFRH/BPD/90010/2012 (to D.M.G.)].

References

Argiles JM, Lopez-Soriano FJ, Toledo M, Betancourt A, Serpe R, Busquets S. The cachexia score (CASCO): a new tool for staging cachectic cancer patients. Journal of Cachexia, Sarcopenia and Muscle 2011;2:87–93.

Atorino L, Silvestri L, Koppen M, Cassina L, Ballabio A, Marconi R, et al. Loss of m-AAA protease in mitochondria causes complex I deficiency and increased sensitivity to oxidative stress in hereditary spastic paraplegia. The Journal of Cell Biology 2003;163:777–87.

Bennani-Baiti N, Walsh D. Animal models of the cancer anorexia–cachexia syndrome. Supportive Care in Cancer: Official Journal of the Multinational Association of Supportive Care in Cancer 2011;19:1451–63.

Blum D, Omlin A, Baracos VE, Solheim TS, Tan BH, Stone P, et al. Cancer cachexia: a systematic literature review of items and domains associated with involuntary weight loss in cancer. Critical Reviews in Oncology/Hematology 2011;80:114–44.

Bonaldo P, Sandri M. Cellular and molecular mechanisms of muscle atrophy. Disease Models & Mechanisms 2013;6:25–39.

Bonetto A, Aydogdu T, Kunzevitzky N, Guttridge DC, Khuri S, Koniaris LG, et al. STAT3 activation in skeletal muscle links muscle wasting and the acute phase response in cancer cachexia. PLoS One 2011;6:e22538.

Bulteau AL, Bayot A. Mitochondrial proteases and cancer. Bioenergetics 2011;1807:595–601.

Buskermolen S, Langius JA, Kruizenga HM, Ligthart-Melis GC, Heymans MW, Verheul HM. Weight loss of 5% or more predicts loss of fat-free mass during palliative chemotherapy in patients with advanced cancer: a pilot study. Nutrition and Cancer 2012;64(6):826–32.

Camargo CA, da Silva ME, da Silva RA, Justo GZ, Gomes-Marcondes MC, Aoyama H. Inhibition of tumor growth by quercetin with increase of survival and prevention of cachexia in Walker 256 tumor-bearing rats. Biochemical and Biophysical Research Communications 2011;406:638–42.

Caseiro A, Vitorino R, Barros AS, Ferreira R, Calheiros-Lobo MJ, Carvalho D, et al. Salivary peptidome in type 1 diabetes mellitus. Biomedical Chromatography 2012;26:571–82.

Cunningham JT, Rodgers JT, Arlow DH, Vazquez F, Mootha VK, Puigserver P. mTOR controls mitochondrial oxidative function through a YY1-PGC-1alpha transcriptional complex. Nature 2007;450:736–40.

Dempsey DT, Buzby GP, Mullen JL. Nutritional assessment in the seriously ill patient. Journal of the American College of Nutrition 1983;2:15–22.

Epstein JI, Amin MB, Reuter VR, Mostofi FK. The World Health Organization/International Society of Urological Pathology consensus classification of urothelial (transitional cell) neoplasms of the urinary bladder. Bladder Consensus Conference Committee. American Journal of Surgical Pathology 1998;22:1435–48.

Fanzani A, Conraads VM, Penna F, Martinet W. Molecular and cellular mechanisms of skeletal muscle atrophy: an update. Journal of Cachexia, Sarcopenia and Muscle 2012;3:163–79.

Fearon KC, Glass DJ, Guttridge DC. Cancer cachexia: mediators, signaling, and metabolic pathways. Cell Metabolism 2012;16:153–66.

Jacobs BL, Montgomery JS, Zhang Y, Skolarus TA, Weizer AZ, Hollenbeck BK. Disparities in bladder cancer. Urologic Oncology 2012;30:81–8.

Julienne CM, Dumas JF, Goupille C, Pinault M, Berri C, Collin A, et al. Cancer cachexia is associated with a decrease in skeletal muscle mitochondrial oxidative capacities without alteration of ATP production efficiency. Journal of Cachexia, Sarcopenia and Muscle 2012;3(4):265–75.

Kawamata H, Kameyama S, Nan L, Kawai K, Oyasu R. Effect of epidermal growth factor and transforming growth factor beta 1 on growth and invasive potentials of newly established rat bladder carcinoma cell lines. International Journal of Cancer 1993;55:968–73.

Laemmli UK. Cleavage of structural proteins during the assembly of the head of bacteriophage T4. Nature 1970;227:680–5.

Lattermann R, Geisser W, Georgieff M, Wachter U, Goertz A, Gnann R, et al. Integrated analysis of glucose, lipid, and urea metabolism in patients with bladder cancer: impact of tumor stage. Nutrition 2003;19:589–92.

Lokireddy S, Wijesoma IW, Bonala S, Wei M, Sze SK, McFarlane C, et al. Myostatin is a novel tumoral factor that induces cancer cachexia. The Biochemical Journal 2012;446(1):23–36.

Maniura-Weber K, Goffart S, Garstka HL, Montoya J, Wiesner RJ. Transient overexpression of mitochondrial transcription factor A (TFAM) is sufficient to stimulate mitochondrial DNA transcription, but not sufficient to increase mtDNA copy number in cultured cells. Nucleic Acids Research 2004;32:6015–27.

Mistry M, Parkin DM, Ahmad AS, Sasieni P. Cancer incidence in the United Kingdom: projections to the year 2030. British Journal of Cancer 2011;105: 1795–803.

Oliveira PA, Palmeira C, Colaco A, de la Cruz LF, Lopes C. DNA content analysis, expression of Ki-67 and p53 in rat urothelial lesions induced by N-butyl-N-(4-hydroxybutyl) nitrosamine and treated with mitomycin C and bacillus Calmette-Guerin. Anticancer Research 2006;26:2995–3004.

Oliveira PA, Adega F, Palmeira CA, Chaves RM, Colaco AA, Guedes-Pinto H, et al. DNA study of bladder papillary tumours chemically induced by N-butyl-N-(4-hydroxybutyl) nitrosamine in Fisher rats. International Journal of Experimental Pathology 2007;88:39–46.

Palmeira C, Oliveira PA, Arantes-Rodrigues R, Colaco A, De la Cruz PL, Lopes C, et al. DNA cytometry and kinetics of rat urothelial lesions during chemical carcinogenesis. Oncology Reports 2009;21:247–52.

Palmeira C, Oliveira PA, Lameiras C, Amaro T, Silva VM, Lopes C, et al. Biological similarities between murine chemical-induced and natural human bladder carcinogenesis. Oncology Letters 2010;1:373–7.

Patra SK, Arora S. Integrative role of neuropeptides and cytokines in cancer anorexia–cachexia syndrome. Clinica Chimica Acta: International Journal of Clinical Chemistry 2012;413:1025–34.

Peluffo GD, Stillitani I, Rodriguez VA, Diament MJ, Klein SM. Reduction of tumor progression and paraneoplastic syndrome development in murine lung adenocarcinoma by nonsteroidal antiinflammatory drugs. International Journal of Cancer 2004;110:825–30.

Romanello V, Sandri M. Mitochondrial biogenesis and fragmentation as regulators of muscle protein degradation. Current Hypertension Reports 2010;12:433–9.

Romanello V, Sandri M. Mitochondrial biogenesis and fragmentation as regulators of protein degradation in striated muscles. Journal of Molecular and Cellular Cardiology 2013;55:64–72.

Roupret M, Zigeuner R, Palou J, Boehle A, Kaasinen E, Sylvester R, et al. European guidelines for the diagnosis and management of upper urinary tract urothelial cell carcinomas: 2011 update. European Urology 2011;59:584–94.

Shum AM, Mahendradatta T, Taylor RJ, Painter AB, Moore MM, Tsoli M, et al. Disruption of MEF2C signaling and loss of sarcomeric and mitochondrial integrity in cancer-induced skeletal muscle wasting. Aging 2012;4:133–43.

Simon N, Papa K, Vidal J, Boulamery A, Bruguerolle B. Circadian rhythms of oxidative phosphorylation: effects of rotenone and melatonin on isolated rat brain mitochondria. Chronobiology International 2003;20:451–61.

Skipworth RJ, Stewart GD, Dejong CH, Preston T, Fearon KC. Pathophysiology of cancer cachexia: much more than host–tumour interaction? Clinical Nutrition 2007;26:667–76.

Springer J, Adams V, Anker SD, Myostatin. Regulator of muscle wasting in heart failure and treatment target for cardiac cachexia. Circulation 2010;121:354–6.

Szarvas T, vom Dorp F, Ergun S, Rubben H. Matrix metalloproteinases and their clinical relevance in urinary bladder cancer. Nature Reviews Urology 2011;8:241–54.

Taylor RW, Birch-Machin MA, Bartlett K, Lowerson SA, Turnbull DM. The control of mitochondrial oxidations by complex III in rat muscle and liver mitochondria. Implications for our understanding of mitochondrial cytopathies in man. The Journal of Biological Chemistry 1994;269:3523–8.

Tisdale MJ. Mechanisms of cancer cachexia. Physiological Reviews 2009;89:381–410.

Tonkonogi M, Sahlin K. Rate of oxidative phosphorylation in isolated mitochondria from human skeletal muscle: effect of training status. Acta Physiologica Scandinavica 1997;161:345–53.

Venkatesh S, Lee J, Singh K, Lee I, Suzuki CK. Multitasking in the mitochondrion by the ATP-dependent Lon protease. Biochimica et Biophysica Acta 2012;1823:56–66.

Wang X, Pickrell AM, Zimmers TA, Moraes CT. Increase in muscle mitochondrial biogenesis does not prevent muscle loss but increased tumor size in a mouse model of acute cancer-induced cachexia. PLoS One 2012;7:e33426.

White JP, Baynes JW, Welle SL, Kostek MC, Matesic LE, Sato S, et al. The regulation of skeletal muscle protein turnover during the progression of cancer cachexia in the Apc(Min/+) mouse. PLoS One 2011;6:e24650.

White JP, Puppa MJ, Sato S, Gao S, Price RL, Baynes JW, et al. IL-6 regulation on skeletal muscle mitochondrial remodeling during cancer cachexia in the ApcMin/+ mouse. Skeletal Muscle 2012;2:14.

Zhou X, Wang JL, Lu J, Song Y, Kwak KS, Jiao Q, et al. Reversal of cancer cachexia and muscle wasting by ActRIIB antagonism leads to prolonged survival. Cell 2010;142:531–43.

CHAPTER V

GENERAL DISCUSSION

General discussion

Mitochondria have considerable plasticity and adapt itself to requirements of the organelle and of the cell (Dimmer and Rapaport 2008). These organelles are very dynamic and respond rapidly and adequately when challenged by physiological or pathological stimuli (Sandri 2008; Romanello and Sandri 2013). Such adaptation is particularly important in striated muscle because it has a high metabolic rate. Because of that, heart and skeletal muscles have a high content of mitochondria to keep up with ATP production for the maintenance of contractile activity (Dorn 2013; Romanello and Sandri 2013). So, changes in mitochondria homeostasis would have deleterious consequences on muscle functionality, playing mitochondrial plasticity a key role in the regulation of cardiac/skeletal muscle cells homeostasis (Romanello and Sandri 2013).

Diabetes mellitus and cancer are common diseases with tremendous impact on health worldwide (Giovannucci, Harlan et al. 2010). Both diabetes mellitus and cancer are prevalent diseases whose incidence is increasing globally. Worldwide, cancer is the 2nd and diabetes mellitus is the 12th leading cause of death (Lopez, Mathers et al. 2006). Moreover, elderly population presents a higher risk for these diseases as well as for cardiovascular ones (Jahangir, Sagar et al. 2007). Considering the aging population in Europe, increasing demands for health care are predicted. So, the better knowledge of these diseases' pathogenesis and the development of new and more effective therapeutic approaches are likely to boost health care conditions, with social and economic impact in countries.

Progressive mitochondrial dysfunction is a common cellular event to the pathogenesis of diseases as cancer (Julienne, Dumas et al. 2012; Shum, Mahendradatta et al. 2012) and diabetes mellitus (Dabkowski, Williamson et al. 2009; Dabkowski, Baseler et al. 2010; Ferreira, Guerra et al. 2013), and also contributes to the aging process (Cadenas and Davies 2000; Kwong and Sohal 2000; Short, Bigelow et al. 2005; Figueiredo, Ferreira et al. 2008; Figueiredo, Powers et al. 2009; Alves, Vitorino et al. 2010). Changes in mitochondria include the appearance of morphological alterations as abnormally rounded mitochondria, increased oxidative damage and reduced oxidative capacity. These morphological, biochemical and bioenergetics changes might ultimately lead to

mitochondrial-mediated apoptosis. Despite numerous studies linking these pathophysiologic conditions to mitochondrial dysfunction, progress in the comprehension of the molecular mechanism(s) involved has been extremely slow. To bring new insights on the molecular pathways underlying mitochondrial dysfunction in pathophysiological conditions, we performed a characterization of mitochondrial plasticity in striated muscle in response to aging, diabetes mellitus and cancer (Studies I, III and IV).

In striated muscles there are two populations of mitochondria with specific biochemical, morphological and functional features, being IMF the most abundant (80%) when compared with SS (20%) mitochondria (Hoppeler 1986). Besides being in higher amount, IMF mitochondrion presents increased OXPHOS activity, which seem related to a lower susceptibility of mitochondrial proteins to carbonylation in heart. Our data highlighted, for the first time, a localization dependence of cardiac OXPHOS activity and susceptibility to post-translational modifications, particularly to carbonylation and nitration. Curiously, the nitration of OXPHOS subunits does not seem to impact respiratory chain activity considering the higher levels observed in IMF mitochondria. However, unlike carbonylation, the role of protein nitration in cell physiology is controversial. Some authors (Aulak, Koeck et al. 2004; Gow, Farkouh et al. 2004) argue that tyrosine nitration is selective, dynamic and reversible, being potentially benefic (Study II).
Unless mitochondrial isolation targets the separation of both populations through the use of density gradients and ultracentrifugation, the biochemical and functional alterations reported in literature might be mainly attributed to IMF mitochondria, considering its greater abundance. According to several authors (Lesnefsky, Gudz et al. 2001; Williamson, Dabkowski et al. 2010; Baseler, Dabkowski et al. 2011; Chomentowski, Coen et al. 2011), IMF mitochondria are more susceptible to external stimuli, to diseases as diabetes mellitus, and to the aging process.

A number of evidences link mitochondria function to signaling pathways that regulate lifespan and the aging process. Decreased mitochondrial size, diminished expression of genes involved in mitochondrial biogenesis, altered mitochondrial activity and oxidative stress are some of the alterations reported in aged striated muscle (Barazzoni, Short et al. 2000; Short, Bigelow et al. 2005; Alves, Vitorino et al. 2010; Koltai, Hart et al. 2012; Cheng, Ito et al. 2013). Nevertheless, the causes of age-related mitochondrial impairment

are still a matter of controversy. In aged heart, we verified an association between the decline in bioenergetic function and the accumulation of oxidatively modified proteins. Among the mitochondrial proteins more prone to carbonylation and nitration we identified OXPHOS subunits, MnSOD and enzymes from lipid metabolism. The high susceptibility of OXPHOS subunits to oxidative damage might justify, at least in part, the lower OXPHOS complexes activity observed in aged heart. This age-related mitochondrial impairment seems to be modulated by lifestyle, with sedentary behavior worsening the functional consequences of aging manifested by an increased content of nitrated mitochondrial proteins and lower OXPHOS activity (Study I).

In an animal model of type 1 diabetes mellitus obtained by the administration of STZ we observed the impairment of OXPHOS activity in skeletal muscle. STZ has a half-life of six hours being readily metabolized, and induces rapid and sustained diabetes. We analyzed *gastrocnemius* muscle after four months of hyperglycemia, a time-point of manifested diabetes-related complications (Topping and Targ 1975) and of 30% loss of muscle mass, with animals evidencing normal cage activity. Regarding previous findings that suggest IMF mitochondria as the mitochondrial population more susceptibility to hyperglycemia (Williamson, Dabkowski et al. 2010), our study focused on the potential modulatory role of PQC system in IMF functionality. Despite the higher content of mitochondria in *gastrocnemius* muscle of STZ-diabetic rats, given by the significant higher mtDNA-to-muscle mass ratio, IMF mitochondria presented lower activity of OXPHOS complexes III and V. Similarly to the observed in aged mitochondria (Study I) and in cardiac mitochondria from diabetics (Ferreira, Guerra et al. 2013), an association between lower ATP production ability and increased carbonylated protein levels was noticed, partially justified by the impairment of PQC system. Besides decreased levels of Lon and paraplegin proteases, a diminished activity of Lon, metalloproteases (PreP, LAP-3 and MIP) and cathepsin D was detected by zymography-LC-MS/MS in isolated IMF mitochondria. Our data highlighted, for the first time, the association between the down-regulation of AAA proteases, particularly of the membranar paraplegin and the matrix Lon protease, and diabetes-related mitochondrial dysfunction in skeletal muscle (Study III).

Muscle wasting is observed in many diseases, being related to poor quality of life and increased risk of mortality (Sakuma and Yamaguchi 2012). Skeletal muscle wasting is the

most prominent feature of cancer cachexia. Actually, increased efforts have been made to understand the mechanisms underlying cancer-induced skeletal muscle wasting aiming to develop strategies to prevent or counteract the loss of muscle mass. Mitochondria dysfunction was previously linked to muscle wasting in peritoneal carcinosis-induced cachexia (Julienne, Dumas et al. 2012). Using an animal model of BBN-induced urothelial carcinoma characterized by a significant loss of body weight and decreased *gastrocnemius* mass, we studied the relationship between mitochondrial dynamics and muscle wasting. The impaired OXPHOS activity observed in the *gastrocnemius* of BBN rats was paralleled by the accumulation of oxidatively modified mitochondrial proteins. Despite the higher proteolytic activity observed in zymo gels, lower levels of the AAA protease paraplegin and the matrix Lon protease were detected in the *gastrocnemius* muscle of BBN rats, suggestive of mitochondrial PQC system impairment. Lower functionality of mitochondrial PQC system seems to be linked to an increased production of ROS, contributing to the accumulation of oxidatively modified mitochondrial proteins and consequently to muscle dysfunction in cancer subjects. Alterations in mitochondria were noticed to occur along with the muscle catabolism induced by the neoplastic growth, further supporting mitochondria as a critical regulator of muscle protein turnover.

The integrated analysis of data retrieved from our experimental studies revealed some similarities in the pattern of disease-related mitochondrial changes (Figure 1). Regarding skeletal muscle (Figure 1A), we studied the impact of type 1 diabetes mellitus and bladder cancer on mitochondrial plasticity and data highlighted: i) the impaired capacity of mitochondria to cope the cellular demands of ATP; ii) the exacerbation of mitochondrial oxidative stress; iii) the increased accumulation of damaged mitochondrial proteins; and iv) the down-regulation of mitochondrial PQC system. All these inter-related processes contribute to mitochondrial dysfunction and ultimately lead to muscle wasting. In aged cardiac muscle we also observed: i) a decreased activity of mitochondrial respiratory chain; ii) enhanced mitochondrial oxidative stress; and iii) increased accumulation of oxidative damaged mitochondrial proteins (Figure 1B). Similar findings were reported in heart from STZ-induced diabetic animals (Ferreira, Guerra et al. 2013).

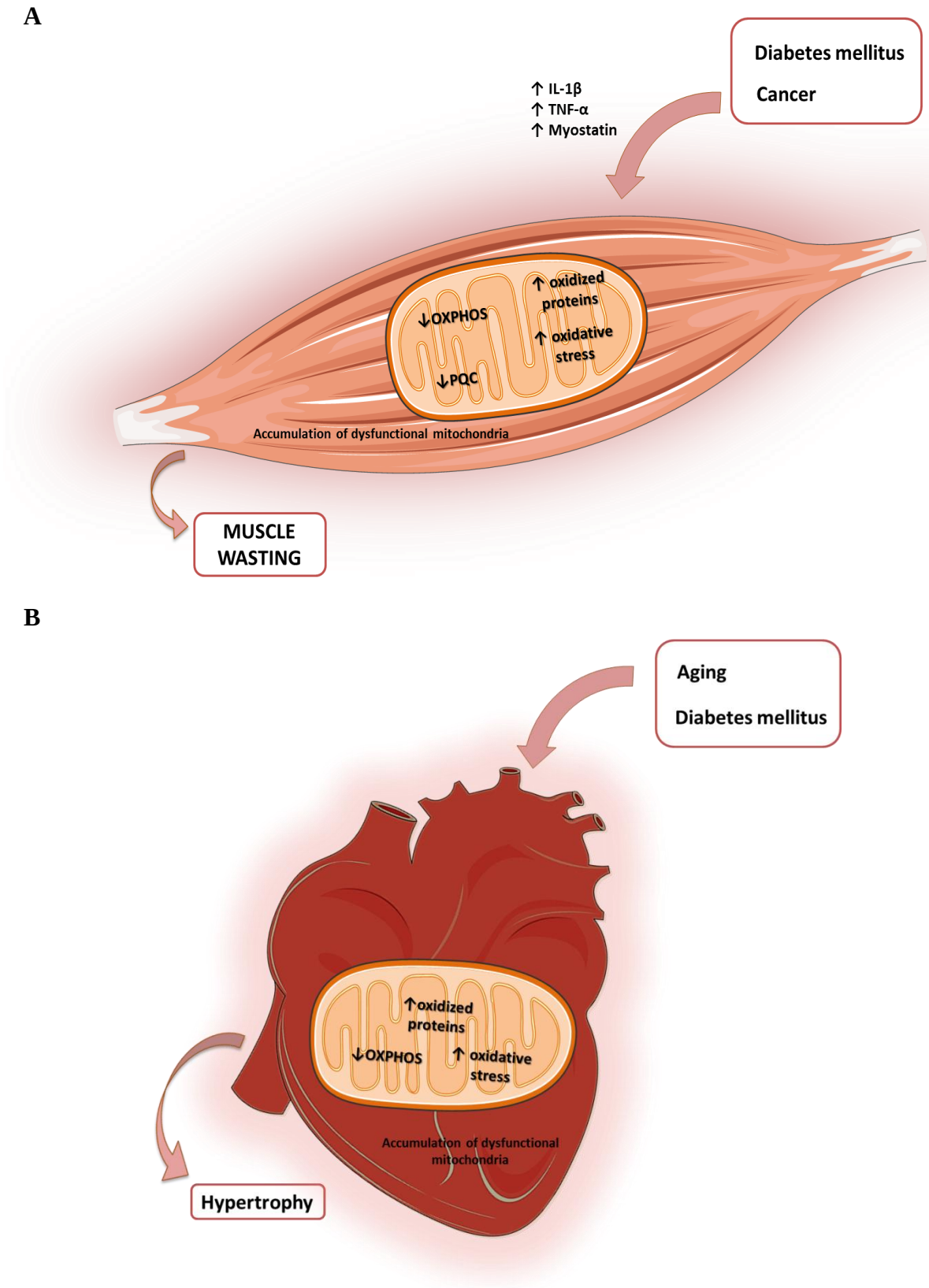

Figure 1: Schematic overview that integrates all data retrieved from the experimental studies. Mechanisms of mitochondrial plasticity in skeletal muscle during diabetes mellitus and cancer (A) and in cardiac muscle during aging and diabetes mellitus (B).
OXPHOS, Oxidative phosphorylation system; PQC, Protein quality control. Figure was made based on Servier Medical Art.

Although the molecular details are far from being clarified, mitochondrial dysfunction in striated muscle, manifested by decreased activity respiratory chain complexes, is due to, at least partially, an increased production of ROS with consequent accumulation of oxidatively modified mitochondrial proteins, not eliminated by the proteases from the mitochondrial PQC system. Independently of stimuli, the mitochondrial proteins more prone to oxidative damage are OXPHOS subunits, metabolic proteins as aconitate hydratase and MnSOD. The accumulation of these oxidized mitochondrial proteins might lead to the exacerbation of ROS production and to the decreased ability to produce ATP, compromising the homeostasis of striated muscle in aging, diabetes mellitus and cancer.

CHAPTER VI
CONCLUSIONS

Conclusions

Mitochondrial dysfunction is known to play a critical role in many pathophysiological conditions; however, the mechanisms involved are not disclosed. To give new insights on this issue, four experimental works were developed targeting striated muscle mitochondrial plasticity in aging, type 1 diabetes mellitus and cancer. Data obtained allowed to conclude that:

i) Age-related impairment of cardiac muscle mitochondria was manifested by decreased OXPHOS activity, paralleled by an increased susceptibility of mitochondrial proteins to oxidation (mainly OXPHOS complexes, MnSOD and enzymes from lipid metabolism), which is worsened by sedentary lifestyle;

ii) Among mitochondrial populations in heart, IMF presented higher OXPHOS activity then SS mitochondria; OXPHOS subunits were more susceptibility to carbonylation in SS and to nitration in IMF mitochondria. Unlike nitration, the increased carbonylation of OXPHOS complexes' subunits seem an underlying mechanism of decreased cardiac mitochondria functionality;

iii) Type 1 diabetes mellitus-related impairment of IMF mitochondria in *gastrocnemius* muscle was associated to decreased activity of mitochondrial PQC system involving the down-regulation of AAA-proteases, namely paraplegin and Lon, with the subsequent accumulation of damaged mitochondrial proteins and decreased OXPHOS activity;

iv) In urothelial carcinoma-related *gastrocnemius* muscle wasting, decreased OXPHOS activity was associated to the accumulation of oxidatively modified mitochondrial proteins due to, at least in part, the down-regulation of mitochondrial proteases from the PQC system. This impaired mitochondrial activity was related to the catabolic profile promoted by pro-inflammatory cytokines and myostatin.

In overall, experimental findings presented in this thesis support the notion that regardless the pathophysiological stimuli that unleash mitochondrial plasticity, the ability for ATP

production is diminished in striated muscle due to increased oxidative damage of biomolecules, being OXPHOS subunits particularly prone. Our data highlighted, for the first time, the impact of PQC system impairment in the accumulation of oxidized proteins, exacerbating mitochondrial dysfunction in pathophysiological conditions. The association between mitochondrial dysfunction due to the accumulation of damaged proteins and bladder cancer cachexia was also reported for the first time.

Future studies focused on the dynamics and functional versatility of mitochondrial PQC system will not only contribute to a better comprehension of the molecular mechanisms that modulate mitochondria functionality but will also allow to define therapeutic targets to prevent or counteract pathophysiologic conditions characterized by mitochondrial dysfunction. The potential non-pharmacological therapeutic effect of exercise should also be more explored envisioning the protection of mitochondrial functionality in striated muscle impacted by pathophysiological conditions.

REFERENCES

References

Abello, N., H. A. Kerstjens, et al. (2009). "Protein tyrosine nitration: selectivity, physicochemical and biological consequences, denitration, and proteomics methods for the identification of tyrosine-nitrated proteins." J Proteome Res **8**(7): 3222-3238.

Acin-Perez, R., P. Fernandez-Silva, et al. (2008). "Respiratory active mitochondrial supercomplexes." Mol Cell **32**(4): 529-539.

Adams, V., H. Jiang, et al. (1999). "Apoptosis in skeletal myocytes of patients with chronic heart failure is associated with exercise intolerance." J Am Coll Cardiol **33**(4): 959-965.

Adhihetty, P. J., V. Ljubicic, et al. (2007). "Effect of chronic contractile activity on SS and IMF mitochondrial apoptotic susceptibility in skeletal muscle." Am J Physiol Endocrinol Metab **292**(3): E748-755.

Adhihetty, P. J., V. Ljubicic, et al. (2005). "Differential susceptibility of subsarcolemmal and intermyofibrillar mitochondria to apoptotic stimuli." Am J Physiol Cell Physiol **289**(4): C994-C1001.

Adhihetty, P. J., M. F. O'Leary, et al. (2008). "Mitochondria in skeletal muscle: adaptable rheostats of apoptotic susceptibility." Exerc Sport Sci Rev **36**(3): 116-121.

Agnetti, G., L. A. Kane, et al. (2007). "Proteomic technologies in the study of kinases: novel tools for the investigation of PKC in the heart." Pharmacol Res **55**(6): 511-522.

Ahn, B. H., H. S. Kim, et al. (2008). "A role for the mitochondrial deacetylase Sirt3 in regulating energy homeostasis." Proc Natl Acad Sci U S A **105**(38): 14447-14452.

Allen, D. L., J. K. Linderman, et al. (1997). "Apoptosis: a mechanism contributing to remodeling of skeletal muscle in response to hindlimb unweighting." Am J Physiol **273**(2 Pt 1): C579-587.

Alves, R. M., R. Vitorino, et al. (2010). "Lifelong physical activity modulation of the skeletal muscle mitochondrial proteome in mice." J Gerontol A Biol Sci Med Sci **65**(8): 832-842.

Amirouche, A., A. C. Durieux, et al. (2009). "Down-regulation of Akt/mammalian target of rapamycin signaling pathway in response to myostatin overexpression in skeletal muscle." Endocrinology **150**(1): 286-294.

Andreu, A. L., M. A. Arbos, et al. (1998). "Reduced mitochondrial DNA transcription in senescent rat heart." Biochem Biophys Res Commun **252**(3): 577-581.

Aponte, A. M., D. Phillips, et al. (2009). "32P labeling of protein phosphorylation and metabolite association in the mitochondria matrix." Methods Enzymol **457**: 63-80.

Argiles, J. M., M. Orpi, et al. (2012). "Myostatin: more than just a regulator of muscle mass." Drug Discov Today **17**(13-14): 702-709.

Arlt, H., R. Tauer, et al. (1996). "The YTA10-12 complex, an AAA protease with chaperone-like activity in the inner membrane of mitochondria." Cell **85**(6): 875-885.

Aulak, K. S., T. Koeck, et al. (2004). "Dynamics of protein nitration in cells and mitochondria." Am J Physiol Heart Circ Physiol **286**(1): H30-38.

Babusikova, E., M. Jesenak, et al. (2008). "Oxidative alternations in rat heart homogenate and mitochondria during ageing." Gen Physiol Biophys **27**(2): 115-120.

Bae, Y. S., H. Oh, et al. (2011). "Regulation of reactive oxygen species generation in cell signaling." Mol Cells **32**(6): 491-509.

Baker, B. M. and C. M. Haynes (2011). "Mitochondrial protein quality control during biogenesis and aging." Trends Biochem Sci **36**(5): 254-261.

Baker, D. J., A. C. Betik, et al. (2006). "No decline in skeletal muscle oxidative capacity with aging in long-term calorically restricted rats: effects are independent of mitochondrial DNA integrity." J Gerontol A Biol Sci Med Sci **61**(7): 675-684.

Balaban, R. S. (2010). "The mitochondrial proteome: a dynamic functional program in tissues and disease states." Environ Mol Mutagen **51**(5): 352-359.

Bao, J. and M. N. Sack (2010). "Protein deacetylation by sirtuins: delineating a post-translational regulatory program responsive to nutrient and redox stressors." Cell Mol Life Sci **67**(18): 3073-3087.

Barazzoni, R. and K. S. Nair (2001). "Changes in uncoupling protein-2 and -3 expression in aging rat skeletal muscle, liver, and heart." Am J Physiol Endocrinol Metab **280**(3): E413-419.

Barazzoni, R., K. R. Short, et al. (2000). "Effects of aging on mitochondrial DNA copy number and cytochrome c oxidase gene expression in rat skeletal muscle, liver, and heart." J Biol Chem **275**(5): 3343-3347.

Barreiro, E., C. Coronell, et al. (2006). "Aging, sex differences, and oxidative stress in human respiratory and limb muscles." Free Radic Biol Med **41**(5): 797-809.

Barreiro, E., B. de la Puente, et al. (2005). "Both oxidative and nitrosative stress are associated with muscle wasting in tumour-bearing rats." FEBS Lett **579**(7): 1646-1652.

Baseler, W. A., E. R. Dabkowski, et al. (2011). "Proteomic alterations of distinct mitochondrial subpopulations in the type 1 diabetic heart: contribution of protein import dysfunction." Am J Physiol Regul Integr Comp Physiol **300**(2): R186-200.

Baumeister, W., J. Walz, et al. (1998). "The proteasome: paradigm of a self-compartmentalizing protease." Cell **92**(3): 367-380.

Benard, G., B. Faustin, et al. (2006). "Physiological diversity of mitochondrial oxidative phosphorylation." Am J Physiol Cell Physiol **291**(6): C1172-1182.

Benard, G. and R. Rossignol (2008). "Ultrastructure of the mitochondrion and its bearing on function and bioenergetics." Antioxid Redox Signal **10**(8): 1313-1342.

Bender, T., C. Leidhold, et al. (2010). "The role of protein quality control in mitochondrial protein homeostasis under oxidative stress." Proteomics **10**(7): 1426-1443.

Beregi, E., O. Regius, et al. (1988). "Age-related changes in the skeletal muscle cells." Z Gerontol **21**(2): 83-86.

Bergmann, O., R. D. Bhardwaj, et al. (2009). "Evidence for cardiomyocyte renewal in humans." Science **324**(5923): 98-102.

Berry, E. A., M. Guergova-Kuras, et al. (2000). "Structure and function of cytochrome bc complexes." Annu Rev Biochem **69**: 1005-1075.

Bodine, S. C., T. N. Stitt, et al. (2001). "Akt/mTOR pathway is a crucial regulator of skeletal muscle hypertrophy and can prevent muscle atrophy in vivo." Nat Cell Biol **3**(11): 1014-1019.

Boffoli, D., S. C. Scacco, et al. (1994). "Decline with age of the respiratory chain activity in human skeletal muscle." Biochim Biophys Acta **1226**(1): 73-82.

Boja, E. S., D. Phillips, et al. (2009). "Quantitative mitochondrial phosphoproteomics using iTRAQ on an LTQ-Orbitrap with high energy collision dissociation." J Proteome Res **8**(10): 4665-4675.

Bonaldo, P. and M. Sandri (2013). "Cellular and molecular mechanisms of muscle atrophy." Dis Model Mech **6**(1): 25-39.

Bonnard, C., A. Durand, et al. (2008). "Mitochondrial dysfunction results from oxidative stress in the skeletal muscle of diet-induced insulin-resistant mice." J Clin Invest **118**(2): 789-800.

Booth, F. W., S. H. Weeden, et al. (1994). "Effect of aging on human skeletal muscle and motor function." Med Sci Sports Exerc **26**(5): 556-560.

Bota, D. A., J. K. Ngo, et al. (2005). "Downregulation of the human Lon protease impairs mitochondrial structure and function and causes cell death." Free Radic Biol Med **38**(5): 665-677.

Bota, D. A., H. Van Remmen, et al. (2002). "Modulation of Lon protease activity and aconitase turnover during aging and oxidative stress." FEBS Lett **532**(1-2): 103-106.

Boudina, S. and E. D. Abel (2007). "Diabetic cardiomyopathy revisited." Circulation **115**(25): 3213-3223.

Boudina, S. and E. D. Abel (2010). "Diabetic cardiomyopathy, causes and effects." Rev Endocr Metab Disord **11**(1): 31-39.

Boudina, S., S. Sena, et al. (2007). "Mitochondrial energetics in the heart in obesity-related diabetes: direct evidence for increased uncoupled respiration and activation of uncoupling proteins." Diabetes **56**(10): 2457-2466.

Boushel, R., E. Gnaiger, et al. (2007). "Patients with type 2 diabetes have normal mitochondrial function in skeletal muscle." Diabetologia **50**(4): 790-796.

Brandt, U. and B. Trumpower (1994). "The protonmotive Q cycle in mitochondria and bacteria." Crit Rev Biochem Mol Biol **29**(3): 165-197.

Brigelius-Flohe, R. (2009). "Commentary: oxidative stress reconsidered." Genes Nutr **4**(3): 161-163.

Bugger, H., S. Boudina, et al. (2008). "Type 1 diabetic akita mouse hearts are insulin sensitive but manifest structurally abnormal mitochondria that remain coupled despite increased uncoupling protein 3." Diabetes **57**(11): 2924-2932.

Bugger, H., D. Chen, et al. (2009). "Tissue-specific remodeling of the mitochondrial proteome in type 1 diabetic akita mice." Diabetes **58**(9): 1986-1997.

Cadenas, E. and K. J. Davies (2000). "Mitochondrial free radical generation, oxidative stress, and aging." Free Radic Biol Med **29**(3-4): 222-230.

Calvani, R., A. M. Joseph, et al. (2013). "Mitochondrial pathways in sarcopenia of aging and disuse muscle atrophy." Biol Chem **394**(3): 393-414.

Campello, S. and L. Scorrano (2010). "Mitochondrial shape changes: orchestrating cell pathophysiology." EMBO Rep **11**(9): 678-684.

Capel, F., C. Buffiere, et al. (2004). "Differential variation of mitochondrial H2O2 release during aging in oxidative and glycolytic muscles in rats." Mech Ageing Dev **125**(5): 367-373.

Capel, F., V. Rimbert, et al. (2005). "Due to reverse electron transfer, mitochondrial H2O2 release increases with age in human vastus lateralis muscle although oxidative capacity is preserved." Mech Ageing Dev **126**(4): 505-511.

Carmeli, E., R. Coleman, et al. (2002). "The biochemistry of aging muscle." Exp Gerontol **37**(4): 477-489.

Carrillo, M. C., S. Kanai, et al. (1992). "Age-related changes in antioxidant enzyme activities are region and organ, as well as sex, selective in the rat." Mech Ageing Dev **65**(2-3): 187-198.

Castelluccio, C., A. Baracca, et al. (1994). "Mitochondrial activities of rat heart during ageing." Mech Ageing Dev **76**(2-3): 73-88.

Cecchini, G. (2003). "Function and structure of complex II of the respiratory chain." Annu Rev Biochem **72**: 77-109.

Chabi, B., B. Mousson de Camaret, et al. (2005). "Random mtDNA deletions and functional consequence in aged human skeletal muscle." Biochem Biophys Res Commun **332**(2): 542-549.

Chacinska, A., C. M. Koehler, et al. (2009). "Importing mitochondrial proteins: machineries and mechanisms." Cell **138**(4): 628-644.

Chan, D. C. (2006). "Mitochondria: dynamic organelles in disease, aging, and development." Cell **125**(7): 1241-1252.

Chang, J., H. Van Remmen, et al. (2003). "Comparative proteomics: characterization of a two-dimensional gel electrophoresis system to study the effect of aging on mitochondrial proteins." Mech Ageing Dev **124**(1): 33-41.

Chao, T. T., C. D. Ianuzzo, et al. (1976). "Ultrastructural alterations in skeletal muscle fibers of streptozotocin-diabetic rats." Cell Tissue Res **168**(2): 239-246.

Chen, V. and C. D. Ianuzzo (1982). "Metabolic alterations in skeletal muscle of chronically streptozotocin-diabetic rats." Arch Biochem Biophys **217**(1): 131-138.

Cheng, Z., S. Ito, et al. (2013). "Characteristics of cardiac aging in C57BL/6 mice." Exp Gerontol **48**(3): 341-348.

Choksi, K. B., J. E. Nuss, et al. (2008). "Age-related alterations in oxidatively damaged proteins of mouse skeletal muscle mitochondrial electron transport chain complexes." Free Radic Biol Med **45**(6): 826-838.

Choksi, K. B., J. E. Nuss, et al. (2011). "Mitochondrial electron transport chain functions in long-lived Ames dwarf mice." Aging (Albany NY) **3**(8): 754-767.

Choksi, K. B. and J. Papaconstantinou (2008). "Age-related alterations in oxidatively damaged proteins of mouse heart mitochondrial electron transport chain complexes." Free Radic Biol Med **44**(10): 1795-1805.

Chomentowski, P., P. M. Coen, et al. (2011). "Skeletal muscle mitochondria in insulin resistance: differences in intermyofibrillar versus subsarcolemmal subpopulations and relationship to metabolic flexibility." J Clin Endocrinol Metab **96**(2): 494-503.

Cimen, H., M. J. Han, et al. (2010). "Regulation of succinate dehydrogenase activity by SIRT3 in mammalian mitochondria." Biochemistry **49**(2): 304-311.

Cocco, T., P. Sgobbo, et al. (2005). "Tissue-specific changes of mitochondrial functions in aged rats: effect of a long-term dietary treatment with N-acetylcysteine." Free Radic Biol Med **38**(6): 796-805.

Coggan, A. R., R. J. Spina, et al. (1992). "Histochemical and enzymatic comparison of the gastrocnemius muscle of young and elderly men and women." J Gerontol **47**(3): B71-76.

Cogswell, A. M., R. J. Stevens, et al. (1993). "Properties of skeletal muscle mitochondria isolated from subsarcolemmal and intermyofibrillar regions." Am J Physiol **264**(2 Pt 1): C383-389.

Cohen, A. (1995). "[Diabetic cardiomyopathy]." Arch Mal Coeur Vaiss **88**(4): 479-486.

Cohen, P. (2002). "The origins of protein phosphorylation." Nat Cell Biol **4**(5): E127-130.

Coleman, R., M. Silbermann, et al. (1987). "Giant mitochondria in the myocardium of aging and endurance-trained mice." Gerontology **33**(1): 34-39.

Conley, K. E., S. A. Jubrias, et al. (2007). "Mitochondrial dysfunction: impact on exercise performance and cellular aging." Exerc Sport Sci Rev **35**(2): 43-49.

Conley, K. E., S. A. Jubrias, et al. (2000). "Oxidative capacity and ageing in human muscle." J Physiol **526 Pt 1**: 203-210.

Cooper, J. M., V. M. Mann, et al. (1992). "Analyses of mitochondrial respiratory chain function and mitochondrial DNA deletion in human skeletal muscle: effect of ageing." J Neurol Sci **113**(1): 91-98.

Corsetti, G., E. Pasini, et al. (2008). "Morphometric changes induced by amino acid supplementation in skeletal and cardiac muscles of old mice." Am J Cardiol **101**(11A): 26E-34E.

Crane, J. D., M. C. Devries, et al. (2010). "The effect of aging on human skeletal muscle mitochondrial and intramyocellular lipid ultrastructure." J Gerontol A Biol Sci Med Sci **65**(2): 119-128.

Crowther, G. J., J. M. Milstein, et al. (2003). "Altered energetic properties in skeletal muscle of men with well-controlled insulin-dependent (type 1) diabetes." Am J Physiol Endocrinol Metab **284**(4): E655-662.

D'Antona, G., M. A. Pellegrino, et al. (2003). "The effect of ageing and immobilization on structure and function of human skeletal muscle fibres." J Physiol **552**(Pt 2): 499-511.

Dabkowski, E. R., W. A. Baseler, et al. (2010). "Mitochondrial dysfunction in the type 2 diabetic heart is associated with alterations in spatially distinct mitochondrial proteomes." Am J Physiol Heart Circ Physiol **299**(2): H529-540.

Dabkowski, E. R., C. L. Williamson, et al. (2009). "Diabetic cardiomyopathy-associated dysfunction in spatially distinct mitochondrial subpopulations." Am J Physiol Heart Circ Physiol **296**(2): H359-369.

Dai, D. F. and P. S. Rabinovitch (2009). "Cardiac aging in mice and humans: the role of mitochondrial oxidative stress." Trends Cardiovasc Med **19**(7): 213-220.

Dalle-Donne, I., R. Rossi, et al. (2003). "Protein carbonyl groups as biomarkers of oxidative stress." Clin Chim Acta **329**(1-2): 23-38.

Das, K. C. and H. Muniyappa (2013). "Age-dependent mitochondrial energy dynamics in the mice heart: Role of superoxide dismutase-2." Exp Gerontol.

Davies, S. M., A. Poljak, et al. (2001). "Measurements of protein carbonyls, ortho- and meta-tyrosine and oxidative phosphorylation complex activity in mitochondria from young and old rats." Free Radic Biol Med **31**(2): 181-190.

de Sagarra, M. R., I. Mayo, et al. (1999). "Mitochondrial localization and oligomeric structure of HClpP, the human homologue of E. coli ClpP." J Mol Biol **292**(4): 819-825.

Delaval, E., M. Perichon, et al. (2004). "Age-related impairment of mitochondrial matrix aconitase and ATP-stimulated protease in rat liver and heart." Eur J Biochem **271**(22): 4559-4564.

Deng, N., J. Zhang, et al. (2011). "Phosphoproteome analysis reveals regulatory sites in major pathways of cardiac mitochondria." Mol Cell Proteomics **10**(2): M110 000117.

Desai, V. G., R. Weindruch, et al. (1996). "Influences of age and dietary restriction on gastrocnemius electron transport system activities in mice." Arch Biochem Biophys **333**(1): 145-151.

Diaz, F., H. Fukui, et al. (2006). "Cytochrome c oxidase is required for the assembly/stability of respiratory complex I in mouse fibroblasts." Mol Cell Biol **26**(13): 4872-4881.

Dimmer, K. S. and D. Rapaport (2008). "Proteomic view of mitochondrial function." Genome Biol **9**(2): 209.

Distler, A. M., J. Kerner, et al. (2008). "Proteomics of mitochondrial inner and outer membranes." Proteomics **8**(19): 4066-4082.

Doria, E., D. Buonocore, et al. (2012). "Relationship between human aging muscle and oxidative system pathway." Oxid Med Cell Longev **2012**: 830257.

Dorn, G. W., 2nd (2013). "Mitochondrial dynamics in heart disease." Biochim Biophys Acta **1833**(1): 233-241.

Drew, B., S. Phaneuf, et al. (2003). "Effects of aging and caloric restriction on mitochondrial energy production in gastrocnemius muscle and heart." Am J Physiol Regul Integr Comp Physiol **284**(2): R474-480.

Droge, W. (2002). "Free radicals in the physiological control of cell function." Physiol Rev **82**(1): 47-95.

Duchen, M. R. (2004). "Mitochondria in health and disease: perspectives on a new mitochondrial biology." Mol Aspects Med **25**(4): 365-451.

Dudkina, N. V., S. Sunderhaus, et al. (2008). "The higher level of organization of the oxidative phosphorylation system: mitochondrial supercomplexes." J Bioenerg Biomembr **40**(5): 419-424.

Duncan, J. G. (2011). "Mitochondrial dysfunction in diabetic cardiomyopathy." Biochim Biophys Acta **1813**(7): 1351-1359.

Duncan, J. G., J. L. Fong, et al. (2007). "Insulin-resistant heart exhibits a mitochondrial biogenic response driven by the peroxisome proliferator-activated receptor-alpha/PGC-1alpha gene regulatory pathway." Circulation **115**(7): 909-917.

Elkina, Y., S. von Haehling, et al. (2011). "The role of myostatin in muscle wasting: an overview." J Cachexia Sarcopenia Muscle **2**(3): 143-151.

Esser, K., B. Tursun, et al. (2002). "A novel two-step mechanism for removal of a mitochondrial signal sequence involves the mAAA complex and the putative rhomboid protease Pcp1." J Mol Biol **323**(5): 835-843.

Faccio, L., C. Fusco, et al. (2000). "Characterization of a novel human serine protease that has extensive homology to bacterial heat shock endoprotease HtrA and is regulated by kidney ischemia." J Biol Chem **275**(4): 2581-2588.

Faist, V., J. Koenig, et al. (1998). "Mitochondrial oxygen consumption, lipid peroxidation and antioxidant enzyme systems in skeletal muscle of senile dystrophic mice." Pflugers Arch **437**(1): 168-171.

Fannin, S. W., E. J. Lesnefsky, et al. (1999). "Aging selectively decreases oxidative capacity in rat heart interfibrillar mitochondria." Arch Biochem Biophys **372**(2): 399-407.

Fanzani, A., V. M. Conraads, et al. (2012). "Molecular and cellular mechanisms of skeletal muscle atrophy: an update." J Cachexia Sarcopenia Muscle **3**(3): 163-179.

Fares, E. and S. E. Howlett (2010). "Effect of age on cardiac excitation-contraction coupling." Clin Exp Pharmacol Physiol **37**(1): 1-7.
Fattoretti, P., J. Vecchiet, et al. (2001). "Succinic dehydrogenase activity in human muscle mitochondria during aging: a quantitative cytochemical investigation." Mech Ageing Dev **122**(15): 1841-1848.
Feng, J., H. Xie, et al. (2008). "Quantitative proteomic profiling of muscle type-dependent and age-dependent protein carbonylation in rat skeletal muscle mitochondria." J Gerontol A Biol Sci Med Sci **63**(11): 1137-1152.
Fermoselle, C., E. Garcia-Arumi, et al. (2013). "Mitochondrial dysfunction and therapeutic approaches in respiratory and limb muscles of cancer cachectic mice." Exp Physiol.
Ferreira, R., G. Guerra, et al. (2013). "Lipidomic characterization of streptozotocin-induced heart mitochondrial dysfunction." Mitochondrion.
Ferreira, R. M., R. Vitorino, et al. (2012). "Spatially distinct mitochondrial populations exhibit different mitofilin levels." Cell Biochem Funct **30**(5): 395-399.
Figueiredo, P. A., R. M. Ferreira, et al. (2008). "Age-induced morphological, biochemical, and functional alterations in isolated mitochondria from murine skeletal muscle." J Gerontol A Biol Sci Med Sci **63**(4): 350-359.
Figueiredo, P. A., S. K. Powers, et al. (2009). "Aging impairs skeletal muscle mitochondrial bioenergetic function." J Gerontol A Biol Sci Med Sci **64**(1): 21-33.
Finley, L. W., W. Haas, et al. (2011). "Succinate dehydrogenase is a direct target of sirtuin 3 deacetylase activity." PLoS One **6**(8): e23295.
Flarsheim, C. E., I. L. Grupp, et al. (1996). "Mitochondrial dysfunction accompanies diastolic dysfunction in diabetic rat heart." Am J Physiol **271**(1 Pt 2): H192-202.
Fontanesi, F., I. C. Soto, et al. (2008). "Cytochrome c oxidase biogenesis: new levels of regulation." IUBMB Life **60**(9): 557-568.
Foster, D. B., J. E. Van Eyk, et al. (2009). "Redox signaling and protein phosphorylation in mitochondria: progress and prospects." J Bioenerg Biomembr **41**(2): 159-168.
Frazier, A. E., C. Kiu, et al. (2006). "Mitochondrial morphology and distribution in mammalian cells." Biol Chem **387**(12): 1551-1558.
Fritz, K. S., J. J. Galligan, et al. (2012). "Mitochondrial acetylome analysis in a mouse model of alcohol-induced liver injury utilizing SIRT3 knockout mice." J Proteome Res **11**(3): 1633-1643.
Gea, J., C. Casadevall, et al. (2012). "Respiratory diseases and muscle dysfunction." Expert Rev Respir Med **6**(1): 75-90.
Gerdes, F., T. Tatsuta, et al. (2012). "Mitochondrial AAA proteases--towards a molecular understanding of membrane-bound proteolytic machines." Biochim Biophys Acta **1823**(1): 49-55.
Gianni, P., K. J. Jan, et al. (2004). "Oxidative stress and the mitochondrial theory of aging in human skeletal muscle." Exp Gerontol **39**(9): 1391-1400.
Gilkerson, R. W., J. M. Selker, et al. (2003). "The cristal membrane of mitochondria is the principal site of oxidative phosphorylation." FEBS Lett **546**(2-3): 355-358.
Giovannucci, E., D. M. Harlan, et al. (2010). "Diabetes and cancer: a consensus report." Diabetes Care **33**(7): 1674-1685.
Glass, D. J. (2003). "Molecular mechanisms modulating muscle mass." Trends Mol Med **9**(8): 344-350.
Goldberg, A. L. (2003). "Protein degradation and protection against misfolded or damaged proteins." Nature **426**(6968): 895-899.
Gomes-Marcondes, M. C. and M. J. Tisdale (2002). "Induction of protein catabolism and the ubiquitin-proteasome pathway by mild oxidative stress." Cancer Lett **180**(1): 69-74.
Gomes, M. D., S. H. Lecker, et al. (2001). "Atrogin-1, a muscle-specific F-box protein highly expressed during muscle atrophy." Proc Natl Acad Sci U S A **98**(25): 14440-14445.
Gomez, L. A., J. S. Monette, et al. (2009). "Supercomplexes of the mitochondrial electron transport chain decline in the aging rat heart." Arch Biochem Biophys **490**(1): 30-35.

Gouspillou, G., I. Bourdel-Marchasson, et al. (2013). "Mitochondrial energetics is impaired in vivo in aged skeletal muscle." Aging Cell.

Gow, A. J., C. R. Farkouh, et al. (2004). "Biological significance of nitric oxide-mediated protein modifications." Am J Physiol Lung Cell Mol Physiol **287**(2): L262-268.

Gray, C. W., R. V. Ward, et al. (2000). "Characterization of human HtrA2, a novel serine protease involved in the mammalian cellular stress response." Eur J Biochem **267**(18): 5699-5710.

Greer, E. L., P. R. Oskoui, et al. (2007). "The energy sensor AMP-activated protein kinase directly regulates the mammalian FOXO3 transcription factor." J Biol Chem **282**(41): 30107-30119.

Grimsrud, P. A., J. J. Carson, et al. (2012). "A quantitative map of the liver mitochondrial phosphoproteome reveals posttranslational control of ketogenesis." Cell Metab **16**(5): 672-683.

Guan, K. L. and Y. Xiong (2011). "Regulation of intermediary metabolism by protein acetylation." Trends Biochem Sci **36**(2): 108-116.

Guerrieri, F., G. Capozza, et al. (1993). "Functional and molecular changes in FoF1 ATP-synthase of cardiac muscle during aging." Cardioscience **4**(2): 93-98.

Hamanaka, R. B. and N. S. Chandel (2010). "Mitochondrial reactive oxygen species regulate cellular signaling and dictate biological outcomes." Trends Biochem Sci **35**(9): 505-513.

Harman, D. (1981). "The aging process." Proc Natl Acad Sci U S A **78**(11): 7124-7128.

Hayat, S. A., B. Patel, et al. (2004). "Diabetic cardiomyopathy: mechanisms, diagnosis and treatment." Clin Sci (Lond) **107**(6): 539-557.

Haynes, C. M., K. Petrova, et al. (2007). "ClpP mediates activation of a mitochondrial unfolded protein response in C. elegans." Dev Cell **13**(4): 467-480.

He, J., S. Watkins, et al. (2001). "Skeletal muscle lipid content and oxidative enzyme activity in relation to muscle fiber type in type 2 diabetes and obesity." Diabetes **50**(4): 817-823.

Hegde, R., S. M. Srinivasula, et al. (2002). "Identification of Omi/HtrA2 as a mitochondrial apoptotic serine protease that disrupts inhibitor of apoptosis protein-caspase interaction." J Biol Chem **277**(1): 432-438.

Hoppel, C. L., B. Tandler, et al. (2009). "Dynamic organization of mitochondria in human heart and in myocardial disease." Int J Biochem Cell Biol **41**(10): 1949-1956.

Hoppeler, H. (1986). "Exercise-induced ultrastructural changes in skeletal muscle." Int J Sports Med **7**(4): 187-204.

Hoppeler, H. and M. Fluck (2003). "Plasticity of skeletal muscle mitochondria: structure and function." Med Sci Sports Exerc **35**(1): 95-104.

Huang, J. H. and D. A. Hood (2009). "Age-associated mitochondrial dysfunction in skeletal muscle: Contributing factors and suggestions for long-term interventions." IUBMB Life **61**(3): 201-214.

Huttemann, M., I. Lee, et al. (2008). "Regulation of oxidative phosphorylation, the mitochondrial membrane potential, and their role in human disease." J Bioenerg Biomembr **40**(5): 445-456.

Ishihara, N., Y. Fujita, et al. (2006). "Regulation of mitochondrial morphology through proteolytic cleavage of OPA1." EMBO J **25**(13): 2966-2977.

Jackson, M. J. (2009). "Redox regulation of adaptive responses in skeletal muscle to contractile activity." Free Radic Biol Med **47**(9): 1267-1275.

Jahangir, A., S. Sagar, et al. (2007). "Aging and cardioprotection." J Appl Physiol **103**(6): 2120-2128.

Janssen, R. J., L. G. Nijtmans, et al. (2006). "Mitochondrial complex I: structure, function and pathology." J Inherit Metab Dis **29**(4): 499-515.

Ji, L. L., D. Dillon, et al. (1990). "Alteration of antioxidant enzymes with aging in rat skeletal muscle and liver." Am J Physiol **258**(4 Pt 2): R918-923.

Ji, L. L., M. C. Gomez-Cabrera, et al. (2006). "Exercise and hormesis: activation of cellular antioxidant signaling pathway." Ann N Y Acad Sci **1067**: 425-435.

Ji, L. L., E. Wu, et al. (1991). "Effect of exercise training on antioxidant and metabolic functions in senescent rat skeletal muscle." Gerontology **37**(6): 317-325.
Jing, E., B. Emanuelli, et al. (2011). "Sirtuin-3 (Sirt3) regulates skeletal muscle metabolism and insulin signaling via altered mitochondrial oxidation and reactive oxygen species production." Proc Natl Acad Sci U S A **108**(35): 14608-14613.
Joseph, A. M., P. J. Adhihetty, et al. (2012). "The impact of aging on mitochondrial function and biogenesis pathways in skeletal muscle of sedentary high- and low-functioning elderly individuals." Aging Cell **11**(5): 801-809.
Joseph, A. M., A. A. Rungi, et al. (2004). "Compensatory responses of protein import and transcription factor expression in mitochondrial DNA defects." Am J Physiol Cell Physiol **286**(4): C867-875.
Judge, S., Y. M. Jang, et al. (2005). "Age-associated increases in oxidative stress and antioxidant enzyme activities in cardiac interfibrillar mitochondria: implications for the mitochondrial theory of aging." FASEB J **19**(3): 419-421.
Judge, S. and C. Leeuwenburgh (2007). "Cardiac mitochondrial bioenergetics, oxidative stress, and aging." Am J Physiol Cell Physiol **292**(6): C1983-1992.
Julienne, C. M., J. F. Dumas, et al. (2012). "Cancer cachexia is associated with a decrease in skeletal muscle mitochondrial oxidative capacities without alteration of ATP production efficiency." J Cachexia Sarcopenia Muscle **3**(4): 265-275.
Julienne, C. M., J. F. Dumas, et al. (2012). "Cancer cachexia is associated with a decrease in skeletal muscle mitochondrial oxidative capacities without alteration of ATP production efficiency." J Cachexia Sarcopenia Muscle.
Kanazawa, A., Y. Nishio, et al. (2002). "Reduced activity of mtTFA decreases the transcription in mitochondria isolated from diabetic rat heart." Am J Physiol Endocrinol Metab **282**(4): E778-785.
Kandarian, S. C. and R. W. Jackman (2006). "Intracellular signaling during skeletal muscle atrophy." Muscle Nerve **33**(2): 155-165.
Kang, S. G., J. Ortega, et al. (2002). "Functional proteolytic complexes of the human mitochondrial ATP-dependent protease, hClpXP." J Biol Chem **277**(23): 21095-21102.
Kanski, J., A. Behring, et al. (2005). "Proteomic identification of 3-nitrotyrosine-containing rat cardiac proteins: effects of biological aging." Am J Physiol Heart Circ Physiol **288**(1): H371-381.
Karata, K., T. Inagawa, et al. (1999). "Dissecting the role of a conserved motif (the second region of homology) in the AAA family of ATPases. Site-directed mutagenesis of the ATP-dependent protease FtsH." J Biol Chem **274**(37): 26225-26232.
Karlberg, T., S. van den Berg, et al. (2009). "Crystal structure of the ATPase domain of the human AAA+ protein paraplegin/SPG7." PLoS One **4**(10): e6975.
Kaser, M. and T. Langer (2000). "Protein degradation in mitochondria." Semin Cell Dev Biol **11**(3): 181-190.
Kelley, D. E., J. He, et al. (2002). "Dysfunction of mitochondria in human skeletal muscle in type 2 diabetes." Diabetes **51**(10): 2944-2950.
Kerner, J., K. Lee, et al. (2011). "Post-translational modifications of mitochondrial outer membrane proteins." Free Radic Res **45**(1): 16-28.
Kerner, J., P. J. Turkaly, et al. (2001). "Aging skeletal muscle mitochondria in the rat: decreased uncoupling protein-3 content." Am J Physiol Endocrinol Metab **281**(5): E1054-1062.
Kirkinezos, I. G. and C. T. Moraes (2001). "Reactive oxygen species and mitochondrial diseases." Semin Cell Dev Biol **12**(6): 449-457.
Kirkwood, T. B. (2005). "Understanding the odd science of aging." Cell **120**(4): 437-447.
Koc, E. C. and H. Koc (2012). "Regulation of mammalian mitochondrial translation by post-translational modifications." Biochim Biophys Acta **1819**(9-10): 1055-1066.
Koehler, C. M. (2000). "Protein translocation pathways of the mitochondrion." FEBS Lett **476**(1-2): 27-31.

Koltai, E., N. Hart, et al. (2012). "Age-associated declines in mitochondrial biogenesis and protein quality control factors are minimized by exercise training." Am J Physiol Regul Integr Comp Physiol **303**(2): R127-134.

Koltai, E., Z. Szabo, et al. (2010). "Exercise alters SIRT1, SIRT6, NAD and NAMPT levels in skeletal muscle of aged rats." Mech Ageing Dev **131**(1): 21-28.

Koppen, M., F. Bonn, et al. (2009). "Autocatalytic processing of m-AAA protease subunits in mitochondria." Mol Biol Cell **20**(19): 4216-4224.

Koppen, M. and T. Langer (2007). "Protein degradation within mitochondria: versatile activities of AAA proteases and other peptidases." Crit Rev Biochem Mol Biol **42**(3): 221-242.

Krebs, H. A. (1940). "The citric acid cycle: A reply to the criticisms of F. L. Breusch and of J. Thomas." Biochem J **34**(3): 460-463.

Krieger, D. A., C. A. Tate, et al. (1980). "Populations of rat skeletal muscle mitochondria after exercise and immobilization." J Appl Physiol **48**(1): 23-28.

Kumaran, S., K. S. Panneerselvam, et al. (2005). "Age-associated deficit of mitochondrial oxidative phosphorylation in skeletal muscle: role of carnitine and lipoic acid." Mol Cell Biochem **280**(1-2): 83-89.

Kumaran, S., M. Subathra, et al. (2004). "Age-associated decreased activities of mitochondrial electron transport chain complexes in heart and skeletal muscle: role of L-carnitine." Chem Biol Interact **148**(1-2): 11-18.

Kwong, L. K. and R. S. Sohal (2000). "Age-related changes in activities of mitochondrial electron transport complexes in various tissues of the mouse." Arch Biochem Biophys **373**(1): 16-22.

Lammi-Keefe, C. J., P. B. Swan, et al. (1984). "Copper-zinc and manganese superoxide dismutase activities in cardiac and skeletal muscles during aging in male rats." Gerontology **30**(3): 153-158.

Langer, T., M. Kaser, et al. (2001). "AAA proteases of mitochondria: quality control of membrane proteins and regulatory functions during mitochondrial biogenesis." Biochem Soc Trans **29**(Pt 4): 431-436.

Lanza, I. R. and K. Sreekumaran Nair (2010). "Regulation of skeletal muscle mitochondrial function: genes to proteins." Acta Physiol (Oxf) **199**(4): 529-547.

Larsen, S., N. Stride, et al. (2011). "Increased mitochondrial substrate sensitivity in skeletal muscle of patients with type 2 diabetes." Diabetologia **54**(6): 1427-1436.

Lashin, O. M., P. A. Szweda, et al. (2006). "Decreased complex II respiration and HNE-modified SDH subunit in diabetic heart." Free Radic Biol Med **40**(5): 886-896.

Lee, I. M., E. J. Shiroma, et al. (2012). "Effect of physical inactivity on major non-communicable diseases worldwide: an analysis of burden of disease and life expectancy." Lancet **380**(9838): 219-229.

Leeuwenburgh, C., C. M. Gurley, et al. (2005). "Age-related differences in apoptosis with disuse atrophy in soleus muscle." Am J Physiol Regul Integr Comp Physiol **288**(5): R1288-1296.

Lenaz, G., C. Bovina, et al. (1997). "Mitochondrial complex I defects in aging." Mol Cell Biochem **174**(1-2): 329-333.

Lenaz, G. and M. L. Genova (2007). "Kinetics of integrated electron transfer in the mitochondrial respiratory chain: random collisions vs. solid state electron channeling." Am J Physiol Cell Physiol **292**(4): C1221-1239.

Lenaz, G. and M. L. Genova (2009). "Structural and functional organization of the mitochondrial respiratory chain: a dynamic super-assembly." Int J Biochem Cell Biol **41**(10): 1750-1772.

Leonhard, K., B. Guiard, et al. (2000). "Membrane protein degradation by AAA proteases in mitochondria: extraction of substrates from either membrane surface." Mol Cell **5**(4): 629-638.

Leonhard, K., J. M. Herrmann, et al. (1996). "AAA proteases with catalytic sites on opposite membrane surfaces comprise a proteolytic system for the ATP-dependent degradation of inner membrane proteins in mitochondria." EMBO J **15**(16): 4218-4229.

Lesnefsky, E. J., T. I. Gudz, et al. (2001). "Aging decreases electron transport complex III activity in heart interfibrillar mitochondria by alteration of the cytochrome c binding site." J Mol Cell Cardiol **33**(1): 37-47.
Lesnefsky, E. J. and C. L. Hoppel (2006). "Oxidative phosphorylation and aging." Ageing Res Rev **5**(4): 402-433.
Lesnefsky, E. J., P. Minkler, et al. (2009). "Enhanced modification of cardiolipin during ischemia in the aged heart." J Mol Cell Cardiol **46**(6): 1008-1015.
Lesnefsky, E. J., S. Moghaddas, et al. (2001). "Mitochondrial dysfunction in cardiac disease: ischemia--reperfusion, aging, and heart failure." J Mol Cell Cardiol **33**(6): 1065-1089.
Lesnefsky, E. J., T. J. Slabe, et al. (2001). "Myocardial ischemia selectively depletes cardiolipin in rabbit heart subsarcolemmal mitochondria." Am J Physiol Heart Circ Physiol **280**(6): H2770-2778.
Lezza, A. M., V. Pesce, et al. (2001). "Increased expression of mitochondrial transcription factor A and nuclear respiratory factor-1 in skeletal muscle from aged human subjects." FEBS Lett **501**(1): 74-78.
Li, Y. P., Y. Chen, et al. (2003). "Hydrogen peroxide stimulates ubiquitin-conjugating activity and expression of genes for specific E2 and E3 proteins in skeletal muscle myotubes." Am J Physiol Cell Physiol **285**(4): C806-812.
Liesa, M., M. Palacin, et al. (2009). "Mitochondrial dynamics in mammalian health and disease." Physiol Rev **89**(3): 799-845.
Lionaki, E. and N. Tavernarakis (2013). "Oxidative stress and mitochondrial protein quality control in aging." J Proteomics.
Lionetti, L., M. P. Mollica, et al. (2007). "Skeletal muscle subsarcolemmal mitochondrial dysfunction in high-fat fed rats exhibiting impaired glucose homeostasis." Int J Obes (Lond) **31**(10): 1596-1604.
Ljubicic, V., A. M. Joseph, et al. (2009). "Molecular basis for an attenuated mitochondrial adaptive plasticity in aged skeletal muscle." Aging (Albany NY) **1**(9): 818-830.
Logan, D. C. (2006). "The mitochondrial compartment." J Exp Bot **57**(6): 1225-1243.
Lombard, D. B., F. W. Alt, et al. (2007). "Mammalian Sir2 homolog SIRT3 regulates global mitochondrial lysine acetylation." Mol Cell Biol **27**(24): 8807-8814.
Lopez, A. D., C. D. Mathers, et al. (2006). "Global and regional burden of disease and risk factors, 2001: systematic analysis of population health data." Lancet **367**(9524): 1747-1757.
Lowell, B. B. and G. I. Shulman (2005). "Mitochondrial dysfunction and type 2 diabetes." Science **307**(5708): 384-387.
Luce, K., A. C. Weil, et al. (2010). "Mitochondrial protein quality control systems in aging and disease." Adv Exp Med Biol **694**: 108-125.
Lumini-Oliveira, J., J. Magalhaes, et al. (2011). "Endurance training reverts heart mitochondrial dysfunction, permeability transition and apoptotic signaling in long-term severe hyperglycemia." Mitochondrion **11**(1): 54-63.
Lyons, C. N., O. Mathieu-Costello, et al. (2006). "Regulation of skeletal muscle mitochondrial content during aging." J Gerontol A Biol Sci Med Sci **61**(1): 3-13.
Mahgoub, M. A. and A. S. Abd-Elfattah (1998). "Diabetes mellitus and cardiac function." Mol Cell Biochem **180**(1-2): 59-64.
Maisch, B., P. Alter, et al. (2011). "Diabetic cardiomyopathy--fact or fiction?" Herz **36**(2): 102-115.
Mammucari, C., S. Schiaffino, et al. (2008). "Downstream of Akt: FoxO3 and mTOR in the regulation of autophagy in skeletal muscle." Autophagy **4**(4): 524-526.
Mandavilli, B. S., J. H. Santos, et al. (2002). "Mitochondrial DNA repair and aging." Mutat Res **509**(1-2): 127-151.
Mansouri, A., F. L. Muller, et al. (2006). "Alterations in mitochondrial function, hydrogen peroxide release and oxidative damage in mouse hind-limb skeletal muscle during aging." Mech Ageing Dev **127**(3): 298-306.

Manzelmann, M. S. and H. J. Harmon (1987). "Lack of age-dependent changes in rat heart mitochondria." Mech Ageing Dev **39**(3): 281-288.

Marcinek, D. J., K. A. Schenkman, et al. (2005). "Reduced mitochondrial coupling in vivo alters cellular energetics in aged mouse skeletal muscle." J Physiol **569**(Pt 2): 467-473.

Marin-Corral, J., C. C. Fontes, et al. (2010). "Redox balance and carbonylated proteins in limb and heart muscles of cachectic rats." Antioxid Redox Signal **12**(3): 365-380.

Marra, G., P. Cotroneo, et al. (2002). "Early increase of oxidative stress and reduced antioxidant defenses in patients with uncomplicated type 1 diabetes: a case for gender difference." Diabetes Care **25**(2): 370-375.

Marzani, B., G. Felzani, et al. (2005). "Human muscle aging: ROS-mediated alterations in rectus abdominis and vastus lateralis muscles." Exp Gerontol **40**(12): 959-965.

Marzetti, E., J. C. Hwang, et al. (2010). "Mitochondrial death effectors: relevance to sarcopenia and disuse muscle atrophy." Biochim Biophys Acta **1800**(3): 235-244.

Marzetti, E. and C. Leeuwenburgh (2006). "Skeletal muscle apoptosis, sarcopenia and frailty at old age." Exp Gerontol **41**(12): 1234-1238.

Maxwell, S. R., H. Thomason, et al. (1997). "Antioxidant status in patients with uncomplicated insulin-dependent and non-insulin-dependent diabetes mellitus." Eur J Clin Invest **27**(6): 484-490.

McClung, J. M., M. A. Whidden, et al. (2008). "Redox regulation of diaphragm proteolysis during mechanical ventilation." Am J Physiol Regul Integr Comp Physiol **294**(5): R1608-1617.

Meex, R. C., V. B. Schrauwen-Hinderling, et al. (2010). "Restoration of muscle mitochondrial function and metabolic flexibility in type 2 diabetes by exercise training is paralleled by increased myocellular fat storage and improved insulin sensitivity." Diabetes **59**(3): 572-579.

Menshikova, E. V., V. B. Ritov, et al. (2006). "Effects of exercise on mitochondrial content and function in aging human skeletal muscle." J Gerontol A Biol Sci Med Sci **61**(6): 534-540.

Miro, O., J. Casademont, et al. (2000). "Aging is associated with increased lipid peroxidation in human hearts, but not with mitochondrial respiratory chain enzyme defects." Cardiovasc Res **47**(3): 624-631.

Mogensen, M., K. Sahlin, et al. (2007). "Mitochondrial respiration is decreased in skeletal muscle of patients with type 2 diabetes." Diabetes **56**(6): 1592-1599.

Moghaddas, S., M. S. Stoll, et al. (2002). "Preservation of cardiolipin content during aging in rat heart interfibrillar mitochondria." J Gerontol A Biol Sci Med Sci **57**(1): B22-28.

Mootha, V. K., C. M. Lindgren, et al. (2003). "PGC-1alpha-responsive genes involved in oxidative phosphorylation are coordinately downregulated in human diabetes." Nat Genet **34**(3): 267-273.

Morino, K., K. F. Petersen, et al. (2005). "Reduced mitochondrial density and increased IRS-1 serine phosphorylation in muscle of insulin-resistant offspring of type 2 diabetic parents." J Clin Invest **115**(12): 3587-3593.

Morley, J. E., A. M. Abbatecola, et al. (2011). "Sarcopenia with limited mobility: an international consensus." J Am Med Dir Assoc **12**(6): 403-409.

Muller, F. L., Y. Liu, et al. (2004). "Complex III releases superoxide to both sides of the inner mitochondrial membrane." J Biol Chem **279**(47): 49064-49073.

Murphy, M. P. (2009). "How mitochondria produce reactive oxygen species." Biochem J **417**(1): 1-13.

Musaro, A., S. Fulle, et al. (2010). "Oxidative stress and muscle homeostasis." Curr Opin Clin Nutr Metab Care **13**(3): 236-242.

Nair, K. S. (2005). "Aging muscle." Am J Clin Nutr **81**(5): 953-963.

Navarro, A. and A. Boveris (2007). "The mitochondrial energy transduction system and the aging process." Am J Physiol Cell Physiol **292**(2): C670-686.

Neupert, W. and J. M. Herrmann (2007). "Translocation of proteins into mitochondria." Annu Rev Biochem **76**: 723-749.

Nolden, M., S. Ehses, et al. (2005). "The m-AAA protease defective in hereditary spastic paraplegia controls ribosome assembly in mitochondria." Cell **123**(2): 277-289.
Nunnari, J. and A. Suomalainen (2012). "Mitochondria: in sickness and in health." Cell **148**(6): 1145-1159.
O'Connell, K. and K. Ohlendieck (2009). "Proteomic DIGE analysis of the mitochondria-enriched fraction from aged rat skeletal muscle." Proteomics **9**(24): 5509-5524.
Oliveira, P. J., A. P. Rolo, et al. (2001). "Decreased susceptibility of heart mitochondria from diabetic GK rats to mitochondrial permeability transition induced by calcium phosphate." Biosci Rep **21**(1): 45-53.
Oliveira, P. J., R. Seica, et al. (2003). "Enhanced permeability transition explains the reduced calcium uptake in cardiac mitochondria from streptozotocin-induced diabetic rats." FEBS Lett **554**(3): 511-514.
Ott, M., V. Gogvadze, et al. (2007). "Mitochondria, oxidative stress and cell death." Apoptosis **12**(5): 913-922.
Pagel-Langenickel, I., D. R. Schwartz, et al. (2007). "A discordance in rosiglitazone mediated insulin sensitization and skeletal muscle mitochondrial content/activity in Type 2 diabetes mellitus." Am J Physiol Heart Circ Physiol **293**(5): H2659-2666.
Pagliarini, D. J., S. E. Calvo, et al. (2008). "A mitochondrial protein compendium elucidates complex I disease biology." Cell **134**(1): 112-123.
Pagliarini, D. J. and J. E. Dixon (2006). "Mitochondrial modulation: reversible phosphorylation takes center stage?" Trends Biochem Sci **31**(1): 26-34.
Palacios, O. M., J. J. Carmona, et al. (2009). "Diet and exercise signals regulate SIRT3 and activate AMPK and PGC-1alpha in skeletal muscle." Aging (Albany NY) **1**(9): 771-783.
Palazzetti, S., M. J. Richard, et al. (2003). "Overloaded training increases exercise-induced oxidative stress and damage." Can J Appl Physiol **28**(4): 588-604.
Palmer, J. W., B. Tandler, et al. (1977). "Biochemical properties of subsarcolemmal and interfibrillar mitochondria isolated from rat cardiac muscle." J Biol Chem **252**(23): 8731-8739.
Pansarasa, O., G. Felzani, et al. (2002). "Antioxidant pathways in human aged skeletal muscle: relationship with the distribution of type II fibers." Exp Gerontol **37**(8-9): 1069-1075.
Papp, Z., D. Czuriga, et al. (2012). "How cardiomyocytes make the heart old." Curr Pharm Biotechnol **13**(13): 2515-2521.
Paradies, G., G. Petrosillo, et al. (2002). "Reactive oxygen species affect mitochondrial electron transport complex I activity through oxidative cardiolipin damage." Gene **286**(1): 135-141.
Paradies, G., F. M. Ruggiero, et al. (1998). "Peroxidative damage to cardiac mitochondria: cytochrome oxidase and cardiolipin alterations." FEBS Lett **424**(3): 155-158.
Pastoris, O., F. Boschi, et al. (2000). "The effects of aging on enzyme activities and metabolite concentrations in skeletal muscle from sedentary male and female subjects." Exp Gerontol **35**(1): 95-104.
Patti, M. E., A. J. Butte, et al. (2003). "Coordinated reduction of genes of oxidative metabolism in humans with insulin resistance and diabetes: Potential role of PGC1 and NRF1." Proc Natl Acad Sci U S A **100**(14): 8466-8471.
Patti, M. E. and S. Corvera (2010). "The role of mitochondria in the pathogenesis of type 2 diabetes." Endocr Rev **31**(3): 364-395.
Penna, F., A. Bonetto, et al. (2010). "Muscle atrophy in experimental cancer cachexia: is the IGF-1 signaling pathway involved?" Int J Cancer **127**(7): 1706-1717.
Perocchi, F., L. J. Jensen, et al. (2006). "Assessing systems properties of yeast mitochondria through an interaction map of the organelle." PLoS Genet **2**(10): e170.
Petrosillo, G., M. Matera, et al. (2009). "Mitochondrial complex I dysfunction in rat heart with aging: critical role of reactive oxygen species and cardiolipin." Free Radic Biol Med **46**(1): 88-94.
Pham, F. H., P. H. Sugden, et al. (2000). "Regulation of protein kinase B and 4E-BP1 by oxidative stress in cardiac myocytes." Circ Res **86**(12): 1252-1258.

Phielix, E., R. Meex, et al. (2010). "Exercise training increases mitochondrial content and ex vivo mitochondrial function similarly in patients with type 2 diabetes and in control individuals." Diabetologia **53**(8): 1714-1721.

Phielix, E., V. B. Schrauwen-Hinderling, et al. (2008). "Lower intrinsic ADP-stimulated mitochondrial respiration underlies in vivo mitochondrial dysfunction in muscle of male type 2 diabetic patients." Diabetes **57**(11): 2943-2949.

Phillips, D., A. M. Aponte, et al. (2011). "Intrinsic protein kinase activity in mitochondrial oxidative phosphorylation complexes." Biochemistry **50**(13): 2515-2529.

Picard, M., D. Ritchie, et al. (2010). "Mitochondrial functional impairment with aging is exaggerated in isolated mitochondria compared to permeabilized myofibers." Aging Cell **9**(6): 1032-1046.

Pickart, C. M. (2001). "Ubiquitin enters the new millennium." Mol Cell **8**(3): 499-504.

Pierce, G. N. and N. S. Dhalla (1985). "Heart mitochondrial function in chronic experimental diabetes in rats." Can J Cardiol **1**(1): 48-54.

Plant, P. J., J. R. Bain, et al. (2009). "Absence of caspase-3 protects against denervation-induced skeletal muscle atrophy." J Appl Physiol **107**(1): 224-234.

Powers, S. K. and M. J. Jackson (2008). "Exercise-induced oxidative stress: cellular mechanisms and impact on muscle force production." Physiol Rev **88**(4): 1243-1276.

Powers, S. K., A. N. Kavazis, et al. (2007). "Oxidative stress and disuse muscle atrophy." J Appl Physiol **102**(6): 2389-2397.

Powers, S. K., A. J. Smuder, et al. (2011). "Mechanistic links between oxidative stress and disuse muscle atrophy." Antioxid Redox Signal **15**(9): 2519-2528.

Powers, S. K., M. P. Wiggs, et al. (2012). "Mitochondrial signaling contributes to disuse muscle atrophy." Am J Physiol Endocrinol Metab **303**(1): E31-39.

Poyton, R. O. and J. E. McEwen (1996). "Crosstalk between nuclear and mitochondrial genomes." Annu Rev Biochem **65**: 563-607.

Price, S. R., J. L. Bailey, et al. (1996). "Muscle wasting in insulinopenic rats results from activation of the ATP-dependent, ubiquitin-proteasome proteolytic pathway by a mechanism including gene transcription." J Clin Invest **98**(8): 1703-1708.

Rabol, R., S. Larsen, et al. (2010). "Regional anatomic differences in skeletal muscle mitochondrial respiration in type 2 diabetes and obesity." J Clin Endocrinol Metab **95**(2): 857-863.

Rabol, R., P. F. Svendsen, et al. (2009). "Reduced skeletal muscle mitochondrial respiration and improved glucose metabolism in nondiabetic obese women during a very low calorie dietary intervention leading to rapid weight loss." Metabolism **58**(8): 1145-1152.

Raha, S. and B. H. Robinson (2000). "Mitochondria, oxygen free radicals, disease and ageing." Trends Biochem Sci **25**(10): 502-508.

Reinders, J., R. P. Zahedi, et al. (2006). "Toward the complete yeast mitochondrial proteome: multidimensional separation techniques for mitochondrial proteomics." J Proteome Res **5**(7): 1543-1554.

Remels, A. H., H. R. Gosker, et al. (2010). "TNF-alpha impairs regulation of muscle oxidative phenotype: implications for cachexia?" FASEB J **24**(12): 5052-5062.

Requena, J. R., C. C. Chao, et al. (2001). "Glutamic and aminoadipic semialdehydes are the main carbonyl products of metal-catalyzed oxidation of proteins." Proc Natl Acad Sci U S A **98**(1): 69-74.

Requena, J. R., R. L. Levine, et al. (2003). "Recent advances in the analysis of oxidized proteins." Amino Acids **25**(3-4): 221-226.

Reznick, R. M., H. Zong, et al. (2007). "Aging-associated reductions in AMP-activated protein kinase activity and mitochondrial biogenesis." Cell Metab **5**(2): 151-156.

Ristow, M., K. Zarse, et al. (2009). "Antioxidants prevent health-promoting effects of physical exercise in humans." Proc Natl Acad Sci U S A **106**(21): 8665-8670.

Ritov, V. B., E. V. Menshikova, et al. (2005). "Deficiency of subsarcolemmal mitochondria in obesity and type 2 diabetes." Diabetes **54**(1): 8-14.

Riva, A., B. Tandler, et al. (2005). "Structural differences in two biochemically defined populations of cardiac mitochondria." Am J Physiol Heart Circ Physiol **289**(2): H868-872.
Rogers, M. A., J. M. Hagberg, et al. (1990). "Decline in VO2max with aging in master athletes and sedentary men." J Appl Physiol **68**(5): 2195-2199.
Romanello, V., E. Guadagnin, et al. (2010). "Mitochondrial fission and remodelling contributes to muscle atrophy." EMBO J **29**(10): 1774-1785.
Romanello, V. and M. Sandri (2010). "Mitochondrial biogenesis and fragmentation as regulators of muscle protein degradation." Curr Hypertens Rep **12**(6): 433-439.
Romanello, V. and M. Sandri (2013). "Mitochondrial biogenesis and fragmentation as regulators of protein degradation in striated muscles." J Mol Cell Cardiol **55**: 64-72.
Rommel, C., S. C. Bodine, et al. (2001). "Mediation of IGF-1-induced skeletal myotube hypertrophy by PI(3)K/Akt/mTOR and PI(3)K/Akt/GSK3 pathways." Nat Cell Biol **3**(11): 1009-1013.
Rooyackers, O. E., D. B. Adey, et al. (1996). "Effect of age on in vivo rates of mitochondrial protein synthesis in human skeletal muscle." Proc Natl Acad Sci U S A **93**(26): 15364-15369.
Rosca, M., P. Minkler, et al. (2011). "Cardiac mitochondria in heart failure: normal cardiolipin profile and increased threonine phosphorylation of complex IV." Biochim Biophys Acta **1807**(11): 1373-1382.
Rosen, P., P. P. Nawroth, et al. (2001). "The role of oxidative stress in the onset and progression of diabetes and its complications: a summary of a Congress Series sponsored by UNESCO-MCBN, the American Diabetes Association and the German Diabetes Society." Diabetes Metab Res Rev **17**(3): 189-212.
Rugarli, E. I. and T. Langer (2012). "Mitochondrial quality control: a matter of life and death for neurons." EMBO J **31**(6): 1336-1349.
Russell, A. P., G. Gastaldi, et al. (2003). "Lipid peroxidation in skeletal muscle of obese as compared to endurance-trained humans: a case of good vs. bad lipids?" FEBS Lett **551**(1-3): 104-106.
Rutter, J., D. R. Winge, et al. (2010). "Succinate dehydrogenase - Assembly, regulation and role in human disease." Mitochondrion **10**(4): 393-401.
Ryan, M. T. and N. J. Hoogenraad (2007). "Mitochondrial-nuclear communications." Annu Rev Biochem **76**: 701-722.
Sack, M. N. (2011). "Emerging characterization of the role of SIRT3-mediated mitochondrial protein deacetylation in the heart." Am J Physiol Heart Circ Physiol **301**(6): H2191-2197.
Sack, M. N. (2012). "The role of SIRT3 in mitochondrial homeostasis and cardiac adaptation to hypertrophy and aging." J Mol Cell Cardiol **52**(3): 520-525.
Sakuma, K. and A. Yamaguchi (2012). "Sarcopenia and cachexia: the adaptations of negative regulators of skeletal muscle mass." J Cachexia Sarcopenia Muscle **3**(2): 77-94.
Sander, G. E. and T. D. Giles (2003). "Diabetes mellitus and heart failure." Am Heart Hosp J **1**(4): 273-280.
Sandri, M. (2008). "Signaling in muscle atrophy and hypertrophy." Physiology (Bethesda) **23**: 160-170.
Sandri, M., C. Sandri, et al. (2004). "Foxo transcription factors induce the atrophy-related ubiquitin ligase atrogin-1 and cause skeletal muscle atrophy." Cell **117**(3): 399-412.
Santagata, S., D. Bhattacharyya, et al. (1999). "Molecular cloning and characterization of a mouse homolog of bacterial ClpX, a novel mammalian class II member of the Hsp100/Clp chaperone family." J Biol Chem **274**(23): 16311-16319.
Sastre, J., M. Asensi, et al. (1992). "Exhaustive physical exercise causes oxidation of glutathione status in blood: prevention by antioxidant administration." Am J Physiol **263**(5 Pt 2): R992-995.
Sauer, R. T. and T. A. Baker (2011). "AAA+ proteases: ATP-fueled machines of protein destruction." Annu Rev Biochem **80**: 587-612.
Schagger, H. (2001). "Respiratory chain supercomplexes." IUBMB Life **52**(3-5): 119-128.

Schagger, H. and G. von Jagow (1991). "Blue native electrophoresis for isolation of membrane protein complexes in enzymatically active form." Anal Biochem **199**(2): 223-231.

Scheede-Bergdahl, C., M. Penkowa, et al. (2005). "Metallothionein-mediated antioxidant defense system and its response to exercise training are impaired in human type 2 diabetes." Diabetes **54**(11): 3089-3094.

Schiaffino, S., K. A. Dyar, et al. (2013). "Mechanisms regulating skeletal muscle growth and atrophy." FEBS J.

Schon, E. A. and N. A. Dencher (2009). "Heavy breathing: energy conversion by mitochondrial respiratory supercomplexes." Cell Metab **9**(1): 1-3.

Seager, M. J., P. K. Singal, et al. (1984). "Cardiac cell damage: a primary myocardial disease in streptozotocin-induced chronic diabetes." Br J Exp Pathol **65**(5): 613-623.

Sena, L. A. and N. S. Chandel (2012). "Physiological roles of mitochondrial reactive oxygen species." Mol Cell **48**(2): 158-167.

Shen, X., S. Zheng, et al. (2006). "Protection of cardiac mitochondria by overexpression of MnSOD reduces diabetic cardiomyopathy." Diabetes **55**(3): 798-805.

Shen, X., S. Zheng, et al. (2004). "Cardiac mitochondrial damage and biogenesis in a chronic model of type 1 diabetes." Am J Physiol Endocrinol Metab **287**(5): E896-905.

Shigenaga, M. K., T. M. Hagen, et al. (1994). "Oxidative damage and mitochondrial decay in aging." Proc Natl Acad Sci U S A **91**(23): 10771-10778.

Short, K. R., M. L. Bigelow, et al. (2005). "Decline in skeletal muscle mitochondrial function with aging in humans." Proc Natl Acad Sci U S A **102**(15): 5618-5623.

Short, K. R., J. L. Vittone, et al. (2003). "Impact of aerobic exercise training on age-related changes in insulin sensitivity and muscle oxidative capacity." Diabetes **52**(8): 1888-1896.

Shoubridge, E. A. (2012). "Supersizing the mitochondrial respiratory chain." Cell Metab **15**(3): 271-272.

Shum, A. M., T. Mahendradatta, et al. (2012). "Disruption of MEF2C signaling and loss of sarcomeric and mitochondrial integrity in cancer-induced skeletal muscle wasting." Aging (Albany NY) **4**(2): 133-143.

Sickmann, A., J. Reinders, et al. (2003). "The proteome of Saccharomyces cerevisiae mitochondria." Proc Natl Acad Sci U S A **100**(23): 13207-13212.

Silva, L. A., C. A. Pinho, et al. (2009). "Physical exercise increases mitochondrial function and reduces oxidative damage in skeletal muscle." Eur J Appl Physiol **105**(6): 861-867.

Singh, K. and D. A. Hood (2011). "Effect of denervation-induced muscle disuse on mitochondrial protein import." Am J Physiol Cell Physiol **300**(1): C138-145.

Siu, P. M., E. E. Pistilli, et al. (2005). "Aging influences cellular and molecular responses of apoptosis to skeletal muscle unloading." Am J Physiol Cell Physiol **288**(2): C338-349.

Smith, M. A. and M. B. Reid (2006). "Redox modulation of contractile function in respiratory and limb skeletal muscle." Respir Physiol Neurobiol **151**(2-3): 229-241.

Sohal, R. S. (2002). "Role of oxidative stress and protein oxidation in the aging process." Free Radic Biol Med **33**(1): 37-44.

Springer, J., V. Adams, et al. (2010). "Myostatin: Regulator of muscle wasting in heart failure and treatment target for cardiac cachexia." Circulation **121**(3): 354-356.

Stadtman, E. R. (2006). "Protein oxidation and aging." Free Radic Res **40**(12): 1250-1258.

Stadtman, E. R. and R. L. Levine (2003). "Free radical-mediated oxidation of free amino acids and amino acid residues in proteins." Amino Acids **25**(3-4): 207-218.

Stahlberg, H., E. Kutejova, et al. (1999). "Mitochondrial Lon of Saccharomyces cerevisiae is a ring-shaped protease with seven flexible subunits." Proc Natl Acad Sci U S A **96**(12): 6787-6790.

Stitt, T. N., D. Drujan, et al. (2004). "The IGF-1/PI3K/Akt pathway prevents expression of muscle atrophy-induced ubiquitin ligases by inhibiting FOXO transcription factors." Mol Cell **14**(3): 395-403.

Stowe, D. F. and A. K. Camara (2009). "Mitochondrial reactive oxygen species production in excitable cells: modulators of mitochondrial and cell function." Antioxid Redox Signal **11**(6): 1373-1414.

Strobel, N. A., J. M. Peake, et al. (2011). "Antioxidant supplementation reduces skeletal muscle mitochondrial biogenesis." Med Sci Sports Exerc **43**(6): 1017-1024.

Sugiyama, S., M. Takasawa, et al. (1993). "Changes in skeletal muscle, heart and liver mitochondrial electron transport activities in rats and dogs of various ages." Biochem Mol Biol Int **30**(5): 937-944.

Suh, J. H., S. H. Heath, et al. (2003). "Two subpopulations of mitochondria in the aging rat heart display heterogenous levels of oxidative stress." Free Radic Biol Med **35**(9): 1064-1072.

Sun, Z., L. Liu, et al. (2008). "Muscular response and adaptation to diabetes mellitus." Front Biosci **13**: 4765-4794.

Suzuki, C. K., K. Suda, et al. (1994). "Requirement for the yeast gene LON in intramitochondrial proteolysis and maintenance of respiration." Science **264**(5156): 273-276.

Suzuki, Y., Y. Imai, et al. (2001). "A serine protease, HtrA2, is released from the mitochondria and interacts with XIAP, inducing cell death." Mol Cell **8**(3): 613-621.

Tait, S. W. and D. R. Green (2010). "Mitochondria and cell death: outer membrane permeabilization and beyond." Nat Rev Mol Cell Biol **11**(9): 621-632.

Takahashi, M. and D. A. Hood (1996). "Protein import into subsarcolemmal and intermyofibrillar skeletal muscle mitochondria. Differential import regulation in distinct subcellular regions." J Biol Chem **271**(44): 27285-27291.

Takasawa, M., M. Hayakawa, et al. (1993). "Age-associated damage in mitochondrial function in rat hearts." Exp Gerontol **28**(3): 269-280.

Tanaka, Y., N. Konno, et al. (1992). "Mitochondrial dysfunction observed in situ in cardiomyocytes of rats in experimental diabetes." Cardiovasc Res **26**(4): 409-414.

Tatarkova, Z., S. Kuka, et al. (2011). "Effects of aging on activities of mitochondrial electron transport chain complexes and oxidative damage in rat heart." Physiol Res **60**(2): 281-289.

Tatsuta, T. (2009). "Protein quality control in mitochondria." J Biochem **146**(4): 455-461.

Tatsuta, T. and T. Langer (2008). "Quality control of mitochondria: protection against neurodegeneration and ageing." EMBO J **27**(2): 306-314.

Tatsuta, T. and T. Langer (2009). "AAA proteases in mitochondria: diverse functions of membrane-bound proteolytic machines." Res Microbiol **160**(9): 711-717.

Terman, A., T. Kurz, et al. (2010). "Mitochondrial turnover and aging of long-lived postmitotic cells: the mitochondrial-lysosomal axis theory of aging." Antioxid Redox Signal **12**(4): 503-535.

Thomas, D. R. (2007). "Loss of skeletal muscle mass in aging: examining the relationship of starvation, sarcopenia and cachexia." Clin Nutr **26**(4): 389-399.

Thompson, L. V. (2009). "Age-related muscle dysfunction." Exp Gerontol **44**(1-2): 106-111.

Tian, M., M. L. Asp, et al. (2011). "Evidence for cardiac atrophic remodeling in cancer-induced cachexia in mice." Int J Oncol **39**(5): 1321-1326.

Tian, M., Y. Nishijima, et al. (2010). "Cardiac alterations in cancer-induced cachexia in mice." Int J Oncol **37**(2): 347-353.

Tisdale, M. J. (2005). "The ubiquitin-proteasome pathway as a therapeutic target for muscle wasting." J Support Oncol **3**(3): 209-217.

Tisdale, M. J. (2009). "Mechanisms of cancer cachexia." Physiol Rev **89**(2): 381-410.

Toledo, F. G., E. V. Menshikova, et al. (2008). "Mitochondrial capacity in skeletal muscle is not stimulated by weight loss despite increases in insulin action and decreases in intramyocellular lipid content." Diabetes **57**(4): 987-994.

Tonkonogi, M., M. Fernstrom, et al. (2003). "Reduced oxidative power but unchanged antioxidative capacity in skeletal muscle from aged humans." Pflugers Arch **446**(2): 261-269.

Topping, D. L. and M. E. Targ (1975). "Time-course of changes in blood glucose and ketone bodies, plasma lipids and liver fatty acid composition in streptozotocin-diabetic male rats." Horm Res **6**(3): 129-137.

Toth, M. J., K. Ward, et al. (2011). "Chronic heart failure reduces Akt phosphorylation in human skeletal muscle: relationship to muscle size and function." J Appl Physiol **110**(4): 892-900.

Trendelenburg, A. U., A. Meyer, et al. (2009). "Myostatin reduces Akt/TORC1/p70S6K signaling, inhibiting myoblast differentiation and myotube size." Am J Physiol Cell Physiol **296**(6): C1258-1270.

Trifunovic, A. and N. G. Larsson (2008). "Mitochondrial dysfunction as a cause of ageing." J Intern Med **263**(2): 167-178.

Turko, I. V., L. Li, et al. (2003). "Protein tyrosine nitration in the mitochondria from diabetic mouse heart. Implications to dysfunctional mitochondria in diabetes." J Biol Chem **278**(36): 33972-33977.

Turrens, J. F. (2003). "Mitochondrial formation of reactive oxygen species." J Physiol **552**(Pt 2): 335-344.

Tzika, A. A., C. C. Fontes-Oliveira, et al. (2013). "Skeletal muscle mitochondrial uncoupling in a murine cancer cachexia model." Int J Oncol.

Ushmorov, A., V. Hack, et al. (1999). "Differential reconstitution of mitochondrial respiratory chain activity and plasma redox state by cysteine and ornithine in a model of cancer cachexia." Cancer Res **59**(14): 3527-3534.

Vafai, S. B. and V. K. Mootha (2012). "Mitochondrial disorders as windows into an ancient organelle." Nature **491**(7424): 374-383.

Van Dyck, L., D. A. Pearce, et al. (1994). "PIM1 encodes a mitochondrial ATP-dependent protease that is required for mitochondrial function in the yeast Saccharomyces cerevisiae." J Biol Chem **269**(1): 238-242.

van Loo, G., M. van Gurp, et al. (2002). "The serine protease Omi/HtrA2 is released from mitochondria during apoptosis. Omi interacts with caspase-inhibitor XIAP and induces enhanced caspase activity." Cell Death Differ **9**(1): 20-26.

Veal, E. A., A. M. Day, et al. (2007). "Hydrogen peroxide sensing and signaling." Mol Cell **26**(1): 1-14.

Verdejo, H. E., A. del Campo, et al. (2012). "Mitochondria, myocardial remodeling, and cardiovascular disease." Curr Hypertens Rep **14**(6): 532-539.

Verdin, E., M. D. Hirschey, et al. (2010). "Sirtuin regulation of mitochondria: energy production, apoptosis, and signaling." Trends Biochem Sci **35**(12): 669-675.

Vicencio, J. M., L. Galluzzi, et al. (2008). "Senescence, apoptosis or autophagy? When a damaged cell must decide its path--a mini-review." Gerontology **54**(2): 92-99.

Vina, J., A. Gimeno, et al. (2000). "Mechanism of free radical production in exhaustive exercise in humans and rats; role of xanthine oxidase and protection by allopurinol." IUBMB Life **49**(6): 539-544.

Voos, W. (2009). "Mitochondrial protein homeostasis: the cooperative roles of chaperones and proteases." Res Microbiol **160**(9): 718-725.

Voos, W. and K. Rottgers (2002). "Molecular chaperones as essential mediators of mitochondrial biogenesis." Biochim Biophys Acta **1592**(1): 51-62.

Wagatsuma, A. and K. Sakuma (2012). "Molecular mechanisms for age-associated mitochondrial deficiency in skeletal muscle." J Aging Res **2012**: 768304.

Wallace, D. C. (1999). "Mitochondrial diseases in man and mouse." Science **283**(5407): 1482-1488.

Wallace, D. C., M. D. Brown, et al. (1999). "Mitochondrial DNA variation in human evolution and disease." Gene **238**(1): 211-230.

Wang, X., A. M. Pickrell, et al. (2012). "Increase in muscle mitochondrial biogenesis does not prevent muscle loss but increased tumor size in a mouse model of acute cancer-induced cachexia." PLoS One **7**(3): e33426.

Weber, J. (2006). "ATP synthase: subunit-subunit interactions in the stator stalk." Biochim Biophys Acta **1757**(9-10): 1162-1170.

Westermann, B. (2010). "Mitochondrial fusion and fission in cell life and death." Nat Rev Mol Cell Biol **11**(12): 872-884.

White, J. P., K. A. Baltgalvis, et al. (2011). "Muscle oxidative capacity during IL-6-dependent cancer cachexia." Am J Physiol Regul Integr Comp Physiol **300**(2): R201-211.

White, J. P., J. W. Baynes, et al. (2011). "The regulation of skeletal muscle protein turnover during the progression of cancer cachexia in the Apc(Min/+) mouse." PLoS One **6**(9): e24650.

Williamson, C. L., E. R. Dabkowski, et al. (2010). "Enhanced apoptotic propensity in diabetic cardiac mitochondria: influence of subcellular spatial location." Am J Physiol Heart Circ Physiol **298**(2): H633-642.

Yaffe, M. P. (1999). "The machinery of mitochondrial inheritance and behavior." Science **283**(5407): 1493-1497.

Yakovlev, V. A. and R. B. Mikkelsen (2010). "Protein tyrosine nitration in cellular signal transduction pathways." J Recept Signal Transduct Res **30**(6): 420-429.

Yan, L., H. Ge, et al. (2004). "Gender-specific proteomic alterations in glycolytic and mitochondrial pathways in aging monkey hearts." J Mol Cell Cardiol **37**(5): 921-929.

Yang, H., T. Yang, et al. (2007). "Nutrient-sensitive mitochondrial NAD+ levels dictate cell survival." Cell **130**(6): 1095-1107.

Yarian, C. S., D. Toroser, et al. (2006). "Aconitase is the main functional target of aging in the citric acid cycle of kidney mitochondria from mice." Mech Ageing Dev **127**(1): 79-84.

Ye, G., N. S. Metreveli, et al. (2004). "Catalase protects cardiomyocyte function in models of type 1 and type 2 diabetes." Diabetes **53**(5): 1336-1343.

Zeviani, M. and S. Di Donato (2004). "Mitochondrial disorders." Brain **127**(Pt 10): 2153-2172.

Zhang, J., A. Lin, et al. (2012). "Perspectives on: SGP symposium on mitochondrial physiology and medicine: mitochondrial proteome design: from molecular identity to pathophysiological regulation." J Gen Physiol **139**(6): 395-406.

Zhao, J., J. J. Brault, et al. (2007). "FoxO3 coordinately activates protein degradation by the autophagic/lysosomal and proteasomal pathways in atrophying muscle cells." Cell Metab **6**(6): 472-483.

Zhao, Q., J. Wang, et al. (2002). "A mitochondrial specific stress response in mammalian cells." EMBO J **21**(17): 4411-4419.

Zhao, X., I. R. Leon, et al. (2011). "Phosphoproteome analysis of functional mitochondria isolated from resting human muscle reveals extensive phosphorylation of inner membrane protein complexes and enzymes." Mol Cell Proteomics **10**(1): M110 000299.

Zick, M., R. Rabl, et al. (2009). "Cristae formation-linking ultrastructure and function of mitochondria." Biochim Biophys Acta **1793**(1): 5-19.

APPENDIX- SUPPLEMENTARY DATA

REVIEW - UNRAVELING THE PHOSPHOPROTEOME DYNAMICS IN MAMMAL MITOCHONDRIAL FROM A NETWORK PERSPECTIVE

Support information is available free of charge via the internet at http://pubs.acs.org/doi/pdf/10.1021/pr4003917.

STUDY I – EFFECT OF LIFESTYLE ON AGE-RELATED MITOCHONDRIAL PROTEIN OXIDATION IN MICE CARDIAC MUSCLE

Supplementary Table S1: Proteins identified in bands reactive for anti-DNP (grey lines) and anti-3-NT (white lines) antibodies by SDS-PAGE and Western blots analysis in whole heart and in mitochondria. (Y - young mice; A - old active mice; S - old sedentary mice).

Band No.	Experimental groups detected			Protein name	UNIPROT Accession no./Entry name			Protein MW	Protein pI	Peptide count	% coverage		Functional cluster
	Y	A	S	Peptide sequence	Modification	Start sequence	End sequence	dMass (ppm)	Prec MW	Theor MW	Conf %	Conf	
1	x	x	x	Very long-chain specific acyl-CoA dehydrogenase	P50544|ACADV_MOUSE			70875,50	8,91	22	42,4		Metabolism
				ELGAFGLQVPSELGGLGLSNTQYAR	Glu->pyro-Glu@N-term	139	163	-6	2558,33	2558,31	99	2	
				NPFGNVGLL**M**GEAGK	Oxidation(M)@10	494	508	0	1518,75	1518,75	99	2	
				EN**M**ASLQSSPQHQELFR	Oxidation(M)@3	617	633	0	2016,93	2016,93	99	1	
				SFAVG**M**FK	Oxidation(M)@6	73	80	-8	901,44	901,44	99	2	
				VASGQALAAF**C**L**T**EPSSGSDVASIR	Trioxidation(C)@11; Thr->Glu@13	206	230	-5	2512,19	2512,18	99	1	
				ATP synthase subunit alpha, mitochondrial	Q03265|ATPA_MOUSE				9,22	19	43,9		OXPHOS
				QGQYSP**M**AIEEQVAVIYAGVR	Gln->pyro-Glu@N-term; Oxidation(M)@7	473	493	1	2307,12	2307,12	99	2	
				EAYPGDVFYLHSR	Glu->pyro-Glu@N-term	335	347	0	1534,72	1534,72	99	2	
				Trifunctional enzyme subunit alpha, mitochondrial	Q8BMS1|ECHA_MOUSE			82669,85	9,24	13	36,3		Metabolism
				SPKPVVAAISGSCLGGGLELAIACQYR	Cys->Dha(C)@13; Dioxidation(C)@24	133	159	7	2657,37	2657,38	99	2	
				Electron transfer flavoprotein-ubiquinone oxidoreductase, mitochondrial	Q921G7|ETFD_MOUSE			68090,93	7,34	11	28,6		Metabolism
				LQINAQN**C**VH**C**K	Dioxidation(C)@8; Cys->Dha(C)@11	578	589	15	1367,64	1367,66	99	1	
				IPVPILPGLP**M**NNHGNYIVR	Oxidation(M)@11	155	174	1	2229,21	2229,21	99	1	
				Long-chain-fatty-acid--CoA ligase 1	P41216|ACSL1_MOUSE			77923,44	6,81	9	29,8		Metabolism
				VKPKPPEPEDLAII**C**FTSGTTGNPK	Propionamide(C)@15	261	285	0	2709,40	2709,40	99	2	
				Sarcalumenin	Q7TQ48|SRCA_MOUSE			99183,99	4,39	10	15,8		Signal transduction
				VYVSSF**W**PQDYKPDTHR	Dioxidation(W)@7	725	741	5	2155,98	2156,00	99	2	
				YQLYTGAEPTTSEFTVL**M**HGPK	Oxidation(M)@18	558	579	-10	2485,21	2485,18	99	1	
				TL**M**LNEDKPADDYSAVLQR	Oxidation(M)@3	478	496	-2	2194,06	2194,06	99	2	

Dihydrolipoyl dehydrogenase, mitochondrial	O08749|DLDH_MOUSE			54272,35	7,99	8	23,8		Metabolism
VVHV**N**GFGK	Deamidated(N)@5	147	155	0	956,51	956,51	99	1	
ALLNNSHYYH**M**AHGK	Oxidation(M)@11	90	104	4	1770,82	1770,83	99	2	
IPNIYAIGDVVAGP**M**LAHK	Oxidation(M)@15	347	365	2	1994,06	1994,07	99	1	
Delta-1-pyrroline-5-carboxylate dehydrogenase, mitochondrial	Q8CHT0|AL4A1_MOUSE			61810,52	8,58	5	16,9		Metabolism
V**A**NEPILAFSQGSPER	Ala->Thr@2	31	46	0	1743,88	1743,88	99	2	
ADP/ATP translocase 1	P48962|ADT1_MOUSE			32883,1	9,73	4	13,4		Transport
EQGFLSF**W**R	Dioxidation(W)@8	64	72	-1	1200,56	1200,56	99	1	
Cytochrome c1, heme protein, mitochondrial	Q9D0M3|CY1_MOUSE			35327,64	9,24	3	39,7		OXPHOS
AANNGALPPDLSYIVR	Deamidated(N)@4	187	202	-3	1670,87	1670,86	99	1	
Methylmalonate-semialdehyde dehydrogenase [acylating], mitochondrial	Q9EQ20|MMSA_MOUSE			57915,63	8,28	3	16,1		Metabolism
IVND**N**PYGNGTAIFTTNGATAR	Deamidated(N)@5	437	458	-3	2267,09	2267,08	99	2	
Dihydrolipoyllysine-residue acetyltransferase component of pyruvate dehydrogenase complex, mitochondrial	Q8BMF4|ODP2_MOUSE			58778,08	5,70	2	10,8		Metabolism
AAPAAAAA**M**APPGPR	Oxidation(M)@9	392	406	1	1334,68	1334,68	99	2	
Cytochrome b-c1 complex subunit 2, mitochondrial	Q9DB77|QCR2_MOUSE			48234,90	9,26	2	12,6		OXPHOS
LP**N**GLVIASLENYAPLSR	Deamidated(N)@3	43	60	24	1927,00	1927,04	99	1	
Calsequestrin-2 OS	O09161|CASQ2_MOUSE			48197,24	4,12	3	8,4		Signal transduction
S**H**PDGYEFLEILK	His->Asp@2	277	289	3	1524,73	1524,73	99	1	
60 kDa heat shock protein, mitochondrial	P63038|CH60_MOUSE			60955,49	5,91	8	23,0		Protein binding/folding
Cytochrome b-c1 complex subunit 1, mitochondrial	Q9CZ13|QCR1_MOUSE			52768,7	5,75	3	18,8		OXPHOS
ATP synthase subunit beta, mitochondrial	P56480|ATPB_MOUSE			55262,41	5,24	20	48,4		OXPHOS
Aconitate hydratase, mitochondrial	Q99KI0|ACON_MOUSE			85463,51	8,08	7	22,8		Metabolism
Acyl-CoA dehydrogenase family member 9, mitochondrial	Q8JZN5|ACAD9_MOUSE			68707,15	7,96	4	7,4		Metabolism
Aldehyde dehydrogenase, mitochondrial	P47738|ALDH2_MOUSE			56537,54	7,53	2	11,8		Metabolism
Amine oxidase [flavin-containing]	Q8BW75|AOFB_MOUSE			58412,55	5,82	3	10,2		Metabolism
Aspartate aminotransferase, mitochondrial	P05202|AATM_MOUSE			44579,04	8,97	1	7,9		Metabolism

	Calcium-binding mitochondrial carrier protein Aralar	Q8BH59|CMC1_MOUSE	74569,62	8,43	1	3,8	Transport
	Calreticulin	P14211|CALR_MOUSE	47994,52	4,33	1	11,8	Protein binding/folding
	Carnitine O-acetyltransferase	P47934|CACP_MOUSE	70839,71	8,63	4	8,9	Metabolism
	Carnitine O-palmitoyltransferase 2, mitochondrial	P52825|CPT2_MOUSE	73927,48	8,46	5	16,1	Metabolism
	Catalase	24270|CATA_MOUSE	59765,29	7,72	4	18,0	Redox
	Citrate synthase, mitochondrial	Q9CZU6|CISY_MOUSE	51736,67	8,72	2	8,2	Metabolism
	Creatine kinase S-type, mitochondrial	Q6P8J7|KCRS_MOUSE	47473,32	8,64	7	23,6	Signal transduction
	Cytochrome c, somatic	P62897|CYC_MOUSE	11605,44	9,61	4	10,5	OXPHOS
	Dihydrolipoyllysine-residue succinyltransferase component of 2-oxoglutarate dehydrogenase complex, mitochondrial	Q9D2G2|ODO2_MOUSE	48994,52	9,10	2	10,8	Metabolism
	Electron transfer flavoprotein subunit beta	Q9DCW4|ETFB_MOUSE	27623,29	8,25	1	4,7	Metabolism
	Glycerol-3-phosphate dehydrogenase, mitochondrial	Q64521|GPDM_MOUSE	80953,74	6,17	1	6,3	Metabolism
	Hydroxyacyl-coenzyme A dehydrogenase, mitochondrial	Q61425|HCDH_MOUSE	34463,87	8,76	1	3,5	Metabolism
	Isocitrate dehydrogenase [NADP], mitochondrial	P54071|IDHP_MOUSE	50906,18	8,88	1	7,1	Metabolism
	Long-chain specific acyl-CoA dehydrogenase, mitochondrial	P51174|ACADL_MOUSE	47907,95	8,53	1	3,0	Metabolism
	Mitochondrial inner membrane protein	Q8CAQ8|IMMT_MOUSE	83900,08	6,18	3	8,3	Signal transduction
	Myosin-7	Q91Z83|MYH7_MOUSE	222878,85	5,59	1	4,1	Structure
	NADH dehydrogenase [ubiquinone] 1 alpha subcomplex subunit 10, mitochondrial	Q99LC3|NDUAA_MOUSE	40603,43	7,63	1	2,8	OXPHOS
	NADH dehydrogenase [ubiquinone] flavoprotein 1, mitochondrial	Q91YT0|NDUV1_MOUSE	50834,20	8,51	3	24,1	OXPHOS
	NADH dehydrogenase [ubiquinone] iron-sulfur protein 2, mitochondrial	Q91WD5|NDUS2_MOUSE	52625,66	6,52	4	25,1	OXPHOS
	NADH-ubiquinone oxidoreductase 75 kDa subunit, mitochondrial	Q91VD9|NDUS1_MOUSE	79748,74	5,51	3	12,1	OXPHOS
	Propionyl-CoA carboxylase beta chain, mitochondrial	Q99MN9|PCCB_MOUSE	58394,00	7,19	1	3,3	Metabolism
	Protein disulfide-isomerase A3	P27773|PDIA3_MOUSE	56678,37	5,88	8	22,4	Redox
	Protein NipSnap homolog 2	O55126|NIPS2_MOUSE	32932,73	9,31	1	8,9	unknown
	Pyruvate kinase isozymes	P52480|KPYM_MOUSE	57844,89	7,17	5	17,3	Metabolism
	Serine protease inhibitor A3M	Q03734|SPA3M_MOUSE	47004,04	5,35	1	6,7	Signal transduction

	Sodium/potassium-transporting ATPase subunit beta-1	P14094|AT1B1_MOUSE				35194,56	8,83	4	16,1		Transport
	Sorting and assembly machinery component 50 homolog	Q8BGH2|SAM50_MOUSE				51863,97	6,34	4	16,0		Signal transduction
	Stress-70 protein, mitochondrial	P38647|GRP75_MOUSE				73528,33	5,91	2	8,1		Protein binding/folding
	Succinate dehydrogenase [ubiquinone] flavoprotein subunit, mitochondrial	Q8K2B3|DHSA_MOUSE				72585,40	7,06	7	15,7		OXPHOS
	Succinyl-CoA:3-ketoacid-coenzyme A transferase 1, mitochondrial	Q9D0K2|SCOT1_MOUSE				55988,57	8,73	6	22,7		Metabolism
	Tripartite motif-containing protein 72	Q1XH17|TRI72_MOUSE				52816,76	6,01	1	3,6		Transport
	Voltage-dependent anion-selective channel protein 1	Q60932|VDAC1_MOUSE				32351,49	8,55	1	3,7		Transport
	Voltage-dependent anion-selective channel protein 2	Q60930|VDAC2_MOUSE				31732,84	7,44	1	2,7		Transport
2 x x x	ATP synthase subunit beta, mitochondrial	P56480|ATPB_MOUSE				55262,41	5,24	25	52,6		
	TIA**M**DGTEGLVR	Oxidation(M)@4		110	121	1	1277,63	1277,63	99	1	OXPHOS
	VALVYGQ**M**NEPPGAR	Oxidation(M)@8		265	279	1	1616,80	1616,80	99	1	
	Creatine kinase S-type, mitochondrial	Q6P8J7|KCRS_MOUSE				47473,32	8,64	24	44,6		
	TFLI**W**INEEDHTR	Dioxidation(W)@5		258	270	4	1704,80	1704,81	99	1	
	GWEFM**W**NER	Dioxidation(W)@6		302	310	1	1285,52	1285,52	99	1	
	LGYILT**C**PSNLGTGLR	Propionamide(C)@7		311	326	5	1747,92	1747,93	99	1	Signal transduction
	LGYILT**C**P**SN**LGTGLR	Trioxidation(C)@7; Deamidated(N)@10	Ser->Asn@9;	311	326	-6	1752,88	1752,87	99	1	
	TFLI**W**INEEDHTR	Trp->Kynurenin(W)@5		258	270	2	1676,81	1676,82	99	1	
	Isocitrate dehydrogenase [NADP], mitochondrial	P54071|IDHP_MOUSE				50906,18	8,88	18	52,4		
	LVPG**W**TKPITIGR	Dioxidation(W)@5		160	172	3	1468,84	1468,84	99	1	Metabolism
	IKVEKPVVE**M**DGDE**M**TR	Oxidation(M)@10; Oxidation(M)@15		44	60	0	2006,96	2006,97	99	2	
	ATP synthase subunit alpha, mitochondrial	Q03265|ATPA_MOUSE				59752,60	9,22	15	43,9		
	EAYPGDVFYLHSR	Glu->pyro-Glu@N-term		335	347	2	1534,72	1534,72	99	2	OXPHOS
	NADH dehydrogenase [ubiquinone] iron-sulfur protein 2, mitochondrial	Q91WD5|NDUS2_MOUSE				52625,66	6,52	15	49,7		
	AVTN**M**TLNFGPQHPAAHGVLR	Oxidation(M)@5		76	96	0	2246,14	2246,14	99	1	OXPHOS
	IDEVEE**M**LTNNR	Oxidation(M)@7		255	266	0	1477,67	1477,67	99	1	
	Cytochrome b-c1 complex subunit 2, mitochondrial	Q9DB77|QCR2_MOUSE				48234,90	9,26	20	41,1		OXPHOS

	ITSEELHYFVQ**N**HFTSAR	Deamidated(N)@12	200	217	0	2179,03	2179,03	99	1	
	LP**N**GLVIASLENYAPLSR	Deamidated(N)@3	43	60	-2	1927,04	1927,04	99	1	
	QVAEQFLNMR	Gln->pyro-Glu@N-term	232	241	-8	1217,60	1217,59	99	1	
	S**M**AASGNLGHTPFLDEL	Oxidation(M)@2	437	453	2	1774,82	1774,82	99	1	
	KS**M**AASGNLGHTPFLDEL	Oxidation(M)@3	436	453	0	1902,91	1902,91	99	2	
	NALANPLY**C**PDYR	Propionamide(C)@9	184	196	1	1579,74	1579,75	99	2	
	3-ketoacyl-CoA thiolase, mitochondrial	Q8BWT1|THIM_MOUSE			41857,92	8,33	14	44,8		Metabolism
	AANEAGYFNEE**M**APIEVK	Oxidation(M)@12	192	209	3	1997,90	1997,90	99	1	
	Trifunctional enzyme subunit beta, mitochondrial	Q99JY0|ECHB_MOUSE			51386,34	9,43	14	32,4		
	IPFLLSGTSYKDL**M**PHDLAR	Oxidation(M)@14	63	82	-2	2289,19	2289,18	99	1	Metabolism
	LNFLSPELPA**V**AEFSTNET**M**GHSADR	Val->Tyr@11; Dethiomethyl(M)@20	205	230	-5	2848,34	2848,33	99	1	
	Cytochrome b-c1 complex subunit 1, mitochondrial	Q9CZ13|QCR1_MOUSE			52768,70	5,75	16	45,2		
	QSVPETQVSILDNGLR	Gln->pyro-Glu@N-term	43	58	2	1737,89	1737,89	99	2	OXPHOS
	EVESIGAHLNAYSTR	Glu->pyro-Glu@N-term	112	126	2	1627,79	1627,80	99	2	
	Medium-chain specific acyl-CoA dehydrogenase, mitochondrial	P45952|ACADM_MOUSE			46481,22	8,60	12	36,6		
	AN**W**YFLLAR	Dioxidation(W)@3	198	206	2	1184,60	1184,60	99	1	Metabolism
	AN**W**YFLLAR	Trp->Kynurenin(W)@3	198	206	-8	1156,61	1156,60	99	1	
	Aspartate aminotransferase, mitochondrial	P05202|AATM_MOUSE			44579,04	8,97	12	29,3		
	ILIRPLYS**N**PPLNGAR	Deamidated(N)@13	310	325	-3	1794,02	1794,02	99	1	Metabolism
	DAG**M**QLQGYR	Oxidation(M)@4	171	180	-2	1153,52	1153,52	99	1	
	NADH dehydrogenase [ubiquinone] 1 alpha subcomplex subunit 10, mitochondrial	Q99LC3|NDUAA_MOUSE			40603,43	7,63	10	29,9		
	LQS**W**LYASR	Dioxidation(W)@4	131	139	1	1154,57	1154,57	99	2	OXPHOS
	QDDWTFHYLR	Gln->pyro-Glu@N-term	286	295	-3	1362,60	1362,60	99	2	
	Acetyl-CoA acetyltransferase, mitochondrial	Q8QZT1|THIL_MOUSE			44816,12	8,71	7	28,1		Metabolism
	EVY**M**GNVIQGGEGQAPTR	Oxidation(M)@4	85	102	1	1920,90	1920,90	99	1	
	Fumarate hydratase, mitochondrial	P97807|FUMH_MOUSE			54370,60	9,12	5	13,4		Metabolism
	MPIPVIQAFGILK	Oxidation(M)@1	85	97	1	1441,83	1441,84	99	2	

	Long-chain specific acyl-CoA dehydrogenase, mitochondrial	P51174|ACADL_MOUSE			47907,95	8,53		6	21,6		Metabolism
	SPAHGISLFLVENG**M**K	Oxidation(M)@15	225	240	4	1714,86	1714,87		99	1	
	ADP/ATP translocase 1	P48962|ADT1_MOUSE			32904,27	9,73		5	22,8		
	EQGFLSF**W**R	Dioxidation(W)@8	64	72	-3	1200,56	1200,56		99	1	Transport
	G**M**GGAFVLVLYDEIKK	Oxidation(M)@2	281	296	0	1754,93	1754,93		99	1	
	Calsequestrin-2	O09161|CASQ2_MOUSE			48197,24	4,12		2	6,5		Protein binding/folding
	S**H**PDGYEFLEILK	His->Asp@2	277	289	1	1524,73	1524,73		99	1	
	Aconitate hydratase, mitochondrial	Q99KI0|ACON_MOUSE			85463,51	8,08		8	25		Metabolism
	Citrate synthase, mitochondrial	Q9CZU6|CISY_MOUSE			51736,67	8,72		9	26,1		Metabolism
	NADH dehydrogenase [ubiquinone] flavoprotein 1, mitochondrial	Q91YT0|NDUV1_MOUSE			50834,20	8,51		7	35,1		OXPHOS
	Actin, alpha cardiac muscle 1	P68033|ACTC_MOUSE			42018,97	5,23		5	29,4		Structure
	Sarcalumenin	Q7TQ48|SRCA_MOUSE			99183,99	4,39		4	12,6		Signal transduction
	Sodium/potassium-transporting ATPase subunit beta-1	P14094|AT1B1_MOUSE			35194,56	8,83		4	18,4		Transport
	Aspartate aminotransferase, cytoplasmic	P05201|AATC_MOUSE			46100,39	6,75		5	19,9		Metabolism
	Very long-chain specific acyl-CoA dehydrogenase, mitochondrial	P50544|ACADV_MOUSE			70875,50	8,91		4	8,1		Metabolism
	Succinate dehydrogenase [ubiquinone] flavoprotein subunit, mitochondrial	Q8K2B3|DHSA_MOUSE			72585,40	7,06		3	14		OXPHOS
	Alpha-sarcoglycan	P82350|SGCA_MOUSE			43286,87	6,00		3	18,1		Structure
	Creatine kinase M-type	P07310|KCRM_MOUSE			43044,97	6,58		3	16		Signal transduction
	Tripartite motif-containing protein 72	Q1XH17|TRI72_MOUSE			52816,76	6,01		3	28,3		Transport
	Fructose-bisphosphate aldolase A	P05064|ALDOA_MOUSE			39224,74	8,40		3	14,6		Metabolism
	Succinate dehydrogenase [ubiquinone] iron-sulfur subunit, mitochondrial	Q9CQA3|DHSB_MOUSE			31813,90	8,96		3	23,8		OXPHOS
	Cytochrome c1, heme protein, mitochondrial	Q9D0M3|CY1_MOUSE			35327,64	9,24		3	24		OXPHOS
	Pyruvate dehydrogenase E1 component subunit alpha, somatic form, mitochondrial	P35486|ODPA_MOUSE			43231,63	8,49		2	21,3		Metabolism
	78 kDa glucose-regulated protein	P20029|GRP78_MOUSE			72422,06	5,07		2	11,3		Protein binding/folding
	Stress-70 protein, mitochondrial	P38647|GRP75_MOUSE			73528,33	5,91		2	15,3		Protein binding/folding
	Malate dehydrogenase, mitochondrial	P08249|MDHM_MOUSE			35611,45	8,93		2	30,5		Metabolism

Elongation factor Tu, mitochondrial	Q8BFR5|EFTU_MOUSE	49508,35	7,23	3	10,4	DNA/RNA/Protein biosynthesis
NADH dehydrogenase [ubiquinone] flavoprotein 2, mitochondrial	Q9D6J6|NDUV2_MOUSE	27285,34	7,00	2	25,4	OXPHOS
NADH dehydrogenase [ubiquinone] iron-sulfur protein 3, mitochondrial	Q9DCT2|NDUS3_MOUSE	30149,33	6,67	2	9,1	OXPHOS
Heat shock cognate 71 kDa protein	P63017|HSP7C_MOUSE	70739,87	5,37	2	13,2	Protein binding/folding
Isocitrate dehydrogenase [NAD] subunit alpha, mitochondrial	Q9D6R2|IDH3A_MOUSE	39638,71	6,27	2	4,9	Metabolism
NADH dehydrogenase [ubiquinone] 1 alpha subcomplex subunit 9, mitochondrial	Q9DC69|NDUA9_MOUSE	42509,15	9,75	2	8,5	OXPHOS
Protein NipSnap homolog 2	O55126|NIPS2_MOUSE	32932,73	9,31	2	24,6	unknown
Acyl-coenzyme A thioesterase 2, mitochondrial	Q9QYR9|ACOT2_MOUSE	49652,02	6,91	2	7,9	Metabolism
Mitochondrial inner membrane protein	Q8CAQ8|IMMT_MOUSE	83900,08	6,18	2	5,7	Signal transduction
ATP synthase subunit d, mitochondrial	Q9DCX2|ATP5H_MOUSE	18749,45	5,52	1	31,1	OXPHOS
Sorting and assembly machinery component 50 homolog	Q8BGH2|SAM50_MOUSE	51863,97	6,34	2	14,5	Protein binding/folding
Myosin light chain 3	P09542|MYL3_MOUSE	22421,56	5,03	1	17,2	Structure
Electron transfer flavoprotein-ubiquinone oxidoreductase, mitochondrial	Q921G7|ETFD_MOUSE	68090,93	7,34	1	5	Metabolism
Acyl-CoA dehydrogenase family member 10	Q8K370|ACD10_MOUSE	118979,21	8,49	1	6,9	Metabolism
Short-chain specific acyl-CoA dehydrogenase, mitochondrial	Q07417|ACADS_MOUSE	44946,70	8,96	1	8,7	Metabolism
Alpha-enolase	P17182|ENOA_MOUSE	47009,63	6,36	1	9,7	Metabolism
Superoxide dismutase [Mn], mitochondrial	P09671|SODM_MOUSE	24602,93	8,80	1	10,4	Redox
Voltage-dependent anion-selective channel protein 1	Q60932|VDAC1_MOUSE	32351,49	8,55	1	3,7	Transport
Cytochrome c, somatic	P62897|CYC_MOUSE	11605,44	9,61	1	10,5	OXPHOS
Electron transfer flavoprotein subunit beta	Q9DCW4|ETFB_MOUSE	27623,29	8,25	1	22	Metabolism
Phosphate carrier protein, mitochondrial	Q8VEM8|MPCP_MOUSE	34843,84	9,11	1	9,5	Transport
Long-chain-fatty-acid--CoA ligase 1	P41216|ACSL1_MOUSE	77923,44	6,81	1	1,7	Metabolism
Phosphoglycerate kinase 1	P09411|PGK1_MOUSE	44419,28	8,02	1	5,5	Metabolism
Cytochrome c oxidase subunit 2	P00405|COX2_MOUSE	25976,40	4,60	1	4,4	OXPHOS
Protein NDRG2	Q9QYG0|NDRG2_MOUSE	40658,01	5,24	1	9,4	Signal transduction

	Cathepsin D	P18242|CATD_MOUSE			38007,47	5,63	1	6,6		Proteolysis
	Actin, cytoplasmic 2	P63260|ACTG_MOUSE			41792,84	5,31	5	26,1		Structure
3 _ x x	Creatine kinase S-type, mitochondrial	Q6P8J7|KCRS_MOUSE			47473,32	8,64	20	56,8		
	GWEF**M**WNER	Dioxidation(M)@5	302	310	6	1285,51	1285,519	99	1	Signal transduction
	TFLI**W**INEEDHTR	Dioxidation(W)@5	258	270	5	1704,80	1704,811	99	1	
	TFLI**W**INEEDHTR	Trp->Kynurenin(W)@5	258	270	1	1676,81	1676,816	99	1	
	Cytochrome b-c1 complex subunit 2, mitochondrial	Q9DB77|QCR2_MOUSE			48234,90	9,26	17	40,4		
	ITSEELHYFVQ**N**HFTSAR	Deamidated(N)@12	200	217	3	2179,03	2179,03	99	1	
	LP**N**GLVIASLENYAPLSR	Deamidated(N)@3	43	60	4	1927,03	1927,04	99	1	OXPHOS
	NALANPLY**C**P**D**YR	Dioxidation(C)@9; Carboxy(D)@11	184	196	-7	1584,70	1584,69	99	1	
	S**M**AASGNLGHTPFLDEL	Oxidation(M)@2	437	453	3	1774,81	1774,82	99	1	
	KS**M**AASGNLGHTPFLDEL	Oxidation(M)@3	436	453	2	1902,91	1902,91	99	2	
	Cytochrome b-c1 complex subunit 1, mitochondrial	Q9CZ13|QCR1_MOUSE			52768,70	5,75	16	37,7		
	N**N**GAGYFLEHLAFK	Deamidated(N)@2	86	99	4	1580,76	1580,76	99	1	
	YETEKN**N**GAGYFLEHLAFK	Deamidated(N)@7	81	99	-7	2231,07	2231,05	99	1	OXPHOS
	QSVPETQVSILDNGLR	Gln->pyro-Glu@N-term	43	58	4	1737,88	1737,89	99	1	
	DIC**S**KYFYDQ**C**PAVAGYGPIEQLPDYNR	Ser->Ala@4; Dioxidation(C)@11	443	470	-2	3240,46	3240,45	99	1	
	NADH dehydrogenase [ubiquinone] 1 alpha subcomplex subunit 10	Q99LC3|NDUAA_MOUSE			40603,43	7,63	13	45,9		
	LQS**W**LYASR	Dioxidation(W)@4	131	139	5	1154,57	1154,57	99	1	OXPHOS
	QDDWTFHYLR	Gln->pyro-Glu@N-term	286	295	4	1362,59	1362,60	99	2	
	Aspartate aminotransferase, mitochondrial	P05202|AATM_MOUSE			44579,04	8,97	12	43,5		
	HFIEQGINV**C**L**C**QSYAK	Cys->Dha(C)@10; Dioxidation(C)@12	263	279	15	1949,90	1949,93	99	1	Metabolism
	NADH dehydrogenase [ubiquinone] iron-sulfur protein 2, mitochondrial	Q91WD5|NDUS2_MOUSE			52625,66	6,52	10	37,4		
	AVTN**M**TLNFGPQHPAAHGVLR	Oxidation(M)@5	76	96	1	2246,14	2246,14	99	1	OXPHOS
	Trifunctional enzyme subunit beta, mitochondrial	Q99JY0|ECHB_MOUSE			51386,34	9,43	11	26,3		
	LNFLSPELPAVAEFSTNET**M**GHSADR	Oxidation(M)@20	205	230	-5	2848,35	2848,33	99	1	Metabolism
	3-ketoacyl-CoA thiolase, mitochondrial	Q8BWT1|THIM_MOUSE			41857,92	8,33	10	33,3		Metabolism

	AANEAGYFNEE**M**APIEVK	Oxidation(M)@12	192	209	2	1997,90	1997,90	99	1	
	VPPETIDSVIVGNV**M**QSSSDAAYLAR	Oxidation(M)@15	46	71	-12	2734,38	2734,35	99	1	
	Fructose-bisphosphate aldolase A	P05064|ALDOA_MOUSE			39224,74	8,40	10	29,1		
	IGEHTPSALAI**M**ENANVLAR	Oxidation(M)@12	154	173	-1	2122,09	2122,08	99	1	Metabolism
	GVVPLAG**TN**GETTTQGLDGLSER	Thr->Pro@8; Deamidated(N)@9	112	134	-2	2268,13	2268,12	99	1	
	Actin, alpha cardiac muscle 1	P68033|ACTC_MOUSE			42018,97	5,23	7	42,4		
	QEYDEAGPSIVHR	Gln->pyro-Glu@N-term	362	374	9	1482,66	1482,67	99	1	Structure
	Isocitrate dehydrogenase [NAD] subunit alpha, mitochondrial	Q9D6R2|IDH3A_MOUSE			39638,71	6,27	7	26,2		
	H**M**GLFDHAAK	Oxidation(M)@2	317	326	7	1141,53	1141,53	99	2	Metabolism
	APIQ**W**EER	Dioxidation(W)@5	59	66	8	1059,49	1059,50	99	1	
	Malate dehydrogenase, mitochondrial	P08249|MDHM_MOUSE			35611,45	8,93	6	38,2		
	GYLGPEQLPD**C**LKG**C**DVVVIPAGVPR	Dehydro(C)@11; Dehydro(C)@15	79	104	1	2692,37	2692,37	99	1	Metabolism
	FVFSLVDA**M**NGK	Oxidation(M)@9	258	269	3	1342,66	1342,66	99	2	
	ADP/ATP translocase 1	P48962|ADT1_MOUSE			32904,27	9,73	9	31,5		
	EQGFLSFWR	Glu->pyro-Glu@N-term	64	72	8	1150,55	1150,56	99	1	
	G**M**GGAFVLVLYDEIKK	Oxidation(M)@2	281	296	1	1754,93	1754,93	99	2	Transport
	EQGFLSF**W**R	Trp->Kynurenin(W)@8	64	72	-4	1172,57	1172,56	99	1	
	Succinate dehydrogenase [ubiquinone] flavoprotein subunit, mitochondrial	Q8K2B3|DHSA_MOUSE			72585,4	7,06	5	16,1		
	HV**N**GQDQIVPGLYACGEAA**C**ASVHGANR	Deamidated(N)@3; Cys->Thr@20	424	451	7	2835,32	2835,34	99	1	OXPHOS
	Voltage-dependent anion-selective channel protein 1	Q60932|VDAC1_MOUSE			32351,49	8,55	5	37,8		
	KLETAVNL**A**WTAGNSNTR	Ala->Cys@9	214	231	-4	1976,98	1976,97	99	1	Transport
	Cytochrome c oxidase subunit 2	P00405|COX2_MOUSE			25976,4	4,60	5	23,4		
	MLISSEDVLHS**W**AVPSLGLK	Dioxidation(W)@12	152	171	4	2213,13	2213,14	99	1	OXPHOS
	ILYM**M**DEINNPVLTVK	Oxidation(M)@5	83	98	5	1907,96	1907,97	99	2	
	Isocitrate dehydrogenase [NADP], mitochondria	P54071|IDHP_MOUSE			50906,18	8,88	13	44		Metabolism
	ATP synthase subunit alpha, mitochondrial	Q03265|ATPA_MOUSE			59752,60	9,22	10	36		OXPHOS
	ATP synthase subunit beta, mitochondrial	P56480|ATPB_MOUSE			55262,41	5,24	21	47,1		OXPHOS

Aconitate hydratase, mitochondrial	Q99KI0|ACON_MOUSE	85463,51	8,08	9	18,2	Metabolism
NADH dehydrogenase [ubiquinone] flavoprotein 1, mitochondrial	Q91YT0|NDUV1_MOUSE	50834,20	8,51	6	23,7	OXPHOS
NADH dehydrogenase [ubiquinone] 1 alpha subcomplex subunit 9, mitochondrial	Q9DC69|NDUA9_MOUSE	42509,15	9,75	5	28,4	OXPHOS
Acetyl-CoA acetyltransferase, mitochondrial	Q8QZT1|THIL_MOUSE	44816,12	8,71	6	26,9	Metabolism
Citrate synthase, mitochondrial	Q9CZU6|CISY_MOUSE	51736,67	8,72	5	14	Metabolism
Medium-chain specific acyl-CoA dehydrogenase, mitochondrial	P45952|ACADM_MOUSE	46481,22	8,60	6	18,3	Metabolism
NADH dehydrogenase [ubiquinone] iron-sulfur protein 3, mitochondrial	Q9DCT2|NDUS3_MOUSE	30149,33	6,67	4	29,7	OXPHOS
Creatine kinase M-type	P07310|KCRM_MOUSE	43044,97	6,58	4	17,1	Signal transduction
Myosin light chain 3	P09542|MYL3_MOUSE	22421,56	5,03	3	30,4	Structure
Succinate dehydrogenase [ubiquinone] iron-sulfur subunit, mitochondrial	Q9CQA3|DHSB_MOUSE	31813,90	8,96	4	28,7	OXPHOS
Myosin-6 OS=Mus musculus	Q02566|MYH6_MOUSE	223565,34	5,57	3	8,8	Structure
Aspartate aminotransferase, cytoplasmic	P05201|AATC_MOUSE	46100,39	6,75	4	22	Metabolism
Long-chain specific acyl-CoA dehydrogenase, mitochondrial	P51174|ACADL_MOUSE	47907,95	8,53	3	16,3	Metabolism
Succinyl-CoA ligase [GDP-forming] subunit alpha, mitochondrial	Q9WUM5|SUCA_MOUSE	36154,76	9,46	3	12,4	Metabolism
ATP synthase subunit d, mitochondrial	Q9DCX2|ATP5H_MOUSE	18749,45	5,52	3	24,2	OXPHOS
Cytochrome c1, heme protein, mitochondrial	Q9D0M3|CY1_MOUSE	35327,64	9,24	4	27,1	OXPHOS
NADH dehydrogenase [ubiquinone] flavoprotein 2, mitochondrial	Q9D6J6|NDUV2_MOUSE	27285,34	7,00	3	30,7	OXPHOS
3-hydroxyisobutyryl-CoA hydrolase, mitochondrial	Q8QZS1|HIBCH_MOUSE	39239,12	6,24	2	9,9	Metabolism
Short-chain specific acyl-CoA dehydrogenase, mitochondrial	Q07417|ACADS_MOUSE	44946,70	8,96	2	12,1	Metabolism
Very long-chain specific acyl-CoA dehydrogenase, mitochondrial	P50544|ACADV_MOUSE	70875,50	8,91	2	8,7	Metabolism
Superoxide dismutase [Mn], mitochondrial	P09671|SODM_MOUSE	24602,93	8,80	2	22,5	Redox
Electron transfer flavoprotein subunit beta	Q9DCW4|ETFB_MOUSE	27623,29	8,25	2	12,9	Metabolism
Calcium-binding mitochondrial carrier protein Aralar1	Q8BH59|CMC1_MOUSE	74569,62	8,43	2	4	Protein binding/folding
Pyruvate dehydrogenase E1 component subunit alpha, somatic form, mitochondrial	P35486|ODPA_MOUSE	43231,63	8,49	2	15,4	Metabolism
Protein NipSnap homolog 2	O55126|NIPS2_MOUSE	32932,73	9,31	2	15,7	unknown

Cytochrome c oxidase subunit 4 isoform 1, mitochondrial	P19783|COX41_MOUSE	19530,46	9,25	2	19,5	OXPHOS
Hydroxyacyl-coenzyme A dehydrogenase, mitochondrial	Q61425|HCDH_MOUSE	34463,87	8,76	2	6,1	Metabolism
Sarcalumenin	Q7TQ48|SRCA_MOUSE	99183,99	4,39	1	14,3	Signal transduction
Voltage-dependent anion-selective channel protein 2	Q60930|VDAC2_MOUSE	31732,84	7,44	2	15,9	Transport
NADH dehydrogenase [ubiquinone] iron-sulfur protein 7, mitochondrial	Q9DC70|NDUS7_MOUSE	24682,87	9,94	1	8	OXPHOS
Malate dehydrogenase, cytoplasmic	P14152|MDHC_MOUSE	36379,97	6,16	1	9	Metabolism
Mitochondrial inner membrane protein	Q8CAQ8|IMMT_MOUSE	83900,08	6,18	1	3,4	Signal transduction
Alpha-sarcoglycan	P82350|SGCA_MOUSE	43286,87	3,00	1	11,4	Structure
D-beta-hydroxybutyrate dehydrogenase, mitochondrial	Q80XN0|BDH_MOUSE	38284,97	9,14	1	9,9	Metabolism
NADH dehydrogenase [ubiquinone] 1 alpha subcomplex subunit 12	Q7TMF3|NDUAC_MOUSE	17086,41	9,38	1	8,3	OXPHOS
NADH dehydrogenase [ubiquinone] 1 alpha subcomplex subunit 4	Q62425|NDUA4_MOUSE	9326,79	9,52	1	14,6	OXPHOS
Cytochrome c, somatic OS=Mus musculus GN=Cycs PE=1 SV=2	P62897|CYC_MOUSE	11605,44	9,61	1	10,5	OXPHOS
Phosphate carrier protein, mitochondrial	Q8VEM8|MPCP_MOUSE	34843,84	9,11	1	3,9	Transport
Sodium/potassium-transporting ATPase subunit beta-1	P14094|AT1B1_MOUSE	35194,56	8,83	1	7,2	Transport
Isocitrate dehydrogenase [NAD] subunit gamma 1, mitochondrial	P70404|IDHG1_MOUSE	42785,44	9,17	1	2,3	Metabolism
Elongation factor Tu, mitochondrial	Q8BFR5|EFTU_MOUSE	49508,35	7,23	1	9,1	DNA/RNA/Protein biosynthesis
Protein NDRG2	Q9QYG0|NDRG2_MOUSE	40658,01	5,24	1	8,9	Signal transduction
NADH dehydrogenase [ubiquinone] iron-sulfur protein 8, mitochondrial	Q8K3J1|NDUS8_MOUSE	24038,33	5,89	1	16,5	OXPHOS
Beta-enolase	P21550|ENOB_MOUSE	46893,69	6,81	1	9,9	Metabolism
Mitochondrial 2-oxoglutarate/malate carrier protein	Q9CR62|M2OM_MOUSE	34023,71	9,95	1	8,6	Metabolism
NADH-ubiquinone oxidoreductase 75 kDa subunit, mitochondrial	Q91VD9|NDUS1_MOUSE	79748,74	5,51	1	2,6	OXPHOS
Pyruvate dehydrogenase E1 component subunit beta, mitochondrial	Q9D051|ODPB_MOUSE	35768,29	5,39	1	12,3	Metabolism
NADH dehydrogenase [ubiquinone] 1 beta subcomplex subunit 10	Q9DCS9|NDUBA_MOUSE	20892,61	8,36	1	14,2	OXPHOS
Cytochrome b-c1 complex subunit Rieske, mitochondrial	Q9CR68|UCRI_MOUSE	29367,64	8,92	1	8,8	OXPHOS

	NADH dehydrogenase [ubiquinone] 1 alpha subcomplex subunit	Q9DCJ5|NDUA8_MOUSE			19860,88	8,80	1	7,6		OXPHOS
	Cytochrome c oxidase subunit 6C	Q9CPQ1|COX6C_MOUSE			8337,81	10,13	1	38,2		OXPHOS
	Actin, cytoplasmic 2	P63260|ACTG_MOUSE			41792,84	5,31	4	29,1		Structure
4 _ x x	Cytochrome b-c1 complex subunit 1, mitochondrial	Q9CZ13|QCR1_MOUSE			52768,70	5,75	33	58,1		
	N**N**GAGYFLEHLAFK	Ammonia-loss(N)@2	86	99	10	1562,74	1562,75	99	2	
	N**N**GAGYFLEHLAFK	Deamidated(N)@2	86	99	4	1580,76	1580,76	99	1	
	IPLAE**W**ESR	Dioxidation(W)@6	424	432	12	1131,54	1131,56	99	1	
	RIPLAE**W**ESR	Dioxidation(W)@7	423	432	10	1287,64	1287,66	99	2	
	YFYD**QC**PAVAGYGPIEQLPDYNR	Gln->Arg@5; Trioxidation(C)@6	448	470	4	2754,23	2754,24	99	2	
	QSVPETQVSILDNGLR	Gln->pyro-Glu@N-term	43	58	6	1737,88	1737,89	99	2	OXPHOS
	EVESIGAHLNAYSTR	Glu->pyro-Glu@N-term	112	126	7	1627,78	1627,80	99	2	
	IQEVDAQ**M**LR	Oxidation(M)@8	433	442	13	1217,59	1217,61	99	1	
	NALVSHLDGTT**P**V**C**EDIGR	Oxidation(P)@12; Cys->Tyr@14	397	415	27	2071,96	2072,02	99	2	
	DIC**S**KYFYDQ**C**PAVAGYGPIEQLPDYNR	Ser->His@4; Cys->Dha(C)@11	443	470	5	3240,48	3240,50	99	2	
	VASEQSSHAT**CT**VGVWIDAGSR	Trioxidation(C)@11; Thr->Glu@12	59	80	-11	2336,06	2336,03	99	2	
	QS**V**PETQVSILDNGLR	Val->Ser@3	43	58	41	1742,81	1742,88	99	1	
	ATP synthase subunit beta, mitochondrial	P56480|ATPB_MOUSE			55262,41	5,24	15	49,7		
	I**M**NVIGEPIDER	Oxidation(M)@2	144	155	9	1400,68	1400,70	99	1	OXPHOS
	GFQQILAGEYDHLPEQAFY**M**VGPIEEAVAK	Oxidation(M)@20	490	519	-11	3365,67	3365,63	99	2	
	VALVYGQ**M**NEPPGAR	Oxidation(M)@8	265	279	8	1616,79	1616,80	99	2	
	ATP synthase subunit b, mitochondrial	Q9CQQ7|AT5F1_MOUSE			28948,83	9,11	14	43,4		OXPHOS
	KEEEH**M**ID**W**VEK	Oxidation(M)@6; Dioxidation(W)@9	210	221	11	1619,70	1619,71	99	2	
	Cytochrome b-c1 complex subunit Rieske	Q9CR68|UCRI_MOUSE			29367,64	8,92	13	51,5		
	AGDFGGYY**C**P**C**HGSHYDASGR	Cys->Dha(C)@9; Dioxidation(C)@11	228	248	13	2216,83	2216,86	99	2	OXPHOS
	E**I**DQEAAVEVSQLR	Glu->pyro-Glu@N-term; Methyl(I)@2	183	196	-57	1581,89	1581,80	99	2	
	Cytochrome c oxidase subunit 2	P00405|COX2_MOUSE			25976,40	4,60	21	44,1		OXPHOS
	MLISSEDVLHS**W**AVPSLGLK	Dioxidation(W)@12	152	171	7	2213,13	2213,14	99	1	

	ML**I**SSEDVLHSWAVPSLGLK	Ile->Asn@3	152	171	-9	2182,13	2182,11	99	1	
	MIPTNDLKPGELR	Oxidation(M)@1	122	134	8	1498,77	1498,78	99	1	
	MLISSEDVLHS**W**	Oxidation(M)@1; Dioxidation(W)@12	152	163	5	1463,65	1463,66	99	2	
	MLISSEDVLHSWAVPSLGLK	Oxidation(M)@1; Dioxidation(W)@12	152	171	2	2229,13	2229,14	99	1	
	ILY**MM**DEINNPVLTVK	Oxidation(M)@4; Oxidation(M)@5	83	98	7	1923,96	1923,97	99	1	
	VVLP**M**ELPIR	Oxidation(M)@5	142	151	8	1181,67	1181,68	99	1	
	NADH dehydrogenase [ubiquinone] flavoprotein 2, mitochondrial	Q9D6J6|NDUV2_MOUSE			27285,34	7,00	11	59,7		OXPHOS
	F**CC**EPAGGLTSLTEPPKGPGFGVQAGL	Cys->Dha(C)@2; Dioxidation(C)@3	222	248	-2	2630,27	2630,27	99	2	
	VAEVLQVPP**M**R	Oxidation(M)@10	100	110	10	1253,67	1253,68	99	1	
	Mitochondrial 2-oxoglutarate/malate carrier protein	Q9CR62|M2OM_MOUSE			34023,71	9,95	11	39,5		Transport
	YEGFFSL**W**K	Dioxidation(W)@8	272	280	8	1207,55	1207,55	99	2	
	EEGVPTL**W**R	Dioxidation(W)@8	174	182	10	1117,53	1117,54	99	1	
	ALIG**M**TAGATGAFVGTPAEVALIR	Oxidation(M)@5	123	146	-1	2302,24	2302,24	99	1	
	Succinate dehydrogenase [ubiquinone] iron-sulfur subunit, mitochondrial	Q9CQA3|DHSB_MOUSE			31813,90	8,96	13	42,2		OXPHOS
	WDPDKTGDKPR	Dioxidation(W)@1	49	59	6	1345,62	1345,63	99	1	
	WDPDKTGDKPR	FormaldehydeAdduct(W)@1	49	59	10	1325,62	1325,64	99	1	
	QQYLQSIEDR	Gln->pyro-Glu@N-term	170	179	6	1261,59	1261,59	99	2	
	MQTYEVDLNK	Oxidation(M)@1	60	69	10	1255,56	1255,58	99	1	
	IYPLPH**M**YVIK	Oxidation(M)@7	129	139	7	1388,74	1388,75	99	2	
	WDPDKTGDKPR	Oxidation(W)@1	49	59	10	1329,62	1329,63	99	1	
	Myosin-6	Q02566|MYH6_MOUSE			223565,34	5,57	9	8,2		Structure
	TVTIKEDQV**M**QQNPPK	Oxidation(M)@10	68	83	1	1870,94	1870,95	99	2	
	Voltage-dependent anion-selective channel protein	Q60932|VDAC1_MOUSE			32351,49	8,55	9	46,3		Transport
	KLETAVNLA**W**TAGNSNTR	Dioxidation(W)@10	214	231	7	1976,98	1976,99	99	2	
	WN**T**DNTLGTEITVEDQLAR	Thr->Pro@3	88	106	22	2171,00	2171,05	99	2	
	ATP synthase subunit d, mitochondrial	Q9DCX2|ATP5H_MOUSE			18749,45	5,52	10	72,7		OXPHOS
	LASLSEKPPAID**W**AYYR	Dioxidation(W)@13	42	58	5	2010,99	2011,01	99	1	

	S**W**NETFHAR	Dioxidation(W)@2	33	41	10	1178,50	1178,51	99	1	
	Creatine kinase S-type, mitochondrial	Q6P8J7|KCRS_MOUSE			47473,32	8,64	8	21,7		
	GI**W**HNYDK	Dioxidation(W)@3	250	257	6	1063,47	1063,47	99	2	Signal transduction
	TFLI**W**INEEDHTR	Dioxidation(W)@5	258	270	6	1704,80	1704,81	99	2	
	ADP/ATP translocase 1	P48962|ADT1_MOUSE			32901,27	9,73	13	24,8		
	EQGFLSF**W**R	Dioxidation(W)@8	64	72	14	1200,54	1200,56	99	1	
	QIFLGGVDR	Gln->pyro-Glu@N-term	97	105	12	986,51	986,52	99	2	
	EQGFLSFWR	Glu->pyro-Glu@N-term	64	72	9	1150,55	1150,56	99	2	Transport
	G**M**GGAFVLVLYDEIK	Oxidation(M)@2	281	295	7	1626,82	1626,83	99	2	
	G**M**GGAFVLVLYDEIKK	Oxidation(M)@2	281	296	6	1754,92	1754,93	99	1	
	EQGFLSF**W**R	Trp->Kynurenin(W)@8	64	72	6	1172,55	1172,56	99	1	
	ATP synthase subunit alpha, mitochondrial	Q03265|ATPA_MOUSE			59752,60	9,22	7	24,1		OXPHOS
	QGQYSP**M**AIEEQVAVIYAGVR	Gln->pyro-Glu@N-term; Oxidation(M)@7	473	493	0	2307,12	2307,12	99	2	
	Protein NipSnap homolog 2	O55126|NIPS2_MOUSE			32932,73	9,31	10	32		
	KNQLLLEFSF**W**NEPVPR	Dioxidation(W)@11	160	176	6	2148,09	2148,10	99	1	
	HG**W**EELVYYTVPLIQE**M**ESR	Dioxidation(W)@3; Oxidation(M)@17	251	270	0	2526,17	2526,17	99	1	unknown
	ENQEFVNFR	Glu->pyro-Glu@N-term	141	149	5	1163,53	1163,54	99	2	
	HGWEELVYYTVPLIQE**M**ESR	Oxidation(M)@17	251	270	0	2494,18	2494,18	99	2	
	KNQLLLEFSF**W**NEPVPR	Trp->Kynurenin(W)@11	160	176	6	2120,09	2120,11	99	1	
	Superoxide dismutase [Mn], mitochondrial	P09671|SODM_MOUSE			24602,93	8,80	9	34,7		
	F**N**GGGHINHTIFWTNLSPK	Ammonia-loss(N)@2	90	108	7	2122,02	2122,04	99	2	
	AIWNVIN**W**ENVTER	Dioxidation(W)@8	203	216	7	1774,85	1774,86	99	1	Redox
	AI**W**NVINWENVTER	Trp->Kynurenin(W)@3	203	216	12	1746,85	1746,87	99	1	
	AI**W**NVIN**W**ENVTER	Trp->Kynurenin(W)@3; Dioxidation(W)@8	203	216	14	1778,83	1778,86	99	1	
	NADH dehydrogenase [ubiquinone] iron-sulfur protein 8, mitochondrial	Q8K3J1|NDUS8_MOUSE			24038,33	5,89	11	37,7		
	LCEAI**C**PAQAITIEAEPR	Cys->Thr@6	118	135	31	1924,93	1924,99	99	2	OXPHOS
	LLN**N**GDKWEAEIAANIQADYLYR	Deamidated(N)@4	190	212	-4	2680,32	2680,31	99	1	

	LLN**N**GDK**W**EAEIAANIQADYLYR	Deamidated(N)@4; Dioxidation(W)@8	190	212	-17	2712,35	2712,30	99	1	
	ILM**W**TELIR	Dioxidation(W)@4	60	68	15	1205,63	1205,65	99	1	
	LLNNGDK**W**EAEIAANIQADYLYR	Dioxidation(W)@8	190	212	5	2711,31	2711,32	99	1	
	IL**M**WTELIR	Oxidation(M)@3	60	68	10	1189,64	1189,65	99	1	
	Cytochrome c1, heme protein, mitochondrial	Q9D0M3|CY1_MOUSE			35327,64	9,24	7	27,1		
	AAN**N**GALPPDLSYIVR	Deamidated(N)@4	187	202	2	1670,86	1670,86	99	1	OXPHOS
	WASEPEHDHR	FormaldehydeAdduct(W)@1	276	285	6	1274,53	1274,54	99	1	
	ATP synthase subunit O, mitochondria	Q9DB20|ATPO_MOUSE			23363,55	10,00	6	45,1		OXPHOS
	VSLAVLNPY**I**K	Ile->Cys@10	74	84	9	1205,64	1205,65	99	2	
	Cytochrome b-c1 complex subunit 2, mitochondrial	Q9DB77|QCR2_MOUSE			48234,9	9,26	7	17,7		
	LP**N**GLVIASLENYAPLSR	Deamidated(N)@3	43	60	7	1927,03	1927,04	99	1	OXPHOS
	L**P**NGLVIASLENYAPLSR	Pro->Ser@2	43	60	-2	1916,04	1916,04	99	2	
	ES1 protein homolog, mitochondrial	Q9D172|ES1_MOUSE			28090,45	9,00	5	27,4		unknown
	GVEVTVGHEQEEGGK**W**PYAGTAEAIK	Dioxidation(W)@16	187	212	1	2773,32	2773,32	99	1	
	NADH dehydrogenase [ubiquinone] 1 beta subcomplex subunit 10 O	Q9DCS9|NDUBA_MOUSE			20892,61	8,36	5	17,6		
	AYDLVVD**W**PVTLVR	Dioxidation(W)@8	36	49	8	1676,86	1676,88	99	1	OXPHOS
	AYDLVVD**W**PVTLVR	Trp->Kynurenin(W)@8	36	49	11	1648,86	1648,88	99	1	
	Dihydrolipoyllysine-residue acetyltransferase component of pyruvate dehydrogenase complex, mitochondrial	Q8BMF4|ODP2_MOUSE			58778,08	5,70	3	12,3		Metabolism
	LQPHEFQGGTFTISNLG**M**FGIK	Oxidation(M)@18	548	569	1	2437,21	2437,209961	99	1	
	Pyruvate dehydrogenase E1 component subunit alpha, somatic form, mitochondrial	P35486|ODPA_MOUSE			43231,63	8,49	2	6,7		Metabolism
	LP**C**IFI**C**ENNR	Cys->Dha(C)@3; Dioxidation(C)@7	216	226	24	1318,60	1318,63	99	2	
	Electron transfer flavoprotein subunit beta	Q9DCW4|ETFB_MOUSE			27623,29	8,25	3	12,9		Metabolism
	GIHV**E**IPGAQAESLGPLQVAR	Glu->Gln@5	86	106	56	2140,05	2140,18	99	2	
	Heat shock cognate 71 kDa protein	P63017|HSP7C_MOUSE			70739,87	5,37	2	5,1		Protein binding/folding
	ATVEDEKLQGKI**N**DEDKQK	Asn->Arg@13	551	569	4	2229,15	2229,16	99	2	
	3-hydroxyacyl-CoA dehydrogenase type-2	O08756|HCD2_MOUSE			27287,45	8,56	2	26,1		Metabolism

	LVAGE**M**GQNEPDQGGQR	Oxidation(M)@6	131	147	7	1800,79	1800,81	99	2	
	ADP/ATP translocase 2	P51881|ADT2_MOUSE			32931,29	9,74	8	28,5		Transport
	GA**W**SNVLR	Dioxidation(W)@3	273	280	15	933,45	933,47	99	1	
	G**M**GGAFVLVLYDEIK	Oxidation(M)@2	281	295	7	1626,82	1626,83	99	1	
	G**M**GGAFVLVLYDEIKK	Oxidation(M)@2	281	296	6	1754,92	1754,93	99	1	
	NADH dehydrogenase [ubiquinone] iron-sulfur protein 3, mitochondrial	Q9DCT2|NDUS3_MOUSE			30149,33	6,67	13	33,5		OXPHOS
	D-beta-hydroxybutyrate dehydrogenase, mitochondrial	Q80XN0|BDH_MOUSE			38284,97	9,14	4	17,2		Metabolism
	NADH dehydrogenase [ubiquinone] 1 beta subcomplex subunit 9	Q9CQJ8|NDUB9_MOUSE			21852,87	7,84	3	18,8		OXPHOS
	Myosin light chain 3	P09542|MYL3_MOUSE			22421,56	5,03	3	25		Structure
	Aconitate hydratase, mitochondrial	Q99KI0|ACON_MOUSE			85463,51	8,08	7	20,8		Metabolism
	Actin, alpha cardiac muscle 1	P68033|ACTC_MOUSE			42018,97	5,23	6	26		Structure
	Succinate dehydrogenase [ubiquinone] flavoprotein subunit, mitochondrial	Q8K2B3|DHSA_MOUSE			72585,4	7,06	5	10,4		OXPHOS
	Trifunctional enzyme subunit alpha, mitochondrial	Q8BMS1|ECHA_MOUSE			82669,85	9,24	4	7,6		Metabolism
	Triosephosphate isomerase	P17751|TPIS_MOUSE			26581,43	7,09	4	19,3		Metabolism
	Metaxin-2	O88441|MTX2_MOUSE			29758,12	5,44	4	22,8		Transport
	Isocitrate dehydrogenase [NADP], mitochondrial	P54071|IDHP_MOUSE			50906,18	8,88	3	15,9		Metabolism
	NADH dehydrogenase [ubiquinone] 1 alpha subcomplex subunit 9, mitochondrial	Q9DC69|NDUA9_MOUSE			42509,15	9,75	3	18,8		OXPHOS
	Cytochrome c oxidase subunit 4 isoform 1, mitochondrial	P19783|COX41_MOUSE			19530,46	9,25	3	20,7		OXPHOS
	NADH dehydrogenase [ubiquinone] flavoprotein 1, mitochondrial	Q91YT0|NDUV1_MOUSE			50834,2	8,51	3	11,6		OXPHOS
	Thioredoxin-dependent peroxide reductase, mitochondrial	P20108|PRDX3_MOUSE			21564,58	5,73	3	10,1		Redox
	Malate dehydrogenase, mitochondrial	P08249|MDHM_MOUSE			35611,45	8,93	3	13,9		Metabolism
	NADH dehydrogenase [ubiquinone] iron-sulfur protein 7, mitochondrial	Q9DC70|NDUS7_MOUSE			24682,87	9,94	2	14,7		OXPHOS
	Mitochondrial inner membrane protein	Q8CAQ8|IMMT_MOUSE			83900,08	6,18	2	7,7		Signal transduction
	Phosphate carrier protein, mitochondrial	Q8VEM8|MPCP_MOUSE			34843,84	9,11	2	14,6		Transport
	NADH dehydrogenase [ubiquinone] 1 alpha subcomplex subunit 8	Q9DCJ5|NDUA8_MOUSE			19860,88	8,80	2	24,4		OXPHOS

Citrate synthase, mitochondrial	Q9CZU6|CISY_MOUSE	51736,67	8,72	2	9,3	Metabolism
Voltage-dependent anion-selective channel protein 3	Q60931|VDAC3_MOUSE	30752,72	8,96	2	21,2	Transport
Voltage-dependent anion-selective channel protein 2	Q60930|VDAC2_MOUSE	31732,84	7,44	2	13,2	Transport
Tripartite motif-containing protein 72	Q1XH17|TRI72_MOUSE	52816,76	6,01	2	10,5	Transport
NADH dehydrogenase [ubiquinone] iron-sulfur protein 2, mitochondrial	Q91WD5|NDUS2_MOUSE	52625,66	6,52	2	6,5	OXPHOS
Cytochrome c, somatic	P62897|CYC_MOUSE	11605,44	9,61	2	23,8	OXPHOS
Cytochrome c oxidase subunit 5A, mitochondrial	P12787|COX5A_MOUSE	12436,10	5,01	2	20,6	OXPHOS
Fructose-bisphosphate aldolase A	P05064|ALDOA_MOUSE	39224,74	8,40	2	7,1	Metabolism
Trifunctional enzyme subunit beta, mitochondrial	Q99JY0|ECHB_MOUSE	51386,34	9,43	1	11,4	Metabolism
Hydroxyacyl-coenzyme A dehydrogenase, mitochondrial	Q61425|HCDH_MOUSE	34463,87	8,76	1	13,4	Metabolism
Adenylate kinase isoenzyme 1	Q9R0Y5|KAD1_MOUSE	21539,60	5,67	1	23,2	Signal transduction
Electron transfer flavoprotein subunit alpha, mitochondrial	Q99LC5|ETFA_MOUSE	35009,44	8,62	1	14,7	Metabolism
Dihydrolipoyllysine-residue succinyltransferase component of 2-oxoglutarate dehydrogenase complex, mitochondrial	Q9D2G2|ODO2_MOUSE	48994,52	9,10	1	15,2	Metabolism
78 kDa glucose-regulated protein	P20029|GRP78_MOUSE	72422,06	5,07	1	7,6	Protein binding/folding
Glutathione S-transferase Mu 1	P10649|GSTM1_MOUSE	25838,8	8,14	1	9,6	Redox
Alpha-actinin-2	Q9JI91|ACTN2_MOUSE	103653,49	5,36	1	6,6	Structure
Sarcalumenin	Q7TQ48|SRCA_MOUSE	99183,99	4,39	1	6,8	Signal transduction
2,4-dienoyl-CoA reductase, mitochondrial	Q9CQ62|DECR_MOUSE	32451,38	8,78	1	12,8	Metabolism
Calcium-binding mitochondrial carrier protein Aralar2	Q9QXX4|CMC2_MOUSE	74466,93	8,77	1	2,8	Signal transduction
Isocitrate dehydrogenase [NAD] subunit alpha, mitochondrial	Q9D6R2|IDH3A_MOUSE	39638,71	6,27	1	4,9	Metabolism
Coiled-coil-helix-coiled-coil-helix domain-containing protein 3, mitochondrial	Q9CRB9|CHCH3_MOUSE	26203,33	8,57	1	14,1	Structure
ATP synthase subunit gamma, mitochondrial	Q91VR2|ATPG_MOUSE	30124,63	8,87	1	7	OXPHOS
Acetyl-CoA acetyltransferase, mitochondrial	Q8QZT1|THIL_MOUSE	44816,12	8,71	1	6,4	Metabolism
Ubiquinone biosynthesis protein COQ9, mitochondrial	Q8K1Z0|COQ9_MOUSE	30240,70	4,93	1	10,5	DNA/RNA/Protein biosynthesis
NADH dehydrogenase [ubiquinone] 1 alpha	Q7TMF3|NDUAC_MOUSE	17086,41	9,38	1	22,8	OXPHOS

	subcomplex subunit 12						
	60S ribosomal protein L10	Q6ZWV3|RL10_MOUSE	24472,7	10,11	1	9,3	DNA/RNA/Protein biosynthesis
	Prohibitin	P67778|PHB_MOUSE	29820,10	5,57	1	7,7	DNA/RNA/Protein biosynthesis
	NADH dehydrogenase [ubiquinone] iron-sulfur protein 6, mitochondrial	P52503|NDUS6_MOUSE	10777,04	6,64	1	12,1	OXPHOS
	3,2-trans-enoyl-CoA isomerase, mitochondrial	P42125|D3D2_MOUSE	29110,72	7,77	1	9	Metabolism
	Stress-70 protein, mitochondrial	P38647|GRP75_MOUSE	73528,33	5,91	1	4,6	Protein binding/folding
	Glutathione S-transferase P 1	P19157|GSTP1_MOUSE	23477,99	8,13	1	12,9	Redox
	Aspartate aminotransferase, mitochondrial	P05202|AATM_MOUSE	44579,04	8,97	1	5,6	Metabolism
	Myosin-binding protein C, cardiac-type	O70468|MYPC3_MOUSE	140632,49	6,06	1	2,3	Signal transduction
	Mitochondrial carnitine/acylcarnitine carrier protein	Q9Z2Z6|MCAT_MOUSE	33026,74	9,24	1	2,7	Transport
	Cytochrome b-c1 complex subunit 7	Q9D855|QCR7_MOUSE	13396,28	9,10	1	9	OXPHOS
	NADH dehydrogenase [ubiquinone] 1 alpha subcomplex subunit 6	Q9CQZ5|NDUA6_MOUSE	15282,80	10,10	1	8,4	OXPHOS
	MACRO domain-containing protein 1	Q922B1|MACD1_MOUSE	35294,69	9,07	1	7,1	unknown
	Electron transfer flavoprotein-ubiquinone oxidoreductase, mitochondrial	Q921G7|ETFD_MOUSE	68090,93	7,34	1	1,8	Metabolism
	Lon protease homolog, mitochondrial	Q8CGK3|LONM_MOUSE	98861,48	5,69	1	0,9	Proteolysis
	Enoyl-CoA hydratase, mitochondrial	Q8BH95|ECHM_MOUSE	28474,72	7,78	1	7,2	Metabolism
	Dapper homolog 2	Q7TN08|DACT2_MOUSE	11710,21	11,20	1	2	Signal transduction
	NADH dehydrogenase [ubiquinone] 1 alpha subcomplex subunit 4	Q62425|NDUA4_MOUSE	9326,79	9,52	1	14,6	OXPHOS
5 x x x	ATP synthase subunit d, mitochondrial	Q9DCX2|ATP5H_MOUSE	18749,45	5,52	29	80,1	OXPHOS
	Cytochrome b-c1 complex subunit 1, mitochondrial	Q9CZ13|QCR1_MOUSE	52768,7	5,75	15	43,3	OXPHOS
	NADH dehydrogenase [ubiquinone] flavoprotein 2, mitochondrial	Q9D6J6|NDUV2_MOUSE	27285,34	7,00	12	65,3	OXPHOS
	ATP synthase subunit O, mitochondrial	Q9DB20|ATPO_MOUSE	23363,55	10,00	12	71,8	OXPHOS
	ATP synthase subunit b, mitochondrial	Q9CQQ7|AT5F1_MOUSE	28948,83	9,11	8	39,5	OXPHOS
	NADH dehydrogenase [ubiquinone] 1 beta subcomplex subunit 9	Q9CQJ8|NDUB9_MOUSE	21852,87	7,84	8	48,6	OXPHOS
	NADH dehydrogenase [ubiquinone] 1 beta subcomplex subunit 10	Q9DCS9|NDUBA_MOUSE	20892,61	8,36	9	47,7	OXPHOS

Mitochondrial 2-oxoglutarate/malate carrier protein	Q9CR62|M2OM_MOUSE	34023,00	9,95	5	24,8	Transport
Cytochrome b-c1 complex subunit Rieske, mitochondrial	Q9CR68|UCRI_MOUSE	34023,71	9,95	7	43,8	OXPHOS
Protein NipSnap homolog 2	O55126|NIPS2_MOUSE	32932,73	9,31	5	30,3	unknown
ATP synthase subunit beta, mitochondrial	P56480|ATPB_MOUSE	55262,41	5,24	4	31,8	OXPHOS
Cytochrome c oxidase subunit 2	P00405|COX2_MOUSE	25976,4	4,60	15	44,1	OXPHOS
ADP/ATP translocase 1	P48962|ADT1_MOUSE	32904,27	9,73	4	24,5	Transport
Superoxide dismutase [Mn], mitochondrial	P09671|SODM_MOUSE	24602,93	8,80	16	48,2	Redox
Thioredoxin-dependent peroxide reductase, mitochondrial	P20108|PRDX3_MOUSE	21564,58	5,73	4	22,6	Redox
Creatine kinase S-type, mitochondrial	Q6P8J7|KCRS_MOUSE	47473,32	8,64	3	19,6	Signal transduction
NADH dehydrogenase [ubiquinone] iron-sulfur protein 8, mitochondrial	Q8K3J1|NDUS8_MOUSE	24038,33	5,89	10	41,5	OXPHOS
Cytochrome c1, heme protein, mitochondrial	Q9D0M3|CY1_MOUSE	35327,64	9,24	4	24,9	OXPHOS
Ferritin light chain 1	P29391|FRIL1_MOUSE	20671,2	5,66	2	25,7	Redox
Cytochrome c oxidase subunit 4 isoform 1, mitochondrial	P19783|COX41_MOUSE	19530,46	9,25	2	24,9	OXPHOS
Aconitate hydratase, mitochondrial	Q99KI0|ACON_MOUSE	85463,51	8,08	2	22,4	Metabolism
NADH dehydrogenase [ubiquinone] iron-sulfur protein 3, mitochondrial	Q9DCT2|NDUS3_MOUSE	30149,33	6,67	2	12,2	OXPHOS
ES1 protein homolog, mitochondrial	Q9D172|ES1_MOUSE	28090,45	9,00	2	19,9	unknown
Adenylate kinase isoenzyme 1	Q9R0Y5|KAD1_MOUSE	21539,6	5,67	1	38,1	Signal transduction
NADH dehydrogenase [ubiquinone] 1 beta subcomplex subunit 8, mitochondrial	Q9D6J5|NDUB8_MOUSE	21875,83	6,15	2	21	OXPHOS
Isocitrate dehydrogenase [NADP], mitochondrial	P54071|IDHP_MOUSE	50906,18	8,88	1	14,6	Metabolism
Isocitrate dehydrogenase [NAD] subunit alpha, mitochondrial	Q9D6R2|IDH3A_MOUSE	39638,71	6,27	1	21,9	Metabolism
Myosin-7	Q91Z83|MYH7_MOUSE	222878,85	5,59	1	15,2	Structure
Actin, cytoplasmic 2	P63260|ACTG_MOUSE	41792,84	5,31	1	9,9	Structure
Malate dehydrogenase, mitochondria	P08249|MDHM_MOUSE	35611,45	8,93	1	9,5	Metabolism
Succinate dehydrogenase [ubiquinone] iron-sulfur subunit, mitochondrial	Q9CQA3|DHSB_MOUSE	31813,9	8,96	1	29,8	OXPHOS

	Dihydrolipoyllysine-residue acetyltransferase component of pyruvate dehydrogenase complex, mitochondrial	Q8BMF4|ODP2_MOUSE	58778,08	5,70	1	13,2	Metabolism
	NADH dehydrogenase [ubiquinone] 1 alpha subcomplex subunit 12	Q7TMF3|NDUAC_MOUSE	17086,41	9,38	1	37,2	OXPHOS
	Acyl-protein thioesterase 1	P97823|LYPA1_MOUSE	24687,69	6,14	1	13,9	Metabolism
	Cytochrome c, somatic	P62897|CYC_MOUSE	11605,44	9,61	1	41,9	OXPHOS
	Cytochrome b-c1 complex subunit 2, mitochondrial	Q9DB77|QCR2_MOUSE	48234,9	9,26	1	9,7	OXPHOS
	60S ribosomal protein L10	Q6ZWV3|RL10_MOUSE	24472,7	10,11	1	19,6	DNA/RNA/Protein biosynthesis
	Voltage-dependent anion-selective channel protein 1	Q60932|VDAC1_MOUSE	32351,49	8,55	1	11,2	Transport
	Electron transfer flavoprotein-ubiquinone oxidoreductase, mitochondrial	Q921G7|ETFD_MOUSE	68090,93	7,34	1	5,7	Metabolism
	Mitochondrial inner membrane protein	Q8CAQ8|IMMT_MOUSE	83900,08	6,18	2	13,7	Signal transduction
	Isocitrate dehydrogenase [NAD] subunit gamma 1, mitochondrial	P70404|IDHG1_MOUSE	42785,44	9,17	1	8,7	Metabolism
	ATP synthase subunit alpha, mitochondrial	Q03265|ATPA_MOUSE	59752,6	9,22	1	5,2	Metabolism
	Pyruvate dehydrogenase E1 component subunit alpha, somatic form, mitochondrial	P35486|ODPA_MOUSE	43231,63	8,49	2	20,5	Metabolism
	Lon protease homolog, mitochondrial	Q8CGK3|LONM_MOUSE	98861,48	5,69	1	9,1	Proteolysis
	D-beta-hydroxybutyrate dehydrogenase, mitochondrial	Q80XN0|BDH_MOUSE	38284,97	9,14	2	12,8	Metabolism
	Long-chain specific acyl-CoA dehydrogenase, mitochondrial	P51174|ACADL_MOUSE	47907,95	8,53	1	12,6	Metabolism
	Transmembrane protein 126A	Q9D8Y1|T126A_MOUSE	21539,22	9,45	1	23	Structure
	NADH dehydrogenase [ubiquinone] iron-sulfur protein 4, mitochondrial	Q9CXZ1|NDUS4_MOUSE	19784,69	10,00	1	10,3	OXPHOS
	NADH dehydrogenase [ubiquinone] 1 alpha subcomplex subunit 8	Q9DCJ5|NDUA8_MOUSE	19860,88	8,80	1	26,7	OXPHOS
	40S ribosomal protein SA	P14206|RSSA_MOUSE	32706,89	4,80	1	9,8	DNA/RNA/Protein biosynthesis
	NADH dehydrogenase [ubiquinone] iron-sulfur protein 7, mitochondrial	Q9DC70|NDUS7_MOUSE	24682,97	9,94	1	13,4	OXPHOS
6 x x x	Cytochrome c oxidase subunit 5A, mitochondrial	P12787|COX5A_MOUSE	12436,1	5,01	25	58,9	OXPHOS
	Cytochrome c oxidase subunit 5B, mitochondrial	P19536|COX5B_MOUSE	10718,18	5,74	10	44,5	OXPHOS
	Cytochrome b-c1 complex subunit 7	Q9D855|QCR7_MOUSE	13396,28	9,10	5	52,3	OXPHOS

Cytochrome c, somatic	P62897|CYC_MOUSE	11605,44	9,61	10	60	OXPHOS
ATP synthase subunit beta, mitochondrial	P56480|ATPB_MOUSE	11605,44	9,61	5	28,5	OXPHOS
Fatty acid-binding protein, heart	P11404|FABPH_MOUSE	14687,66	6,15	8	36,8	Metabolism
ADP/ATP translocase 1	P48962|ADT1_MOUSE	32904,27	9,73	7	23,5	Transport
NADH dehydrogenase [ubiquinone] 1 alpha subcomplex subunit 6	Q9CQZ5|NDUA6_MOUSE	15282,8	10,10	3	43,5	OXPHOS
NADH dehydrogenase [ubiquinone] iron-sulfur protein 6, mitochondrial	P52503|NDUS6_MOUSE	10777,04	6,64	3	34,5	OXPHOS
ATP synthase subunit delta, mitochondrial	Q9D3D9|ATPD_MOUSE	15023,87	4,46	3	22,6	OXPHOS
Cytochrome c oxidase subunit 6A2, mitochondrial	P43023|CX6A2_MOUSE	9421,68	8,13	3	38,1	OXPHOS
Cytochrome c oxidase subunit 6A1, mitochondrial	P43024|CX6A1_MOUSE	9619,83	6,63	2	41,4	OXPHOS
NADH dehydrogenase [ubiquinone] iron-sulfur protein 5	Q99LY9|NDUS5_MOUSE	12516,49	9,12	2	25,5	OXPHOS
Cytochrome c oxidase subunit 6C	Q9CPQ1|COX6C_MOUSE	8337,81	10,13	2	34,2	OXPHOS
NADH dehydrogenase [ubiquinone] 1 subunit C2	Q9CQ54|NDUC2_MOUSE	14163,66	9,24	1	22,5	OXPHOS
Cytochrome b-c1 complex subunit 8	Q9CQ69|QCR8_MOUSE	9637,06	10,26	1	29,3	OXPHOS
Enoyl-CoA hydratase, mitochondrial	Q8BH95|ECHM_MOUSE	28474,72	7,78	1	16,2	Metabolism
Acyl-coenzyme A thioesterase 13	Q9CQR4|ACO13_MOUSE	15182,84	8,95	1	18,6	Metabolism
Aconitate hydratase, mitochondrial	Q99KI0|ACON_MOUSE	85463,51	8,08	1	4	Metabolism
Mitochondrial carrier homolog 2	Q791V5|MTCH2_MOUSE	33367,92	8,60	1	9,6	Transport
Voltage-dependent anion-selective channel protein 1	Q60932|VDAC1_MOUSE	32351,49	8,55	1	11,5	Transport
Very long-chain specific acyl-CoA dehydrogenase, mitochondrial	P50544|ACADV_MOUSE	70875,5	8,91	1	3,7	Metabolism
NADH dehydrogenase [ubiquinone] 1 alpha subcomplex subunit 7	Q9Z1P6|NDUA7_MOUSE	12444,39	10,17	1	9,7	OXPHOS
Microsomal glutathione S-transferase 3	Q9CPU4|MGST3_MOUSE	16957,77	9,54	1	9,2	Redox
ATP synthase subunit g, mitochondrial	Q9CPQ8|ATP5L_MOUSE	11293,32	9,74	1	18,5	OXPHOS
Trifunctional enzyme subunit beta, mitochondrial	Q99JY0|ECHB_MOUSE	51386,34	9,43	1	2,3	Metabolism
CDGSH iron-sulfur domain-containing protein 1 O	Q91WS0|CISD1_MOUSE	12096,96	9,17	1	12	Signal transduction

NADH dehydrogenase [ubiquinone] 1 alpha subcomplex subunit 4	Q62425|NDUA4_MOUSE	9326,79	9,52	1	14,6	OXPHOS
ATP synthase subunit e, mitochondrial	Q06185|ATP5I_MOUSE	8104,41	9,35	1	9,9	OXPHOS
ADP/ATP translocase 2	P51881|ADT2_MOUSE	32931,29	9,74	3	18,8	Transport

STUDY II - OXPHOS SUSCEPTIBILITY TO OXIDATIVE MODIFICATIONS: THE ROLE OF HEART MITOCHONDRIAL SUBCELLULAR LOCATION

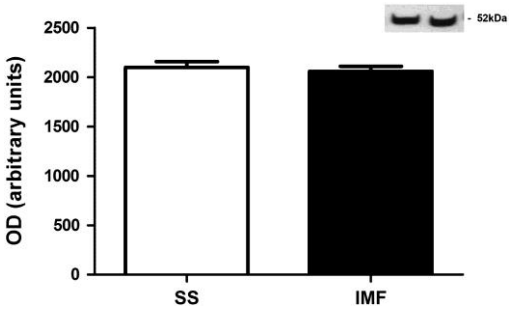

Supplementary Figure S1: Comparison of relative quantities of ATP synthase subunit β in cardiac mitochondrial populations determined by Western blotting analysis. A representative panel of immunoblot is presented above the histogram. Results represent the mean ± SEM for five pools of IMF and SS fractions

STUDY III - IMPAIRED PROTEIN QUALITY CONTROL SYSTEM UNDERLIES MITOCHONDRIAL DYSFUNCTION IN SKELETAL MUSCLE OF STREPTOZOTOCIN-INDUCED DIABETIC RATS

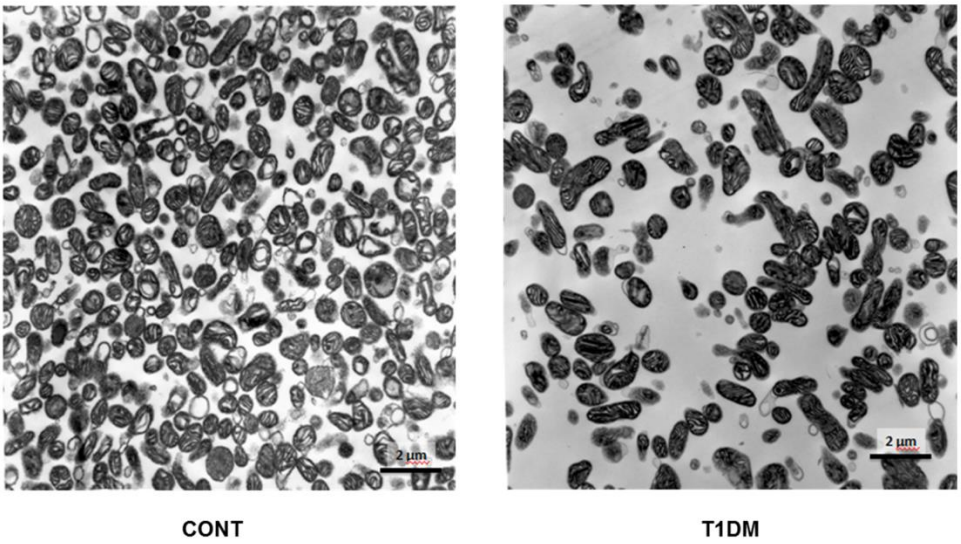

Supplementary Figure S1: Representative TEM micrographs of IMF mitochondria isolated from CONT (A) and T1DM (B) gastrocnemius muscle.

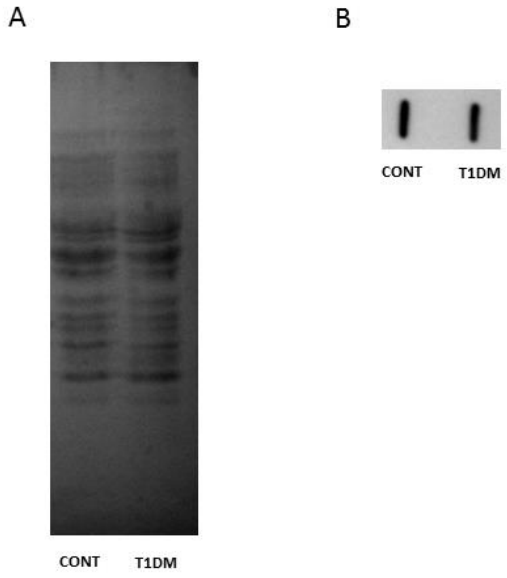

Supplementary Figure S2: Representative profile of Ponceau S stained western (A) and slot (B) blots.

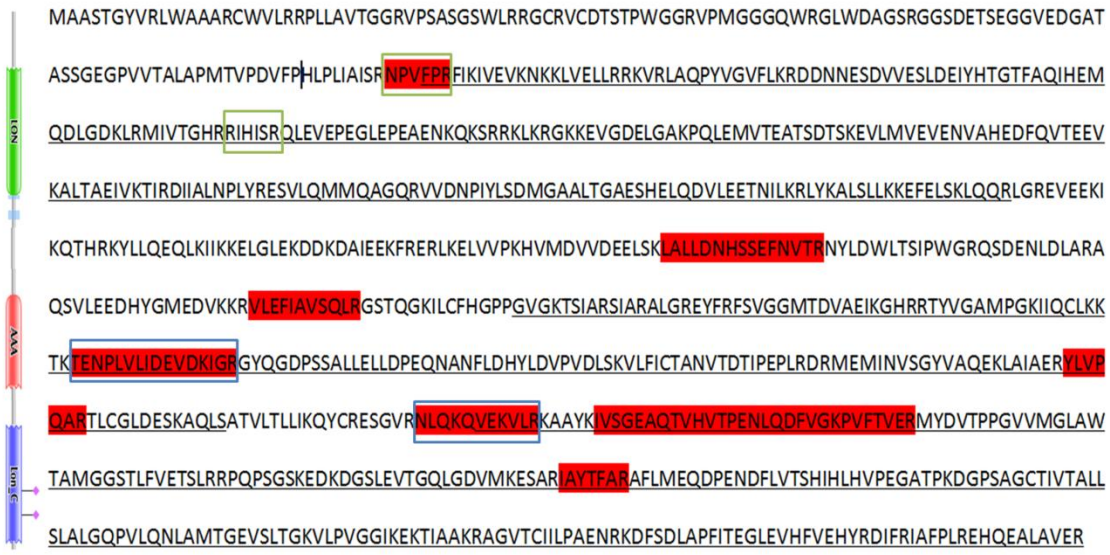

Supplementary Figure S3: Lon protease sequence (accession #LONM_RAT) evidencing the domains (underlined) assigned according to*MEROPS* with the identified peptides annotated: in red the ones identified in band 1, in blue boxes the ones observed in band 5 and in green boxes the peptides identified in band 6.

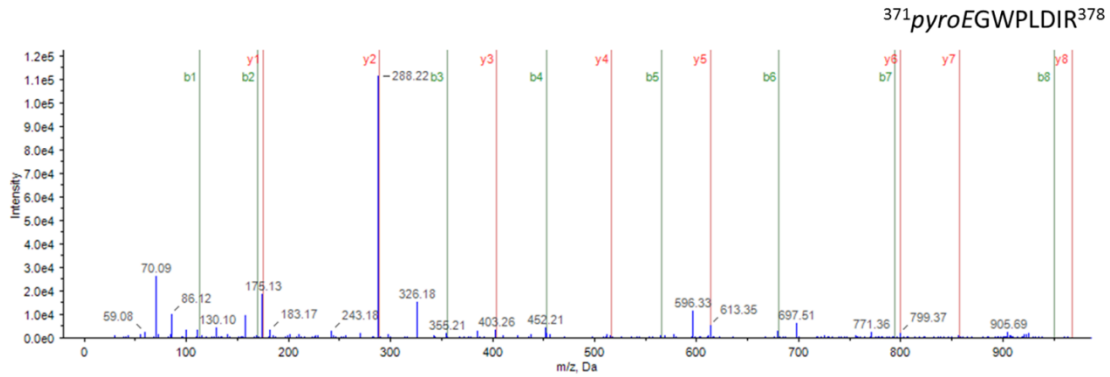

Supplementary Figure S4: MS/MS spectrum of the peptide 371EGWPLDIR378 derived from tryptic digestion of aconitate hydratase (accession #ACON_RAT) containing a pyro-Glu@N-term (annotated as pyroE), which analysis was performed following the methodological approach previously described [33]. The b and y ion series are annotated.

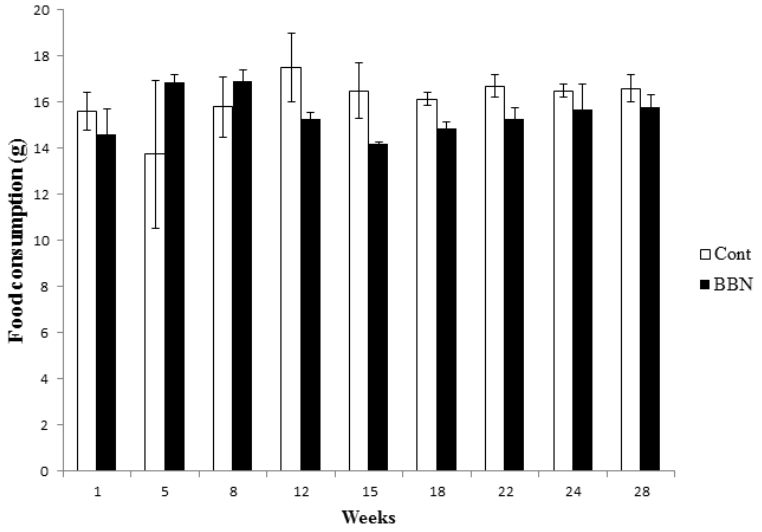

Supplementary Figure S1: Food intake over the course of the experimental protocol**.**

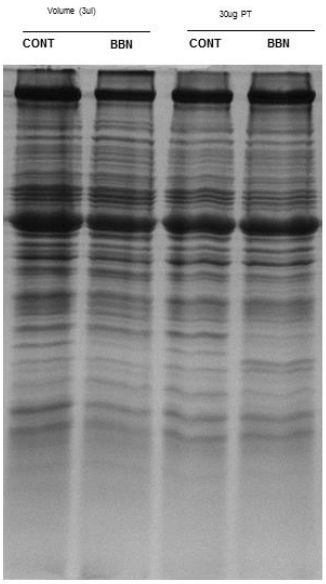

Supplementary Figure S2: Separation of mitochondrial proteins by 12 5% SDS-PAGE (considering sample volumes and protein content).